Luminescence dating of loess from the island of Susak in the Northern Adriatic Sea and the "Gorjanović loess section" from Vukovar in eastern Croatia

LARA WACHA

Luminescence dating of loess from the island of Susak in the Northern Adriatic Sea and the "Gorjanović loess section" from Vukovar in eastern Croatia

Inaugural-Dissertation
zur
Erlangung des Doktorgrades
im Fachbereich Geowissenschaften
der Freien Universität Berlin

vorgelegt von

LARA WACHA
aus Zagreb,
Kroatien

2011.

Erster Gutachter: Prof. Dr. Manfred Frechen

Zweiter Gutacher: Prof. Dr. Goran Durn

Eingereicht am: 08.02.2011.

Tag der Disputation: 17.05.2011.

CONTENTS

Summary

Loess-palaeosol sequences are an excellent high-resolution archive for palaeoenvironmental changes. They hide information about the past climate and climatic changes. To be able to reconstruct the palaeoenvironment it is common practice to investigate these deposits with a multidisciplinary approach. A detailed and reliable geochronology is mandatory to be able to interpret the results of such investigations.

The aim of this study was to establish a reliable chronological framework of loess-palaeosol sequences from Croatia. In Croatia two major loess regions can be distinguished, the North Adriatic loess region related to the river Po in North Italy and its tributaries and the Danube loess region in eastern Croatia. From both regions the most representative loess-palaeosol sequences were selected for investigations; the loess-palaeosol sequence on the island of Susak, where up to 90 m of Quaternary deposits, predominantly loess and loess derivatives were determined, and the "Gorjanović loess section" in Vukovar, which is the matter of scientific interest since the last centuries. These two genetically similar but in many ways different remains of climatic fluctuations during the Pleistocene were selected to be the topic for a detailed multi-proxy research for this PhD.

This geochronological framework is the first step in high-resolution investigations which is in progress. The dating was performed using infrared stimulated luminescence (IRSL) dating method, which is the method of choice for dating of Quaternary aeolian deposits, as well as radiocarbon dating. Throughout this PhD several luminescence dating protocols were used; the multiple aliquot additive (MAAD) dose protocol which is a somewhat old-fashioned protocol was used for polymineral fine grain material separated from the loess from Susak for an easier correlation with older published data in this area; the single aliquot regenerative (SAR) protocol which is a widely used measuring protocol, with fading tests and fading corrections performed on the measured samples as well, to obtain more reliable dating results. For the "Gorjanović loess section" the post-IR IRSL protocol, which is a modified SAR protocol developed recently for dating of older deposits (Middle Pleistocene) was introduced. This protocol has the advantage that it can overcome the performance of fading tests and fading corrections since in this protocol more stable luminescence signals from feldspars are registered.

Using the above mentioned laboratory measuring protocols which were supported by numerous experiments and performance tests good and reliable geochronological frameworks for the sections under study were established. The results from the loess-palaeosol sequences on Susak show us that a very detailed record correlating to OIS5 (and possibly OIS6 or older) is preserved, unique in this region. Furthermore, based on the dating results as well as mineralogical and geochemical investigations the three tephra layers were correlated to South Italian volcanic provinces. The luminescence dating results are supported by the radiocarbon dating as well. The "Gorjanović loess section" is an example of the penultimate glacial- last interglacial – last glacial period (OIS6 – OIS2), as seen from the dating results, and can easily be correlated to similar loess-palaeosol sections in the region.

In this thesis a detailed and reliable chronological framework of prominent loess-palaeosol sequences in Croatia is established as well as a milestone for a stratigraphy of Quaternary deposits in Croatia.

Zusammenfassung

Löss-/Paläobodenabfolgen sind ausgezeichnete Sedimentarchive, die Paläoumwelt-Veränderungen detailliert aufzeichnen. Um diese Umweltveränderungen der Vergangenheit rekonstruieren zu können, werden Sedimentabfolgen multidisziplinär untersucht. Hierbei ist ein detaillierter und verlässlicher chronologischer Rahmen eine notwendige Voraussetzung, um die Ergebnisse der Paläoumwelt-Veränderungen quantitativ interpretieren zu können.

Das Ziel dieser Doktorarbeit ist die Erstellung eines verlässlichen chronologischen Rahmens für Löss-/Paläobodenabfolgen aus Kroatien. In Kroatien können zwei wichtige Lößregionen unterschieden werden, die zum einen in Verbindung mit dem Po-Flusssystem und Norditalien und zum anderen mit dem Donau-Flusssystem in Ostkroatien stehen. Aus beiden Lößregionen wurden die repräsentativsten Löss-/Paläobodensequenzen für die chronologischen Untersuchungen ausgewählt: a) die Löß-/Paläobodenabfolge der Insel Susak, die aus bis zu 90 m mächtigen quartären Ablagerungen besteht, darunter vor allem Lösse und Lößderivate, und b) das Gorjanović-Löss-Profil in Vukovar. Das Gorjanović Löss-Profil ist in Kroatien von besonderem wissenschaftlichem Interesse und seit dem letzten Jahrhundert intensiv untersucht worden. Die Abfolgen auf Susak und in Vukovar sind genetisch ähnlich aber unterscheiden sich in vielen Eigenschaften, darunter die Ausprägung der klimatischen Fluktuationen.

Im Rahmen dieser Arbeit wurde ein verlässlicher chronologischer Rahmen mittels infrarot optisch stimulierte Lumineszenz (IRSL)-Datierungen erstellt. Die Lumineszenz (hier: IRSL) ist die Methode der Wahl, um quartäre minerogene Sedimente zu datieren und das Sedimentationsalter zu bestimmen. Die Radiokohlenstoff (^{14}C)-Methode wird für die Altersbestimmung von organischem Material (z.B. Holzkohle, Mollusken) angewendet und datiert den Zeitpunkt der seit dem Ableben des Organismus vergangen ist.

Im Rahmen dieser Dissertation wurden verschiedene Lumineszenz-Protokolle erstellt und angewendet: das „Multiple-Aliquot-Additiv“ (MAAD) Dosis Protokoll wurde für polymineralisches Feinkornmaterial (4-11 μm) angewendet, welches aus dem Löss von Susak aufbereitet wurde, um die Korrelation und Vergleichbarkeit mit alten Datierungsstudien zu erleichtern, in denen vorwiegend die MAAD-Protokolle angewendet wurden; desweiteren wurde das „Single Aliquot Regenerative“ (SAR) Protokoll angewendet, welches das heutzutage am weitesten verbreitete Messprotokoll ist, dies schließt die aus methodischen

Gründen wichtigen Fading-Tests und die Fading-Korrektur ein. Letztere sind notwendige Untersuchungen, um verlässlichere Datierungsergebnisse zu bestimmen.

Das post-IR IRSL–Protkoll ist ein modifiziertes SAR-Protokoll, das für die Datierung älterer Sedimente (Mittelpleistozän) eingeführt wurde, und für das Gorjanović-Profil verwendet wurde. Dieses Protokoll hat den Vorteil, dass Fading-Tests und Fading-Korrekturen nicht notwendig sind weil hier stabilere Lumineszenz-Signale aus Feldspat gemessen werden. Die Anwendung des post-IR IRSL-Protokolls wurde durch zahlreiche Experimente und „Performance Tests“ unterstützt, um auf diese Weise einen verlässlicheren chronologischen Rahmen für die untersuchten Sedimentabfolgen zu erstellen.

Die Ergebnisse für die Löss-/Paläobodenabfolgen aus Susak zeigen, dass eine sehr detaillierte Sequenz für das Sauerstoffisotopenstadium (OIS) 5 und 3 vorliegt. Das Vorkommen von Sedimenten, die mit OIS 6 oder älter korrelieren, sind ebenfalls nicht auszuschließen. Diese Löß-/Paläobodenabfolge ist für die Region nördliche Adria einzigartig.

Basierend auf den Datierungsergebnissen und mineralogischen und geochemischen Untersuchungen konnten drei dem Löss bzw. einem Paläoboden zwischen geschaltete Tephralagen mit der süditalienischen Vulkanprovinz korreliert werden.

Die Lumineszenz-Datierungen wurden durch ^{14}C-Altersbestimmungen unterstützt und bestätigt. Das Gorjanović-Profil ist ein Beispiel für die vorletztglaziale/letztinterglaziale bis letztglaziale Periode (OIS 6-2), wie durch Datierungsergebnisse bestätigt wurde, und kann sehr gut mit anderen bedeutenden Löss-/Paläobodenabfolgen der Nachbargebiete (Ungarn und Serbien) korreliert werden.

Im Rahmen dieser Doktorarbeit wurden zum ersten Mal ein detaillierter und verlässlicher chronologischer Rahmen für besonders wichtige Löss-/Paläobodenabfolgen aus Ostkroatien und der nördlichen Adria erstellt und somit ein bedeutender Fortschritt für die Quartärstratigraphie in Kroatien erreicht.

LIST OF FIGURES

LIST OF TABLES

CHAPTER 1

Introduction

1.1. The general background and the study sites

The Quaternary is a period of oscillating climate extremes; the climate changed from extremely cold with ice sheets covering most of the northern hemisphere to warm periods resulting in the recession of the ice. During the cold stages south of the margins of the ice extensions, in the mid-latitudes an extended loess cover accumulated in the periglacial area spreading from Northwest and Central Europe through Southeast Europe, the Russian Plain (Haase et al., 2007) and Central Asia (Dodonov, 1991). The most important and most extended loess region is in China (the Loess Plateau) where loess-palaeosol sequences are up to 300 m thick and represent a very detailed climate archive enabling an excellent correlation with the marine record (e.g. Guo et al., 1998; Frechen, 1999; Donghuai et al., 2004). Loess can also be found in northern and southern America (e.g. Roberts et al., 2003; Carter-Stiglitz et al., 2006), Alaska (e.g. Muhs et al., 2003) and New Zealand (e.g. Berger et al., 2002; Pillans and Wright, 1990). Since loess is a periglacial sediment directly dependant to climatic changes during the Quaternary high resolution investigation of these deposits are mandatory for unravelling climate information and climate reconstructions (e.g. Bokhorst and Vandenberghe, 2009; Bokhorst et al., 2009; Bokhorst et al., 2011). Nowadays climate changes are a matter of discussion and public interest and the general attitude is that investigating the past helps understanding the present and predicting the future. For a detailed investigation of a loess-palaeosol sequence a detailed and robust chronology is mandatory.

While the loess in China can be categorised to be desert loess, loess in Europe is usually associated with large river systems such as the Rhine and the Danube which flowed away from the Alpine ice margins through a tundra-steppe environment (Litt et al., 2008; Smalley et al., 2009). In the middle part of the Danube basin, several large rivers converse with the Danube, such as the Sava, the Drava and the Tisza. Due to that reason a lot of sediment material is available which is eventually deposited in the form of loess. In the Carpathian

basin along the Danube, thick (up to 60 m) loess sequences are exposed. Beside this classical loess region along the Danube, there is another loess region, related to the river Po in North Italy (Fig. 1.1.). In this area loess and loess derivatives can be found along the fringes of the Alps, covering the carbonate basement or filling caves and shelters (Coudé-Gaussen, 1990). The thickness of these deposits is not as impressive as the thickness of loess in the Carpathian basin, but an usually discontinuous loess coverage up to a few meters is present. However, on the island of Susak in Croatia (North Adriatic Sea) a very thick loess-palaeosol sequence is exposed. On this isolated island the thickness of Quaternary sediments is reported to be up to 90 m. Loess and loess derivatives from the North Adriatic region are often neglected for major palaeoclimatic reconstructions and regional correlation, partly because of their small thickness and partly owing to the lack of published data in international literature.

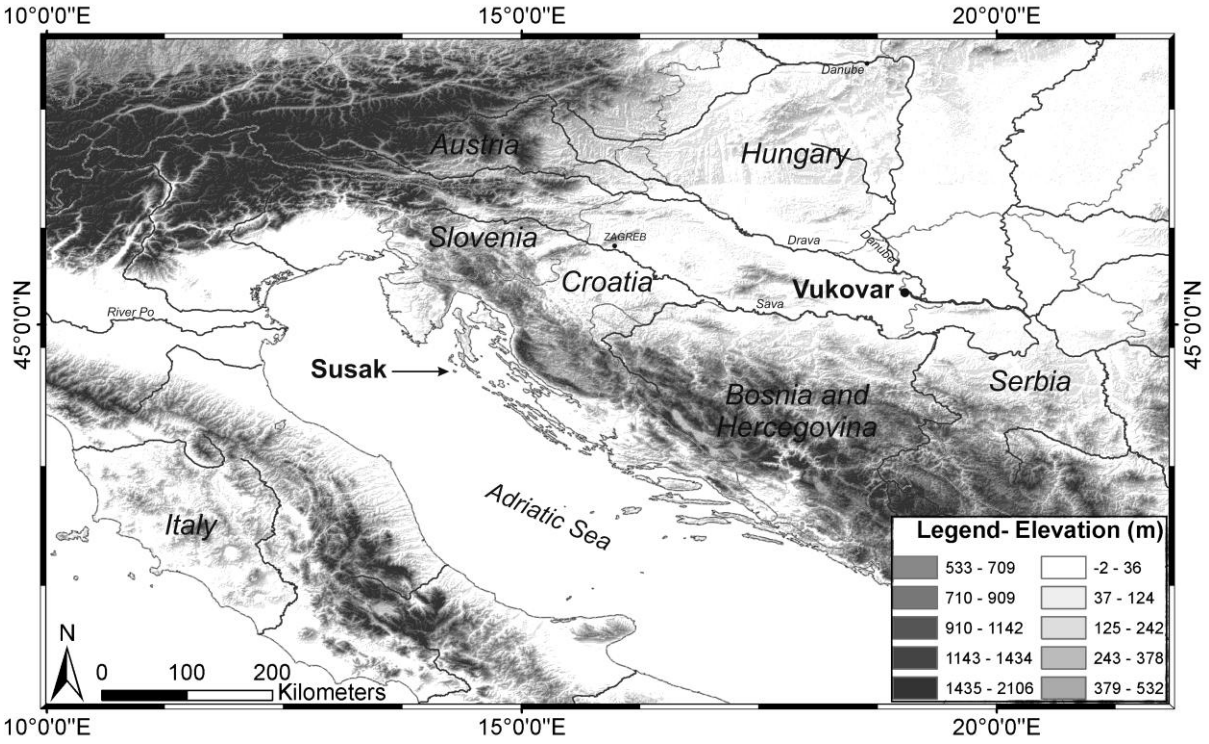

Figure 1.1. Map of Croatia and the neighbouring countries with indicated locations which were the topic of the research (the Island of Susak and the "Gorjanović loess section" in Vukovar. Elevation map for the area is prepared using the DEM image obtained from ASTER GDEM (product of METI and NASA).

Very oversimplified, the geology of Croatia can be divided into two major palaeogeographical units; the Adriatic Carbonate Platform (AdCP, Vlahović et al., 2005; Korbar, 2009) and the Croatian part of the Pannonian basin system (Pavelić, 2001, 2002, 2005). The AdCP is characterised by up to 8000 m thick carbonate succession ranging from the Middle Permian (or even Upper Carboniferous) to the Eocene (Vlahović et al., 2005). The Quaternary deposits

in this region are usually transgressive on the older sediments and are represented by moraine remains in the Velebit Mountain, glacio-fluvial deposits as well as aeolian deposits found on the coast and on the islands along the Adriatic Sea. During the Pleistocene the sea level of the Mediterranean Sea was up to 100 m lower than today (Van Straaten, 1970; Cremaschi, 1987; Amorosi et al., 1999) making the North Adriatic a closed basin with a large input of fluvial material carried by the river Po and its tributaries. During the glacials this fluvial material was exposed to wind activity and was subsequently deposited to form loess and aeolian sand interrupted by soil forming processes during the interglacials and interstadials. In this region volcanism was active as well, as evidenced by the three tephra layers detected on Susak (Mikulčić Pavlaković et al., 2011). Probably, a widely distributed small loess plateau, as evidenced by loess and loess derivatives on the island of Susak and neighbouring islands came into existence during glacial times but was eroded to a great extend again owing to the rising sea-level at the end of the last glaciations. The thick and in many ways unique loess-palaeosol sequence on the island of Susak made of loess, loess derivatives and sand intercalated by numerous palaeosols and (at least) three tephra layers is one of the topics of this thesis.

In Eastern Croatia the sediment record is more or less continuous from the Neogene to the Quaternary related to the sedimentary evolution of the Pannonian basin (Pavelić, 2005) with active tectonics during the Quaternary (Prelogović et al., 1998). The Pleistocene is characterised by alluvial sediments related to the major rivers of this area (Sava, Danube and Drava) and their tributaries. Besides alluvial deposits, eastern Croatia is characterised by thick loess deposits along the Danube. The thickness of loess and loess-like deposits in eastern Croatia ranges from 0.5 to 60 m (Bognar, 1979) with the thickest loess-palaeosols found on the loess plateaus, for example in the Vukovar loess plateau where the "Gorjanović loess section" was described (Wacha and Frechen, 2011b). Furthermore, the loess and loess-like deposits from eastern Croatia are genetically related to similar deposits in Vojvodina and Hungary where a detailed stratigraphy and geochronology already exists (e.g Marković et al., 2007; Fuchs et al., 2008; Schmidt et al., 2010; Novothny et al., 2002, 2009, 2010, 2011) which significantly helps the correlation.

This PhD thesis is an important contribution to the research of loess in Croatia. For the first time a systematic and very detailed dating approach was presented on the prominent loess-palaeosol sections from both loess regions in Croatia; i. e. on Susak from the river Po loess region and from Vukovar which belongs to the Danube loess region. Furthermore, these

investigated sections were correlated with the nearby surrounding loess sections and a regional chronology based correlation is presented. These first results are a basis for future high-resolution multi-proxy investigations as well as for establishing a detailed stratigraphy of the Croatian loess, which is a part of an ongoing post-PhD research project.

1.2. Loess stratigraphy in Croatia

In Croatia the tripartite Alpine geochronological distribution of the Late Pleistocene (Würm) was usually used for sediments although it often proved to be inappropriate (Rukavina, 1983) especially for loess-palaeosol sequences (Poje, 1985). Such stratigraphy was supported by several radiocarbon dating results of carbonate concretions and molluscs collected from loess (Galović and Mutić, 1984; Pikija et al., 1995). The radiocarbon dating method can only be used for ages up to 50,000 years (see Chapter 1.3.2.). The most detailed stratigraphy based on malacological investigations of loess-palaeosol sequences in eastern Croatia was presented by Poje (1985, 1986, 1988). With the application of more recent and precise nummerical dating methods this old Quaternary stratigraphy is more or less discarded and a correlation with oxygen isotope stages (OIS) is introduced.

The first systematic subdivision of loess-palaeosol sequences in Croatia was given by Gorjanović-Kramberger in 1922. He investigated morphological and hydrographical properties of several loess-palaeosol sequences from Eastern Croatia and while describing them he separated loess (L) from "laimen-zones" (S). While describing he counted the palaeosols from the stratigraphically oldest to the youngest (counting from the bottom) calling the lower-most exposed palaeosol S_1. He noticed the problem of counting from the bottom because not all loess-palaeosol sequences have the same number of palaeosols which was a problem for correlation. Nevertheless, he recognized the dependence of the deposits to palaeoclimatic changes and ice expansion and retreats. He also concluded that the loess-palaeosol sequences in eastern Croatia (and Vojvodina) belong to the upper Pleistocene (upper Diluvium) or if correlated to the Alpine Pleistocene division it can be correlated with the Würmian glacial period. Bronger (1976) made a detailed palaeopedological study of key loess sections from the Carpathian (Pannonian) basin, among others from Croatia (the Vukovar and Erdut section) with the purpose of reconstructing the Quaternary climate and landscape evolution. Based on his palaeopedological results he correlated the investigated

sections and assumed that the F_5 palaeosol (the fifth palaeosol from the top – a Braunerde type palaeosol) represents the last interglacial. This conclusion was revised after the first thermoluminescence (TL) dating results of the same sections presented by Singhvi et al. (1989). Singhvi et al. (1989) concluded that the F_3 and F_2 palaeosols can be correlated to the last interglacial period. A revised pedostratigraphy for the SE Central Europe was given by Bronger (2003). The first IRSL-based chronostratigraphy of three Middle and Upper Pleistocene loess-palaeosol sequences from eastern Croatia was given by Galović et al. (2009).

A detailed stratigraphy of the Danube loess from Vojvodina was presented by Marković et al. (2004). This stratigraphy follows the Chinese loess stratigraphic system (Kukla, 1987) and is supported by detailed geochronological, palaeomagnetic and other data (Marković et al., 2005, 2006, 2007, 2008, 2009; Fuchs et al., 2008; Buggle et al., 2009; Schmidt et al., 2010). Using the dating results of loess-palaeosol sequences from Croatia enables the correlation with the loess stratigraphy from Vojvodina.

In Hungary the stratigraphy of loess can generally be divided into the old and young loess series (Pécsi, 1993). The old loess series is characterised by red, reddish mediterranean type palaeosols and with the Brunhes-Matuyama palaeomagnetic boundary (0.78 Ma) detected in it. The young loess series relates to loess intercalated with numerous brown, well-developed steppe-like and forest palaeosols. The palaeosols found intercalating the loess are usually named after the type localities (key sections) in Hungary where they had been described in detail. Furthermore, there are two tephra layers which are good marker horizons for correlation; the Bag tephra (Horváth, 2001) found in the old loess series and the Paks tephra from the young loess series. The numerous geochronological investigations of loess-palaeosol sequences in Hungary enable correlation between the Hungarian (Novothny et al., 2002, 2009, 2010) and Serbian loess stratigraphy (Fuchs et al., 2008, Schmidt et al., 2010) which also relates to the Croatian loess (Chapter 5).

The first stratigraphy of loess on Susak from the North Adriatic region is presented in Chapters 2 and 4.

Since no loess stratigraphy was developed in Croatia the results of the detailed investigations presented in this study are used for correlation with both Serbian and Hungarian loess stratigraphies.

1.3. Dating methods

Various Quaternary dating methods are available, both numerical and relative. There are numerous publications and books regarding individual methods available (e.g Walker, 2005; Bradley, 1999). To establish an absolute chronology for the investigated Quaternary loess-palaeosol sequences from Croatia the luminescence dating method and the radiocarbon dating method were applied in these studies. Both will be briefly described in the next chapters. As luminescence dating methods are the central part of this PhD, a brief overview of the methodological background will be presented.

1.3.1. Luminescence dating

Luminescence dating belongs to the radiation exposure dating methods, along with electron spin resonance dating and fission track dating (see Walker, 2005; Bradley, 1999). These methods are based on measuring the cumulative effect of natural radioactivity on the crystal structure of minerals or fossils. The basic principle of such dating methods is that the larger the number of trapped electrons or crystal damage, the longer has been the time of exposure to radiation, and hence the older the material being dated (Walker, 2005). Luminescence dating can determine the time elapsed since the last exposure of the sediment to direct sunlight, which reduces the latent luminescence signal in minerals (Wintle and Huntley, 1979). Luminescence dating has the advantage that the sediments deposition age is dated directly (Fig. 1.2.). The equivalent dose (D_e) is a measure of the past radiation and, if divided by the dose rate (measured by gamma spectrometry), gives the time elapsed since the sediment was exposed to daylight or sunlight prior to deposition.

The age of a sample is calculated using the formula:

$$Age\ [a] = \frac{De}{Dose\ rate} \frac{(Gy)}{(Gy/a)};$$

where D_e is the equivalent dose measured in the luminescence laboratory and the dose rate is the annual dose rate of the surrounding sediment including the cosmic radiation. Detailed descriptions of the physical background and the principles of the luminescence dating method

are given in Wintle (1997), Aitken (1998), Bøtter-Jensen et al. (2003), Wintle (2008 and papers within) and Preusser et al. (2008).

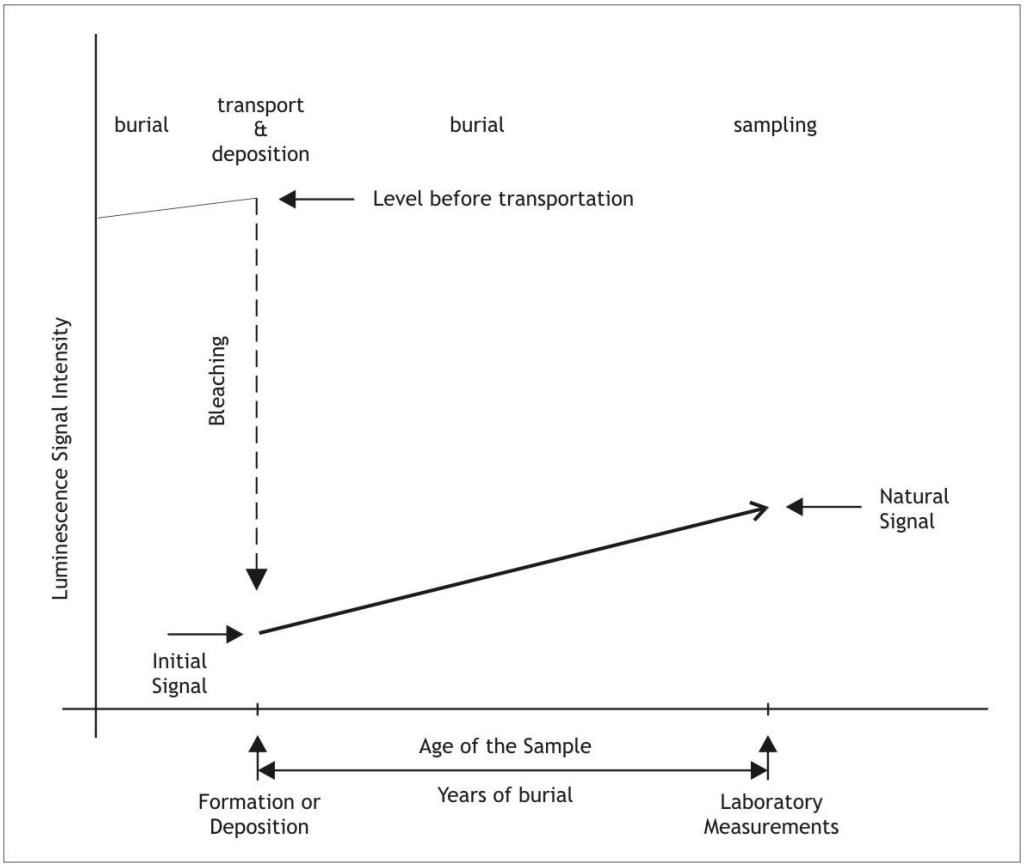

Figure 1.2. The principle of luminescence dating (modified after Aitken, 1998 and Walker, 2005).

That minerals when heated emit light was already described in 1663 by Sir Robert Boyle (Boyle, 1664). He noted that diamonds glow in dark when heated. This effect is called thermoluminescence and was used for mineral identification until the 1950s when this effect was applied for dating of archaeological and geological materials as well as for many other dosimetric applications (Aitken, 1985, 1998). Thermoluminescence dating (TL) as well as the optically stimulated luminescence dating (OSL – when stimulated with a light source, a diode or a laser) are widespread methods for dating archaeological materials and Quaternary sediments. There are several types of OSL which depends on the wavelength of the applied light. For the stimulation of quartz the blue or the green light is used while for feldspars the infrared stimulation is used (infrared stimulated luminescence - IRSL).

OSL dating proved to be successful for dating aeolian sediments, such as loess (as presented in this thesis) and dunes (e.g. Kunz et al., 2010; Alappat et al., submitted), and shallow marine sediments (Alappat et al., 2010; Thiel et al., 2010a; Jacobs, 2008). Furthermore, OSL dating is applied for fluvial (Lauer et al., 2010) and glacial (Ou et al., 2010) deposits as well; although the basic assumption of the method is not always fulfilled for these sedimentary environments, i.e. there is insufficient sediment exposure to sunlight prior to deposition which means that these deposits suffer from incomplete bleaching and hence the dating results are age overestimated, if appropriate statistical methods are not applied. Experiments and methodological improvements are trying to overcome this problem.

The two mostly used minerals for TL and OSL dating (which are the two most abundant minerals in sediments, as well) are quartz and feldspars. Quartz saturates at lower doses than feldspar, usually at ~ 200 Gy and can hence be used for dating of samples up to about 50-70 ka depending of the dose rate of the sediment. On the other hand, feldspar can be used for dating older sediments, up to several hundred thousand years because it saturates at ~ 2000 Gy (Schmidt et al., 2010, submitted; Thiel et al., 2011; Lauer et al., 2010). But feldspar has the disadvantage that it suffers from anomalous fading (Wintle, 1973), an athermal loss of signal which can cause age underestimation. To overcome this problem Huntley and Lamothe (2001) presented a solution for corrections of ages. These fading corrections are possible only for the linear part of the growth curve, which means samples up to ~ 50 ka. Fading corrections for feldspar in saturation field is under investigation (Lamothe et al., 2003; Kars et al., 2008). Recently new measuring protocols were developed which measure more stable luminescence signals which show less fading (Thomsen et al., 2008; Buylaert et al., 2009; Reimann et al., 2010; Thiel et al., 2010a, b, c, 2011, submitted; Wacha et al., 2010b, 2011b; Schmidt et al., submitted).

1.3.1.1. Measuring protocols

There are several types of measuring protocols for establishing the equivalent dose (D_e) used in more recent research. Therefore, different protocols were applied in order to compare and correlate the results with previously published data. Furthermore, the used measuring procedures presented in this thesis are an interesting summary of a fast evolution of the dating method towards more precise and accurate results. Because of that reason the protocols will be mentioned here and shortly described.

1.3.1.1.1. Multiple aliquot additive dose protocol (MAAD)

Using the multiple aliquot additive dose protocol (MAAD) many aliquots (subsamples) are measured for calculating a single D_e value. The principle of this protocol is shown in Fig. 1.3.a. For this measurement several (48) aliquots are prepared and divided into groups. One group of aliquots is used for the measurement of the natural luminescence signal while the other groups are irradiated with different doses prior to any measurements. Usually seven increasing doses are given, which are used for the construction of the growth curve. Prior to the measurements the aliquots are preheated at 230°C for 1 minute in order to eliminate the unstable part of the signal. The D_e of the unknown sample is calculated by extrapolation of the growth curve. The advantage of the MAAD measuring protocol is that the sample was not often heat treated during the protocol which reduces the sensitivity changes of the sample which is often a problem of other measuring protocols.

Another problem of this protocol is that the error depends on the scatter of the growth curve (the bigger the scatter, the bigger the error) and that the ages are usually underestimated if compared to other protocols, because the measurements took place four weeks after the irradiation of the aliquots. Furthermore, no fading corrections were developed for the MAAD.

In this thesis the MAAD protocol was used as presented by Galović et al. (2009), Novothny et al. (2002) and Wintle (1997).

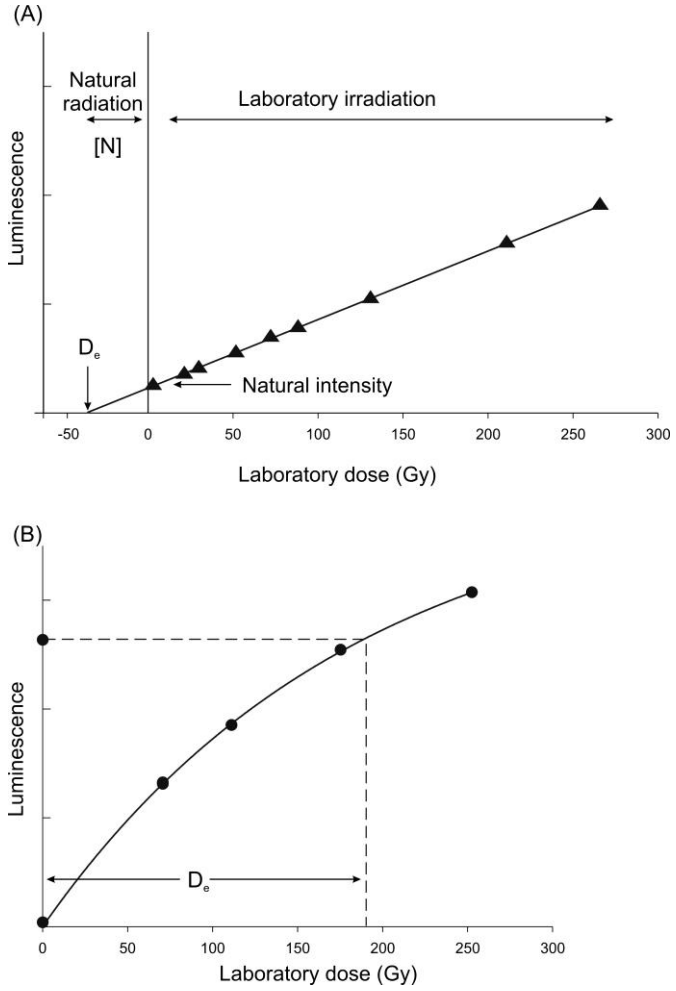

Figure 1.3. (A) The multiple aliquot additive (MAAD) dose evaluation. After measuring the natural luminescence signal same aliquots are irradiated in the laboratory with several increasing doses. The D_e is obtained by extrapolation of the curve. (B) The single aliquot regenerative (SAR) dose evaluation. The natural signal is compared to the artificially constructed growth curve. (from Walker, 2005).

1.3.1.1.2. Single aliquot regenerative dose protocol (SAR)

The advantage of this protocol, compared to the MAAD, is that only one aliquot is needed to obtain a D_e-value. Another advantage of the SAR protocol is that the D_e-value is determined by the interpolation of the growth curve. The SAR protocol comprises a series of cycles. In the first cycle the natural luminescence signal of the aliquot is registered. In the next few steps the aliquot is exposed to several steps of artificial radiation and the luminescence signal is measured afterwards. All of these measurements of luminescence are preceded by a preheat which understands heating the sample to a fixed temperature, usually between 160°C and 300°C and holding it there for a short period of time (e.g. 10 s). This procedure removes unstable charges from shallow traps so that the luminescence signal comes only from stable

traps. After repeating this procedure for several regeneration doses the dose response curve can be constructed and the unknown natural signal can be interpolated and the D_e estimated (Fig. 1.3.b). The disadvantage of the SAR protocol are the numerous heating and optical stimulation steps which can cause sensitivity changes in the sample. Sensitivity changes are monitored and used for corrections in the protocol which minimize this problem (Duller, 2008).

In this study the SAR protocol after Wallinga et al. (2007) was used for the D_e measurements as well as all the necessary performance tests prior to the measurements.

1.3.1.1.3. Elevated temperature post-IR IRSL protocol

Both the MAAD and the SAR protocol are used for measurements of the quartz and feldspar luminescence signal. Since feldspar suffers from anomalous fading, an athermal loss of signal through time (Wintle, 1973; Spooner, 1994) causing age underestimation, time consuming fading corrections are required (Huntley and Lamothe, 2001). But also new protocols, such as the post-IR IRSL, are being developed to overcome this problem. The elevated temperature post-IR IRSL protocol is based on measuring more stable luminescence signals of feldspar which are supposed to show less fading. Thomsen et al. (2008) made tests on various sedimentary feldspar samples using different stimulation and detection conditions and concluded that stimulation at elevated temperatures reduces the fading rate. Based on this study Buylaert et al. (2009) tested a modified SAR protocol which involved stimulation at 50°C (which is the standard temperature for feldspar) as well as stimulation at 225°C afterwards (post-IR IRSL signal). In their study they concluded that the post-IR IRSL fading rates are significantly lower than the fading rates for the IRSL signal at 50°C and that this signal is bleachable in nature and can hence be used for dating of sediments.

1.3.2. Radiocarbon dating

Radiocarbon dating is probably the most widely used radiometric dating technique although it has a relatively short age span, up to about 50 000 years (Geyh, 2005). It is also one of the first radiometric dating techniques which resulted from Willard Libby's investigations of the possibility that radiocarbon might exist in biological materials (Walker, 2005).

^{14}C (radiocarbon), along with ^{12}C and ^{13}C, is one of the three isotopes of carbon. The most abundant of those is ^{12}C which comprises around 98.9% of all naturally occurring carbon, the rest is ^{13}C and ^{14}C. ^{14}C is a naturally occurring radioisotope which occurs in trace amounts on Earth of up to 1 part per trillion (0.0000000001%). ^{14}C decays to a stable nitrogen isotope, ^{14}N, through the emission of beta (β) particles. One β particle is released from the nucleus for every atom of ^{14}C that decays. Atoms of ^{14}C are formed in the upper atmosphere through the interaction of cosmic rays with nitrogen. During this reaction the neutrons from the cosmic radiation are captured by the nitrogen (^{14}N) atom and the lost proton creates ^{14}C. This ^{14}C is rapidly oxidised to form carbon dioxide ($^{14}CO_2$) which becomes a part of the global carbon cycle of the earth and eventually assimilates into plants through the photosynthesis and subsequently animals as well. The major part of ^{14}C is absorbed into the oceans. Although ^{14}C is constantly decaying it is also continuously added from the atmosphere, which means that the amount of ^{14}C is constant through time. Eventually, the carbon in living beings is in isotopic equilibrium with the atmosphere. This situation is constant until the death of the organism which triggers the "radiocarbon clock" (Walker, 2005). The radioactive decay occurs at a constant rate which means that if we measure the amount of ^{14}C remained in a fossil or sample and compare it to modern ^{14}C in standard materials, an age for the death of the organism can be determined. For this purpose it is necessary to know the rate at which ^{14}C decays. The half-life of a ^{14}C atom is 5730±40 years which means that the upper age limit is around 45000 years. Samples older than 45000 years are defined as being of "infinite age" (Walker, 2005; Geyh, 2005).

There are several error sources in radiocarbon dating. Contamination refers to addition of younger or older carbon to the sample material. It can happen prior to field sampling, due to e.g. bioturbation, during sampling or in the laboratory. There are physical and chemical pretreatments to remove some of the contaminants but if the contaminant has the same chemical characteristic as the sample, separation of the contaminant may be impossible. Isotopic fractionation understands preferential incorporating of lighter C isotopes into a material. This can be corrected in the laboratory by measuring the $^{13}C/^{12}C$ ratio using mass spectrometry and comparing it with the ratio of the PDB limestone standard. Another problem is the marine reservoir effect. This is a problem for marine materials because sea water often shows an apparent age due to longer residence time of ^{14}C in intermediate and deep waters. But one of the major problems in radiocarbon dating is the long-term variation in the production of ^{14}C appearing naturally and influenced by human activity (Walker, 2005; Bradley, 1999).

1.4. Outline of the dissertation

This dissertation is composed of six chapters. In **Chapter 1** the general outline of the thesis and introductory notes are presented. **Chapters 2** to **5** are articles which were all submitted to peer-reviewed journals. **Chapters 2** and **3** are articles published in *Quaternary International*, **Chapter 4** is in press in *Quaternary Science Journal (Eiszeitalter und Gegenwart)*, **Chapter 5** is in press in *Quaternary International* and **Chapter 6** provides a conclusion and a summary of the previous chapters and an overview of all the results.

Chapter 2: Luminescence Dating of Upper Pleistocene Loess from the Island of Susak in Croatia (Wacha et al., 2011a).

In this chapter the first attempt of dating of loess in the Croatian North Adriatic loess region (the island of Susak) is presented. In this study the luminescence dating method was applied on both coarse-grained quartz and fine-grained feldspar minerals separated from loess, with the purpose to find the appropriate dating protocol for the measurements. Both the SAR and the MAAD protocol were applied for the measurements of the D_e-s for better comparison with older published dating results from Croatia. Luminescence dating results were compared with radiocarbon data. The first interpretation of the geochronology and stratigraphy of the loess-palaeosol sequence on Susak was provided.

Chapter 3: Mineralogical and Geochemical Characteristics of Quaternary Sediments from the Island of Susak (Northern Adriatic, Croatia) (Mikulčić Pavlaković et al., 2011)

This chapter deals with mineralogical and geochemical properties of Quaternary sediments from the island of Susak. A part of this research was luminescence dating of a further loess-palaeosol section, not described in Wacha et al. (2011a). This research is related to the research presented in **Chapter 2** and was hence included in this dissertation. In this chapter a correlation of four investigated sections was presented. Based on the mineralogical and geochemical properties of the tephra layers found in the loess-palaeosol sequence on Susak island and luminescence dating results of the loess below and above the tephra layer, a possible provenance of the volcanic events was proposed.

Chapter 4: The Loess Chronology of the Island of Susak, Croatia. (Wacha et al., 2010a).

A high-resolution infrared stimulated luminescence (IRSL) and radiocarbon dating study of the loess-palaeosol sequence on Susak is presented in **Chapter 4**. In this chapter the research of the previous two chapters was summarized and improved with more data. A more complete geochronology of the sections under study is presented. The investigated loess-palaeosol sequences from the Island of Susak in the river Po plain loess region were compared and correlated with contemporaneous sequences from the Carpathian basin and the river Danube loess region.

Chapter 5: The Geochronology of the "Gorjanović loess section" in Vukovar. (Wacha and Frechen, 2011b)

In this study a detailed geochronological framework was presented for the "Gorjanović loess section" in eastern Croatia. This section has been a matter of interest since the last centuries and is considered as one of the key loess sections in Croatia. For this study the post-IR IRSL protocol was tested and applied for equivalent dose (D_e) calculations. This protocol proved to be successful for dating of older sediments. A geochronological interpretation of the investigated section and the correlation with other loess sections in the region is presented. This chapter contributed unravelling the evolution of the loess-palaeosol region of the river Danube area.

1.5. References

Aitken, M.J., 1985. Thermoluminescence dating. Academic Press, London, 351 pp.

Aitken, M.J., 1998. An Introduction to Optical Dating. Oxford University Press, Oxford, 280 pp.

Alappat, L., Vink., A., Tsukamoto, S., Frechen, M., 2010. Establishing the Late Pleistocene–Holocene sedimentation boundary in the southern North Sea using OSL dating of shallow continental shelf sediments. Proceedings of the Geologists' Association 121, 43-54.

Alappat, L., Frechen, M., Ramesh, R., Tsukamoto, S., Srinivasalu, S., submitted. Evolution and chronology of late Holocene coastal dunes in the Cauvery delta region of Tamil Nadu, India. Journal of Asian Earth Sciences.

Amorosi, A., Colalongo, M.L., Pasini, G., Preti, D., 1999. Sedimentary response to Late Quaternary sea-level changes in the Romagna plain (northern Italy). Sedimentology 46, 99-121.

Berger, G.W., Pillans, B.J., Bruce, J.G., McIntosh, P.D., 2002. Luminescence chronology of loess-paleosol sequences from southern South Island, New Zealand. Quaternary Science Review 21, 1899-1913.

Bognar, A., 1979. Distribution, properties and types of loess and loess-like sediments in Croatia. Acta Geologica Academiae Scientiarium Hungaricae 22, 267-286.

Bokhorst, M., Vandenberghe, J., 2009. Validation of wiggle matching using a multi-proxy approach and its palaeoclimatic significance. Journal of Quaternary Science 24/8, 937-947.

Bokhorst, M.P., Beets, C.J., Marković, S.B., Gerasimenko, N.P., Matviishina, Z.N., Frechen, M., 2009. Pedo-chemical climate proxies in Late Pleistocene Serbian–Ukranian loess sequences. Quaternary International 198, 113-123.

Bokhorst, M.P., Vandenberghe, J., Sümegi, P., Łanczont, M., Gerasimenko, N.P., Matviishina, Z.N., Marković, S.B., Frechen, M., 2011. Atmospheric circulation patterns in central and eastern Europe during the Weichselian Pleniglacial inferred from loess grain-size records. Quaternary International 234, 1-2, 62-74.

Bøtter-Jensen, L., McKeever, S.W.S., Wintle, A.G., 2003. Optically Stimulated Luminescence Dosimetry. Elsevier, Amsterdam, 355 pp.

Boyle, R., 1664. Experiments and Considerations Touching Colours. Herringham, London. http://www.gutenberg.net.

Bradley, R.S., 1999. Palaeoclimatology – Reconstructing Climates of the Quaternary. Academic Press, San Diego, XV + 614 pp.

Bronger, A., 1976. Zur quartären Klima- und Landschaftsentwicklung des Karpatenbeckens auf (palaeo)-pedologischer und bodengeographischer Grundlage. Kieler Geographische Schriften 45, 268 pp.

Bronger, A., 2003. Correlation of loess-paleosol sequences in East and Central Asia with SE Central Europe: towards a continental Quaternary pedostratigraphy and paleoclimatic history. Quaternary International 106/107, 11–31.

Buggle, B., Hambach, U., Glaser, B., Gerasimenko, N., Marković, S., Glaser, I., Zöller, L., 2009. Stratigraphy, and spatial and temporal paleoclimatic trends in Southeastern/Eastern European loess-paleosol sequences. Quaternary International 196, 86-106.

Buylaert, J.P., Murray, A.S., Thomsen, K.J., Jain, M., 2009. Testing the potential of an elevated temperature IRSL signal from K-feldspar. Radiation Measurements 44, 560-565.

Carter-Stiglitz, B., Banerjee, S.K., Gourlan, A., Oches, E., 2006. A multi-proxy study of Argentina loess: Marine oxygen isotope stage 4 and 5 environmental record from pedogenic hematite. Palaeogeography, Palaeoclimatology, Palaeoecology 239, 45-62.

Coudé -Gaussen, G., 1990. The loess and loess-like deposits along the sides of the western Mediterranean Sea: genetic and palaeoclimatic significance. Quaternary International 5, 1–8.

Cremaschi, M., 1987. Loess deposits of the Po plain and the adjoining Adriatic basin (Northern Italy). In: Pécsi, M. and French, H.D. (eds.): Loess and Periglacial Phenomena: 125-140, Budapest (Akademiai Kiado).

Duller, G.A.T., 2008. Luminescence dating: Guidelines on using luminescence dating in archaeology. English Heritage, Swindon, 43 pp.

Dodonov, A.E., 1991. Loess of Central Asia. GeoJurnal 24.2, 185-194.

Donghuai, S., Bloemendal, J., Rea, D.K., Zhisheng, A., Vandenberghe, J., Huayu, L., Ruixia, S., Tungsheng, L., 2004. Bimodal grain-size distribution of Chinese loess, and its palaeoclimatic implications. Catena 55, 325-340.

Frechen, M., 1999. Luminescence dating of loessic sediments from the Loess plateau, China. Geologische Rundschau 87, 675-684.

Fuchs, M., Rousseau, D.-D., Antoine, P., Hatté, C., Gauthier, C., Marković, S., Zoeller, L. 2008. Chronology of the Last Climatic Cycle (Upper Pleistocene) of the Surduk loess sequence, Vojvodina, Serbia. Boreas 37, 66-73.

Galović, I., Mutić, R., 1984. Gornjopleistocenski sediment istočne Slavonije (Hrvatska). Rad JAZU 411, 299–356, Zagreb.

Galović, L., Frechen, M., Halamić, J., Durn, G., Romić, M., 2009. Loess chronostratigraphy in Eastern Croatia - A first luminescence dating approach. Quaternary International 198 (1-2), 85 -97.

Geyh, M.A., 2005. ^{14}C dating – still a challenge for users? Zeitschift fur Geomorphologie, NF Supplementband 139, 63–85.

Gorjanović-Kramberger, D., 1922. Morfologijske i hidrografijske prilike prapornih predjela Srijema, te pograničnih česti županije virovitičke. Glasnik hrvatskoga prirodoslovnog društva XXXIV, 111-164, Zagreb.

Guo, Z., Liu, T., Fedoroff, N., Wei, L., Ding, Z., Wu, N., Lu, H., Jiang, W., An, Z., 1998. Climate extremes in Loess of China coupled with the strength of deep-water formation in the North Atlantic. Global and Planetary Change 18, 113-128.

Haase, D., Fink, J., Haase, G., Ruske, R., Pécsi, M., Richter, H., Altermann, M., Jäger, K.D., 2007. Loess in Europe – its spatial distribution based on a European Loess Map, scale 1:2,500,000. Quaternary Science Reviews 26, 1301-1312.

Horváth, E., 2001. Marker horizons in the loesses of the Carpathian Basin. Quaternary International 76/77, 157-163.

Huntley, D.J., Lamothe, M., 2001. Ubiquity of anomalous fading in K-feldspars, and the measurement and correction for it in optical dating. Canadian Journal of Earth Sciences 38, 1093-1106.

Jacobs, Z., 2008. Luminescence chronologies for coastal and marine sediments. Boreas 37, 508-535.

Kars, R.H., Wallinga, J., Cohen, K.M., 2008. A new approach towards anomalous fading correction for feldspar IRSL dating – tests on samples in field saturation. Radiation Measurements 43, 786-790.

Korbar, T., 2009. Orogenic evolution of the External Dinarides in the NE Adriatic region: a model constrained by tectonostratigraphy of Upper Cretaceous to Paleogene carbonates. Earth-Science Review 96/4, 296-312.

Kukla, G., 1987. Loess stratigraphy in Central China. Quaternary Science Reviews 6, 191-219.

Kunz, J.A., Frechen, M., Ramachandran, R., Urban, B., 2010. Revealing the coastal event-history of the Andaman Islands (Bay of Bengal) during the Holocene using radiocarbon and OSL dating. International Journal of Earth Sciences 99/8, 1741-1761.

Lamothe, M., Auclair, M., Hanazaoui, C., Huot, S., 2003. Towards a prediction of long-term anomalous fading of feldspar IRSL. Radiation Measurements 37, 493-498.

Lauer, T., Frechen, M., Hoselmann, C., Tsukamoto, S., 2010. Fluvial aggradation phases in the Upper Rhine Graben—new insights by quartz OSL dating. Proceedings of the Geologists' Association 121, 154–161.

Litt, T., Schminke, H.-U., Frechen, M., Schlüchter, C., 2008. Quaternary. In: McCann, T. (ed.): The Geology of Central Europe: Mesozoic and Cenozoic. pp. 1287-1340, Geological Society of London.

Marković, S.B., Kostić, N.S., Oches, E.A., 2004. Palaeosols in the Ruma loess section (Vojvodina, Serbia). Revista Mexicana de Ciencias Geológicas 21, 79–87.

Marković, S.B., McCoy, W.D., Oches, E.A., Savić, S., Gaudenyi, T., Jovanović, M., Stevens, T., Walther, R., Ivanisević, P., Galić, Z. 2005. Paleoclimate record in the upper Pleistocene loess-palaeosol sequence at Petrovaradin brickyard (Vojvodina, Serbia). Geologica Carpathica 56, 545–552.

Marković, S.B., Oches, E., Sümegi, P., Jovanović, M., Gaudenyi, T. 2006. An introduction to the middle and upper Pleistocene loess-palaeosol sequence at Ruma brickyard, Vojvodina, Serbia. Quaternary International 149, 80–86.

Marković, S.B., Oches, E.A., McCoy, W.D., Frechen, M., Gaudenyi, T., 2007. Malacological and sedimentological evidence for ''warm'' glacial climate from the Irig loess sequence, Vojvodina, Serbia. Geochemistry Geophysics Geosystems 8/9, Q09008.

Marković, S.B., Bokhorst, M.P., Vandenberghe, J., McCoy, W.D., Oches, E.A., Hambach, U., Gaudenyi, T., Jovanović, M., Stevens, T., Zöller, L., Machalett, B., 2008. Late Pleistocene loess-palaeosol sequences in the Vojvodina region, North Serbia. Journal of Quaternary Science 23/1, 73–84.

Marković, S.B., Hambach, U., Catto, N., Jovanović, M., Buggle, B., Machalett, B., Zöller, L., Glaser, B., Frechen, M., 2009. The middle and late Pleistocene loess palaeosol sequences at Batajanica, Vojvodina, Serbia. Quaternary International 198, 255–266.

Mikulčić Pavlaković, S., Crnjaković, M., Tibljaš, D., Šoufek, M., Wacha, L., Frechen, M., Lacković, D., 2011. Mineralogical and geochemical characteristics of Quaternary sediments

from the Island of Susak (Northern Adriatic, Croatia), Quaternary International 234, 1-2, 32-49.

Muhs, D.R., Ager, T.A., Bettis III, E.A., McGeehin, J., Been, J.M., Begét, J.E., Pavich, M.J., Stafford Jr., T.W., Stevens, De A.S.P., 2003. Stratigraphy and palaeoclimatic significance of Late Quaternary loess–palaeosol sequences of the Last Interglacial–Glacial cycle in central Alaska. Quaternary Science Reviews 22, 1947–1986.

Novothny, Á., Horváth, E., Frechen, M., 2002. The loess profile at Albertirsa, Hungary - improvements in loess stratigraphy by luminescence dating. Quaternary International 95–96, 155–163.

Novothny, Á., Frechen, M., Horváth, E., Bradák, B., Oches, E.A., McCoy, W.D., Stevens, T., 2009. Luminescence and amino acid recemization chronology of the loess-palaeosol sequence at Sütto, Hungary. Quaternary International 198/1-2, 62-76.

Novothny, Á., Frechen, M., Horváth, E., Krbetschek, M., Tsukamoto, S., 2010. Infrared stimulated luminescence and radiofluorescence dating of aeolian sediments from Hungary. Quaternary Geochronology 5, 114-119.

Novothny, Á., Frechen, M., Horváth, E., Wacha, L., Rolf, Ch., 2011. Investigating the penultimate and last glacial cycles of the Süttő loess section (Hungary) using luminescence dating, high resolution grain size, and magnetic susceptibility data. Quaternary International 234, 1-2, 75-85.

Ou, X.J., Xu, L.B., Lai, Z.P., Long, H., He, Z., Fan, Q.S., Zhou, S.Z., 2010. Potential of quartz OSL dating on moraine deposits from eastern Tibetan Plateau using SAR protocol. Quaternary Geochronology 5, 257-262.

Pavelić, D., 2001. Tectonostratigraphic model for the North Croatian and North Bosnian sector of the Miocene Pannonian Basin System. Basin Research 12, 359-376.

Pavelić, D., 2002. The South-Western Boundary of Central Paratethys. Geologia Croatica 55/1, 83-92.

Pavelić, D., 2005. Cyclicity in the evolution of the Neogene North Croatian basin (Pannonian basin system). In: Mabesoone, J.M., Neumann, V.H. (eds.): Cyclic Development of Sedimentary Basins. Developments in Sedimentology 57, 273-283.

Pécsi, M., 1993. Quaternary and loess research. In: Bassa, L., Keresztesi, Zs., Lóczy, D. (eds.): Loess in Form 2, Hungarian Academy of Science, Budapest, 82 pp.

Pikija, M., Šikić, K., Sarkotić-Šlat, M., Magaš, N., 1995. Geologija hrvatskog dijela Baranje. In: Vlahović, I., Velić, I., Šparica, M. (Eds.), First Croatian Geological Congress, Opatija, Proceedings 2, Institute of Geology and Croatian Geological Society, Zagreb, 447-451.

Pillans, B., Wright, I., 1990. 500,000-year paleomagnetic record from New Zealand loess. Quaternary Research 33, 178-187.

Poje, M., 1985. Praporne naslage vukovarskog profila i njihova stratigrafska pripadnost. Geološki Vjesnik 38, 45-66.

Poje, M., 1986. Ekološke promjene na vukovarskom prapornom ravnjaku proteklih cca 500.000 godina. Geološki Vjesnik 39, 19-42.

Poje, M., 1988. Malakocenoze graničnog područja između tipičnog karbonatnog i smeđeg beskarbonatnog prapora Slavonije. Rad JAZU 441, 169-180, Zagreb.

Prelogović, E., Saftić, B., Kuk, V., Velić, J., Dragaš, M., Lučić, D., 1998. Tectonic activity in the Croatian part of the Pannonian basin. Tectonophysics 297, 283-293.

Preusser, F., Degering, D., Fuchs, M., Hilgers, A., Kadereit, A., Klasen, N., Krbetschek, M., Richter, D., Spencer, J.Q.G., 2008. Luminescence dating: basics, methods and applications. Quaternary Science Journal (E&G) 57/1-2, 95-149.

Reimann, T., Tsukamoto, S., Naumann, M., Frechen, M., 2011. The potential of using feldspars for optical dating of young coastal sediments – a test case from Darss-Zingst peninsula (southern Baltic Sea coast). Quaternary Geochronology 6/2, 207-222.

Roberts, H.M., Muhs, D.R., Wintle, A.G., Duller, G.A.T., Betis III, E.A., 2003. Unprecedented last-glacial mass accumulation rates determined by luminescence dating of loess from western Nebraska. Quaternary Research 59, 411-419.

Rukavina, D., 1983. O stratigrafiji gornjeg pleistocena s osvrtom na topla razdoblja i njihov odraz u naslagama na području Jugoslavije. Rad JAZU 19, 199-221, Zagreb.

Schmidt, E., Machalett, B., Marković, S.B., Tsukamoto, S., Frechen, M., 2010. Luminescence chronology of the upper part of the Stari Slankamen loess sequence (Vojvodina, Serbia). Quaternary Geochronology 5, 137-142.

Schmidt, E.D., Semmel, A., Frechen, M., submitted. Luminescence dating of the loess/palaeosol sequence at the gravel quarry Gaul/Weilbach. Quaternary Science Journal (E&G).

Singhvi, A.K., Bronger, A., Sauer, W., Pant, R.K., 1989. Thermoluminescence dating of loess-paleosol sequences in the Carpathian basin (East-Central Europe): a suggestion for a revised chronology. Chemical Geology (Isotope Science Section) 73, 307–317.

Spooner, N.A., 1994. The anomalous fading of infrared-stimulated luminescence from feldspars. Radiation Measurements 23 2/3, 625-632.

Smalley, I., O'Hara-Dhand, K., Wint, J., Machalett, B., Jary, Z., Jefferson, I., 2009. Rivers and loess: The significance of long river transportation in the complex event-sequence approach to loess deposit formation. Quaternary International 198, 7-18.

Thiel, C., Coltorti, M., Tsukamoto, S., Frechen, M., 2010a. Geochronology for some key sites along the coast of Sardinia (Italy). Quaternary International 222, 36-47.

Thiel, C., Terhorst, B., Jaburová, I., Buylaert, J.-P., Murray, A.S., Fladerer, F.A., Damm, B., Frechen, M., Ottner, F., 2010b. Sedimentation and erosion processes to late Pleistocene sequences exposed in the brickyard of Langenlois/Lower Austria. Geomorphology, doi: 10.1016/j.geomorph.2011.02.011.

Thiel, C., Buylaert, J.-P., Murray, A.S., Terhorst, B., Tsukamoto, S., Frechen, M., 2010c. Investigating the chronostratigraphy of prominent palaeosols in Lower Austria using post-IR IRSL dating. Quaternary Science Journal (E&G).

Thiel, C., Buylaert, J.-P., Murray, A., Terhorst, B., Hofer, I., Tsukamoto, S., Frechen, M., 2011. Luminescence dating of the Stratzing loess profile (Austria) – Testing the potential of an elevated temperature post-IR IRSL protocol. Quaternary International 234, 1-2, 23-31.

Thiel, C., Buylaert, J.-P., Murray, A.S., Tsukamoto, S., submitted. On the applicability of post-IR IRSL dating to Japanese loess. Geochronometria.

Thomsen, K.J., Murray, A.S., Jain, M., Bøtter-Jensen, L., 2008. Laboratory fading rates of various luminescence signals from feldspar-rich sediment extracts. Radiation Measurements 43, 1474-1486.

Van Straaten, L.M.J.U., 1970. Holocene and Late Pleistocene sedimentation in the Adriatic Sea. Geologische Rundschau 60, 106-131.

Vlahović, I., Tišljar, J., Velić, I., Matičec, D., 2005. Evolution of the Adriatic Carbonate Platform: Palaeogeography, main events and depositional dynamics. Palaeogeography, Palaeoclimatology, Palaeoecology 220, 330-360.

Wacha, L., Mikulčić Pavlaković, S., Frechen, M., Crnjaković, M., 2010a. The Loess Chronology of the Island of Susak, Croatia. Quaternary Science Journal (E&G).

Wacha, L., Koloszár, L., Chikán, G., Galović, L., Magyari, Á., Marsi, I., Tsukamoto, S., 2010b. IRSL Dating of a Quaternary Sediment Succession in Šarengrad, Eastern Croatia. In: Horvat, M.: Abstracts book, 4th Croatian Geological Congress, 380-381, Croatian Geological Survey, Zagreb.

Wacha, L., Mikulčić Pavlaković, S., Novothny Á., Crnjaković, M., Frechen, M., 2011a. Luminescence Dating of Upper Pleistocene Loess from the Island of Susak in Croatia. Quaternary International 234, 1-2, 50-61.

Wacha, L., Frechen, M., 2011b. The geochronology of the "Gorjanović loess section" in Vukovar, Croatia. Quaternary International, doi: 10.1016/j.quaint.2011.04.010.

Walker, M., 2005. Quaternary Dating Methods. John Wiley & Sons, London, 286 pp.

Wallinga, J., Bos, A.J.J., Dorenbos, P., Murray, A.S., Schokker, J., 2007. A test case for anomalous fading correction in IRSL dating. Quaternary Geochronology 2, 216-221.

Wintle, A.G., 1973. Anomalous fading of thermoluminescence in mineral samples. Nature 245, 143-144.

Wintle, A.G., 1997. Luminescence dating: laboratory procedures and protocols. Radiation Measurements 27, 769–817.

Wintle, A.G., 2008. Luminescence dating of Quaternary sediments – Introduction. Boreas 37, 469-470.

Wintle, A.G., Huntley, D.J., 1979. Thermoluminescence dating of a deep-sea sediment core. Nature 279, 710-712.

CHAPTER 2

Quaternary International (2011), 234 (1-2), 50-61.

Luminescence dating of Upper Pleistocene loess from the Island of Susak in Croatia

Lara Wacha[1, 2], Snježana Mikulčić Pavlaković[3], Ágnes Novothny[1], Marta Crnjaković[3], Manfred Frechen[1]

[1]Leibniz Institute for Applied Geophysics, S3 Geochronology and Isotope Hydrology, Stilleweg 2, D-30655 Hannover, Germany

[2] Croatian Geological Survey, Sachsova 2, HR-10000 Zagreb, Croatia

[3] Croatian Natural History Museum, Department of Mineralogy and Petrography, Demetrova 1, HR-10000 Zagreb, Croatia

Abstract

The loess-palaeosol sequence on the island of Susak is a detailed Late Pleistocene archive of climate change in the North Adriatic Sea of Croatia. Quaternary deposits on Susak are up to 90 m thick and consist of loess, loess derivatives and sand, intercalated by numerous palaeosols and at least three tephra layers. Infrared stimulated luminescence (IRSL) dating was carried out on polymineral fine-grained material. Thirteen samples were collected from two sections on Susak to study the timing of loess accumulation and soil formation. The single aliquot regenerative (SAR) protocol, as well as the multiple aliquot additive-dose (MAAD) protocol, were applied for equivalent dose (D_e) determination. The IRSL ages were fading corrected. Independent age control is provided by radiocarbon dating of charcoal remains. The results show that loess and loess derivatives from the investigated sections represent a very detailed record correlating to the Marine Isotope Stage (MIS) 3, with short periods of stronger sand deposition and occasional volcanic activity. The extraordinary thickness of the deposits is very likely related to the vicinity of the River Po plain which extended to the southeast due to marine regressions of the Adriatic Sea during the cold periods of the Pleistocene.

Keywords: loess, Susak, Croatia, luminescence dating, geochronology, Late Pleistocene

2.1. Introduction

Loess and loess derivatives are important records of climate and environmental changes and variations of atmospheric dust flux (Frechen et al., 2003; Machalett et al., 2008). In order to set up a more reliable chronological framework, luminescence dating of numerous loess-palaeosol sequences along major European river systems has been carried out. During the 1980s, loess from Croatia was dated by thermoluminescence (TL) (Singhvi et al., 1989) and recently by infrared stimulated luminescence (IRSL) (Galović et al., 2009). Loess is often associated with major river systems, because rivers supply material to geographical regions from which they are subsequently transported and deposited by wind (Smalley et al., 2009). Along with the "classic" loess region along the river Danube, loess can be found on the carbonate platform (Coudé-Gaussen, 1990) along the Adriatic coast and on the islands, where it covers the carbonate basement and fills caves and shelters. The most representative example of such loess deposits is the well developed loess-palaeosol sequence on the Island of Susak, North Adriatic Sea. Loess on Susak has been investigated by different approaches including mineralogy and sedimentology (Mutić, 1967; Cremaschi, 1987a, b, 1990). Bognar and Zámbó (1992) studied paleomagnetic properties, and Bognar et al. (2003) applied a multidisciplinary approach and made an environmental reconstruction of the loess island. According to Coudé-Gaussen (1990), the source area of loess from Susak is the Po plain and its catchment area. On the basis of pedostratigraphic data from Cremaschi (1990), loess sedimentation along the Adriatic Sea is referred to the late Pleniglacial period of the Upper Pleistocene (Cremaschi, 1990).

Loess on Susak is not typical loess, as defined by Pécsi (1990). It is coarser-grained than "normal" loess. After Mutić (1967), it is a sandy silt but with all the characteristics of loess. Furthermore, Mutić (1967) concluded that the coarse fraction is a result of the stronger wind dynamics during glacial times and the vicinity to the source area. According to granulometric analysis presented in Mutić (1967) and Mikulčić Pavlaković et al. (2011) which show a higher sand content in loess, Susak loess is termed sandy loess, after Pye's (1987, 1995) nomenclature.

The aim of this paper is to set up a more reliable and precise chronological framework for the loess-palaeosol sequence on Susak using fading corrected infrared stimulated luminescence

(IRSL) and radiocarbon dating. Furthermore, the loess deposits from Susak will be correlated with classical loess sites in Croatia, Serbia and Hungary.

2.2. Geological setting

The Island of Susak is the outermost island of the Kvarner Archipelago in the North Adriatic Sea of Croatia (Fig. 2.1.). It is situated south of the Istrian Peninsula and 7 km southwest of the island of Mali Lošinj, which is the nearest large island. Susak is located between 44.50° and 44.52° N and 14.28° and 14.32° E. The island has a surface of 3.8 km^2, and is 3 km long and 1.5 km wide. Its highest point is 98 m a.s.l. The island has all characteristics of a loess plateau developed on a flat basement (Bognar et al., 2003). Its flat Upper Cretaceous and, in a smaller amount, Eocene limestone surface is covered by up to 90 m of Quaternary sediments, predominantly by loess, loess derivatives and sand, intercalated with many palaeosols and at least three tephra layers. According to Bognar et al. (2003), the sediment succession has normal magnetization and thus correlates to the Brunhes paleomagnetic epoch. Susak, along with the islands of Unije, Velike and Male Srakane, belongs to the Unije-Susak tectonic unit (Mamužić, 1973). This unit is characterised by faulting with the typical northwest to southeast Dinaridic spreading direction. Susak is an exception because it dips towards the east. This orientation is the same as the West Istrian tectonic structures, making it very likely that Susak belongs to the West Istrian autochthon of the Northern Adriatic Carbonate Platform (Mamužić, 1973).

Loess and loess-like deposits are characteristic for the eastern part of Croatia along the Danube River, whereas along the Adriatic coast these deposits are less abundant. The origin of the loessic material has been often related to cryoclastic processes. Glaciofluvially reworked sediments from the Alps were deposited in the piedmont area of the Po River (Coudé-Gaussen, 1990) and the finegrained deposits were subsequently taken up by wind. During the cold periods of the Pleistocene, the Po River flood plain expanded towards the south into the Adriatic Sea, owing to lower sea level in that time. Due to the regression of the Adriatic Sea, continental climatic characteristics prevailed in the Po plain, and caused increased accumulation of silty and sandy aeolian material and loess formation. The climate in which the Mediterranean loess was deposited was less severe compared to that in north–western Europe (Coudé-Gaussen, 1990; Marković et al., 2007, 2008). The numerous thin

brown weakly developed palaeosols intercalated in the loess from Susak are evidence of climate variations.

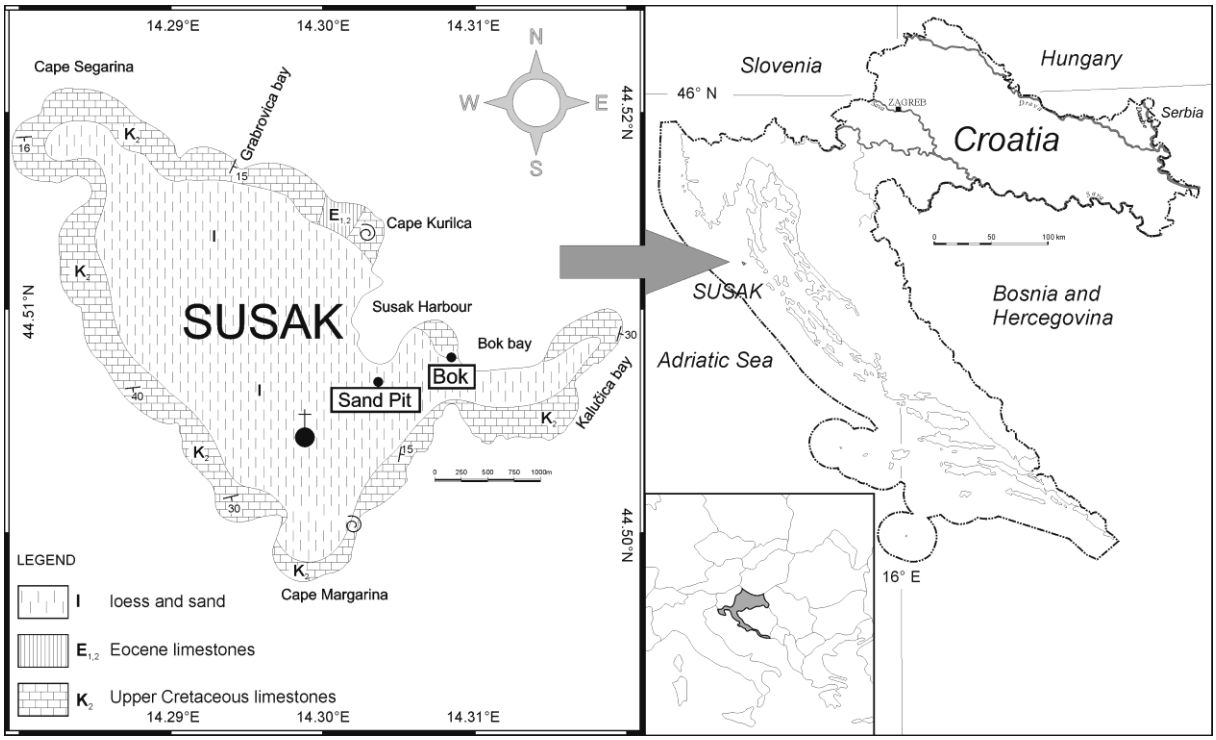

Figure 2.1. Location and geological map (simplified after Mamužić, 1965) of the island of Susak showing the position of the loess-palaeosol sections under study.

Due to the steep loess cliffs induced by slope erosion, rich vegetation and human impact, it is not possible to describe a continuous and complete sediment succession from only one location on the island. Several smaller outcrops, which could be correlated by means of intercalated tephra layers and palaeosol horizons, were studied. Two major sections were described on Susak, both located on the easternmost part of the island. The Bok section is situated along Bok Bay (44.50809 N, 14.31557E) (Figs. 2.1. and 2.2.) and the Sand Pit section is situated in a small quarry, about 1 km southeast of the village (44.5071 N, 14.31092E) (Figs. 2.1. and 2.3.).

Figure 2.2. Picture showing Bok Bay where the Bok section is located. Terraced morphology is clearly distinguishable. a) Red palaeosol covering Cretaceous limestones. On top of the red palaeosols a horizon of lithified loess (sandstone bench) and the oldest loess is visible. In this loess the oldest tephra (TF1) was found (not visible on this picture). The picture was taken about 20m east of the major outcrop. b) The brown palaeosols from the middle part of the section. The upper, thinner palaeosol contains accumulations of the middle tephra (TF2). c) The upper part of the section with the thin brown weakly developed palaeosols and the upper, youngest tephra (TF3).

Figure 2.3. The East Wall of the sand pit near the Lower Village where the Sand Pit section is located. The picture was taken in 2008 when the SouthWall does not exist any more in its former shape due to human activity. a) The thick brown palaeosol from the bottom of the section (behind the vegetation on the picture). b) The middle part of the section with the weakly developed, thin brown palaeosols containing charcoal remains.

2.2.1. Bok section

In the Bay of Bok, the flat plateau-like bedrock consists of Senonian rudist limestones. In the eastern part of the island the bedrock is at sea level, rising in elevation westwards up to about 10 m (Cremaschi, 1990). The bedrock surface is erosional with numerous cracks and cavities which are filled by terra rossa, or according to Bognar et al. (2003) fossil reddish clay. Terra rossa is a polygenetic reddish clayey to silty-clayey soil formed during the Neogene and/or warm and humid periods of the Quaternary. In some isolated karst terrains, terra rossa may have formed exclusively from the insoluble residue of limestone and dolomite, but it more frequently comprises a span of parent materials including, for example, aeolian dust, volcanic material or sedimentary clastic rocks which arrived on the carbonate terrain via different transport mechanisms (Durn et al., 1999; Durn, 2003). Two red well-developed palaeosols of unknown age, about 80–100 cm-thick, cover the carbonate bedrock (Figs. 2.2.a and 2.4.). On the southern part of the island the palaeosols are widely distributed, but they thin towards Bok Bay. According to Bognar et al. (2003), such reddish clays are as a rule intercalated in old loess. Such palaeosols are not typical red clay, but are rather steppe soils formed under warm and dry or subhumid climates (Bognar et al., 2003). The palaeosols are separated with carbonate (septarian) concretions, differing in shape, up to 20 cm in diameter, indicating strong carbonate dissolution, leaching and precipitation owing to warm climatic conditions and the resulting soil formation processes. The terra rossa and the red palaeosol covering the carbonate bedrock are of Pliocene age according to Bognar et al. (2003). The palaeosol is covered by about 150 cm of sandy loess. In the lowermost part of the loess, a horizon of lithified sandy loess (sandstone bench according to Bognar et al., 2003; Figs. 2.2.a and 2.4.) about 30 cm-thick is intercalated. A yellow tephra layer (TF1) few cm thick is intercalated in the oldest loess. The tephra layer is easily recognizable at many locations of the island. The upper part of this loess has abundant vertical carbonate concretions, i.e. root channels filled with secondary carbonate. This is supposed to be the oldest loess on the island. According to Bognar et al. (2003), in correlating the palaeosols on Susak with those from Hungary, the tephra is suggested to be significantly older than the last interglacial.

The loess is covered by an orange–brown palaeosol, about 100 cm-thick. The transition from the oldest loess to the orange–brown palaeosol is gradual in places where the carbonate concretions from the layer below are missing. The lowermost part of the palaeosol has a reddish colour and has abundant iron and manganese rich nodules. The upper 25 cm of the palaeosol is enriched with small carbonate concretions and vertical root channels filled with

secondary carbonate up to few cm in length. The palaeosol is covered by a 20 cm-thick loess layer, which has a gradual transition into a brown palaeosol. The brown palaeosol is 100 cm-thick: its lower part is enriched in Fe–Mn nodules and is darker in colour than the upper part. In the upper part, carbonate concretions up to few cm in diameter are intermingled.

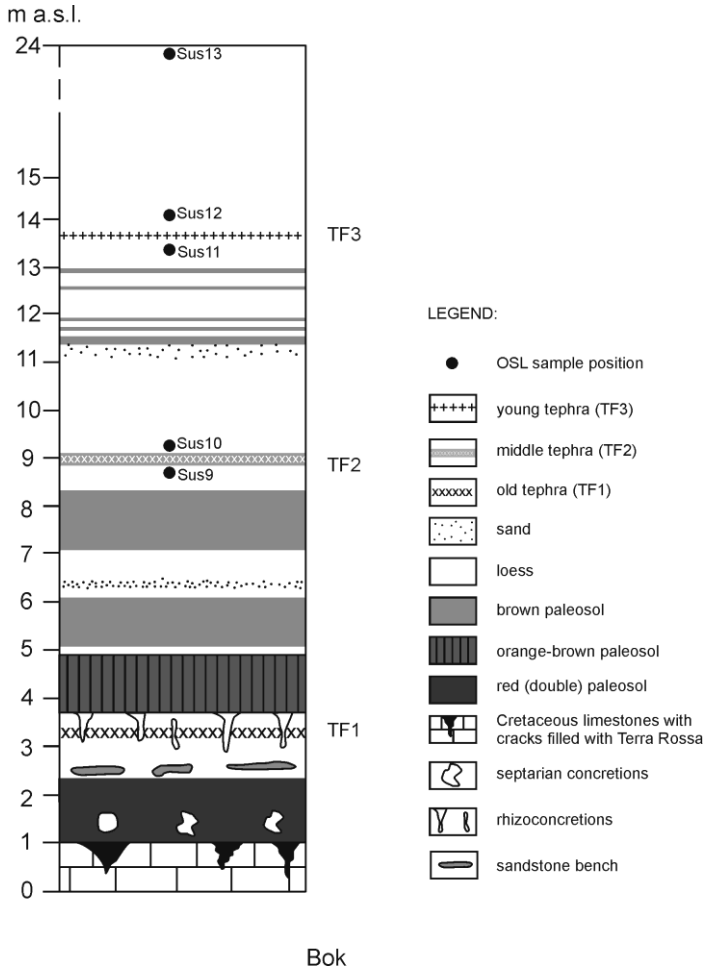

Figure 2.4. The sketch of the Bok loess-palaeosol sequence with indicated luminescence samples names and position.

The palaeosol is covered by loess about 100 cm-thick with abundant secondary carbonate enrichment. The transition between palaeosol and loess is abrupt, and the boundary is erosional and bioturbated. The lower part of this loess is intercalated by a 30 cm thick sand layer. On top of the loess layer a 100–120 cm-thick chocolate brown palaeosol (Figs. 2.2.b and 2.4.) is developed, which is again covered by a 60 cm-thick loess layer. There is a gradual transition from the loess into a 15–20 cm-thick brown, probably redeposited palaeosol (Figs. 2.2.b and 2.4.). Small pockets filled with an orange–yellow tephra (TF2) are intercalated in the brown palaeosol. The tephra is laterally discontinuously exposed. The thin brown

palaeosol with the tephra is covered by 210 cm of loess. The loess is overlain by a 35 cm-thick fine sand layer which again fines upwards into loess. The uppermost loess is about 300 cm-thick and intercalated with five weakly developed or redeposited palaeosols (Figs. 2.2.c and 2.4.) up to a few cm thick with many pieces of charcoal. A 2 cm-thick olive green tephra layer (TF3), is also intercalated in the loess, about 50 cm above the uppermost described palaeosol horizon (Figs. 2.2.c and 2.4.). The loess is homogenous and enriched with secondary carbonate.

Four luminescence samples (Sus12, Sus11, Sus10 and Sus9) were collected from this section, on top and below both tephras, at depths of 15.8 m, 16.3 m, 20.8 m and 21.3 m, and one (Sus13) at the highest reachable position, the supposed youngest loess, at about 8 m depth below surface (Fig. 2.4.).

2.2.2. Sand Pit section

The Sand Pit section is located about 1 km east of the Lower village of Susak (Fig. 2.1.). Material is occasionally being quarried for building purposes from this location.

Two sections were described in the quarry, one at the south wall and the second at the east wall. The loess-palaeosol sequence from the east wall is about 36 m thick and consists of loess, sandy loess and sand intercalated by six thin, brown, weakly developed or redeposited palaeosols, one thick chocolate brown, strongly developed palaeosol and a tephra layer. The loess-palaeosol sequence from the south wall is about 12m high. It consists of loess and laminated sand, intercalated with six weakly developed or redeposited palaeosols up to a few cm thick and two tephra layers (Fig. 2.5.). These palaeosols are excellent marker horizons for correlating the loess record of the two sections.

At the base of the east wall of the Sand Pit section, the chocolate brown palaeosol is about 170 cm-thick (Figs. 2.3.a and 2.5.). The palaeosol is carbonate-free and covered by a 180 cm-thick loess layer. The lower part of this loess is carbonate-free, but in the upper part secondary carbonate occurs and a few small molluscs were found.

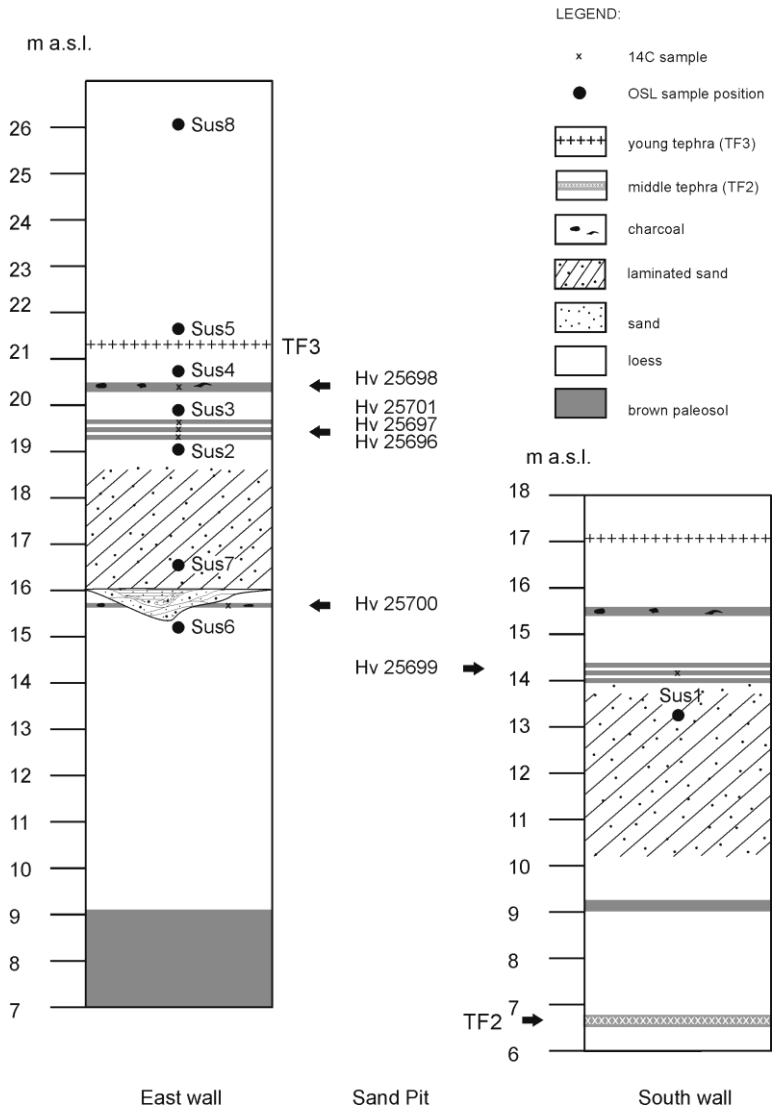

Figure 2.5. The investigated Sand Pit sections with indicated luminescence and radiocarbon samples names and position.

During field-work describing and sampling was not possible between 10.5 m and 12.4 m owing to debris. Homogenous loess with secondary carbonate is exposed between 12.4 m and 13.6 m height. A few secondary carbonate concretions, up to 5 mm in diameter, are intermingled. Loess gradually becomes sandier to the top, and again fines upwards into loess, which has the same properties as the loess below. In the upper part of the loess, laterally a brown palaeosol up to 5 cm-thick is intercalated, containing many charcoal pieces. The upper part of the loess and the brown palaeosol are eroded and a 50 cm deep incised wedge is visible. The wedge is filled with a laminated mixture of coarse-grained to fine-grained sand

including abundant mollusc fragments, which very likely give evidence for water activity. The loess and the sand from the wedge are covered by coarse-grained laminated sand.

Between 16.5 m and 18.5 m the wall was not accessible but it was clearly visible that the sediment succession is continuous. At 18.5 m a.s.l., a 170 cm-thick laminated sand is exposed. The sand has abundant secondary carbonates, carbonate coatings and remains of root channels filled with carbonate. The sand gradually fines upwards into silt. The loess on top of this sand horizon is 330 cm-thick. This loess is homogenous with abundant secondary carbonates and with rare molluscs. Loess is intercalated with 5 brown palaeosols up to 5 cm-thick. In the lower part of this loess horizon, four brown palaeosols with charcoal remains are distinguishable (Figs. 2.3.b and 2.5.). The palaeosols are bioturbated and their thickness varies. Laterally the uppermost palaeosol thins out. About 50 cm above the four palaeosols, another brown palaeosol with charcoal pieces is intercalated. This palaeosol is up to 10 cm-thick, its thickness changes laterally. This palaeosol shows a lot of bioturbation features. About 50 cm above the palaeosol, a 3–5 cm-thick olive–brown tephra layer (TF3) is intercalated, which is widely distributed on the island.

The section at the south wall of the quarry starts with loess, which is in its lower part, intercalated by a few cm-thick brown palaeosol containing orange–yellow material of the middle tephra (TF2). The 3 m thick loess covering the palaeosol gradually coarsens upwards into sand and laminated sand. The upper part of this loess horizon is intercalated by a few cm-thick brown palaeosol. The sand is intercalated with carbonate-rich root channels up to 30 cm long and 2–3 cm in diameter and intermingled by weakly lithified sand concretions. The sand is covered by homogeneous loess about 2 m thick. In the lower part of this horizon, three weakly developed brown palaeosols with charcoal remains are recognized. These palaeosols are similar to those from the upper part of the east wall and thus can be correlated with each other (Fig. 2.5.). This section was described during field-work in 2003 and 2004 and is no longer fully exposed.

Eight samples were taken from the Sand Pit section, one from the south wall (Sus1) at a depth of 18.0m and seven samples (Sus2, Sus3, Sus4, Sus5, Sus6, Sus7, Sus8) from the east wall at depths of 17.0 m, 16.2 m, 15.3 m, 14.5 m, 20.7 m, 19.5 m and 10.0 m, respectively. Sampling took place in summer 2007.

2.3. Luminescence dating

The optically stimulated luminescence (OSL) dating method is widely used for determining the depositional age or the burial time of the sediment. This method can determine the time elapsed since the last exposure of the sediment to direct sunlight. The exposure of the sediment to direct sunlight is described as bleaching, which means that the sunlight releases all the trapped electrons in the crystal lattice of the minerals in the sediment and thus resets the "clock" to zero. After deposition and after the material was buried, the minerals are again exposed to natural radioactivity of the surrounding sediment. This ionizing radiation moves electrons from their original position into electron traps caused by impurities or crystal lattice defects, from where they can only be released by additional energy. Releasing these electrons from the traps and the recombination with positive charges in the crystal lattice results in emission of light (luminescence), and can be measured with a photomultiplier in the laboratory. With time the amount of such dislocated electrons grows, meaning that the luminescence signal is proportional to the depositional age of the sediment. The intensity of the luminescence signal increases with the deposition age of the sediment. The equivalent dose (De) is a measure of the past radiation and, if divided by the dose rate, gives the time elapsed since the last exposure of the sediment to sunlight i. e. deposition.

The principles of luminescence dating are given by Aitken (1985, 1998) and Wintle (1997). This method is applicable and widely used for dating aeolian sediments, especially loess (Frechen et al., 1997; Novothny et al., 2002, 2009; Lu et al., 2007; Roberts, 2008; Galović et al., 2009). Luminescence ages from a few years (Ballarini et al., 2003; Kunz et al., 2010) up to a few hundred thousand years can be dated (Wang et al., 2006, 2007), and thus expanding the age range far beyond radiocarbon dating. During the 1970s and 1980s, thermoluminescence had been used as a method for dating aeolian deposits such as loess. In the mid 1980s, optically stimulated luminescence (OSL) and infrared stimulated luminescence (IRSL) were developed for dating monomineralic quartz and potassium-rich feldspar grains, respectively (Huntley et al., 1985; Hütt et al., 1988). The quartz signal saturates at lower doses than the feldspar signal, which means that feldspar is apparently more suitable for dating older sediments. However, feldspars have the disadvantage of being affected by nomalous fading (Wintle, 1973), which causes age underestimation. Huntley and Lamothe

(2001) presented a model, which makes fading correction possible for samples younger than w20–50 ka. Fading correction for older samples is still under investigation (Lamothe et al., 2003; Kars et al., 2008). In this study the single aliquot regenerative-dose (SAR) protocol, including fading tests and fading corrections were applied, as well as the multiple aliquot additive-dose (MAAD) protocol, for better correlation and understanding of existing dating results of loess in Croatia which could suffer from anomalous fading resulting in age underestimation (Galović et al., 2009). A detailed description of these protocols and their advantages and disadvantages can be found in Aitken (1985, 1998), Wintle (1997), Bøtter-Jensen et al. (2003) and Lian and Roberts (2006). Radiocarbon dating was used as an independent age control.

2.3.1. Sample preparation

Thirteen luminescence samples were taken in light-proof metal tubes, which were hammered in the previously cleaned loess wall. Laboratory preparation took place under subdued red light. The samples were first dried and sieved. The sieved coarse- and finegrained material was treated with 10% HCl to remove carbonates, H_2O_2 to remove organic material and Na-oxalate against coagulation. The 100–150 mm grain-size fraction was separated into coarsegrained quartz and feldspar minerals using sodium-polytungstate. Quartz was etched with 30% hydrofluoric acid for 1 h to get rid of the outer alpha-irradiated rim and potential feldspar contamination. The <100 mm fraction was refined to 4–11 mm fraction (Frechen et al., 1996). The coarse-grains were mounted on stainless-steel discs using silicon spray. The fine-grain polymineral material (4–11 mm) was mounted on aluminium discs by settling in acetone. All measurements were performed using an automated Risø TL/OSL-DA15 reader equipped with a 90Sr/90Y beta source, with the dose rate of 0.124 Gy/s, (Bøtter-Jensen et al., 2000) at the Leibniz Institute for Applied Geophysics (LIAG). The feldspar luminescence signal was detected through a Schott BG-39 and Corning 7–59 filter combination emitting blue light; whereas the quartz luminescence signal was detected through a 7.5 mm thick U-340 filter transmitting the UV wavelength range. Coarse-grained quartz was discarded for measurements because of the weak luminescence signal and feldspar contamination, even after several cycles of etching.

2.3.2. Performance tests for polymineral fine-grain IRSL measuring

Luminescence properties were investigated before any equivalent dose (D_e) measurements. Preheat tests for determining the appropriate preheat temperature, and dose recovery tests with different preheat temperatures were performed. As the source material of the loess has very likely the same origin, the tests were made for two samples on each section, one sample from the bottom of the profile and one from the upper part of the profile, i.e. on samples Sus5 and Sus6 for the Sand Pit section and Sus9 and Sus12 for the Bok section.

For the preheat tests 24 aliquots of each sample were used. The temperatures were measured in steps of 20°C ranging from 160°C to 300°C. The results of the preheat tests are shown in Fig. 2.6. All samples show a continuous increase in equivalent dose with temperature, with a plateau in the high temperature part of the curve. A temperature of 260°C was found to be the most suitable and was taken for the measurement of D_e.

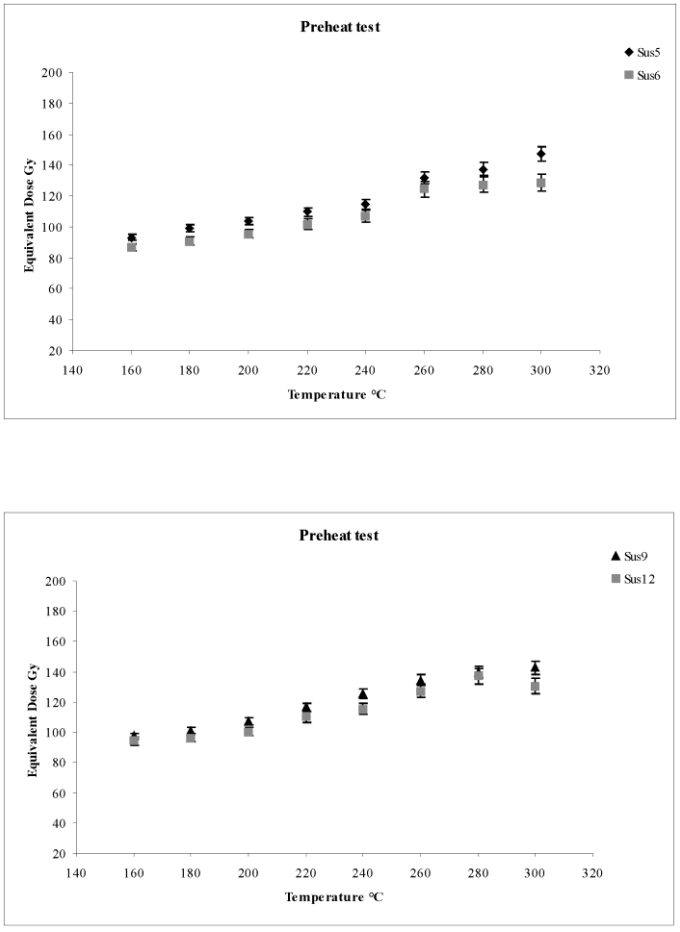

Figure 2.6. Results of the preheat plateau tests for samples Sus5 and Sus6 from the Bok section and Sus9 and Sus12 from the Sand Pit section. For each sample the mean of three aliquots and the standard deviation is shown.

The dose recovery test is a test to show the quality of recovering a known dose successfully. Dose recovery tests were performed on 24 aliquots for each of the four selected samples, which were bleached for 3 h in a Dr. Hönle SOL 2 solar simulator prior to the irradiation with a fixed beta-dose close to the expected equivalent dose. Different preheat temperature were used, same as in the preheat tests. The dose recovery ratios ranged from 0.98 to 1.11, as shown in Fig. 2.7.

After plotting the test results (the D_e, the recycling ratio and the recuperation) against the different preheat temperatures, the most suitable preheat temperature (260°C) was selected for further measurements. This temperature is still in the plateau region and recovers given doses. Dose recovery tends to overestimate on temperatures higher than 280°C (Fig. 2.7). Doses were successfully recovered for all samples.

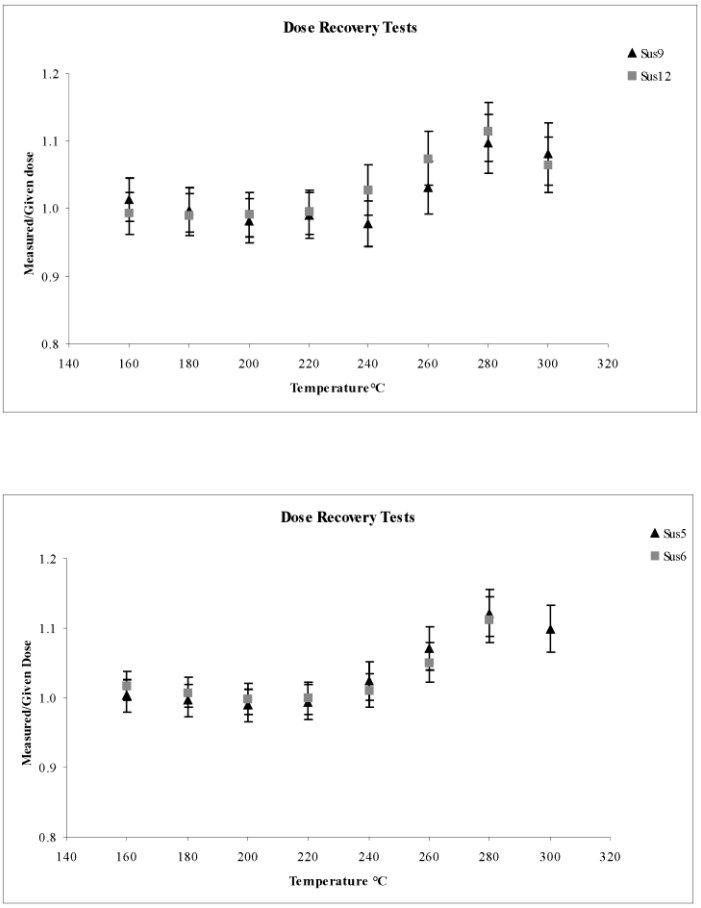

Figure 2.7. Results of the dose recovery tests for samples Sus5 and Sus6 from the Bok section and Sus9 and Sus12 from the Sand Pit section. Applied doses were 123 Gy for Sus5 and Sus6 and 136 Gy for Sus9 and Sus12.

2.3.3. Equivalent dose (D_e) determination

The equivalent dose (D_e) values, which is the dose the sample has absorbed since the last exposure to sunlight prior to deposition, were measured using a simple, slightly modified single aliquot regenerative-dose (SAR) protocol for feldspar (Wallinga et al., 2007). A 10 s preheat at 260°C and cutheat same as preheat conditions were used to estimate the De values for feldspar. IR stimulation at 50°C for 300 s was used for background subtraction. Twelve aliquots per sample were used for the measurements. The scatter between aliquots was very low. The uncertainty of the D_e values was given by a standard error. The equivalent doses are given in Table 2.1.

2.3.4. Dose rate determination

The dose rates of the sediment, necessary for age calculation, were measured by gamma spectrometry with an HPGe (High-Purity Germanium) N-type coaxial detector in the laboratory. 50 g of dried and homogenized sample material was filled in round plastic beaker, cap sealed to avoid the loss of ^{222}Rn in the ^{238}U decay chain and stored for at least four weeks for re-establishing radioactive equilibrium. Measuring time was three days. The measured activities of ^{40}K and radionuclides from the ^{238}U and ^{232}Th decay chains were used for calculation of potassium, thorium and uranium content. Radioactive equilibrium was assumed for the decay chain, which is normally the case for loess. Cosmic dose rates were corrected for altitude and sediment thickness (Prescott and Hutton, 1994). Alpha efficiency was estimated to a mean value of 0.08 ± 0.02 for all samples (Rees-Jones, 1995). Water content was assumed to be 15 ± 5% for all samples (Pécsi, 1990). The total dose rates, the cosmic dose rates and the uranium, thorium and potassium contents are given in Table 2.1.

2.3.5. Fading tests

IRSL of feldspars suffers from anomalous fading, which is an unwanted loss of signal, resulting in age underestimation (Wintle, 1973). Fading tests were carried out on six aliquots per sample for all samples. The data were corrected using the method of Huntley and Lamothe (2001) and Auclair et al. (2003). Same measurement conditions were used and given doses were chosen close to the natural ones. Different delaying time between 0.03 and 32 h were used. The mean of the g-values from 6 aliquots was used for calculation and their standard errors. The g-values are given in Table 2.1.

Table 2.1. Results from the dosimetry, the SAR IRSL measurements, g-values, the uncorrected and corrected ages. The dose rate is the sum of the dose rates from the alpha, beta, gamma and cosmic radiation. For the calculation of the total dose rate the conversion factors published by Adamiec and Aitken (1998) were used. A systematic error of 2 % is included for the gamma spectrometry. An error of 10 % is estimated for the cosmic dose.

	Sample name	Sample ID	Depth below surface (m)	U (ppm)	Th (ppm)	K (%)	Cosmic dose (mGy/a)	Doserate (mGy/a)	De (Gy)	g-value	Uncorrected age (ka)	Corrected age(ka)
Sand Pit section	Sus1	1426	18.00	2.31 ± 0.04	8.12 ± 0.09	1.15 ± 0.02	0.024 ± 0.002	2.50 ± 0.15	96.1 ± 0.4	2.0 ± 0.1	38.5 ± 2.3	46.4 ± 2.7
	Sus2	1427	17.00	2.32 ± 0.04	7.77 ± 0.11	1.31 ± 0.02	0.027 ± 0.003	2.61 ± 0.15	92.3 ± 0.6	1.9 ± 0.1	35.4 ± 2.1	42.2 ± 2.4
	Sus3	1428	16.20	4.30 ± 0.05	12.81 ± 0.12	1.68 ± 0.03	0.028 ± 0.003	4.02 ± 0.22	120.0 ± 0.7	1.6 ± 0.1	29.9 ± 1.7	34.5 ± 1.9
	Sus4	1429	15.30	4.40 ± 0.05	13.44 ± 0.10	1.71 ± 0.02	0.030 ± 0.003	4.14 ± 0.23	123.0 ± 0.7	1.5 ± 0.2	29.7 ± 1.6	34.1 ± 1.9
	Sus5	1430	14.50	4.74 ± 0.05	14.99 ± 0.14	1.73 ± 0.03	0.032 ± 0.003	4.40 ± 0.24	128.6 ± 0.6	2.0 ± 0.1	29.2 ± 1.6	35.1 ± 1.9
	Sus6	1431	20.70	3.71 ± 0.05	11.09 ± 0.12	1.40 ± 0.03	0.022 ± 0.002	3.42 ± 0.20	116.6 ± 1.7	1.9 ± 0.1	34.1 ± 2.0	40.7 ± 2.4
	Sus7	1432	19.50	3.57 ± 0.04	11.03 ± 0.11	1.37 ± 0.02	0.023 ± 0.002	3.35 ± 0.19	111.2 ± 0.6	2.4 ± 0.5	33.2 ± 1.9	41.6 ± 3.2
	Sus8	1433	10.00	4.16 ± 0.05	13.32 ± 0.14	1.60 ± 0.03	0.050 ± 0.005	3.97 ± 0.22	97.3 ± 0.5	2.0 ± 0.1	24.5 ± 1.4	29.5 ± 1.6
Bok section	Sus9	1434	21.30	3.50 ± 0.05	10.04 ± 0.12	1.40 ± 0.02	0.021 ± 0.002	3.26 ± 0.19	131.8 ± 1.1	2.3 ± 0.4	40.4 ± 2.4	50.3 ± 3.5
	Sus10	1435	20.80	4.19 ± 0.08	13.33 ± 0.14	1.76 ± 0.03	0.021 ± 0.002	4.09 ± 0.22	156.7 ± 1.3	2.3 ± 0.4	38.3 ± 2.1	47.5 ± 3.2
	Sus11	1436	16.30	4.15 ± 0.05	13.26 ± 0.13	1.68 ± 0.03	0.027 ± 0.003	4.01 ± 0.22	127.2 ± 1.0	1.9 ± 0.1	31.7 ± 1.8	37.8 ± 2.0
	Sus12	1437	15.80	4.52 ± 0.05	14.48 ± 0.12	1.70 ± 0.02	0.028 ± 0.003	4.26 ± 0.23	128.6 ± 1.0	2.0 ± 0.1	30.2 ± 1.7	36.3 ± 1.9
	Sus13	1438	8.00	3.84 ± 0.05	11.90 ± 0.13	1.28 ± 0.02	0.062 ± 0.006	3.48 ± 0.20	78.8 ± 0.9	2.1 ± 0.1	22.7 ± 1.3	27.5 ± 1.6

2.3.6. Multiple aliquot additive-dose method (MAAD)

Additionally, the multiple aliquot additive-dose method (MAAD) was employed on polymineral 4–11 mm grains, detecting IRSL signals with a Schott BG-39/Corning 7–59 filter combination. Ten out of thirteen samples were measured (Sus4–Sus13). Beside the natural signal, seven increasing dose steps ranging from 45 to 750 Gray (Gy) were applied to determine the D_e value. All discs were stored at room temperature for at least four weeks after irradiation. The samples were preheated at 230°C for 1 min in order to eliminate the unstable part of the signal. A 10 s IR exposure was carried out to obtain their IRSL signal. Subsamples (3 discs each sample) were exposed to an unfiltered solar simulator lamp (Dr Hönle SOL 2) for 3 h, preheated and measured to obtain background subtraction. Equivalent dose values were obtained by integrating the 1–10s region of the IRSL decay curves using the Analyst program, version 3.24 (Risø). An exponential growth curve was fitted to the data and compared with the natural luminescence signal to estimate equivalent dose. Only one D_e is obtained with this method, and the error depends on the scatter of the growth curve. This method was used for comparison with data from similar locations in the nearby region, such as the Danube loess in Croatia (Galović et al., 2009) and Hungary (Novothny et al., 2002, 2009). The D_e values and the ages are presented in Table 2.2.

Table 2.2. Equivalent doses, dose rates and age results using MAAD protocol.

	Sample name	Sample ID	Dose rate (Gy/ka)	De (Gy)	Age (ka)
Sand Pit section	LUM-1429	Sus 4	4.14 ± 0.23	97.6 ± 2.7	23.6 ± 1.5
	LUM-1430	Sus 5	4.40 ± 0.24	118.2 ± 4.7	26.8 ± 1.8
	LUM-1431	Sus 6	3.42 ± 0.20	102.1 ± 2.3	29.8 ± 1.8
	LUM-1432	Sus 7	3.35 ± 0.19	108.9 ± 4.9	32.5 ± 2.4
	LUM-1433	Sus 8	3.97 ± 0.22	116.1 ± 7.0	29.2 ± 2.4
Bok section	LUM-1434	Sus 9	3.26 ± 0.19	103.5 ± 2.6	31.7 ± 2.0
	LUM-1435	Sus 10	4.09 ± 0.22	155.4 ± 3.2	38.0 ± 2.2
	LUM-1436	Sus 11	4.01 ± 0.22	84.4 ± 2.5	21.0 ± 1.3
	LUM-1437	Sus 12	4.26 ± 0.23	80.9 ± 2.9	19.0 ± 1.2
	LUM-1438	Sus 13	3.48 ± 0.20	52.5 ± 2.6	15.1 ± 1.1

2.4. Radiocarbon dating

In this study, six charcoal samples from the Sand Pit section were taken for radiocarbon dating and used as independent age control. The specific activity of ^{14}C was measured radiometrically by proportional counters (Geyh, 1990, 2005) at the Leibniz Institute for Applied Geophysics (LIAG). Radiocarbon ages were converted into calibrated calendar ages using the radiocarbon calibration curve based on coral samples and program after Fairbanks et al. (2005). The sample positions and the calibrated and uncalibrated ages are shown in Figs. 2.5. and 2.8. and Table 2.3.

Table 2.3. Uncalibrated and calibrated radiocarbon dating results. The results were calibrated using the Fairbanks et al. (2005) calibration curve spanning from 0 to 50,000 years BP and transferred in ka BP in order to make the radiocarbon results better comparable with luminescence ages.

Sample Name	Uncalibrated radiocarbon age ka B.P.	Calendar age ka cal. B.P.
Hv 25696	24.2 ± 0.8	29.0 ± 0.9
Hv 25697	26.8 ± 1.0	32.2 ± 1.0
Hv 25698	26.8 ± 0.2	32.1 ± 0.3
Hv 25699	23.0 ± 0.6	27.7 ± 0.7
Hv 25700	27.2 ± 0.9	32.5 ± 1.0
Hv 25701	25.5 ± 1.2	30.6 ± 1.4

2.5. Results

Results from the dosimetry, the equivalent doses, g-values, and the uncorrected and corrected ages are given in Table 2.1., results from the MAAD measurements are presented in Table 2.2. The ages are summarized in Fig. 2.8.

Uranium, thorium and potassium content range from 3.3 to 4.7 ppm, 7.8 to 14.5 ppm and from 1.15 to 1.73%, respectively, resulting in a dose rate between 2.50 and 4.40 mGy/a. The

mean dose rate is 3.65 ± 0.21 mGy/a, and is typical for European loess. Mean dose rate from the Danubian loess in Eastern Croatia is 3.80 mGy/a (Galović et al., 2009), from Hungary 3.43 (Novothny et al., 2009), from Serbia 3.92 mGy/a (Schmidt et al., 2010).

Fading corrections were done for all samples. All polymineral IRSL signals show fading, which results in age underestimation. The fading tests revealed low fading rates, the g-values range from 1.5 to 2.3%/decade. The fading corrected ages are presented in Table 2.1.

The De values range from 78.8 ± 0.9 to 156.7 ± 1.3 Gy measured with the SAR protocol and they do not show a systematic increase in D_e with depth. The D_e values from the samples from Sand Pit section are very uniform and the time span is within the 1-sigma standard deviation of the age estimates. The distribution of equivalent dose obtained for samples Sus1 to Sus8 from Sand Pit section displays three clusters which can be associated with different granulometric features of the deposits. The sand was deposited between 46.4 ± 2.7 ka and 42.2 ± 2.4 ka, indicating a short period of intensive sand accumulation. Loess covering the sand, from 19 m height to the youngest tephra (TF3), was deposited between 35.1 ± 1.9 ka and 34.5 ± 1.9 ka. The sample taken at 26 m height is 29.5 ± 1.6 ka old and is stratigraphically the youngest loess from this section. Based on the dating results of the loess below and on top of the youngest tephra layer (TF3), the age of the tephra spans between 35.1 ± 1.9 and 34.1 ± 1.9 ka. The loess below the tephra and on top of the palaeosol containing charcoal could be bioturbated resulting in age inversion.

At the Bok section the lowermost sample taken from loess below the middle tephra (TF2) gave an IRSL age of 50.3 ± 3.5 ka. The uppermost loess sample taken from 24 m height gave an age of 27.5 ± 1.6 ka, making it the stratigraphically youngest loess at this section. The age of the middle tephra (TF2) is between 50.3 ± 3.5 ka and 47.5 ± 3.2 ka. The age of the youngest tephra (TF3) spans from 37.8 ± 2.0 ka to 36.3 ± 1.9 ka.

The D_e measured with the MAAD protocol range from 52.5 ± 2.6 Gy to 155.4 ± 3.2 Gy. Some of the D_e-s obtained with the SAR protocol are in good agreement with those obtained by the MAAD protocol. The age results are underestimated comparing with SAR measurements, what is expected, since the IRSL measurements for MAAD were conducted after a four weeks delay after irradiation and no fading corrections were applied (Table 2.2., Fig. 2.8.). The calibrated radiocarbon dating results are presented in Fig. 2.8. and Table 2.3.

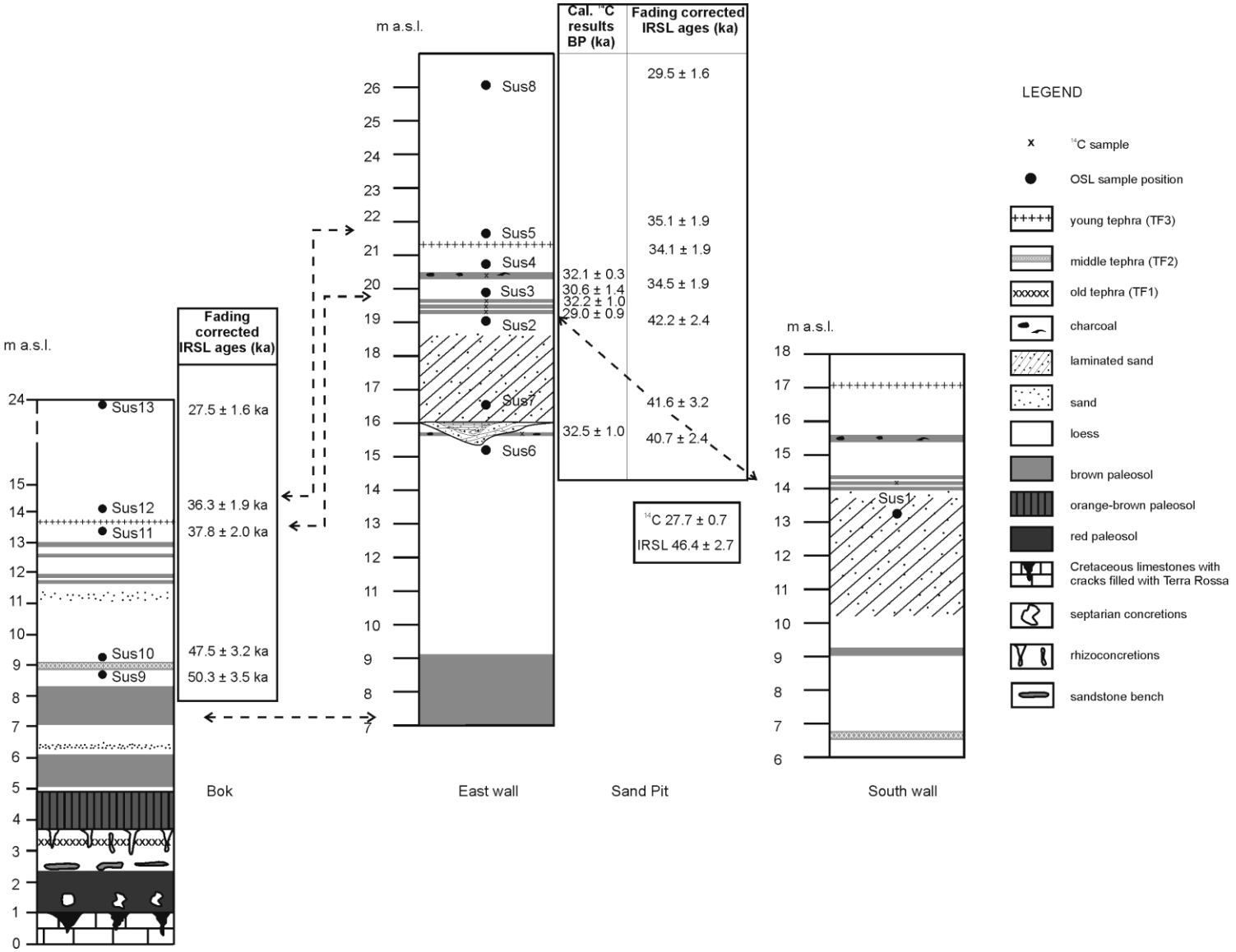

Figure 2.8. Correlation of luminescence and radiocarbon age estimates and the investigated profiles.

2.6. Discussion

2.6.1. Susak loess stratigraphy

The island of Susak is unique because of the great thickness of Quaternary sediments on such a small surface and represents the most detailed loess-palaeosol record in the North Adriatic area including the Po plain region. Besides the detailed mineralogical investigations of Mutić (1967), sedimentological work of Cremaschi (1990) and paleomagnetic measurements by Bognar and Zámbó (1992), no detailed geochronological investigation has been done of the loess and loess derivatives from this island. Bognar et al. (2003) gave an overview of paleoecological and paleogeomorphological evolution in the Carpathian Basin and its southern surroundings including Susak as a result of climatic changes during the Pliocene and Pleistocene epochs. Their correlation was based on describing palaeosol properties and finding equivalents in the Hungarian loess stratigraphy. In addition to radiocarbon data, paleomagnetic measurements indicate that the entire loess sequence from Susak has normal magnetization, and so correlates most likely to the Brunhes epoch. Malacological investigation suggests a last glacial age, as discussed in Bognar et al. (2003). The latter stratigraphic interpretation is not based on numerical dating and so remains under discussion.

The terra rossa and the strongly developed red palaeosol (termed SAV according to Bognar et al., 2003) found at the contact with the Cretaceous limestone basement (Fig. 2.8) are the result of Mediterranean climate in the North Adriatic region. In this area, climate conditions were generally milder than in Central and Western Europe (Cremaschi, 1987b; Coudé-Gaussen, 1990). The strong red colour of both palaeosols is a result of rubification, a process of preferential formation of haematite over goethite, associated with the Mediterranean climate, high internal drainage due to the karst nature of the limestone basement and neutral pH conditions (Durn, 2003). According to Bognar et al. (2003), the red palaeosol covering the basement is a steppe-like soil formed under warm and dry or subhumid conditions, and it represents the lower or the lowermost Pleistocene. Based on soil properties, they correlated it with the Hungarian PD (Paks Double) type palaeosol.

Paleomagnetic measurements presented in Bognar et al. (2003) showed negative inclination in the red palaeosol, and so the Brunhes-Matuyama boundary (0.78 Ma) was placed in it. Durn et al. (2007) assumed the age of the red palaeosol on Susak, as well as similar palaeosols found in Istria, to be of Eemian age. They also showed that the parent material of these soils

had a mixed origin, with a predominant aeolian component. They also assumed that the aeolian component was probably loess older than the Late Pleistocene. Septarian concretions which can be seen in the red palaeosol are the result of capillary upwards movement of water enriched in dissolved carbonate from the limestone below, as suggested by Bognar and Zámbó (1992). According to Mikulčić Pavlaković et al. (2011), it is more likely that the concretions are a result of dissolution of carbonate from the upper part of the sequence and accumulation on the less permeable horizon below. The loess covering the red palaeosol (Fig. 2.8.) is probably the oldest loess on the island. The sandstone bench is a result of strong circulation of water enriched with $CaCO_3$ through the overlying deposits and calcite crystallisation on the top of the impermeable red palaeosol below (Bognar and Zámbó, 1992). Because of the difference in permeability of the two contacting layers, the bench has a platy shape and lateral spreading. The characteristics and dimensions suggest drastic oscillations of humid and dry periods during pedogenesis of the overlying reddish–brown palaeosol (Mikulčić Pavlaković et al., 2011).

The lowermost yellow tephra layer, which is very likely the oldest one found on the island, is described in more detail by Mikulčić Pavlaković et al. (2011). The tephra has not been dated. A correlation of the orange–brown palaeosol from Susak with the Mende Base (MB)-type palaeosol from Hungarian stratigraphy, as suggested by Bognar et al. (2003), is not based on any evidence and is therefore discarded. The MB palaeosol is significantly older than the last interglacial (Wintle and Packman, 1988; Frechen et al., 1997) i.e. older than Marine Isotope Substage 5e (MIS 5e), correlated with the deep sea record. Rhizoconcretions which can also be found in this oldest loess layer are the result of vertical water movements along root channels and carbonate precipitation. The abundance of these three different types of concretions in the old loess layer indicates a high precipitation alternatively a high water table and very humid and warm climate conditions.

Overlying the orange–brown palaeosol is a thin loess layer, covered by a brown palaeosol. The small thickness of the loess between the two well-developed palaeosols is probably a result of erosional processes, indicating a hiatus. The brown palaeosol covering the thin loess horizon is described by Bognar et al. (2003) as a chernozem palaeosol, of BA type (Basaharc Lower) from Hungarian loess stratigraphy. According to Frechen et al. (1997), the BA palaeosol is also older than the last interglacial and was formed during the antepenultimate interglacial. At present, no numerical dating is available for this part of the sequence.

Loess intercalated by a sand horizon covers the brown palaeosol. According to radiocarbon dating results from Bognar et al. (2003) this horizon should be older than 35 000 BP. A chocolate brown palaeosol overlies the loess, which is covered by another loess horizon intercalated by a brown palaeosol with small patches of orange–yellow tephra (TF2). The IRSL dating results indicate that the palaeosol with the tephra is younger than 50.3 ± 3.5 ka, making the loess and palaeosol belong to MIS 3. The appearance of the tephra in the palaeosol means that the tephra was probably reworked and partly bioturbated during the soil forming processes in the period between 50.3 ± 3.5 and 47.5 ± 3.2 ka. This also indicates a short period of warm climate during an interstadial, with soil formation and evidence of volcanic activity.

Dating results of the loess and loess derivatives overlying the brown palaeosol with tephra patches indicate that the whole upper part of the section was formed during MIS 3. The great thickness of the loess indicates a very high accumulation rate during MIS 3 and a dry and cold climate. The numerous thin brown palaeosols, which can be seen intercalated in the loess, are the result of climate fluctuations, periods of short warm climatic conditions with pedogenetic processes. Based on the luminescence dating results of the loess below and above the tephra layer, the upper tephra (TF3) found in the upper part of the Bok section is between 37.8 ± 2.0 ka and 36.3 ± 1.9 ka. In the uppermost part of the Bok section, the luminescence results estimate an age of 27.5 ± 1.6 ka, representing the youngest IRSL dated loess sample of the sequence under study.

At the Sand Pit section, the contact with the carbonate basement and the red palaeosols was not exposed during field-work (Fig. 2.8.). The lowermost visible palaeosol in the Sand Pit section is a carbonate-free brown palaeosol. The brown palaeosol is covered by loess, gradually becoming sandier upwards and subsequently followed by the next fining-up cycle resulting again in loess. The upper part of this loess is intercalated by a few cm thick brown palaeosol with charcoal remains. The calibrated radiocarbon age of 32.5 ± 1.0 ka (Hv 25 700), can be correlated with luminescence dating results of the loess directly from below the palaeosol, which gave an IRSL age estimate of 40.7 ± 2.4 ka.

The wedge filled with laminated coarse-grained material and mollusc fragments is probably a result of a short and strong water activity and erosion. The age of the sand directly covering the wedge gave an IRSL age of 41.6 ± 3.2 ka, which is in agreement with the age of the loess from below the water induced erosion, and gives evidence for the relative short duration of the erosion period. The IRSL age of the loess covering the sand is 42.2 ± 2.4 ka. This age

correlates well with the ages from the sand below and indicate a period of intense sand mobility between around 40 and 46 ka. The luminescence dating results of the sample from the South wall are in good agreement with the results from the East wall. The loess covering the sand is intercalated by four few cm-thick brown palaeosols with charcoal remains. Three of the palaeosols group together and can be followed in several locations. The calibrated radiocarbon results of the palaeosols gave ages of 29.0 ± 0.9 ka (Hv 25 696), 32.2 ± 1.0 ka (Hv 25 697), 30.6 ± 1.4 ka (Hv 25 701) and 32.1 ± 0.3 ka (Hv 25 698), from top to bottom (Fig. 2.8.). The age of the uppermost tephra (TF3) layer spans between 34.1 ± 1.9 ka and 35.1 ± 1.9 ka, based on the result of the sample from the loess below the tephra and directly covering the tephra. The uppermost collected sample from this section gave an age of 29.5 ± 1.6 ka and represents the youngest loess on this section and can be correlated with the loess from the Bok section.

The sediment succession from the Bok section between the second brown palaeosol and the upper tephra (TF3) and the Sand Pit section are not identical. At the Sand Pit section sand prevails, while at the Bok section sand can be found only as a 30 cm-thick layer intercalated in the loess. The sand and the laminated sand are the result of the deflation of the sediments from a proximal source. The number and the position of the thin brown palaeosols (chernozem-like soils, according to Bognar et al., 2003) are not identical. At both sections there is a small "pedocomplex"/triple palaeosol of three such thin brown palaeosols, which are exposed at several locations on the island indicating an island-wide distribution. Laterally at some locations, one of the palaeosols thins out and disappears, and on other locations four of the palaeosols are visible. It is even possible that more of such palaeosols are present in this loess succession, very likely depending on the paleorelief and short warm interstadials and erosional periods. The uppermost tephra layer (TF3) has the same colour and mineralogical composition (Mikulčić Pavlaković et al., 2011) at both profiles. At the Sand Pit section, evidence for water activity is present as a coarse sand-filled wedge. From the dating results from the Sand Pit section, between 40.7 and 46.4 ka intensive sand accumulation took place, and around 35.0 ka a period of increased dust accumulation and loess formation started. At the Bok section, loess accumulation dominated. The difference between these two relatively nearby sections is probably triggered by the different paleorelief, but more investigation and data is necessary for a detailed paleorelief reconstruction. The triple palaeosols with the charcoal remains and the uppermost tephra layer (TF3) are exposed at both sections and hence can be correlated.

Deposits correlating to MIS2 and younger were not sampled at the two sections under study because of inaccessible vegetation-covered steep loess walls. The landscape and the relief of Susak are dominated by numerous artificial terraces and terraced slopes, which are the result of frequent reworking of the surface due to agricultural and other human activities, especially wine grape production. Because of that reason, it is very likely that the youngest deposits are not in their primary position, making it difficult to find appropriate outcrops for sampling.

2.6.2. Correlation with the Danube basin

In Eastern Croatia, along the banks of the Danube, impressive loess-palaeosol sequences can be found in Slavonia and Baranja. The loess successions are intercalated by at least four palaeosols or pedocomplexes, which correlate with Middle and Upper Pleistocene interstadials and interglacials (Galović et al., 2009). At Erdut and Zmajevac sections, the uppermost palaeosol intercalated in the loess gave an IRSL age estimate ranging from 46.5 ± 4.7 ka to 48.9 ± 5.0 ka. Galović et al. (2009) correlated this palaeosol to the last middle pleniglacial (MIS3), or maybe to an early glacial interstadial (MIS5). As fading correction was not applied in this study, the IRSL age underestimation cannot be ruled out and has to be checked. The IRSL age of the first palaeosol from the top in Zmajevac and Erdut could be correlated with the IRSL age estimates of 46.0 ± 3.2 ka from below the brown palaeosol with tephra patches (TF2) on Susak. Palaeosols younger than the MIS3 have not been found yet in the loess-palaeosol sections in Eastern Croatia. The uncorrected MAAD dating results from below the tephra bearing palaeosol on Susak of 29.1 ± 1.8 ka is most likely in agreement with TL results from the uppermost palaeosol from Erdut (palaeosol F1, 45–29 ka; Bronger, 2003). This age can also be correlated with the IRSL age range of 46.9 ± 4.8 to 19.8 ± 2.1 ka from the uppermost palaeosol from Erdut provided in Galović et al. (2009). At Zmajevac section, the uppermost palaeosol is younger than 48.9 ± 5.0 and was also correlated to the F1 palaeosol from Erdut (Bronger, 1976, 2003). At Zmajevac, this palaeosol is covered by about 5m of loess, which gave IRSL age estimates ranging from 20.2 ± 2.1 to 17.8 ± 1.9 ka and correlating to the last pleniglacial (MIS2). In Eastern Croatia the chronological position of the last interglacial palaeosol (MIS5e) is still under discussion. At the Zmajevac section, the second pedocomplex from the top probably correlates to the last interglacial soil (MIS5e) (Galović et al., 2009).

According to Serbian chronostratigraphic interpretation (Marković et al., 2004, 2007, 2008, 2009) the last interglacial-early glacial palaeosol S1 (equivalent to fossil soil F2 of Bronger's nomenclature (Bronger, 2003), and to MF2 palaeosol from the Hungarian loess chronostratigraphy (Wintle and Packman, 1988; Frechen et al., 1997)) correlates with MIS 5 (Schmidt et al., 2010; Marković et al., 2007, 2009; Fuchs et al., 2008). This palaeosol is overlain by a composite loess unit L1, correlated with MIS 4–2 (Schmidt et al., 2010; Marković et al., 2007, 2009; Fuchs et al., 2008). The last glacial loess (L1) is subdivided in this region by a weakly developed interstadial palaeosol complex (L1S1), which appears as a single pedohorizon (Ruma section, Marković et al., 2004) or as double (Irig section, Marković et al., 2007, 2009; Batajnica section) or as multiple (Stari Slankamen section, Schmidt et al., 2010; Surduk section, Antoine et al., 2009) palaeosols, and is correlated to MIS3. MIS3 is represented by weakly developed chernozem palaeosols, reflecting slightly warmer and drier conditions during that interval (Marković et al., 2007). Recently, the upper part of the Stari Slankamen section in Vojvodina was investigated by Schmidt et al. (2010). There, the chernozem-like pedocomplex (V-L1S1) yielded age estimates ranging from 35.0 ± 2.2 to 31.3 ± 1.9 ka. The youngest loess from Susak is contemporaneous with the V-L1 loess unit from Stari Slankamen in Serbia. MIS3 in Hungary is represented by the MF1 palaeosol (Frechen et al., 1997; Novothny et al., 2002), a weakly developed chernozem-like palaeosol. At Zmajevac and Erdut sections, the upper weakly developed pedocomplex is correlated to MIS3 (Galović et al., 2009). In Hungary two weak humic horizons, h_1 and h_2, correlate to MIS2. Such horizons have not been found in Croatian and Serbian loess deposits. Susak loess-palaeosol sequence is unique and differs in many ways from the Danubian loess sequences. A more detailed chronological study is required and in progress to determine the MIS5 palaeosol because correlating palaeosols based only on their physical properties may result in wrong conclusions.

During the Middle and Upper Pleistocene the Po plain was an important sedimentation basin, surrounded by the Alps, Apennines and the Adriatic Sea. During glacial periods, the sea level in the Mediterranean Sea was about 100 m lower than today. It caused a quick progradation of alluvial deposits of the Po river which created wide barren and poorly protected areas from which large amounts of fine-grained material could have been removed by wind (Cremaschi, 1990). During MIS2 and 3 loess accumulation rates were very high in Europe (Frechen et al., 2003). The same situation occurred in the North Adriatic Sea and the evidence of these dramatic climatic changes and processes are found in the loess-palaeosol sequence on Susak.

These first results have started unravelling the complex Last Glacial evolution on the island of Susak, and a first chronological framework has been established.

2.7. Conclusion

A first chronological framework was set up for the loess-palaeosol sequence on the island of Susak using an IRSL dating approach. A simple SAR protocol with fading corrections was used successfully for establishing the De values. The SAR results were compared to MAAD results. The SAR protocol provided more reliable age estimates. Within error limits, the calculated ages are in stratigraphic order, correlating the investigated loess-palaeosol successions to the last glacial–interglacial cycle. The results indicate a very detailed loess-palaeosol record correlating with MIS3. Most of the Late Glacial loess record is probably missing and loess-palaeosols older than the MIS3 have been often eroded. At Susak, the great thickness of the loess correlating with MIS3 indicates a strong accumulation rate during that time and the vicinity of the source area. The climate on Susak and the vicinity of the deposits source area, the River Po plain, resulted in deposition of thick loess and loess derivatives during glacial periods, and soil formation during interstadial or interglacial periods. The Upper Pleistocene loess succession on Susak is more detailed and more complex than in the Danube basin. IRSL ages estimates of two tephra layers have been determined. The middle tephra (TF2) is sandwiched by IRSL ages of 50.3 ± 3.5 ka and 47.5 ± 3.2 ka, based on loess from below and above the tephra layer. This tephra can be correlated to several central and south Italian volcanic provinces. The possible source area of the uppermost tephra layer (TF3), which was deposited between 37.8 ± 2.0 ka and 34.1 ± 1.9 ka, could be the Campanian Province in South Italy (Mikulčić Pavlaković et al, 2011). It is necessary to extend the geochronological framework with dating of loess from the lowermost and uppermost parts of the sections. According to the fading-corrected luminescence dating results, it can be concluded that a very detailed MIS3 record is exposed on the island of Susak. Loess on Susak differs in many ways from contemporaneous deposits in other loess regions, such as the loess along the Danube in Eastern Croatia, Serbia and Hungary.

2.8. Acknowledgements

This research has been financed by the DAAD (German Academic Exchange Service), Leibniz Institute for Applied Geophysics (LIAG), Hannover, Germany; Croatian Ministry of Science, Education and Sports, Projects Nr. 0181001, 0183008 and 183-0000000-3201. This work could not be possible without the help from the colleagues from the S3 from LIAG. The authors wish to thank to Dr. Lidija Galović for fruitful discussions and support, to Ivo Suša for technical support and to Ira Wacha-Biličić for correcting the English. The valuable comments and guidelines from Prof. Dr. Goran Durn and Dr. Sumiko Tsukamoto are appreciated.

2.9. References

Adamiec, G., Aitken, M., 1998. Dose-rate conversion factors: update. Ancient TL 16, 37-50.

Aitken, M.J., 1985. Thermoluminescence Dating. Academic Press, London, 351 pp.

Aitken, M.J., 1998. An introduction to optical dating. Oxford University Press, Oxford, 280 pp.

Antoine, P., Rousseau, D.D., Fuchs, M., Hatté, C., Gauthier, C., Marković, S.B., Jovanović, M., Gaudenyi, T., Moine, O., Rossignol, J., 2009. High-resolution record of the last climatic cycle in the southern Carpathian Basin (Surduk, Vojvodina, Serbia). Quaternary International 198, 19-36.

Auclair, M., Lamothe, M., Huot, S., 2003. Measurement of anomalous fading for feldspar IRSL using SAR. Radiation Measurements 37, 487–492.

Ballarini, M., Wallinga, J., Murray, A.S., Heteren, S.v., Oost, A.P., Bos, A.J.J., Eijk, C.W.E.v., 2003. Optical dating of young coastal dunes on a decadal time scale. Quaternary Science Reviews 22, 1011-1017.

Bognar, A., Zámbó, L., 1992. Some new data of the loess genesis on Susak island. In: Bognar, A. (Ed.), Proceedings of the International Symposium “Geomorphology and Sea”. University of Zagreb, Croatia, 65-72.

Bognar, A., Schweitzer, F., Szöőr, G., 2003. Susak – environmental reconstruction of a loess island in the Adriatic. Geographical Research Institute, Hungarian Academy of Sciences, Budapest, 141 pp.

Bøtter-Jensen, L., Bulur, E., Duller, G.A.T., Murray A.S., 2000. Advances in luminescence instrument systems. Radiation Measurements 32, 523-528.

Bøtter-Jensen, L., McKeever, S.W.S., Wintle, A.G., 2003. Optically stimulated luminescence dosimetry. Elsevier, Amsterdam, 355 pp.

Bronger, A., 1976. Zur quartaeren Klima- und Landschaftsentwicklung des Karpatenbeckens auf (palaeo)-pedologischer und bodengeographischer Grundlage. Kieler Geographische Schriften 45, 268 pp.

Bronger, A., 2003. Correlation of loess-paleosol sequences in East and Central Asia with SE Central Europe: towards a continental Quaternary pedostratigraphy and paleoclimatic history. Quaternary International 106/107, 11–31.

Coudé-Gaussen, G., 1990. The loess and loess-like deposits along the sides of the western Mediterranean Sea: genetic and palaeoclimatic significance. Quaternary International 5, 1–8.

Cremaschi, M., 1987a. Paleosols and Vetusols in the Central Po plain, a study in Quaternary Geology and Soil Development.– Edizioni Unicopli, Milano, 306 pp.

Cremaschi, M., 1987b. Loess deposits of the Po plain and the adjoining Adriatic basin (Northern Italy). In: Pécsi, M., French, H.D. (Eds.), Loess and Periglacial Phenomena, pp. 125-140, Akademiai Kiado, Budapest.

Cremaschi, M., 1990. Stratigraphy and palaeoenviromental significance of the loess deposits on Susak Island (Dalmatian archipelago). Quaternary International 5, 97–106.

Durn, G., Ottner, F., Slovenec, D., 1999. Mineralogical and geochemical indicators of the polygenetic nature of terra rossa in Istria, Croatia. Geoderma 91 (1–2), 125–150.

Durn, G., 2003. Terra rossa in the Mediterranean region: Parent materials, composition and origin. Geologia Croatica 56 (1), 83-100.

Durn, G., Aljinović, D., Crnjaković, M., Lugović, B., 2007. Heavy and light mineral fractions indicate polygenesis of extensive terra rossa soils in Istria, Croatia. In: Mange, M., Wright, D. (Eds.), Heavy Minerals in Use, Developments in Sedimentology, vol. 58. Elsevier, Amsterdam, 701–737.

Fairbanks, R.G., Mortlock, R.A., Chiu, T.-C., Cao, L., Kaplan, A., Guilderson, T.P., Fairbanks, T.W., Bloom, A.L., 2005. Marine radiocarbon calibration curve spanning 0 to 50,000 years B.P. based on paired 230Th/234U/238U and 14C dates on pristine corals. Quaternary Science Reviews 24, 1781–1796.

Frechen, M., Schweitzer, U., Zander, A., 1996. Improvements in sample preparation for the fine grain technique. Ancient TL 14 (2), 15–17.

Frechen, M., Horváth, E., Gábris, Gy., 1997. Geochronology of Middle and Upper Pleistocene loess sections in Hungary. Quaternary Research 48, 291–312.

Frechen, M., Oches, E.A., Kohfeld, K.E., 2003. Loess in Europe - mass accumulation rates during the Last Glacial Period. Quaternary Science Reviews 22 (18–19), 1835–1857.

Fuchs, M., Rousseau, D.-D., Antoine, P., Hatté, C., Gauthier, C., Marković, S., Zoeller, L. 2008. Chronology of the Last Climatic Cycle (Upper Pleistocene) of the Surduk loess sequence, Vojvodina, Serbia. Boreas 37, 66-73.

Galović, L., Frechen, M., Halamić, J., Durn, G., Romić, M., 2009. Loess chronostratigraphy in Eastern Croatia - A first luminescence dating approach. Quaternary International 198 (1-2), 85 -97.

Geyh, M.A., 1990. ^{14}C dating of loess. Quaternary International 7/8, 115-118.

Geyh, M.A., 2005. ^{14}C dating - still a challenge for users? Z Geomorph NF Suppl 139:63-85.

Huntley, D.J., Godfrey-Smith, D.I., Thewalt, M.L.W., 1985. Optical dating of sediments. Nature 313, 105–107.

Huntley, D.J., Lamothe, M., 2001. Ubiquity of anomalous fading in K-feldspars, and the measurement and correction for it in optical dating. Canadian Journal of Earth Sciences 38, 1093-1106.

Hütt, G., Jaek, I., Tchonka, Y., 1988. Optical dating: K-feldspars optical response stimulation spectra. Quaternary Science Reviews 7, 381–386.

Kars, R.H., Wallinga, J., Cohen, K.M., 2008. A new approach towards anomalous fading correction for feldspar IRSL dating - tests on samples in field saturation. Radiation Measurements 43, 786-790.

Kunz, A., Frechen, M., Ramesh, R., Urban, B., 2010. Luminescence dating of Late Holocene dunes showing remnants of early settlement in Cuddalore and evidence of monsoon activity in south east India. Quaternary International 222, 194-208.

Lamothe, M., Auclair, M., Hanazaoui, C., Huot, S., 2003. Towards a prediction of long-term anomalous fading of feldspar IRSL. Radiation Measurements 37, 493–498.

Lian, O.B., Roberts, R.G., 2006. Dating the Quaternary: progress in luminescence dating of sediments. Quaternary Science Reviews 19/20, 2449-2675.

Lu, Y.C., Wang, X.L., Wintle, A.G., 2007. A new OSL chronology for dust accumulation in the last 130,000 yr for the Chinese Loess Plateau. Quaternary Research 67, 152–160.

Machalett, B., Oches, E.A., Frechen, M., Zöller, L., Hambach, U., Mavlyanova, N.G., Marković, S.B., Endlicher, W., 2008. Aeolian dust dynamics in central Asia during the Pleistocene: Driven by the long-term migration, seasonality, and permanency of the Asiatic polar front. Geochemistry, Geophysics, Geosystems 9, Q08Q09.

Mamužić, P., 1965. Osnovna geološka karta SFRJ 1:100 000. List Lošinj L 33-155, Institut za geološka istraživanja, Zagreb, Savezni geološki zavod, Beograd.

Mamužić, P., 1973. Osnovna geološka karta SFRJ 1:100 000. Tumač za list Lošinj. Institut za geološka istraživanja, Zagreb, Savezni geološki zavod, Beograd, 34 pp.

Marković, S.B., Kostic, N.S., Oches, E.A., 2004. Paleosols in the Ruma loess section (Vojvodina, Serbia). Revista Mexicana de Ciencias Geológicas 21, 79-87.

Marković, S.B., Oches, E.A., McCoy, W.D., Frechen, M., Gaudenyi, T., 2007. Malacological and sedimentological evidence for “warm” glacial climate from the Irig loess sequence, Vojvodina, Serbia. Geochemistry, Geophysics, Geosystems 8, Q09008.

Marković, S.B., Bokhorst, M., Vandenberghe, J., Oches, E.A., Zöller, L., McCoy, W.D., Gaudenyi, T., Jovanović, M., Hambach, U., Machalett, B., 2008. Late Pleistocene loess-paleosol sequences in the Vojvodina region, North Serbia. Journal of Quaternary Science 23, 73-84.

Marković, S.B., Hambach, U., Catto, N., Jovanović, M., Buggle, B., Machalett, B., Zöller, L., Glaser, B., Frechen, M., 2009. Middle and Late Pleistocene loess sequences at Batajnica, Vojvodina, Serbia. Quaternary International 198, 255-266.

Mikulčić Pavlaković, S., Crnjaković, M., Tibljaš, D., Šoufek, M., Wacha, L., Frechen, M., Lacković, D., 2011. Mineralogical and Geochemical Characteristics of Quaternary Sediments from the Island of Susak (Northern Adriatic, Croatia). Quaternary International 234 (1-2), 32-49.

Mutić, R., 1967. Pijesak otoka Suska. Geološki vjesnik 20, 41-57.

Novothny, Á., Horváth, E., Frechen, M., 2002. The loess profile at Albertirsa, Hungary - improvements in loess stratigraphy by luminescence dating. Quaternary International 95–96, 155–163.

Novothny, Á., Frechen, M., Horváth, E., Bradák, B., Oches, E.A., McCoy, W.D., Stevens, T., 2009. Luminescence and amino acid recemization chronology of the loess-paleosol sequence at Sütto, Hungary. Quaternary International 198 (1-2), 62-76.

Pécsi, M., 1990. Loess is not just the accumulation of dust. Quaternary International 7/8, 1-21.

Prescott, J.R., Hutton, J.T., 1994. Cosmic ray contributions to dose rates for luminescence and ESR dating: large depths and long-term time variations. Radiation Measurements 23**,** 497-500.

Pye, K., 1987. Aeolian Dust and Dust Deposits. Academic Press, London, 335 pp.

Pye, K., 1995. The nature, origin and accumulation of loess. Quaternary Science Reviews 14, 653–667.

Roberts, H.M., 2008. The development and application of luminescence dating to loess deposits: a perspective on the past, present and future. Boreas 37**,** 483-507.

Rees-Jones, J., 1995. Optical dating of young sediments using fine-grain quartz. Ancient TL 13, 9–14.

Schmidt, E., Machalett, B., Marković, S.B., Tsukamoto, S., Frechen, M., 2010. Luminescence chronology of the upper part of the Stari Slankamen loess sequence (Vojvodina, Serbia). Quaternary Geochronology 5, 2-3, 137-142.

Singhvi, A.K., Bronger, A., Sauer, W., Pant, R.K., 1989. Thermoluminescence dating of loess-paleosol sequences in the Carpathian basin (East-Central Europe): a suggestion for a revised chronology. Chemical Geology (Isotope Science Section) 73, 307-317.

Smalley, I., O´Hara-Dhand, K., Wint, J., Machalett, B., Jary, Z., Jefferson, I., 2009. Rivers and loess: The significance of long river transportation in the complex event-sequence approach to loess deposit formation. Quaternary International 198, 7-18.

Wallinga, J., Bos, A.J.J., Dorenbos, P., Murray, A.S., Schokker, J., 2007. A test case for anomalous fading correction in IRSL dating. Quaternary Geochronology 2, 216-221.

Wang X.L., Lu Y.C., Wintle A.G., 2006. Recuperated OSL dating of fine-grained quartz in Chinese loess. Quaternary Geochronology 1, 89-100.

Wang X.L., Wintle A.G., Lu Y.C., 2007. Testing a single-aliquot protocol for recuperated OSL dating. Radiation Measurements 42, 380-391.

Wintle, A.G., 1973. Anomalous fading of thermoluminescence in mineral samples. Nature 245, 143–144.

Wintle, A.G., 1997. Luminescence dating: laboratory procedures and protocols. Radiation Measurements 27, 769–817.

Wintle, A.G., Packman, S.C., 1988. Thermoluminescence ages for three sections in Hungary. Quaternary Science Reviews 7, 315–320.

CHAPTER 3

Quaternary International (2011), 234 (1-2), 32-49.

Mineralogical and Geochemical Characteristics of Quaternary Sediments from the Island of Susak (Northern Adriatic, Croatia)

Snježana Mikulčić Pavlaković[1], Marta Crnjaković[1], Darko Tibljaš[2], Marin Šoufek[1], Lara Wacha[3, 4], Manfred Frechen[4], Damir Lacković[1]

[1] Croatian Natural History Museum, Department of Mineralogy and Petrography, Demetrova 1, HR-10000 Zagreb, Croatia

[2] University of Zagreb, Faculty of Science, Horvatovac 95, HR-10000 Zagreb, Croatia

[3] Croatian Geological Survey, Sachsova 2, HR-10000 Zagreb, Croatia

[4] Leibniz Institute for Applied Geophysics, S3 Geochronology and Isotope Hydrology, Stilleweg 2, D-30655 Hannover, Germany

Abstract

Middle and Upper Pleistocene loess-palaeosol sequences up to 90 m thick are exposed on the Island of Susak located in the Northern Adriatic Sea in Croatia. During glacial times the sea level was up to about 120 m lower and a significant part of the Adriatic became land. The source area of the primary aeolian sediments was in the vicinity of the island and is related to the southward extended River Po plain. The loess has a mainly clayey to sandy silt or sand grain-size and is intercalated by at least three tephras, numerous palaeosols and calcareous segregations. The heavy mineral association points to metamorphic and igneous rocks from Alpine regions as source material of the loess. Geochemical and mineralogical properties of loess and palaeosols differentiate one from another and reflect the intensity of weathering and pedogenesis. The oldest tephra contains vitroclasts and serrated clinopyroxene while the middle and the youngest tephra along with vitroclasts, contain idiomorphic augite as diagnostic volcanic features. Based on bulk rock and vitroclast chemistry, morphology of pyroxenes, and the age of the loess sandwiching the tephra, the potential source of this volcanic material could very likely be the Campanian or Aeolian volcanic province in southern Italy. Infrared stimulated luminescence dating-results show that the major part of the aeolian deposits including the tephra layers correlates to MIS 3 - MIS 5.

Keywords: Northern Adriatic Sea, Quaternary, loess, palaeosol, tephra

3.1.Introduction

Quaternary aeolian deposits are widely distributed on Adriatic islands and along the Croatian and Italian coasts. In the Kvarner region, aeolian sediments including loess, its derivatives and sand have been found on the islands of Unije, Vele and Male Srakane and Lošinj. The most impressive and thickest loess-palaeosol sequence is exposed on the Island of Susak.

Susak Island is situated in the western part of the Kvarner archipelago (Fig. 3.1.) and covers an area of 3.8 km^2 with the highest peak at 96 m above sea level (asl). The landform is characterized by specific loess plateaus, and steep, mostly inapproachable loess bluffs and gorges covered by vegetation. Two sandy beaches are located along Susak Bay near to Susak harbour and along Bok Bay (Fig. 3.2.). Most of the bedrock is made of Senonian rudist limestone and Cenomanian-Turonian limestone in the southeast part and northwest part of the island, respectively. On the northern coast, Eocene limestone is found in a narrow zone between two faults (Mamužić, 1973). Geotectonically, Susak and the southwestern part of Unije Island are part of the Istrian autochton of the Northern Adriatic platform (Bognar et al., 2003).

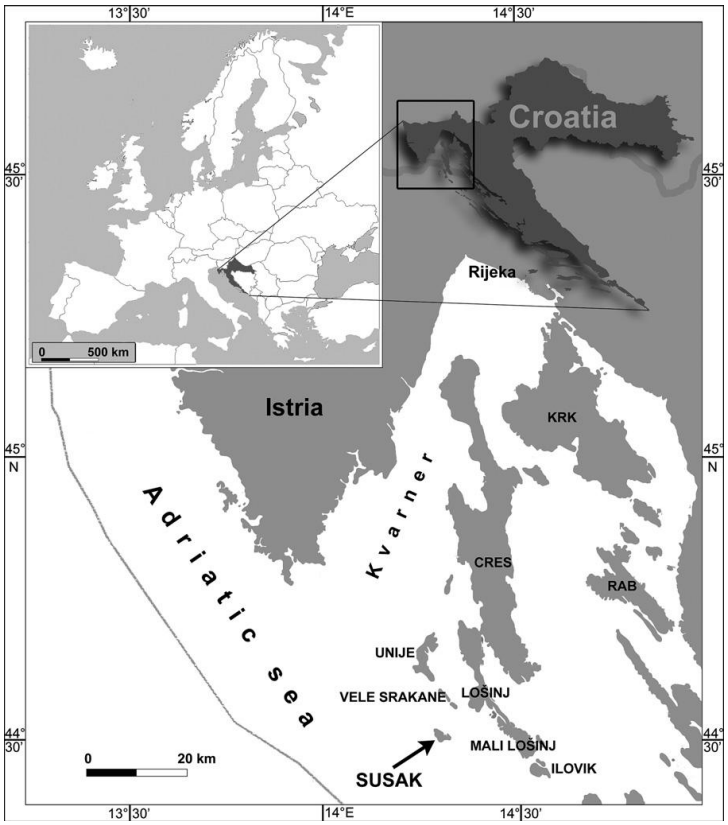

Figure 3.1. Geographical setting of the Island of Susak, Croatia.

Susak loess deposits provide a very detailed record of climate and environment change and are one of the most impressive geomorphological phenomena on the Adriatic islands. According to Bognar et al. (2003) they are thickest in the northwest part of the Island (up to 90 m in Garba area, Fig. 3.2.). However, deposits of the lower southeast part, being more accessible, have been the subject of most previous studies. Stache (1872), Marchesetti (1882), Salmojraghi (1907), Kišpatić (1910), Šandor (1912), Mutić (1967), Bognar et al. (1983) and Cremaschi (1990b) investigated provenance and mineral composition of loess. Based on the heavy mineral association, which is typical for metamorphic rocks of Alpine regions, most of the previous researches concluded that the source area of the aeolian sediments from Susak is the ancient alluvial plain formed by River Po and today submerged by the Adriatic Sea. These sediments were most likely accumulated by fluvial and aeolian transport mechanisms during the glacio-eustatic regression in Middle and Late Pleistocene. Marković-Marjanović (1966), Wein (1977), and Bognar (1997) studied the palaeosols, whereas Bognar et al. (2003) recorded the tephra horizons. The fossil terra rossa (FTR) in limestone cracks, which is considered the oldest palaeosol on the island, is probably of Pliocene age (Bognar et al., 2003).

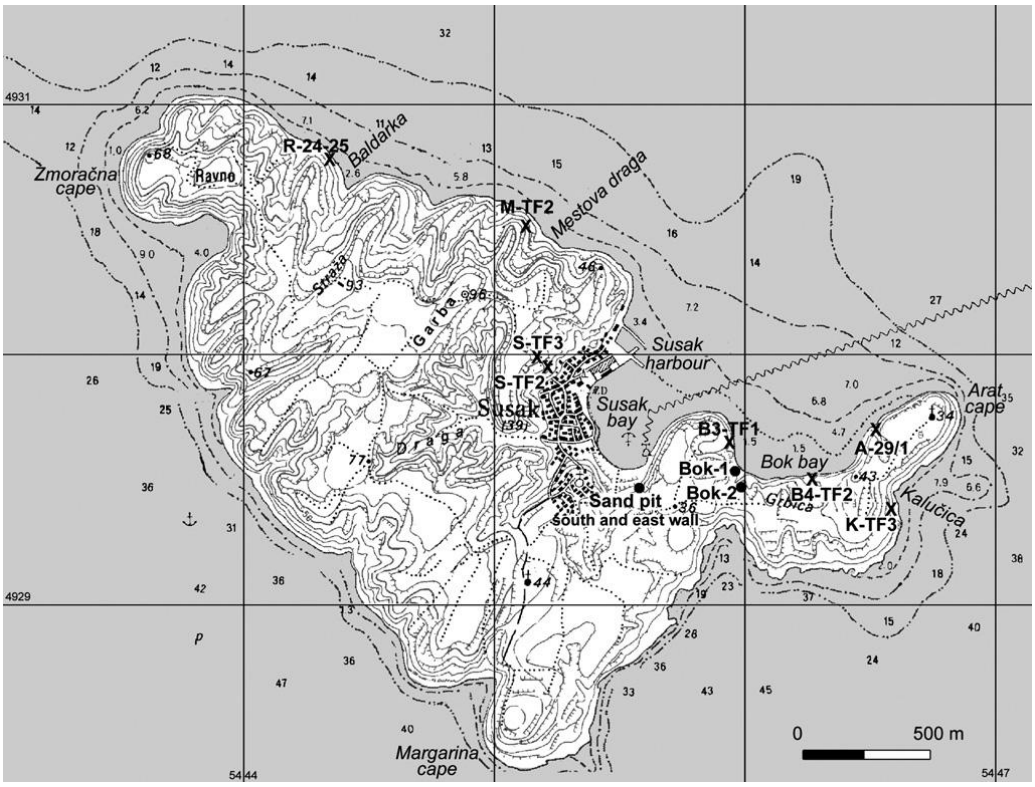

Figure 3.2. Topographic map of the Island of Susak showing locations of studied loess sections (circles) and sampling sites (crosses); Gauss-Krüger coordinates are shown (modified after MGI, 1977).

In spite of numerous investigations of the lowermost 30 m of the sediment record from Susak, the exact age of the deposits is still under discussion. Marković-Marjanović (1976) suggested that the loess is of last glacial (Würmian) age. Cremaschi (1990a, b) studied three loess profiles (Margarina, Arat and Harbour sequences, Fig. 3.2.) and correlated the loess-palaeosol record to the Middle and Late Pleistocene sediments of northern and central Italy and the River Po plain. Based on palaeomagnetic investigations and palaeopedological similarities with Hungarian palaeosols, Bognar et al. (2003) suggested that the palaeosol horizons from Susak have ages between 800 000 years and 120 000 years; the younger loess taken from 26 to 29 m asl gave uncalibrated radiocarbon ages of 16 730 ± 210 - 18 490 ± 155 years (Bognar et al., 2003). Štamol and Poje (1998) carried out malacological studies and concluded that the loess overlying the red palaeosol in the base of the sequence was deposited during the last glaciation (Würmian), with the uppermost investigated sediment correlating to the Dryas. More recent studies, based on infrared stimulated luminescence and radiocarbon dating showed that loess from the investigated sequence of 8-26 m asl represents a very detailed record correlating to MIS 3 with short periods of increased sediment accumulation rates (Wacha et al., 2011).

The aim of this study is to provide new data on mineralogical and geochemical properties of these sediments, primarily tephras and palaeosols, and to provide deposition ages of four stratigraphically important loess horizons by infrared stimulated luminescence dating.

3.2. Methods

Particle size analysis of the grain-size fractions 63-125 μm and >125 μm was carried out by wet sieving and the grain-size fraction <63 μm was analyzed by SediGraph 5100 (Micromeritics, 2002). Samples were dispersed in a solution of 0.05% $(NaPO_3)_6$ and additionally kept in ultrasonic bath prior to analysis. The carbonate ($CaCO_3$) content was calculated from the weight difference before and after cold hydrochloric acid (3%) treatment.

Heavy minerals were separated using bromoform (density: 2.89 g/cm^3) from the <50 μm and 50-125 μm fractions of loess, palaeosols and concretions, and from 32 to 125 μm fraction of tephra. Heavy minerals were mounted on glass slides and the heavy mineral spectra were determined by ribbon counting 300-500 grains for each sample using polarizing light

microscope (Mange and Maurer, 1992). Four groups of heavy mineral species were distinguished: opaque, micaceous, other transparent minerals and lithic fragments (including vitroclasts).

Thin sections were prepared from calcareous concretions and, for this purpose, artificially epoxy-cemented loess samples. Thin sections were used to investigate calcite, ferrous iron-bearing calcite and dolomite following the method after Friedman (Allman and Lawrence, 1972).

Chemical analyses were performed in order to get insight into possible differences in geochemical composition between loess and palaeosols and to examine the element behaviour during pedogenesis as well as to chemically characterize volcanic material i.e. tephra horizons. Chemical analyses were carried out in commercial laboratories in Canada (ACME Analytical Laboratories Ltd., Vancouver). Eleven major elements were determined by the ICP-AES method. Analysis of trace elements, including rare earth elements (REE), was carried out by ICP-MS. Samples for determination of REE and incompatible elements were prepared by $LiBO_2$ fusion while precious and base metals were digested in aqua regia.

For identification and quantification of secondary Fe-oxides in soils, dithionite-citrate bicarbonate treatment, proposed by Mehra and Jackson (1960), was used. Iron extracted (Fe_d), was measured with Pye-Unicam SP9 atomic absorption spectrophotometer. This parameter, when compared with the total iron content (Fe_{tot}) reflects a degree of weathering of Fe-containing primary silicates (Boero and Schwertmann, 1987). Fe_{tot} was calculated from Fe_2O_3 concentration obtained by major element analysis. Colour of the palaeosols was determined using Munsell Soil Color Charts (1994).

Analysis of volcanic vitroclasts was performed by SEM-Energy Dispersive Spectrometer (EDS) and the results were stoichiometrically normalized to number of oxygen. Analysis was carried out in high vacuum on Vega©Tescan TS5136MM scanning electron microscope (SEM) equipped with Oxford INCA EDS detector using an acceleration voltage of 20.0 kV. Due to uneven surface and high porosity of particles, detection of major elements of lower atomic number such as sodium was problematic. Therefore, in order to accomplish identical analytical conditions on each particle an area of 2500 μm^2 was analyzed.

Phase composition of bulk rock and light mineral fraction of loess, palaeosols, calcareous segregations and tephra was determined by X-ray powder diffraction (XRD) using Philips X'Pert Pro instrument equipped with X'celerator detector (CuKα radiation, 45 kV, 40 mA).

Phases were determined by comparison of obtained data with those from JCPDS (1996) database using Philips X'Pert HighScore software (Philips Analytical B.V., 2001).

Highly oriented samples of <2 μm fraction of selected palaeosols have been prepared for clay mineral identification on air-dried, ethylene-glycol saturated, and heated (at 400 and 550°C, respectively) samples according to the procedure described by Starkey et al. (1984). On selected samples, enriched in clay minerals, the illite and chlorite crystallinities, expressed as Kübler (KI) (Kübler, 1967) and Árkai (ÁI) (Árkai, 1991) indices, respectively, were measured in order to determine origin of clay minerals. The Kübler index (KI) and Árkai Index (ÁI) are widely applied for determining the grade of diagenesis and low temperature regional metamorphism of clastic rocks, which are usually devoid of metamorphic indicator minerals and assemblages (Kübler, 1967, 1968; Árkai, 1991; Árkai et al., 1995). Sample preparation and X-ray powder pattern recording was undertaken according to Kisch (1991). Full widths at half maxima (FWHM) were read manually. XRD measurements of KI and ÁI were carried out on the same instrument as the bulk rock samples. Instrumental conditions were: 40 kV, 40 mA, step 0.02°2θ, and the measuring time was 5 s. Correlation of KI and ÁI values measured in the laboratory, to the values of Kübler's laboratory, taken as reference values, was made using eight Kisch standards (Kisch, 1990, 1991). Changes in FWHM caused by instrumental conditions (tube ageing) were monitored with time measurement of Crystallinity Index Standards (CIS) (Warr and Rice, 1994) which were for the first time measured together with Kisch standards.

The infrared stimulated luminescence (IRSL) dating method has proven to be an excellent method for dating Quaternary sediments, especially aeolian sediments like loess (Frechen et al., 1997; Novothny et al., 2002, 2009; Galović et al., 2009). The principles of luminescence dating are given by Aitken (1998) and Wintle (1997). Four samples were taken in light-proof plastic tubes, by pushing or hammering into a previously cleaned loess wall. Additional material was taken for dose rate determination by gamma spectrometry. Sampling took place in 2008. Sample preparation of the polymineral, fine-grain fraction (4-11 μm), luminescence measurements and dose rate determination are explained in detail in Wacha et al. (2011).

3.3. Results

This study was carried out between 2003 and 2008 (Mikulčić Pavlaković et al., 2005; Mikulčić Pavlaković, 2006). Four Susak loess sections, two located in Bok Bay - Bok-1 (Gauss-Krüger coordinates 5445962, 4929604) and Bok-2 (5445960, 4929552) and the other two in the hinterland of Susak Bay at local sand pit (5445561, 4929415) - Sand Pit-south wall and Sand Pit-east wall were investigated (Fig. 3.2.). A list of samples including sediment description is shown in Table 3.1.

3.3.1. Loess sections

3.3.1.1.Bok-1 (Fig. 3.3.)

In this study, the lowermost 11 m of the 31 m high section was investigated. At the bottom of the sequence two distinct red palaeosols (B1-5/3-lower and B1-5/5-upper), often intercalated by horizontally layered calcareous (septarian) concretions (B1-5/4), are exposed covering the limestone base. These palaeosols are covered by loess (B1-5/6/2) intercalated by a discontinuous, solid layer of lithified sandy loess (B1-5/6/1) (sandstone benches sensu Bognar et al., 2003) in its lower part and abundant calcareous rhizoconcretions (B1-5/6/3) above it. The lower part of this unit, the part where sandstone benches are absent, shows horizontal layering and cross-bedding, with irregular and abrupt laminae rhythmically changing in colours, often bioturbated and cryoturbated. In this unit, the stratigraphically oldest tephrawas found (B3-TF1). This loess is superimposed by a distinct, well-developed reddish-brown palaeosol (B1-5/7/1, B1-5/7/2). Alternations of loess and sandy sediment intercalated by at least two brown palaeosol horizons (B1-5/8/2 with charcoal pieces and double palaeosol (B1-5/10/1-3)) are found in the upper part of the sequence. The overlying loess is intercalated by brown palaeosol (B1-5/12) with patchy distributed yellow-orange tephra material (middle tephra (B1-TF2)). Throughout the section under study, except in sandy layers, calcified root channels ranging in diameter from 1 to 20 mm can be found more or less abundantly.

Table 3.1. List of samples and sediment description (for location of sampling sites see Fig. 3.2.).

	m asl	Sample	Sediment description
	10.2-10.3	B1-TF2	Middle tephra (TF2)
	8.0-8.5	B1-5/11	Sand
	7.2-8.0	B1-5/10/1-3	Brown (double) palaeosol
	6.7-7.2	B1-5/9/3	Sand
	6.3-6.7	B1-5/9/2	Loess
	5.9-6.3	B1-5/9/1	Loess (sandy-clayay silt)
	5.5-5.9	B1-5/8/2	Brown palaeosol with charcoal pieces
	5.0-5.5	B1-5/8/1	Loess (sandy silt) containing two slightly humified horizons
Bok-1 section	4.5-5.0	B1-5/7/2	Reddish-brown palaeosol (well-developed) - upper part
	3.6-4.5	B1-5/7/1	Reddish-brown (well-developed) - lower part
	2.4-3.6	B1-5/6/3	Calcareous rhizoconcretions
	2.9	B3-TF1	Oldest tephra (TF3)
	2.3-3.5	B1-5/6/2	Loess (clayey silt)
	1.8-2.3	B1-5/6/1	Sandstone bench
	1.4-1.8	B1-5/5	Upper red palaeosol (well-developed)
	1.4-1.6	B1-5/4	Septarian nodules
	1.0-1.4	B1-5/3	Lower red palaeosol (well-developed)
	13.7	B2-TF3	Youngest tephra (TF3)
	9.0	B2-TF2	Middle tephra (TF2)
Bok-2 section	8.9-9.1	B2-32/3/2	Brown palaeosol
	8.3-8.9	B2-32/2	Loess (sandy silt)
	7.0-8.3	B2-32/1/1-2	Brown palaeosol (well-developed)
	17.0	P-TF3	Youngest tephra (TF3)
	15.4-15.5	P-19/6	Brown palaeosol with charcoal peaces
	14.0-14.2	P-19/4	Brown palaeosol horizon (possibly redeposited)
	10.0-14.0	P-19/5	Cross-laminated sandy sediment
	9.2-10.0	P-19/3	silty sand
	9.0-9.2	P-19/2	Brown palaeosol with charcoal pieces (possibly redeposited)
	6.6-9.0	P-19/1	Loess (sandy-clayey silt)
Sand Pit-south wall section	6.6	P-TF2	Middle tephra (TF2)
	ca. 13	S-TF2	Middle tephra (TF2)
	ca. 12	M-TF3	
	9.0	B4-TF2	
	ca. 20	S-TF3	Youngest tephra (TF3)
	ca. 11	K-TF3	
	ca. 0.5	A-29/1	Fossil terra rossa (FTR) in limestone cracks
	ca. 1	R-24-25	Rudist limestone (Cretaceous limestone base)

3.3.1.2.Bok-2 (Fig. 3.3.)

At the Bok-2 section, the sediment sequence between 7 and 24 m asl was investigated. It starts with well-developed brown palaeosol (B2-32/1/1-2) with calcified root channels and bioturbations (crotovinas). The palaeosol is covered by loess, which is intercalated by a brown palaeosol with the middle tephra (B2- TF2) and several thinner brown, humic-rich horizons, possibly pedosediments. These humified horizons are covered by loess sandwiching the youngest tephra (B2-TF3) in the upper part of the section.

3.3.1.3.Sand Pit – south wall (Fig. 3.3)

The Sand pit-south wall section was investigated in 2003 and 2004 on the southern side of the Susak sand pit, which is no longer fully exposed. The sequence starts approximately 6 m asl with a brown palaeosol containing the middle tephra (P-TF2). The overlying loess (P-19/1, P-19/3), sandwiching a thin, brown palaeosol (P-19/2), is covered by cross-bedded sand and a redeposited brown palaeosol (P-19/4) showing 3-4 charcoal-rich humified horizons. The overlying loess is intercalated by a thin brown palaeosol (P-19/6), which also contains charcoal pieces and a distinctive layer of the youngest tephra (P-TF3).

3.3.1.4.Sand Pit – east wall (Fig. 3.3.)

The Sand pit-east wall section is located in the eastern part of the Susak sand pit and was investigated in 2008. The sequence starts with well-developed brown palaeosol. Above the overlying loess, cross-bedded sand is visible, containing lenses of laminated coarse to fine-grained sand and pebbles consisting of calcareous concretions and mollusc fragments indicating short-term running water activity. The thin brown palaeosol in the same horizon was affected by this erosional event. The overlying sediment sequence is the same as on Sand Pit-south wall section. Due to similarity between the east wall and the south wall sections, no detailed mineralogical and geochemical analyses of east wall section were performed. Because the south wall section is no longer fully exposed samples for luminescence dating were collected only from the east wall and its results (Wacha et al., 2011) are presented for correlation purposes. The middle (TF2) and youngest (TF3) tephras were also found at other locations on the Island (Fig. 3.2., M-TF2, B4-TF2, S-TF2-middle tephra and S-TF3, K-TF3-youngest tephra).

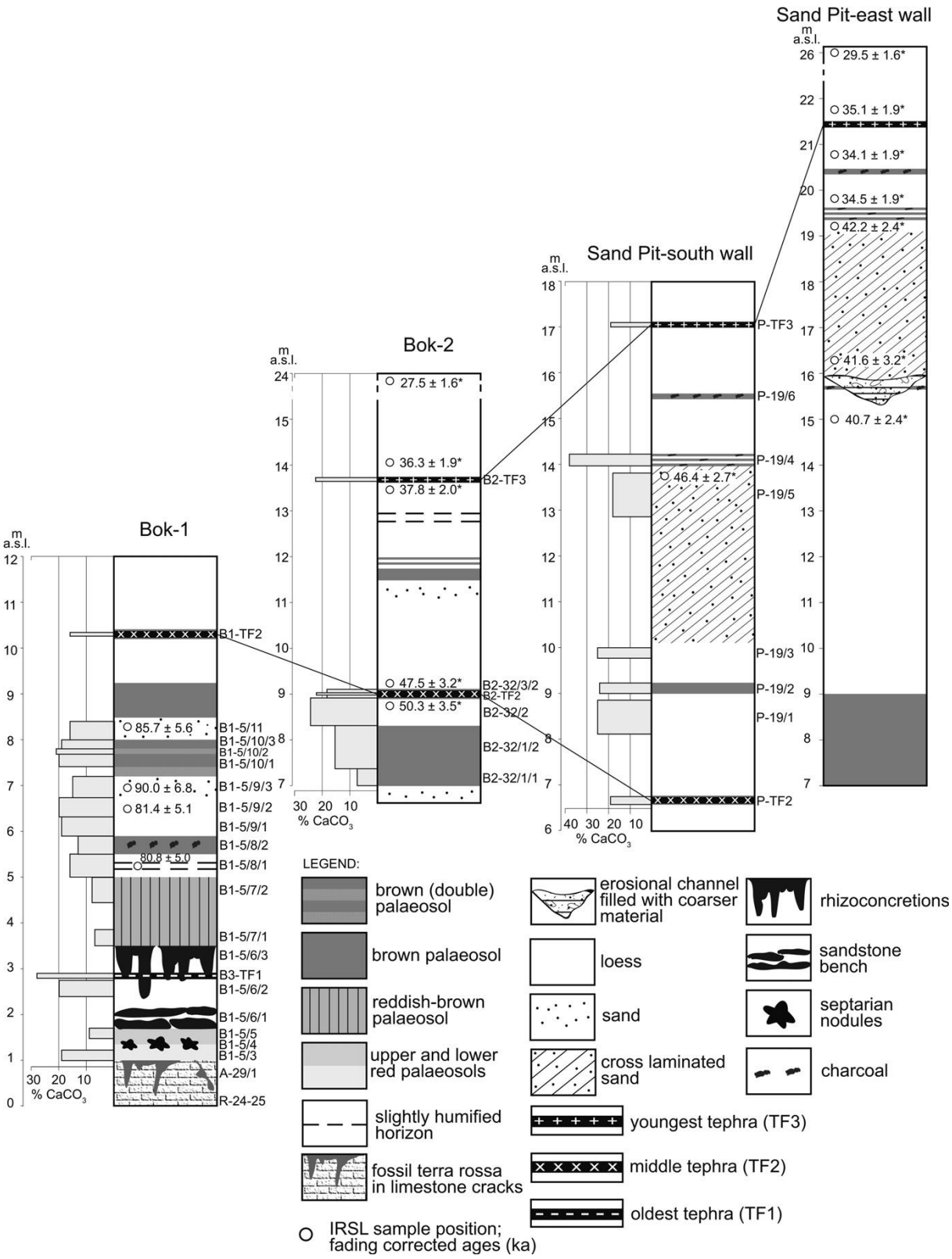

Figure 3.3. Stratigraphic sequences of Susak loess sections at Bok Bay (Bok-1, Bok-2) and Susak's sand pit (Sand Pit-south wall, Sand Pit-east wall) and $CaCO_3$ content of sediments; *IRSL ages after Wacha et al. (2011).

3.3.2. Loess and sand

In most horizons, silt (sandy-clayey, clayey and sandy silt) is the dominant grain-size fraction (Fig. 3.4., Table 3.2.). Sandy and clayey silt, from coefficients calculated according to Folk and Ward (1957), is poorly sorted, sandy-clayey silt is very poorly sorted and all have very positive skewness, i.e. they are weighted towards the coarse end-member (Table 3.2.). Although loess is mostly siliciclastic, carbonate particles (detritic and diagenetic) are also present (14.9-25 weight % of $CaCO_3$ content, Fig. 3.3.). They are mostly composed of micritic or microsparitic limestone fragments, while sparitic fragments and individual bigger grains are composed of dolomite. Siliciclastic constituents are quartz, micaceous minerals, feldspars and lithic fragments (Fig. 3.5.a).

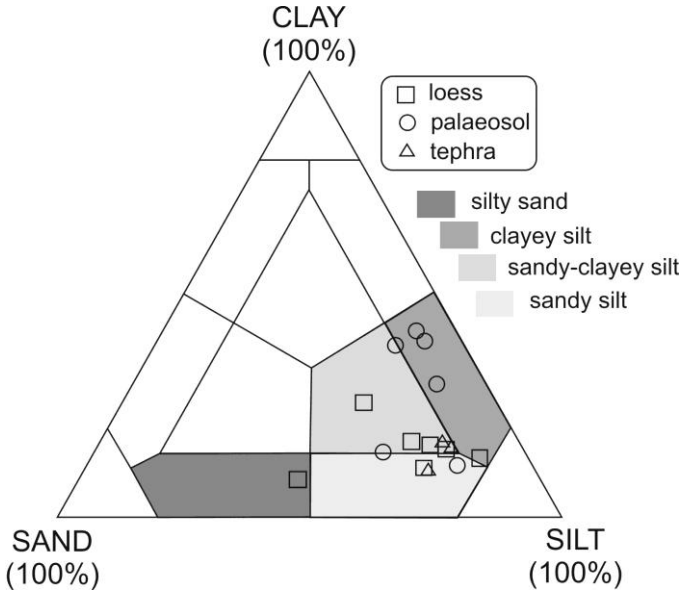

Figure 3.4. Grain-size distribution of loess, palaeosol and tephra (sediment description after Trefethen, 1950).

Quartz is angular, only the bigger grains are slightly rounded. The quartz is mostly clear with rare inclusions. Many grains show undulose extinction. Composite quartz with two or three subgrains showing extinction in different positions is also found. Feldspars occur as monocrystals (probably potassium feldspars) and polysynthetic plagioclase twins. The feldspars are mostly colourless and relatively clear but some grains show traces of weathering along cleavage planes.

Four groups of heavy mineral species are represented as follows (Fig. 3.5.b): lithic fragments (3-7%), opaque grains (4-12%), micaceous (muscovite, chlorite, biotite) (14-63%), and other transparent minerals (32-72%) (Table 3.3.).

Figure 3.2. Particle size analysis of sediments (Md - median, M - Mean, s - standard deviation, Sk - skewness, K - kurtosis).

	m a.s.l.	Sample	Granulometric composition (%) (Wentworth, 1922)			Granulometric parameters in Φ units (Folk and Ward, 1957)					Skewness	Sorting	Sediment description (Trefethen, 1950)
			Sand	Silt	Clay	Md	M	s	Sk	K			
Loess	9.8-10.0	P-19/3	48.6	43.9	7.6	4.04	4.17	1.58	0.46	2.26	Very positive	Poor	Silty sand
	8.1-8.9	P-19/1	22.0	61.9	16.1	4.87	5.53	2.20	0.50	1.55	Very positive	Very poor	Sandy-clayey silt
	8.3-8.9	B2-32/2	16.0	69.6	14.4	4.98	5.51	1.99	0.49	1.75	Very positive	Poor	Sandy silt
	5.9-6.4	B1-5/9/1	18.7	66.2	15.1	4.95	5.52	2.11	0.47	1.55	Very positive	Very poor	Sandy-clayey silt
	5.0-5.5	B1-5/8/1	22.7	67.4	10.0	4.79	5.04	1.84	0.39	1.71	Very positive	Poor	Sandy silt
	2.4-2.8	B1-5/6/2	10.2	77.5	12.3	5.30	5.54	1.80	0.36	1.70	Very positive	Poor	Clayey silt
Palaeosols	9.0-9.2	P-19/2	15.7	73.7	10.6	4.98	5.26	1.76	0.41	1.78	Very positive	Poor	Sandy silt
	7.4-8.3	B2-32/1/2	10.2	60.7	29.2	5.82	6.78	2.60	0.42	0.72	Very positive	Very poor	Clayey silt
	7.0-7.4	B2-32/1/1	26.7	48.2	25.1	5.32	6.32	2.78	0.44	0.76	Very positive	Very poor	Sandy-clayey silt
	5.5-5.9	B1-5/8/2	29.0	57.4	13.6	4.83	5.29	2.17	0.41	1.24	Very positive	Very poor	Sandy silt
	4.5-5.0	B1-5/7/2	14.3	47.9	37.8	5.97	6.83	2.75	0.33	0.57	Very positive	Very poor	Clayey silt
	1.4-1.8	B1-5/5	8.0	53.2	38.8	6.84	7.30	2.49	0.17	0.66	Positive	Very poor	Clayey silt
	1.0-1.4	B1-5/3	8.5	50.4	41.1	7.17	7.41	2.51	0.05	0.69	Symmetrical	Very poor	Clayey silt
Tephra	17.0	P-TF3	21.9	68.3	9.9	5.06	5.20	1.88	0.30	1.57	Positive	Poor	Sandy silt
	9.0	B2-TF2	14.4	70.5	15.1	5.80	5.94	2.05	0.21	1.23	Positive	Very poor	Clayey silt
	2.8	B3-TF1	16.1	67.8	16.1	5.27	5.76	2.15	0.38	0.70	Very positive	Very poor	Sandy-clayey silt

Table 3.3. Heavy mineral composition of sediments; RL – rudist limestone, Op – opaque, LF – lithic fragments, Mic – micaceous, OT – other transparent, Grt – garnet, Ep – epidote, Tr – tremolite, Act – actinolite, Gln – glaucophane, Rbk – ribeckite, Aug – augite, Zrn – zircon, Tur – tourmaline, Rt – rutile, Ttn – titanite, Ky – kyanite, St – staurolite, Cld – chloritoid, Brk – brookite, And – andalusite (Kretz, 1983), Gr/Br Hbl – green/brown hornblende, Hyp – hyperstene, Cpx – clinopyroxene, Cr-spl – chrom-spinel, Cr-Chl – chrom-chlorite, N-unknown.

	sample	All= 100%				Other transparent = 100%																				
		Op	LF	Mic	OT	Grt	Ep-Zo	Tr-Act	Br Hbl	Grn Hbl	Gln-Rbk	Aug	Hyp	Cpx	Zrn	Tur	Rt	Ttn	Ky	St	Cld	Brk	And	Sil	Cr-sp	Cr-Chl	N
loess	P-19/5	11	4	14	72	28	30	10	-	16	-	2	1	6	-	2	1	5	-	1	1	1	-	-	-	-	-
	P-19/3	4	4	46	46	14	28	18	-	18	2	4	3	4	-	1	1	4	3	1	1	1	-	-	-	1	-
	P-19/1	7	3	49	42	17	43	13	2	9	-	1	2	5	1	1	1	4	3	-	1	-	1	-	-	1	-
	B2-32/2	7	3	36	53	20	39	11	1	14	+	+	+	6	-	3	1	1	+	1	1	-	-	-	-	-	-
	B1-5/11	4	7	37	52	18	39	10	2	15	1	3	2	5	-	2	2	2	-	1	1	-	-	-	-	-	-
	B1-5/9/3	12	6	16	66	26	24	10	1	17	2	2	2	5	1	2	1	5	1	1	1	1	1	-	-	-	-
	B1-5/9/1	5	4	37	54	21	34	12	1	16	3	2	1	5	1	-	-	3	2	1	1	-	1	-	-	-	-
	B1-5/8/1	4	3	63	32	15	37	16	1	12	-	2	2	4	2	2	4	2	1	1	1	1	-	-	-	-	1
	B1-5/6/2	7	3	49	41	13	38	14	1	17	1	6	2	3	-	2	1	3	1	-	-	2	-	1	-	-	-
palaeosols	P-19/4	11	4	14	72	28	30	10	1	15	-	2	1	6	+	2	1	5	+	1	1	1	-	-	-	-	-
	P-19/2	7	3	49	42	17	43	13	3	8	-	1	2	5	1	1	1	4	3	-	1	-	1	-	-	1	-
	B2-32/3/2	9	4	33	54	25	28	13	1	15	-	1	3	5	1	1	1	4	1	2	1	-	-	-	-	-	-
	B2-32/1/2	5	2	34	59	18	30	16	2	18	1	2	3	3	1	-	1	3	2	2	1	-	-	-	-	-	-
	B2-32/1/1	7	3	26	64	10	37	15	-	16	-	1	3	9	-	2	2	3	1	1	-	1	1	-	-	-	-
	B1-5/10/3	7	5	34	54	16	31	9	3	21	3	2	1	5	-	3	1	4	2	1	1	-	-	-	-	-	-
	B1-5/10/1	6	4	45	46	16	30	14	1	24	1	2	2	6	-	2	-	1	2	-	1	1	1	-	-	-	-
	B1-5/8/2	5	3	45	48	24	36	14	1	9	+	1	2	2	-	3	1	2	1	1	1	-	-	-	1	-	-
	B1-5/7/1	6	4	35	55	14	47	13	1	9	1	1	2	4	1	2	1	2	1	1	1	1	-	-	-	-	-
	B1-5/5	14	3	22	61	21	30	10	-	11	-	4	4	8	1	1	3	3	2	2	-	1	-	-	-	-	-
	B1-5/3	15	1	22	62	22	31	7	-	14	-	2	6	1	-	2	1	4	3	1	1	1	-	1	-	-	6
	A-29/1 (terra rossa)	63	1	2	34	23	15	1	-	10	-	1	4	1	4	17	12	3	5	1	1	1	-	-	1	-	-
calcareous segregations	B1-5/6/3/1 (rhyzoconcretion)	6	2	36	56	17	41	13	-	14	-	2	2	3	1	3	-	3	3	-	1	2	-	-	-	-	-
	B1-5/6/1 (sandstone bench)	8	4	60	28	13	35	17	-	19	2	3	1	3	1	3	-	1	-	2	2	1	-	-	-	-	-
	B1-5/4 (septarian nodule)	7	3	25	65	21	33	13	-	16	1	3	1	4	-	2	1	3	1	-	-	1	-	1	-	1	-
RL	R-24-25	14	26	20	41	33	25	4	2	8	-	-	-	4	4	2	4	4	4	-	-	2	-	2	-	-	-

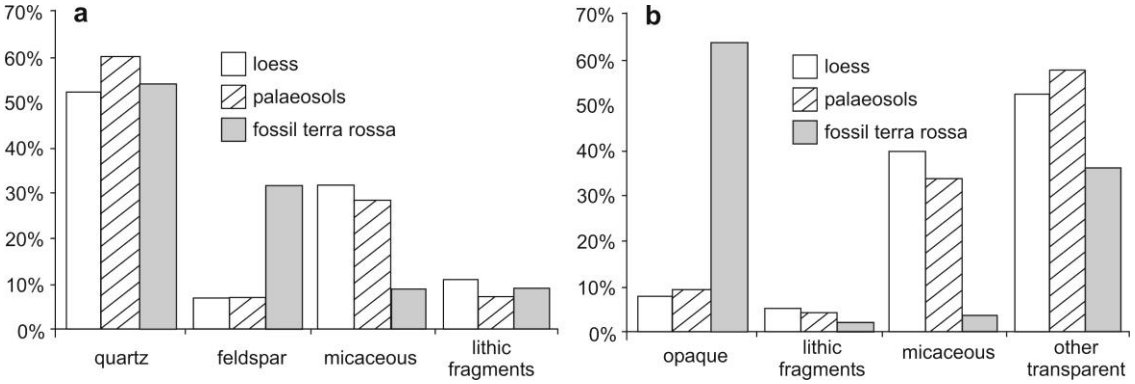

Figure 3.5. Average content of main groups of minerals and other particles in the (a) light and (b) heavy mineral fraction of loess, palaeosol and fossil terra rossa.

Lithic fragments are mostly schist grains built of micaceous minerals and quartz, epidote or zoisite and sericite. Quartzite or microquartzite, chert and pelitic fragments are rare. Opaque grains are magnetite, secondary hematite, and other Fe- and Mn-oxides and hydroxides, limonitized grains and some unknown opaque grains. Micaceous minerals are generally rounded. The most abundant is muscovite (9-42%) often with numerous acicular inclusions. Chlorite (8-21%) is usually green or brown with yellow rims, but blue and bluish-purple variety, possibly Cr-chlorite (Tröger, 1967) is also found. Many flakes show rutile needles, some in the form of sagenite aggregates. Biotite (3-17%) has a light-brown to yellowish-brown colour. Some biotites are very pale or golden yellow, almost isotropic. Greenish patches or hexagonally arranged yellow rutile inclusions are visible on some grains, most likely as a result of chloritisation (Tröger, 1967). Among the other transparent minerals, the most abundant are epidote/zoisite (24-43%). Epidote is short-prismatic, greenish-yellow, whereas zoisite is colourless with a bit more elongated grains having characteristic anomalous blue interference colours. Garnets (13-28%) are mostly colourless and angular or slightly rounded. Idiomorphic or hipidiomorphic grains are rare. Amphiboles (24-38%) are represented by hornblende-type amphiboles (11-18%), tremolite-actinolite (10-18%) and glaucophane-riebeckite (3%). Hornblende-type amphiboles are dark-green, olive-green or bluish-green. Brown hornblende is very rare and is found as irregular, elongated, weathered grains with yellowish-brown to dark brown pleochroic colours. Glaucophane-riebeckite amphibols show typical pleochroic scheme in bluish-purple colours. Pyroxenes (6-11%) consist mostly of clinopyroxene including augite. Hyperstene is rare, with serrated edges and weak pleochroism. Zircon is very rare (1-2%). Idiomorphic to hypidiomorphic grains with sharp, angular edges, as well as some idiomorphic and isometrical well-rounded grains, are found.

Tourmaline (1-3%) is mostly elongated and hypidiomorphic, but terminations on one or both ends can be found. Grains show strong pleochroism ranging in colour from brown to colourless. The greyish-green variety is rare. Rutile (1-4%) is mostly prismatic, yellow, and yellowish to reddish-brown. Dark, almost opaque grains probably have undergone alteration (leucoxinisation). Interference colours are obscured by the strong inherent mineral colour. High relief and extreme birefringence are diagnostic. Titanite and kyanite content is less than 5% each. Staurolite, chloritoid, andalusite, sillimanite and brookite were found only in some samples with less than 2%. Ultrastable minerals (zircon, tourmaline and rutile), whose content is represented by the ZTR index (Hubert, 1962), are present in low percentages (1-8%), and are present throughout the sequence. These mineral characteristics are the same in palaeosols and calcareous segregations.

A comparative study of coarse (50-125 μm) and fine (<50 μm) grain-size fractions of the same sediment was conducted in order to determine interrelation between mineral and granulometric composition (Fig. 3.6.). The coarse fraction contains significantly more micaceous minerals and, due to overall silty composition of the sediment, only slightly more lithic fragments. The fine fraction has significantly higher ZTR index, garnet content and more opaque minerals.

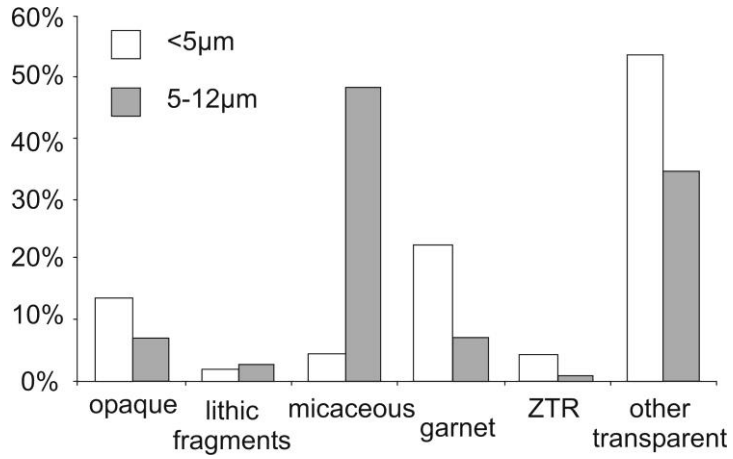

Figure 3.6. Correlation between mineral and granulometric composition in heavy mineral fraction of loess (sample P-19/1).

X-ray diffraction analysis of bulk sample and light mineral fraction revealed quartz, calcite, muscovite, chlorite, albite and amphibole. Other minerals (pyroxene group), which were determined using polarizing light microscope, were not identified with certainty owing to their low amounts.

Low SiO_2 content (47.72-55.14 weight %; Table 3.4.) in loess is typical for silty sediments (Pettijohn, 1957). The overall chemistry puts this sediment in graywacke field with the exception of three coarse-grained (B1-5/9/3, B1-5/11 and P-19/5) that are close to litharenites (Fig. 3.7., Table 3.4.). These sandy members also contain more SiO_2 (up to 62.25 weight %) while fine-grained sediment (B1-5/6/2-clayey silt, Table 3.4.) has more Al_2O_3, Fe_2O_3, MgO, CaO and K_2O. The concentration of REE is also grain-size dependent, being lower in sand than in silt (Table 3.7.).

Results from the dosimetry, the equivalent doses, g values, and the uncorrected and corrected ages of four analyzed samples from Bok-1 section are given in Table 3.5. The calculation of the equivalent doses (D_e), the dose rates and the ages are discussed in detail in Wacha et al. (2011). Uranium, thorium and potassium content range from 2.17 to 3.83 ppm, from 7.63 to 12.80 ppm and from 1.36 to 1.50%, respectively, resulting in a dose rate between 2.58 and 3.70 mGy/a. The mean dose rate is 3.31 ± 0.18 mGy/a and is in agreement with dose rates presented in Wacha et al. (2011). Fading tests were carried out using the approach of Huntley and Lamothe (2001) and Auclair et al. (2003). Fading tests gave small g values ranging from 2.3 ± 0.15 to 2.70 ± 0.20 indicating low fading rates. The De values range from 174.7 ± 4.3 to 241.3 ± 6.7 Gy and show a systematic increase with depth. The D_e value from sample B1-5/9/3, which was collected from a sand layer, has a little higher value. Independent age control has not yet been available. The obtained ages of the sequence under study range from 80.8 ± 5.0 to 90.0 ± 6.8 ka (Table 3.5., Fig. 3.3.).

3.3.3. Palaeosols

On the Island of Susak, the loess is intercalated by numerous palaeosol horizons. They differ significantly in colour from the other units. The most distinctive are red palaeosols (B1-5/3-lower, 7.5YR5/8 and B1-5/5-upper, 10YR5/8) at the bottom of the sequence ranging in thickness from 10 to 120 cm, but on some elevated parts of the limestone coast may be absent. The reddish-brown (10YR5/8) palaeosol (B1-5/7/1, B1-5/7/2) is considered the thickest (up to 200 cm) on the Island and covers a zone of abundant rhizoconcretions. Several younger brown palaeosol horizons (10YR4/6, 10YR3/4, 10YR4/4) with various degree of pedogenesis (B1-5/8/2, B2-32/1/1-2, B2-32/3/2, B1-5/10/1-3, P-19/2, P-19/4, P-19/6), some of them very likely redeposited, range in thickness from 20 to 120 cm are found throughout the overlying sequence.

Table 3.4. Bulk rock analysis of sediments (weight%); LOI – loss on ignition.

	Sample	SiO_2	Al_2O_3	Fe_2O_3	MgO	CaO	Na_2O	K_2O	TiO_2	P_2O_5	MnO	Cr_2O_3	LOI	SUM
loess	P-19/5*	60.78	9.65	3.19	3.66	8.69	1.91	1.53	0.61	0.17	0.07	0.01	9.90	100.17
	P-19/3	52.72	10.29	3.82	5.07	10.97	1.71	1.72	0.69	0.19	0.08	0.01	12.90	100.17
	P-19/1	51.02	10.65	4.10	5.28	11.02	1.64	1.84	0.68	0.19	0.08	0.01	13.80	100.31
	B2-32/2	47.72	10.50	3.61	5.94	11.77	1.76	1.90	0.65	0.18	0.07	0.01	16.20	100.31
	B1-5/11*	62.25	10.46	3.22	3.49	7.67	1.96	1.72	0.54	0.14	0.07	0.01	8.80	100.33
	B1-5/9/3*	62.24	10.57	3.68	3.50	7.35	1.94	1.72	0.66	0.15	0.08	0.01	8.40	100.30
	B1-5/9/1	53.21	11.91	4.44	4.35	9.84	1.84	1.97	0.77	0.20	0.09	0.02	11.70	100.34
	B1-5/8/1	55.14	11.72	4.04	3.96	9.42	2.01	1.95	0.77	0.22	0.08	0.01	9.50	98.82
	B1-5/6/2	52.91	12.07	3.90	4.48	8.33	2.86	2.20	0.65	0.18	0.07	0.01	12.70	100.36
palaeosols	P-19/4	40.13	8.52	3.07	7.87	14.46	1.74	1.52	0.55	0.13	0.06	0.01	22.20	100.26
	P-19/2	51.72	11.38	4.12	4.82	10.50	1.83	1.96	0.70	0.20	0.08	0.02	13.00	100.33
	B2-32/3/2	55.61	14.71	4.64	2.61	5.66	2.51	2.28	0.75	0.20	0.11	0.01	11.30	100.39
	B2-32/1/2	57.35	13.23	4.86	2.57	5.14	2.44	2.36	0.78	0.23	0.09	0.02	11.20	100.27
	B2-32/1/1	62.59	13.70	5.12	3.02	4.11	2.02	2.31	0.82	0.20	0.09	0.02	6.40	100.40
	B1-5/10/3	53.50	12.05	4.33	3.41	10.37	1.70	2.02	0.71	0.17	0.08	0.02	12.00	100.36
	B1-5/10/1	53.10	11.64	4.26	3.99	10.06	1.64	1.98	0.68	0.18	0.08	0.01	12.60	100.22
	B1-5/8/2	58.17	12.50	4.61	2.72	7.64	2.03	2.11	0.79	0.18	0.09	0.01	11.70	102.55
	B1-5/7/2	63.46	13.99	4.88	1.68	3.47	2.17	2.38	0.81	0.08	0.09	0.02	7.40	100.43
	B1-5/5	55.97	14.52	5.38	3.00	4.70	2.81	2.51	0.81	0.10	0.11	0.01	10.40	100.32
	B1-5/3	51.03	13.99	5.28	2.50	7.90	2.45	2.26	0.77	0.09	0.12	0.02	13.90	100.31
	A-29/1 (fossil terra rossa)	16.03	5.19	2.28	0.49	39.76	0.27	0.49	0.33	0.05	0.05	0.02	35.10	100.06
calcareous segregations	B1-5/6/3 rhizoconcretion	24.30	5.13	1.73	2.09	34.17	1.01	0.93	0.30	0.07	0.03	0.01	30.40	100.17
	B1-5/6/1 sandstone bench	24.59	5.36	1.82	3.04	31.92	1.34	1.05	0.34	0.08	0.03	0.01	30.60	100.18
	B1-5/4 septarian	26.98	7.19	2.68	1.55	30.27	1.22	1.20	0.41	0.07	0.05	0.01	28.60	100.23
tephra	P-TF3 (youngest)	51.68	14.64	5.05	3.60	8.96	1.89	1.85	0.77	0.29	0.09	0.01	11.50	100.33
	B2-TF3 (youngest)	46.54	16.19	5.83	3.29	10.06	1.61	1.52	0.76	0.33	0.11	0.01	13.90	100.15
	S-TF2 (middle)	44.21	20.42	5.02	1.59	3.41	1.71	2.12	0.64	0.34	0.12	0.01	20.80	100.39
	B2-TF2 (middle)	44.04	19.13	4.79	1.71	3.91	3.08	1.84	0.64	0.38	0.11	0.01	20.80	100.44
	B3-TF1 (oldest)	46.09	11.76	4.32	4.35	12.03	2.03	1.57	0.62	0.21	0.08	0.01	17.20	100.27

Table 3.5. Results from the dosimetry, the SAR IRSL measurements, g values, the uncorrected and corrected ages. The dose rate is the sum of the dose rates from the alpha, beta, gamma and cosmic radiation. For the calculation of the total dose rate the conversion factors published by Adamiec and Aitken (1998) were used. A systematic error of 2% is included for the gamma spectrometry. An error of 10% is estimated for the cosmic dose.

Sample name	Sample ID	Depth (m)	U (ppm)	Th (ppm)	K (%)	Cosmic dose (mGy/a)	Doserate (mGy/a)	De (Gy)	g-value	Uncorrected age (ka)	Corrected age(ka)
B1-5/11	1741	21.90	2.17 ± 0.01	7.63 ± 0.04	1.36 ± 0.01	0.020 ± 0.003	2.58 ± 0.15	174.71 ± 4.29	2.3 ± 0.2	67.6 ± 4.3	85.7 ± 5.6
B1-5/9/3	1740	23.00	3.48 ± 0.03	12.02 ± 0.06	1.44 ± 0.01	0.019 ± 0.002	3.47 ± 0.19	241.27 ± 6.72	2.5 ± 0.4	69.5 ± 4.3	90.0 ± 6.8
B1-5/9/2	1739	23.50	3.55 ± 0.03	11.92 ± 0.06	1.43 ± 0.01	0.019 ± 0.002	3.47 ± 0.19	220.85 ± 5.85	2.4 ± 0.2	63.6 ± 3.9	81.4 ± 5.1
B1-5/8/1	1738	24.70	3.83 ± 0.02	12.80 ± 0.06	1.50 ± 0.01	0.019 ± 0.002	3.70 ± 0.20	226.29 ± 5.45	2.7 ± 0.2	61.1 ± 3.7	80.8 ± 5.0

The grain-size distribution of palaeosols is similar to that of loess. However, a higher clay content is noticeable in well-developed palaeosols (Fig. 3.4., Table 3.2.; B1-5/3, B1-5/5, B1-5/7/2, and B2-32/1/2). The carbonate content is lower in well-developed palaeosols than in loess, ranging from 6.6 to 14.8 weight %. In weakly humified or redeposited horizons this difference is not so obvious (13.3-20.4 weight %) (Fig. 3.3.). According to chemical composition, the palaeosols are considered geochemically as graywacke (Fig. 3.7.).

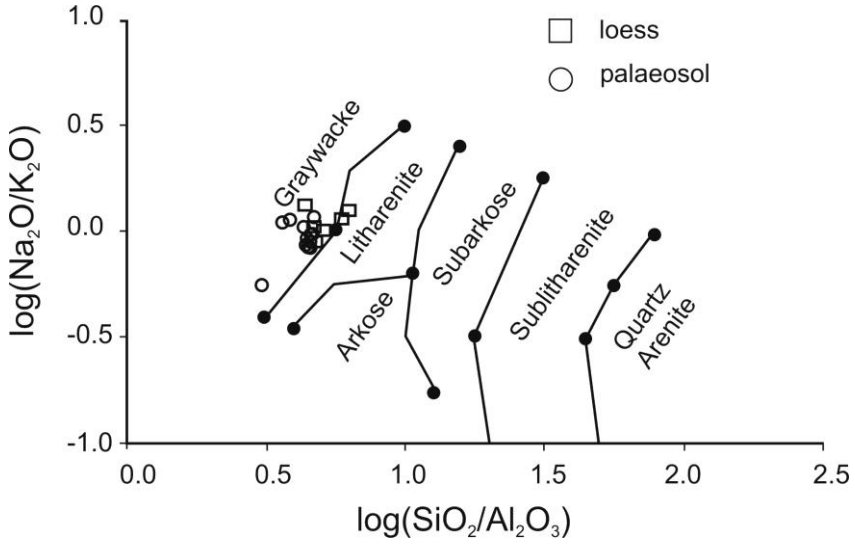

Figure 3.7. SiO_2/Al_2O_3 vs Na_2/K_2O ratios of loess and palaeosol (after Pettijohn et al., 1972, taken from Rollinson, 1993).

Loess and palaeosols do not differ significantly in mineral composition. However, palaeosols generally have more quartz (often with limonite coatings) and less lithic fragments (Fig. 3.5.a and b).

Heavy mineral associations as well as ZTR indices (4%) are practically the same (Table 3.3.). The content of opaque grains is significantly higher in well-developed red palaeosols (Table 3.3.) consisting mostly of pedogenic particles - yellow, brown or almost black concentric globule about 0.1 mm in diameter. Those particles are probably Fe- and Mn-oxides or hydroxides and are responsible for the red colour of this palaeosol.

Compared to loess, SiO_2, Al_2O_3, FeO, K_2O as well as trace element content (especially Ba, Rb, V, Y and Zr) are a bit higher in well-developed palaeosols, while CaO and Sr concentrations are lower (Fig. 3.8., Tables 3.4. and 3.6.).

Palaeosols, similar to loess, show a rather flat European Shale-normalized REE pattern, but with a bit higher concentration of all elements due to REE immobility during the pedogenesis.

A small negative Eu anomaly is present in almost all horizons. Lower REE concentration is observed in redeposited horizon P-19/4 (Table 3.7.).

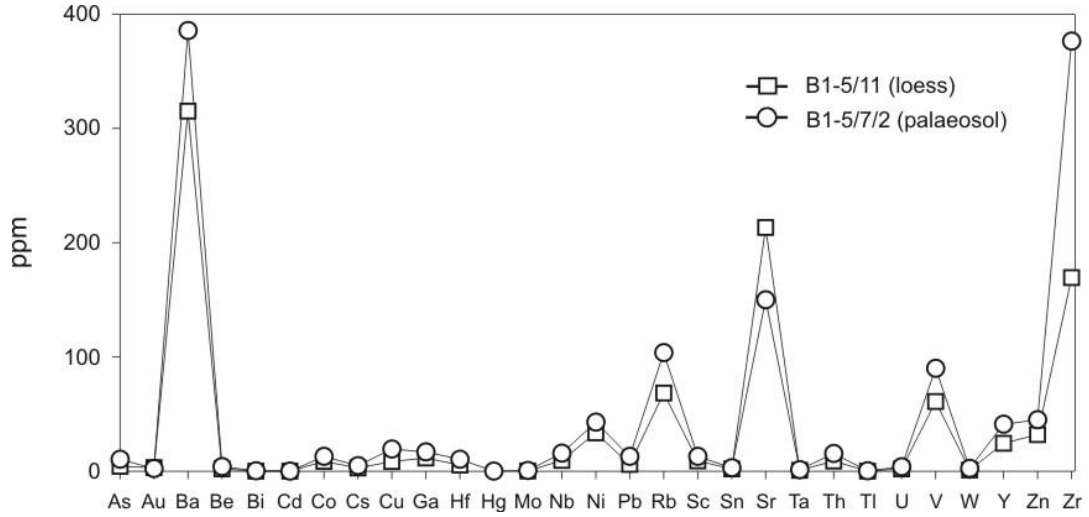

Figure 3.8. Trace element composition of loess and well-developed palaeosol.

The Fe_d/Fe_{tot} ratio, which is taken as an index of weathering (e.g. Boero and Schwertmann, 1987), varies between 0.2 and 0.4 and reflects a certain degree of weathering of Fe-containing primary silicates. This ratio is slightly higher in well-developed palaeosols B1-5/3, B1-5/5 and B1-5/7/1 than in the younger brown palaeosol B1-5/10/1 (Table 3.8.).

XRD powder analysis revealed the same phases as in loess including quartz, calcite, muscovite, chlorite, albite and amphibole. Measured values of Kübler and Árkai indices are characteristic for illite and chlorite originating from terrains affected by very-low grade metamorphism (Fig. 3.9.b). Taking into account the asymmetry and width of chlorite (002) maximum (due to kaolinite having (001) maximum on the same position), ÁI (002) index was not taken into consideration.

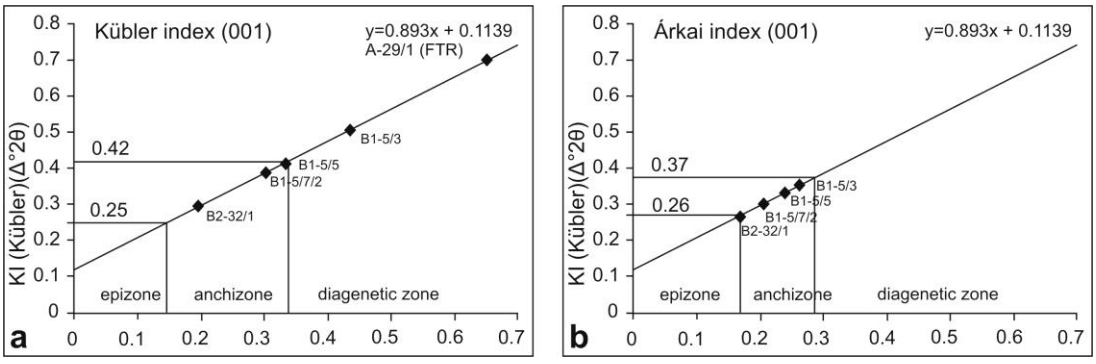

Figure 3.9. Graphical representation of the degree of thermal alteration according to the data of Kübler and Árkai indices for: a – KI (001) and b – ÁI (001). KI and ÁI values are expressed in Δ°2θ (CuKα). Boundaries of the anchizone were taken from Kübler (1968, 1990) for KI and from Árkai et al. (1995) for ÁI; FTR – fossil terra rossa.

Table 3.6. Trace element composition of sediments (in ppm), as measured by ICP-MS**.**

	Sample	As	Au	Ba	Be	Bi	Cd	Co	Cs	Cu	Ga	Hf	Hg	Mo	Nb	Ni	Pb	Rb	Sc	Sn	Sr	Ta	Th	Tl	U	V	W	Y	Zn	Zr
loess	P-19/5	3.2	42.4	248.8	3.0	0.1	0.1	7.2	2.3	6.1	9.8	6.8	<0.01	0.2	9.7	23.0	4.5	56.4	9.0	2.0	201.4	1.0	8.7	0.1	2.6	54.0	1.9	26.1	25.0	248.6
	P-19/3	4.5	6.3	305.0	2.0	0.1	0.1	9.4	3.2	9.6	13.4	8.3	<0.01	0.3	12.1	31.1	5.6	68.3	11.0	3.0	225.0	1.1	11.7	0.1	3.3	71.0	2.0	31.3	35.0	303.2
	P-19/1	5.0	13.0	316.4	2.0	0.1	0.1	10.9	3.8	15.5	13.1	9.9	<0.01	0.3	12.6	39.3	7.3	77.0	11.0	2.0	222.3	1.1	11.1	0.1	3.6	78.0	1.8	34.8	44.0	346.7
	B2-32/2	5.6	1.6	333.6	2.0	0.1	0.1	9.0	3.6	8.8	13.6	8.5	0.0	0.3	12.2	21.6	6.6	78.9	10.0	3.0	194.0	1.1	11.3	0.1	3.4	72.0	1.8	31.2	36.0	300.5
	B1-5/11	4.3	3.1	315.2	2.0	0.1	0.1	8.6	2.9	8.5	11.5	5.4	<0.01	0.2	9.4	33.5	5.9	68.5	9.0	2.0	213.3	0.8	8.9	0.1	2.1	61.0	1.0	24.4	32.0	169.5
	B1-5/9/3	4.3	<0.5	320.6	3.0	0.1	<0.1	10.5	2.9	9.3	12.8	8.8	0.0	0.2	11.3	32.2	5.7	68.8	10.0	2.0	217.3	1.0	11.0	0.1	3.1	67.0	1.8	32.1	31.0	309.8
	B1-5/9/1	6.0	1.6	331.5	3.0	0.2	0.1	11.4	3.7	16.3	13.9	10.4	0.0	0.3	12.4	40.6	7.8	77.0	12.0	3.0	203.2	1.2	14.0	0.1	3.7	83.0	2.2	36.8	42.0	349.7
	B1-5/8/1	6.2	2.2	355.3	1.0	0.2	0.1	10.0	3.7	11.8	15.2	10.0	0.0	0.3	13.5	32.3	7.0	80.0	11.0	3.0	211.2	1.3	14.1	0.1	3.8	75.0	2.2	36.1	37.0	362.1
	B1-5/6/2	6.7	15.9	380.9	2.0	0.2	<0.1	9.8	3.8	14.3	15.8	8.8	0.0	0.3	12.3	32.3	8.4	90.8	10.0	3.0	205.1	1.2	13.4	0.2	3.8	74.0	2.0	34.4	41.0	314.1
paloesols	P-19/4	4.3	82.5	239.5	2.0	0.1	0.1	7.7	3.3	12.3	10.5	7.1	0.0	0.3	9.4	22.0	7.0	59.1	8.0	2.0	175.6	0.8	10.0	0.1	3.1	62.0	1.6	24.2	35.0	254.5
	P-19/2	5.1	34.0	347.8	2.0	0.1	0.1	10.5	3.8	18.1	14.7	9.5	0.0	0.2	12.9	38.4	7.1	79.3	11.0	3.0	230.3	1.2	12.4	0.1	3.7	80.0	2.1	33.5	47.0	325.1
	B2-32/3/2	14.4	6.7	493.8	6.0	0.3	0.2	9.6	8.0	29.9	16.9	11.4	0.0	0.3	27.4	44.7	18.2	101.2	11.0	4.0	208.3	2.2	21.9	0.3	3.8	83.0	2.6	39.6	60.0	384.5
	B2-32/1/2	9.8	14.7	417.1	2.0	0.2	0.1	12.9	4.7	20.6	16.8	9.2	0.0	0.3	14.6	38.8	9.0	100.0	13.0	6.0	209.5	1.2	13.1	0.2	3.7	96.0	4.8	37.4	59.0	336.8
	B2-32/1/1	8.2	13.5	407.6	3.0	0.2	0.1	14.1	5.0	15.6	17.3	10.9	0.0	0.3	14.8	52.2	9.7	97.3	14.0	4.0	171.8	1.3	16.1	0.2	3.8	102.0	2.6	40.0	58.0	387.8
	B1-5/10/3	7.2	4.3	383.8	3.0	0.2	0.1	11.2	4.4	14.8	15.5	8.0	0.0	0.2	13.1	40.3	8.3	87.5	12.0	4.0	185.7	1.2	12.1	0.1	3.3	85.0	2.4	36.8	45.0	300.6
	B1-5/10/1	5.9	2.0	374.4	3.0	0.2	0.1	11.1	4.4	21.2	14.1	8.0	0.0	0.2	12.8	41.9	8.4	86.8	11.0	3.0	191.8	1.2	12.0	0.2	3.2	83.0	2.3	33.7	47.0	284.9
	B1-5/8/2	7.7	5.5	393.9	4.0	0.2	0.1	12.1	4.5	16.2	15.8	10.5	0.0	0.3	14.3	38.5	9.0	88.6	12.0	3.0	186.1	1.3	15.0	0.2	3.8	86.0	2.5	38.6	44.0	353.5
	B1-5/7/2	10.4	2.3	385.6	4.0	0.3	0.1	12.9	4.8	19.4	16.9	10.5	0.0	0.6	15.8	43.0	12.9	103.7	13.0	3.0	150.0	1.4	15.5	0.3	3.9	90.0	2.4	41.1	45.0	376.4
	B1-5/5	10.5	5.5	445.7	3.0	0.4	0.2	15.0	6.6	20.6	18.3	9.0	0.0	0.5	16.9	41.5	16.7	116.8	13.0	3.0	148.7	1.3	16.6	0.4	3.6	101.0	3.2	40.1	59.0	310.1
	B1-5/3	9.6	2.5	442.8	4.0	0.4	0.3	16.0	7.0	19.6	17.6	8.3	0.0	0.5	16.1	42.4	19.6	111.3	13.0	3.0	164.0	1.3	18.1	0.4	3.3	100.0	3.2	37.5	57.0	289.3
	A-29/1 (terra rossa)	4.1	10.8	92.8	1.0	0.2	0.9	8.4	3.8	15.6	6.3	3.1	0.0	0.8	6.7	17.3	9.8	39.1	6.0	<01	55.0	0.5	5.7	0.2	1.4	67.0	1.3	20.1	20.0	135.3
calcareous segregations	B1-5/6/3/1 rhizoconcretion	2.1	5.7	172.8	1.0	0.1	0.1	4.4	1.6	5.8	6.9	3.6	<0.01	0.2	5.0	12.9	3.3	36.6	5.0	1.0	146.1	0.5	6.3	0.1	1.9	32.0	0.7	19.8	13.0	132.5
	B1-5/6/1 sandstone bench	3.4	18.1	178.0	1.0	0.1	0.1	4.5	2.1	8.5	6.6	4.2	0.0	0.2	5.7	12.4	4.3	40.7	5.0	1.0	131.0	0.5	6.7	0.1	1.9	38.0	1.0	17.4	17.0	152.6
	B1-5/4 (septarian)	4.0	3.7	251.4	2.0	0.2	0.3	7.5	3.1	8.9	9.3	4.3	0.1	0.3	7.9	18.1	7.8	56.7	7.0	2.0	135.7	0.7	8.4	0.1	3.5	51.0	1.9	19.9	26.0	150.2
tephra	P-TF3	13.3	8.8	675.3	4.0	0.2	0.1	11.2	3.8	23.1	14.5	10.0	0.0	0.3	18.3	36.3	14.7	76.0	11.0	4.0	413.0	1.6	16.9	0.1	4.0	101.0	2.1	37.8	42.0	341.6
	B2-TF3	17.3	3.6	1216.6	5.0	0.3	0.3	13.3	3.3	30.3	12.8	6.9	0.0	0.4	21.7	35.5	22.1	54.5	9.0	3.0	573.0	1.8	18.9	0.1	3.2	119.0	2.5	34.4	47.0	273.3
	S-TF2	33.6	5.5	574.3	17.0	0.6	0.1	5.5	6.6	39.2	11.9	15.9	0.0	0.3	53.9	61.4	50.0	73.1	6.0	7.0	208.2	6.0	56.0	0.2	5.1	59.0	3.4	43.0	61.0	516.6
	B2-TF2	34.6	4.9	477.5	20.0	0.6	0.1	6.0	7.3	36.6	13.5	14.4	0.0	0.3	50.6	51.5	46.2	79.3	7.0	7.0	250.8	5.4	53.1	0.3	4.6	63.0	4.5	44.0	60.0	501.9
	B3-TF1	9.6	8.5	450.9	5.0	0.4	0.1	12.7	5.7	23.1	12.4	8.8	0.0	0.3	13.2	49.9	22.6	67.4	10.0	3.0	317.0	1.2	21.3	0.2	4.9	88.0	2.9	32.1	41.0	296.8

Table 3.7. Rare earth element (REE) composition of sediments (in ppm), as measured by ICP-MS.

	sample	La	Ce	Pr	Nd	Sm	Eu	Gd	Tb	Dy	Ho	Er	Tm	Yb	Lu
loess	P-19/5	30.30	60.90	7.38	26.30	5.60	1.17	4.78	0.78	4.65	0.93	2.60	0.45	2.56	0.50
	P-19/3	39.60	79.50	9.35	35.80	7.40	1.32	6.03	0.93	5.63	1.02	3.24	0.47	2.94	0.43
	P-19/1	41.70	82.50	10.03	37.40	7.70	1.32	6.29	1.05	6.50	1.31	3.59	0.59	3.28	0.52
	B2-32/2	37.50	74.20	8.87	32.60	7.30	1.32	6.09	1.00	5.41	1.04	2.92	0.50	2.86	0.46
	B1-5/11	29.70	60.10	7.11	27.20	5.40	1.04	4.61	0.78	4.36	0.88	2.48	0.38	2.46	0.38
	B1-5/9/3	36.50	72.00	8.66	33.80	6.70	1.35	5.61	0.95	5.62	1.01	3.15	0.50	3.12	0.49
	B1-5/9/1	42.80	88.10	10.52	41.30	8.00	1.50	6.68	1.22	6.78	1.24	3.63	0.66	3.29	0.57
	B1-5/8/1	44.00	88.50	10.45	39.30	7.60	1.55	6.34	1.22	6.35	1.18	3.56	0.57	3.59	0.53
	B1-5/6/2	42.60	87.80	10.60	38.90	7.70	1.50	6.21	1.05	6.40	1.22	3.49	0.56	3.27	0.50
palaeosols	P-19/4	30.30	61.50	7.17	27.20	5.80	1.16	4.45	0.77	4.42	0.82	2.38	0.34	2.39	0.37
	P-19/2	39.10	81.50	9.68	35.60	7.10	1.42	6.09	1.13	5.79	1.29	3.43	0.55	2.99	0.50
	B2-32/3/2	60.50	128.90	13.50	49.30	9.70	1.53	7.85	1.36	7.44	1.37	4.08	0.59	4.03	0.58
	B2-32/1/2	43.60	88.80	10.62	39.10	8.10	1.50	7.12	1.14	6.30	1.23	3.79	0.60	3.40	0.53
	B2-32/1/1	47.70	95.90	11.06	41.90	8.60	1.60	7.45	1.22	7.21	1.38	3.96	0.63	3.78	0.62
	B1-5/10/3	41.20	83.30	9.87	38.60	7.70	1.45	6.34	1.10	6.10	1.18	3.54	0.60	3.63	0.50
	B1-5/10/1	39.20	78.40	9.03	37.60	7.50	1.33	5.64	0.98	5.65	1.12	3.39	0.58	3.19	0.50
	B1-5/8/2	47.20	94.40	11.46	41.40	8.60	1.54	6.85	1.16	6.90	1.32	3.66	0.60	3.75	0.57
	B1-5/7/2	51.70	106.00	12.43	47.60	9.20	1.66	7.18	1.36	7.23	1.44	3.96	0.70	4.22	0.60
	B1-5/5	50.00	107.30	12.15	43.60	9.10	1.73	6.75	1.23	6.57	1.33	3.83	0.62	3.86	0.55
	B1-5/3	49.40	109.70	11.57	43.20	8.30	1.77	6.81	1.16	6.53	1.21	3.58	0.61	3.33	0.55
	A-29/1 (fossil terra rossa)	24.30	38.30	5.40	21.40	4.20	0.84	3.38	0.55	2.99	0.51	1.62	0.26	1.75	0.24
calcareous segregations	B1-5/6/3/1 rhzoconcretion	18.60	36.00	4.57	17.00	3.50	0.56	2.74	0.49	2.88	0.46	1.64	0.26	1.66	0.23
	B1-5/6/1 sandstone bench	20.50	40.40	4.56	17.70	3.20	0.68	3.22	0.53	2.92	0.47	1.87	0.28	1.60	0.33
	B1-5/4 septarian nodule	26.60	52.80	6.23	23.30	4.40	0.87	3.37	0.60	3.50	0.55	1.90	0.40	2.00	0.29
tephra	P-TF3	51.80	102.30	12.21	46.10	9.00	1.80	7.66	1.23	6.95	1.31	3.80	0.60	3.57	0.67
	B2-TF3	53.00	107.20	12.07	45.70	9.10	1.95	7.23	1.09	6.14	1.07	3.30	0.52	3.29	0.47
	S-TF2	89.20	191.20	19.60	69.90	13.00	1.64	9.89	1.63	8.99	1.63	4.69	0.71	4.49	0.81
	B2-TF2	80.60	180.90	18.11	63.40	12.30	1.54	9.98	1.59	8.78	1.66	4.51	0.74	5.07	0.77
	B3-TF1	55.70	116.80	12.58	47.50	8.90	1.67	7.01	1.07	5.55	1.09	3.14	0.44	2.99	0.49

Table 3.8. Total (tot) and dithionite extractable (d) iron in palaeosols; FTR-fossil terra rossa.

sample	Fe_{tot} (%)	Fe_d (%)	Mn_d (ppm)	Fe_d / Fe_{tot}
B1-5/10/1	3.45	0.60	187	0.17
B1-5/7/2	3.67	1.32	343	0.36
B1-5/5	4.18	1.16	429	0.28
B1-5/3	4.27	1.48	487	0.35
A-29/1 (FTR)	2.45	1.39	355	0.57

Fossil terra rossa (FTR) (A-29/1; Figs. 3.2. and 3.3.) can be found in limestone cracks as a red coloured palaeosol (2.5YR4/6) interlocked with calcite veins. In contrast to the younger palaeosols, the FTR is lithified, owing to high $CaCO_3$ content (70.2 weight %).

Compared to loess and other palaeosols, the heavy mineral spectrum of FTR shows significantly more authigenic opaque minerals, mainly Fe-oxides and -hydroxides (hematite and goethite) including up to 20% of magnetite (Fig. 3.5.b, Table 3.3.). Lithic fragments and micaceous minerals occur in negligible amounts. Other transparent heavy minerals in general are not as numerous as they are in loess and younger palaeosols which is especially visible in lower epidote/zoisite and actinolite-tremolite content (Table 3.3.). Another major difference is in significantly higher content of ultrastable minerals (ZTR = 31%) in FTR. The weathering index (Fe_d/Fe_{tot}) is 0.6 and reflects a quite high degree of weathering of Fe-containing primary silicates (Table 3.8.).

The XRD powder analysis of the <2 μm fraction revealed kaolinite and illite, the later showing the highest KI index of all palaeosols (0.652 $\Delta°2\theta$) (Fig. 3.9.a) which is characteristic for diagenetic illite.

3.3.4. Calcareous segregations

Calcareous segregations are very abundant in loess. The lowest horizon of concretions (B1-5/4) is situated in red palaeosols, mostly but not exclusively, in a horizontal layer separating the lower red palaeosol (B1-5/3) from the upper red palaeosol (B1-5/5) (Fig. 3.3.). They are irregularly-shaped or rounded, concentric, often showing star-like cracks, therefore termed septaria or septarian nodules (Pettijohn, 1957).

Directly on top of the upper red palaeosol another calcareous horizon can be observed (Fig. 3.3.). This lithified sandy loess (or sandstone bench sensu Bognar et al. (2003)) is a discontinuous layer (B1-5/6/1), ranging from 20 to 70 cm in thickness, formed by the precipitation of $CaCO_3$ in oversaturated water migrating from upper parts of the section. The overlying loess unit contains vertical to subvertical rhizoconcretions of different sizes up to 50 cm in length that sometimes may coalesce into somewhat continuous layers.

The carbonate content ranges from 57.5 to 65.1 weight %. All three types of segregations have similar mineral composition as the surrounding sediment (Table 3.3.). REE patterns of all three types are also similar and show lower concentrations compared to European Shale (ES) due to high $CaCO_3$ content (Table 3.7.). Siliciclastic constituents are quartz, micaceous

minerals, lithic fragments and feldspars. Quartz is angular, much like in loess. Carbonate particles are present as detritic grains and microsparitic to sparitic cement. Rare tiny calcite grains surrounding carbonate particles look like border cement of first generation, while larger ferrous calcite crystals might be cement of a second generation formed in reductive microenvironment.

Septarian nodules have micritic to microsparitic calcite matrix, smudged with clay and ferrous minerals. After staining, larger grains were identified as ferrous calcite.

3.3.5. Tephra

Three tephra layers (Figs. 3.2. and 3.3.) macroscopically differ from each other as well as from surrounding sediment. The stratigraphically oldest tephra (B3-TF1), intercalated in loess unit B1-5/6/2, has a pale orange colour and ranges from 2 to 4 cm in thickness showing diffuse transition to the sediment. The middle tephra (Fig. 3.2. - S-TF2, M-TF2, B4-TF2; Fig. 3.3. - B1-TF2, B2-TF2, P-TF2) intercalated in a brown palaeosol is yellow to orange and has a patchy distribution. The stratigraphically youngest tephra (Fig. 3.2. - S-TF3, K-TF3; Fig. 3.3. - B2-TF3, P-TF3) has a distinct greyish colour and is 2-3 cm thick. This tephra is more compact than the other tephras and has a sharp but sometimes irregular transition to the surrounding loess most likely due to bioturbation.

Particle size analysis showed similarity with loess. Silt is the dominant grain-size fraction (sandy-clayey and sandy silt) (Fig. 3.4., Table 3.2.).

The carbonate content of youngest tephra ranges from 18.9 to 22.6% and in the middle tephra from 16.1 to 22.0%. The highest carbonate content found in the oldest tephra (28.3%) is probably related to higher carbonate content of the surrounding sediment (Fig. 3.3.).

Light mineral fraction (Fig. 3.10.a) is composed mainly of quartz (31-50%), vitroclasts (11-45%), while the presence of lithic fragments is lower than in loess (1-4%). Vitroclasts reach up to 45% in the light mineral fraction of the middle tephra. Vitroclasts appear also in heavy mineral fraction and are the most abundant in the youngest tephra (Fig. 3.10.b). Vitroclasts from all three tephras are often weathered and mostly coated with secondary alteration products. They are yellowish to brownish-grey in colour, irregularly-shaped but mostly elongated and more or less tubular. Tubular shape and vesicular textures are more pronounced in vitroclasts of the middle tephra (Fig. 3.11.). During grain-mount preparation, for some

reason, the reaction with Canada balsam caused change in colour from yellowish-brown to reddish-violet in vitroclasts from the middle tephra.

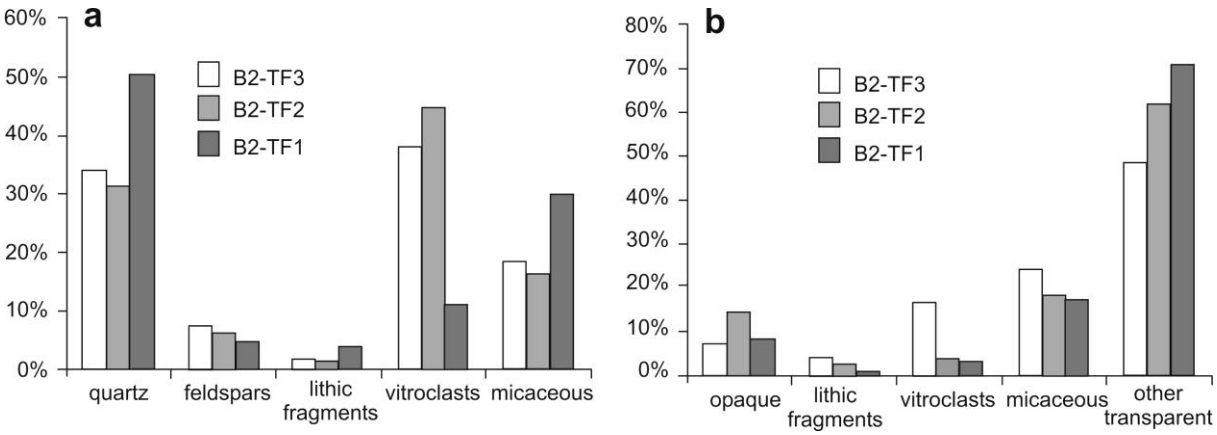

Figure 3.10. Average content of main groups of minerals and other particles in the (a) light and (b) heavy mineral fraction in tephra (B3-TF1-oldest, B2-TF2-middle, B2-TF3-youngest).

The heavy mineral association shows similarity with loess but with significantly higher pyroxene content (Table 3.3.). Higher content of serrated clinopyroxene grains is particularly emphasised in the oldest tephra (B3-TF1). Idiomorphic, green augite crystals are typical for the middle (B2-TF2) and the youngest tephra (B2-TF3). Phase composition of all three tephras is similar to loess showing quartz, calcite, muscovite, chlorite, albite, pyroxenes and amphiboles as detected phases.

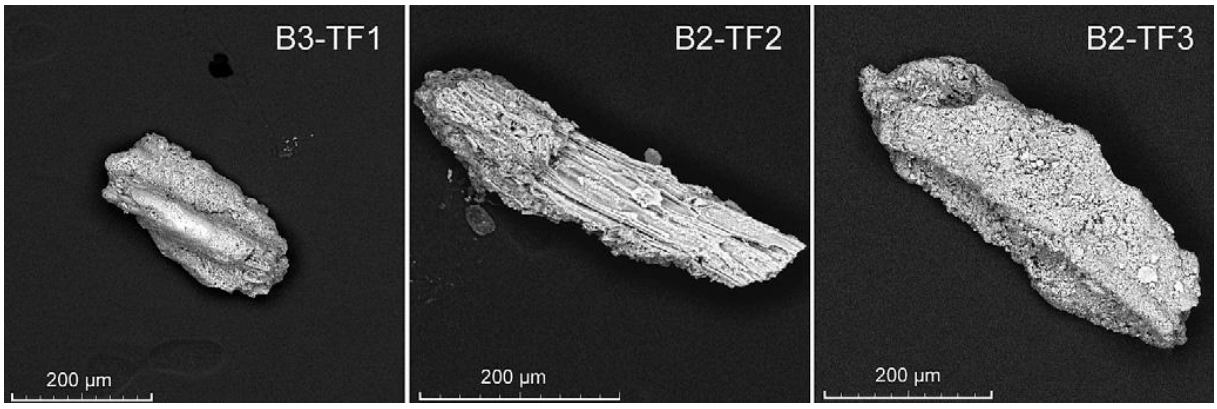

Figure 3.11. BSE images of vitroclasts from tephra (B3-TF1-oldest, B"-TF2-middle, B2-TF3-youngest).

Major and trace element concentrations including REE are shown in Tables 3.4., 3.6. and 3.7. SiO_2 content in the oldest (B3-TF1) and the middle tephra (B2-TF3) is 46.09% and 46.54%, respectively. A value of 51.68% SiO_2 for the P-TF3 is probably a result of stronger mixing with loess, therefore this sample is not included in the classifications. The middle tephra

contains lower SiO_2 (44.04-44.21%) but higher Al_2O_3 content (19.30-20.42%) than the other two tephras.

The lateral continuity of the middle and the youngest tephra horizons allows their correlation on distant localities on the island. All tephras have similar chemical properties. Based on SiO_2 content they are neutral with low alkali content (Na and K). However, the middle tephra contains less SiO_2, MgO and CaO, and more Al_2O_3, Na_2O and K_2O than the oldest (TF1) and the youngest (TF3) tephra (Table 3.4.). Trace element concentrations in the oldest and the youngest tephra are also similar, whereas the middle tephra shows higher trace element concentrations with the exception of Ba, Co, Sr and V (Table 3.6., Fig. 3.12.). The primordial mantle-normalized trace element diagram is characterized by positive anomalies for Cs and Th and negative anomalies for Ba, Sr and Ti (Fig. 3.13.). All three tephras show fractionated REE pattern (LREE concentrations being higher) and negative Eu anomaly (Fig. 3.14.).

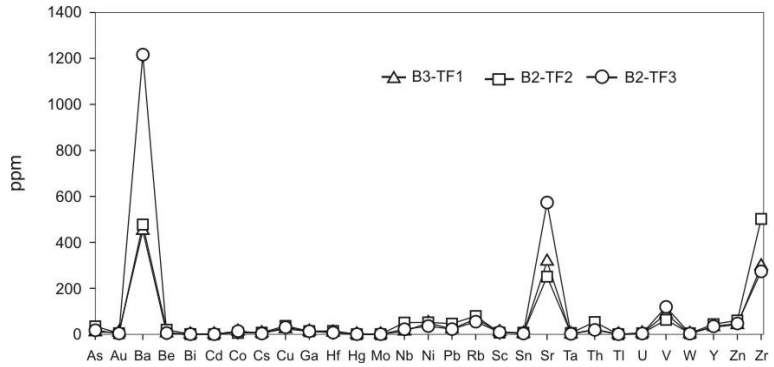

Figure 3.12. Trace element composition of tephra (B3-TF1-oldest, B2-TF2-middle, B2-TF3-youngest).

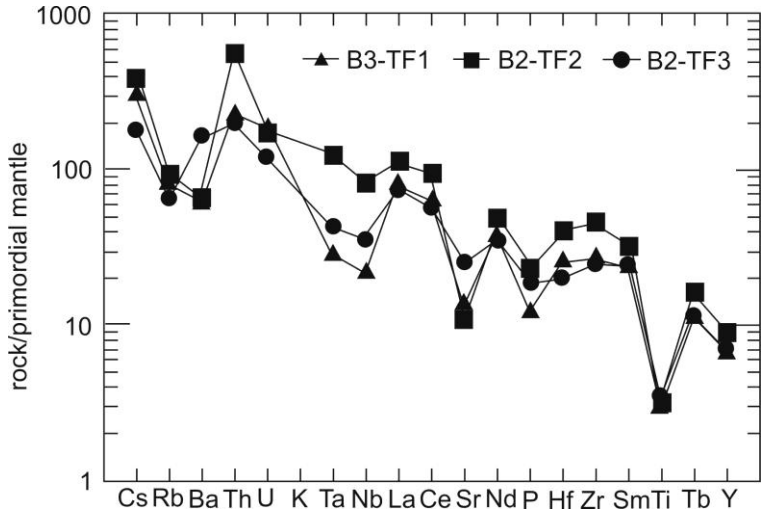

Figure 3.13. Primordial mantle-normalized trace element composition of tephra (Wood, 1979) (B3-TF1 - oldest, B2 - TF2 - middle, B2-TF3- youngest).

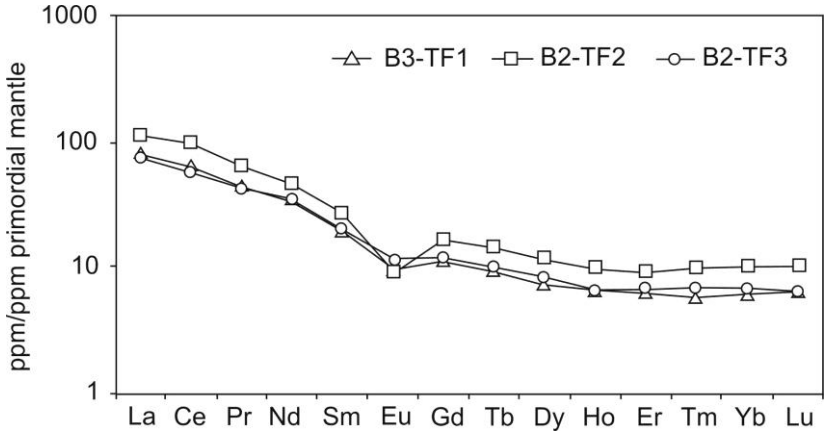

Figure 3.14. Primordial mantle-normalized REE patterns for tephra (McDonough et al., 1992) (B3-TF1 - oldest, B2-TF2 - middle, B2-TF3 - youngest).

3.4. Discussion

The majority of the sediments from Susak have a maximum in the silt-size fraction. Nevertheless, sandy sediments, sometimes cross-bedded, can also be found. Susak aeolian deposits are mainly poorly sorted which is in accordance with description of unweathered loess by Folk and Ward (1957). Poor to very poor sorting of fine sediments is most probably the result of granulometric composition, namely, when the mean grain-size decreases the transporting fluid is better able to transport particles of all sizes (Folk and Ward, 1957). Furthermore, the tendency of poor sorting can be stimulated by particle mixing due to turbulence during aeolian transport (Nickling, 1983). In addition, after the coarser material has settled out, the sorting of dust grains is enhanced only after further transport downwind (Clemens, 1998). Very positive skewness of Susak sediments reflects higher content of coarser material, which implies close vicinity of the source area. Therefore, short-distance transport of fluvial and aeolian accumulations from the Po river plain to Susak resulted in poor sorting.

The mineral composition is similar throughout the whole loess sequence. Some differences have been observed in sediments owing to different grain-size and different lithologies such as palaeosols and tephras.

The large number of opaque grains in the fine-grained fraction (<5 μm) is a consequence of Fe- and Mn-oxide and –hydroxide formation which is a result of weathering primary Fe-containing silicates and associated grain-size degradation.

In the Susak sediments, the heavy mineral association, along with lithic fragments (although present in low percentages) is very suitable for provenance studies. Lithic fragments include schists, chert, quartzite, pelite rocks, micritic and microsparitic limestone. Heavy minerals studied derive (Pettijohn et al., 1972) from the same metamorphic rocks: green and blue schists (epidote/zoisite, amphiboles, brown tourmaline, glaucophane and chloritoid); highgrade metamorphic rocks (garnet, amphiboles, kyanite, andalusite and staurolite). In addition, heavy minerals from igneous rocks (hornblende-type amphiboles, augite, hypersthene, titanite, zircon) were also recognized. Brown hornblende (oxyhornblende) could originate from high-grade metamorphic rocks or could be of volcanic origin (Tröger, 1967; Mange and Maurer, 1992). This kind of association fits the petrographic province of the

Alpine region, which is in accordance with most previous research (Salmojraghi, 1907; Mutić, 1967; Bognar et al., 1983).

Heavy minerals of Italian loess consist mostly of minerals from metamorphic parageneses (amphibole, epidote, disthene, garnet) and this association is characteristic of the fluvial and fluvioglacial Late Pleistocene deposits of the Po plain which represented the source of the aeolian dust (Cremaschi, 1990a). Comparison of the Monte Conero plateau and Susak island deposits, located on the opposite sides of the Adriatic Sea, but derived from that same deflation area, showed that they have the same heavy mineral composition (Cremaschi, 1990a).

According to Ferraro's (2009) studies of Val Sorda loess sequence in Northern Italy, ultradense fraction of heavy minerals (garnet, anatase, brookite, rutile, barite, chrome spinel, zircon, xenotime, monazite and opaques) represents a wind proxy, fitting with the identified coarser grain-size zones, higher percentages indicating higher wind intensities. Val Sorda, being a proximal loess, is relatively coarse-grained and rich in ultradense minerals. Susak loess, being more distal, shows an increase of ultradense minerals, especially garnets, only in the coarse-grained cross-laminated layer (P-19/5, Table 3.3.), thus directly indicating higher wind intensities during accumulation of this unit.

Grouping the transparent heavy minerals after Garzanti and Andò (2007) showed certain analogy with Alpine collision orogen sources and River Po sediments, the minor deviation is very likely a consequence of mixing with material from other sediment sources, like the northern Apennines, during fluvio-aeolian transport (Fig. 3.15.).

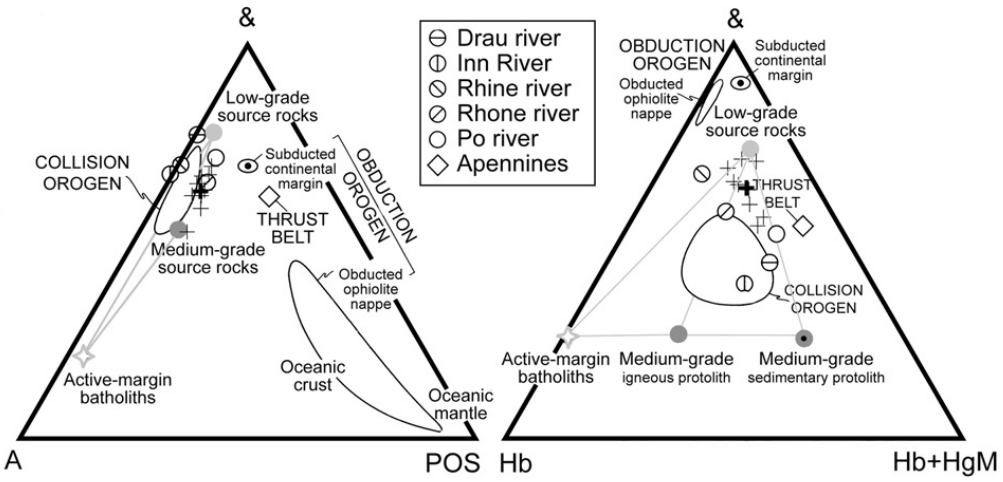

Figure 3.15. Orogenic provenance and heavy mineral suites of loess (bolded cross = average value); &-all transparent heavy minerals not included in the other two poles; A – total amphiboles; POS - pyroxenes, olivine and spinel; Hb - hornblende; HgM - high-grade metasedimentary minerals (staurolite, andalusite, kyanite, sillimanite) (modified after Garzanti and Andò, 2007).

Cremaschi (1990a, b) correlated the lower part of the Susak loess deposits to the late Middle and Upper Pleistocene accumulation phases. Marković-Marjanović (1966, 1976) and Wein (1977) mentioned Würm glacial as the main period of loess deposition. Based on malacological investigations, Štamol and Poje (1998) presumed a Dryas age for the upper part of the investigated loess sequence. The chronostratigraphical correlation and interpretation of the palaeosols from Susak with those of the Hungarian record, as suggested by Bognar et al. (2003), are not valid following the studies of Wintle and Packman (1988), Frechen et al. (1997) and Novothny et al. (2002, 2009). Wacha et al. (2011) set up a more reliable chronological framework according to IRSL dating of the loess sequence (8-26 m asl) resulting in detailed record correlating to MIS 3 (Fig. 3.3.). The loess-palaeosol sequence between B2-32/2 brown palaeosol (Bok-2 section) and B1-5/11 sandy layer (Bok-1 section) was not dated, but could possibly be a part of MIS 4 record. Underlying sequence belongs to the period between 80.8 ± 5.0 and 90.0 ± 6.8 ka and can be correlated with middle or late MIS 5 with a few shorter interstadials indicated by brown palaeosols (B1-5/8/2 and B1-5/10/1-3). Considering the thickness and high degree of pedogenesis, the underlying well-developed reddish-brown palaeosol (B1-5/7/1, B1-5/7/2) could be of Riss/Würm interglacial and its parent material along with underlying loess, therefore related to aeolian accumulation phase during the Middle Pleistocene (MIS 6 record or older). Such interpretation supports conclusion of previous studies made by Cremaschi (1990a, b) who suggested that most of the Susak loess deposits accumulated during the Last Glacial period whereas only lower unit of the Susak sedimentary sequence is related to the aeolian sedimentation of the late Middle Pleistocene and to the Last Interglacial weathering. As there is a significant part of loess overlying the studied sequences (26-90 m asl), the younger loess could belong to the MIS 2 record, which supports suggestions made by Cremaschi (1990b) and conclusions of Štamol and Poje (1998) about the presence of Dryas in the upper part of Susak loess deposits.

Chemical weathering of loess occurred during interglacials and interstadials resulting in soil formation. Palaeosols from Susak contain more fine-grained particles than loess and are almost all very poorly sorted. The influence of pedogenesis is evident in the reduction of lithic fragments and formation of authigenic particles, Fe-oxides and -hydroxides resulting in a higher content of opaque grains, especially in the fine-grain fraction (<5 μm). The coefficient of weathering (Na_2O/K_2O) distinguishes strongly evolved palaeosols from loess only in the upper part of the succession; in the lower parts the sodium content is higher, most probably owing to an influence of sea-water. The [$(CaO + Na_2O + MgO + K_2O)/Al_2O_3$] ratio, taken as an estimation of the loss of bases, correlates with the duration of pedogenesis and internal

drainage of palaeosols and is most evident in the red (B1-5/5-upper) and reddish-brown (B1-5/7/2) palaeosols. Palaeosols also show a higher Ba/Sr ratio (taken as intensity of leaching and weathering) due to larger susceptibility of Sr to weathering and Ba being stronger retained to clay.

The oldest red palaeosols at the base of the loess sequence, in contrast to FTR, is not lithified. The red colour derives from amorphous Fe-oxides and -hydroxides. Bognar (1997) suggested that this palaeosol is a forest-type soil and was partly formed during karstification of underlying limestone under warm and humid climate predating the Pleistocene. However, this study showed that the heavy mineral association is similar to that in the loess, and REE concentrations are similar to those in other younger palaeosols. This indicates prevailing origin from loess, although a minor influence of material remained after limestone karstification is possible, thus making it similar to Istrian terra rossa (Durn et al., 1999, 2001, 2007; Durn, 2003). A systematic pedological investigation characterising the type of palaeosols is still missing.

The heavy mineral association of FTR is significantly different from those of the stratigraphically younger palaeosols and loess (Table 3.3.). Therefore, the insoluble residues of Cretaceous limestone containing the same minerals could represent the source material for FTR. The same heavy mineral association was determined in limestones of the Croatian karst area by Tućan (1911), and almost the same results with somehow different interpretation of genesis were obtained by a re-investigation of this material (Crnjaković, 1994). Negligible amounts of micaceous minerals in FTR indirectly imply a genetic connection to limestone rather than to loess and palaeosols. The difference is especially evident in the ZTR index of FTR, a magnitude higher than in loess and palaeosols. Nevertheless, based on minerals found in both FTR and loess, in spite of the significantly smaller amounts in FTR, a possible additional aeolian contribution should be mentioned. Mineral maturity of FTR is a consequence of stable mineral association inherited from older sediment (Cretaceous limestone) on one hand, and of long-term and intense diagenesis on the other. Hematite, responsible for the prevailing red colour, along with magnetite and goethite, as the major opaque minerals, was formed during interglacial periods and is the dominant pedogenetic mineral phase. Relatively high Fe_d/Fe_{tot} ratio (0.6) taken as a weathering index (Table 3.8.) reflects a quite high degree of weathering of Fe-containing primary silicates and is similar to Istrian terra rossa, which gave 0.7 (Durn et al., 2001; Durn, 2003). The FTR formation at Susak indicates a Mediterranean climate with strong internal drainage due to high porosity of

the underlying limestone, as well as neutral pH conditions (Boero and Schwertmann, 1989). REE concentrations are usually higher in palaeosols, whereas in FTR, these values are lower due to significant $CaCO_3$ content. FTR contains kaolinite and illite with the highest measured KI (0.652 Δ°2θ) (Fig. 3.9.a). This KI value indicates diagenetic origin of illite in contrast to illite and chlorite from the younger palaeosols which have KI and ÁI values characteristic for anchizone, and therefore they are not authigenic but detrital (originating from loess or better to say from loess source area) (Fig. 3.9.b). However, kaolinite in all palaeosols is most likely of diagenetic origin.

On the Island of Susak three types of calcareous segregations can be recognized. Although similar in heavy mineral composition, septarian nodules (septaria) show a lesser amount of opaque grains than the surrounding sediment. Since most of the Fe-oxides and -hydroxides (as opaque grains) in palaeosols are of pedogenetic origin, lower amount of those hydroxides in septarian concretions indicates that they were formed in the early stage of pedogenesis. Ferrous calcite in the matrix is an indicator for crystallization in reductive surrounding. Higher Al_2O_3 content could be related to the presence of aluminous gel involved in the formation of septaria (Pettijohn, 1957; Ruchin, 1958). Bognar and Zámbó (1992) explained their genesis through the upward capillary movement of $CaHCO_3$-rich water from the underlying limestone and precipitation of $CaCO_3$ on the horizontal contact with the upper, impermeable part of the red palaeosol. However, due to the lower carbonate content in the upper part of the red palaeosol, dissolution of carbonate from the upper part and its precipitation on the contact with the lower more clayey part of the red palaeosol are also likely.

Calcareous rhizoconcretions and sandstone benches occur in the overlying loess unit. Calcium carbonate was leached out from the overlying reddish-brown palaeosol and precipitated in the underlying horizon during the soil forming process. These two types of concretions were formed most likely by downward percolation of water rich in Ca-hydrogen carbonate from the upper parts of the sediment succession, and by precipitation on the border with lower, less permeable red palaeosol horizon, or around the roots of plants. Considering their redundancy and dimensions, it can be concluded that during pedogenesis of the overlying reddish-brown palaeosol, the climate of the interglacial was characterized by oscillations of humid and dry periods.

On the Island of Susak the aeolian deposits have been affected by pyroclastic input derived from Pleistocene volcanic activity. Tephra horizons provide excellent isochronous markers to

correlate between marine and terrestrial records. Considering the stratigraphy in loess sequence and IRSL dating of overlying loess, the oldest tephra below reddish-brown palaeosol (older than 90.0 ± 6.8 ka) is most likely much older than the Last Interglacial. The loess sandwiching the middle tephra (TF2) gave IRSL ages between 47.5 ± 3.2 and 50.3 ± 3.5 ka. The IRSL age of the youngest tephra (B2-TF3) on Sand Pit-east wall section is between 34.1 ± 1.9 and 35.1 ± 1.9 ka old and in Bok-2 section between 37.8 ± 2.0 and 36.3 ± 1.9 ka old (Wacha et al., 2011) which is in good correlation. The mineral and chemical composition of the oldest and youngest tephra are modified due to contamination with loess material or, in the case of the middle tephra, due to mixing with palaeosol material. Although chemical characterization and precise determination of the volcanic provenance are still under discussion, the tephras from Susak can be correlated macroscopically, chemically and chronologically.

The influence of pedogenesis on the primary chemical composition is shown for the middle tephra, for which it is more evident than for the oldest and youngest tephras. Based on SiO_2/K_2O ratio these tephras belong to high-K calc-alkaline series (Fig. 3.16.). Based on total alkali vs silica (TAS) diagram, TF1 and TF3 belong to basaltic andesite whereas TF2 is of basaltic andesite to basaltic trachyandesite composition and considering SiO_2 content all three are neutral (Fig. 3.17.). Immobile element ratios, Zr/TiO_2 and Nb/Y, correspond to trachyandesitic composition for TF2, whereas TF1 and TF3 are of rhyodacite and dacite composition (Fig. 3.18.).

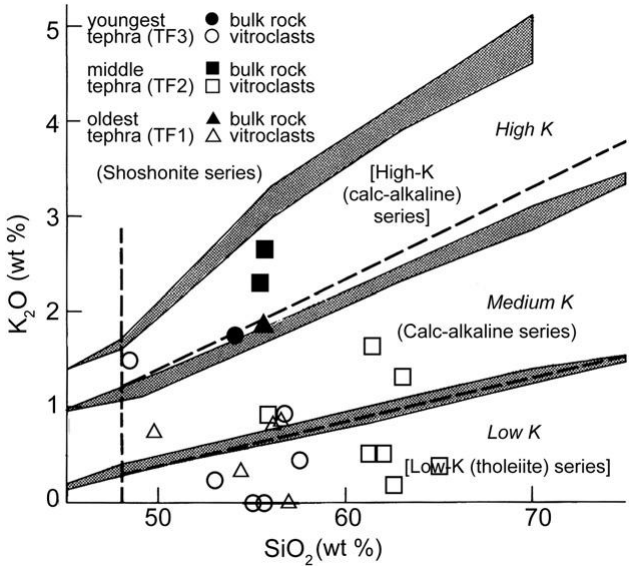

Figure 3.16. SiO_2 vs K_2O (weight %) diagram for tephra (bulk rock) and vitroclasts (Le Maitre, 1989).

Chemical composition of the vitroclasts differs from the bulk rock chemistry of tephra mostly by lower alkali content (Na and K). The differences could be a consequence of vitroclast weathering and difficulties in the analysis of very porous particles having uneven surfaces (hardly detectable light elements, especially Na). Vitroclasts from the middle tephra are of basaltic andesite, andesite and dacite composition, whereas TF1 and TF3 correspond to basaltic andesite and basalt (Fig. 3.17.). The difference of middle tephra is also visible in the subalkali series diagram (Fig. 3.16.). The similarity of the oldest and the youngest tephra vitroclasts points to the same type of volcanism. The elongated and tubular vitroclasts of the middle tephra could be indicative for a strong eruption of Plinian-type.

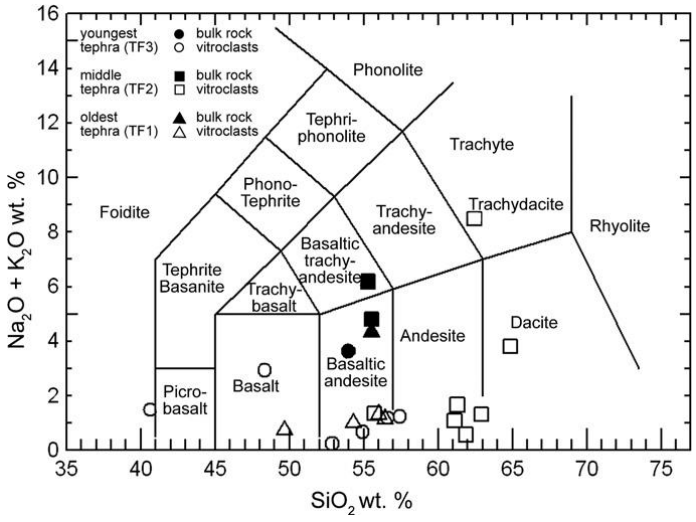

Figure 3.17. Total alkali vs silica (TAS) diagram for tephra (bulk rock) and vitroclasts (Le Maitre, 1989).

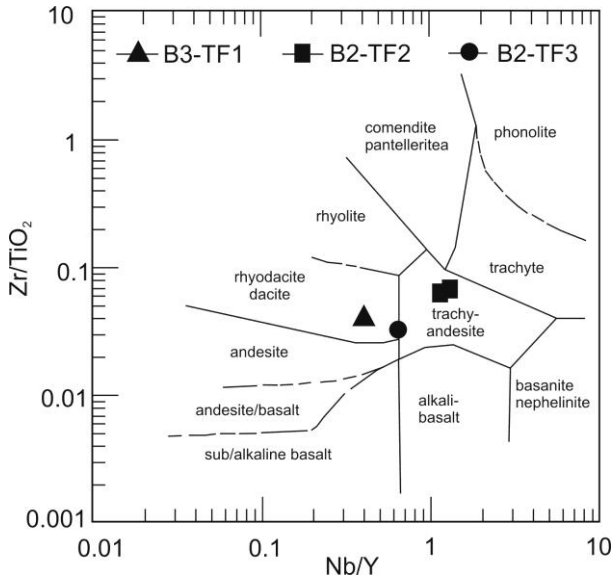

Figure 3.18. Bulk rock trace element plot for tephras (Winchester and Floyd, 1977) (B3-TF1 - oldest, B2-TF2 - middle, B2-TF3 - youngest).

In spite of the similarity in mineral composition of tephra and loess, a significantly higher content of pyroxene in all three tephras (especially in the oldest) was found. Particularly indicative are idiomorphic augite crystals in middle and youngest tephras. Serration of clinopyroxenes in the oldest tephra could be a result of diagenetic processes in the lower (the oldest) unit of the loess sequence. The appearance of large hypidiomorphic augite grains in beach sands on the southern side of the Island of Hvar (Central Dalmatian archipelago) is considered a direct contribution of Middle and South Italian volcanic provinces (Lužar-Oberiter et al., 2007, 2008). Serrated augite in Quaternary sands near Stari Grad (Island of Hvar) shows distinct similarity with weathered augite of the oldest tephra from Susak (Crnjaković, unpublished data). As far as augite is concerned, green augite is widespread in the heavy mineral-rich beach sands of the Aeolian arc (Garzanti and Andò, 2007) which could also point out a potential source for augite from Susak and Hvar.

According to the study of heavy mineral association of Upper Pleistocene deposits in the Paglicci Cave (SE Italy) (Cremaschi and Ferraro, 2007), a significant increase in pyroxene (green) was also recognized in Campanian ignimbrite pyroclastic material (34 ka radiocarbon age), confirming the persistence of westerly winds in the area thus making the same eruption a possible source for Susak's youngest tephra (TF3).

It is interesting to mention that in the Italian Northern Adriatic area, three tephra layers were recorded in the Marche province, Italy (Chiesa et al., 1990). Of those tephras the middle one has also been described as of Plinian-type and mineral association has been comparable to Y5 layer that is related to Campanian ignimbrite eruption of the Phlegraean Fields (Thunell et al., 1979) dated around 39 ka (De Vivo et al., 2001). The oldest tephra (TF1) is probably much older than Campanian ignimbrite eruption so it could possibly originate from another, still unidentified source. Considering abundance and frequency of Italian volcanic activity during Pleistocene (Peccerillo, 2005) the additional analyses are required for further characterization of tephra horizons and correlation with possible sources of this volcanic material.

3.5. Conclusion

Quaternary sediments of the Island of Susak consist of loess, sandy loess and sand, palaeosols, three tephra layers and three distinctive horizons of calcareous segregations.

Upwards, throughout the sequence, loess generally becomes sandier and sometimes it is cross-laminated. Cross-laminated sandy sediments in the upper part of the succession represent dune sediments, while sporadically present small channels with graduated layers indicate the presence of occasional ephemeral water transport.

According to heavy mineral association source material originates from provenances in the area of Alpine collisional orogen and the River Po sediments, with slight deviations, caused by addition of material originating from the northern Apennines (Garzanti and Andò, 2007).

Based on recent IRSL and radiocarbon dating of loess, very detailed MIS 3 (Wacha et al., 2011) and MIS 5a-d records are exposed on Susak Island. Furthermore, considering the still not dated sediment sequence sandwiching the loess sections under study, interglacial MIS 5e palaeosol and much older loess record on one hand, as well as much younger MIS 2 records on the other, might also be present.

Numerous palaeosols and humified horizons are clear evidence for considerate chemical weathering and pedogenesis of loess on the Island of Susak during interglacial/interstadial periods. Differences between palaeosols and loess are not only evident in colours but also in granulometric, mineral and chemical composition and depend on duration and intensity of pedogenesis.

Pyroclastic material related to at least three Pleistocene volcanic events has been studied. Three tephra layers are macroscopically different from each other and from the surrounding sediment, and can be correlated on different localities on the island. The oldest (TF1) and youngest (TF3) tephras, situated in loess, show certain similarities, whereas middle (TF2) tephra is a bit different not only by its geochemical characteristics but also by vitroclasts morphology and field appearance being situated in brown palaeosol. The main characteristics of these distinct volcanic layers are vitroclasts, higher content of pyroxenes compared to surrounding sediment and, although rare, presence of idiomorphic biotite. The middle tephra (TF2) and the youngest tephra (TF3) show similar morphology of some pyroxenes, namely idiomorphic clinopyroxene crystals (possibly augite) which is quite different from the oldest tephra (TF1) that contains serrated clinopyroxene grains.

The source of tephra based on bulk rock and vitroclasts chemistry is not certain, due to the fact that their chemistry is modified by mixing of volcanic material with the surrounding sediment (loess and palaeosol) and by weathering. However, additionally having in mind mineral composition, morphology of volcanic particles and eruption age, possible sources are

very likely Middle and South Italian volcanic provinces (Campanian Province and Aeolian arc).

3.6. Acknowledgements

We would like to thank Goran Durn and Marta Mileusnić of the Faculty of Mining, Geology and Petroleum Engineering, University of Zagreb for AAS measurements and helpful consultations as well as Kristina Pikelj for help in particle size analysis. Special appreciation goes to Lidija Galović for providing extended insight in loess research as well as for many useful discussions. Dragan Bukovec is greatly thanked for constructive comments. This study was supported by the Ministry of Science, Education and Sports, projects no. 0183008 and 183-0000000-3201.

3.7. References

Adamiec, G., Aitken, M., 1998. Dose-rate conversion factors: update. Ancient TL 16, 37-50.

Aitken, M.J., 1998. An introduction to optical dating. Oxford University Press, Oxford, 280 p.

Allman, M., Lawrence, D.F., 1972. Geological Laboratory Techniques. Blandford Press, London, 335 pp.

Árkai, P., 1991. Chlorite crystallinity: An empirical approach and correlation with illite crystallinity, coal rank and mineral facies as exemplified by Paleozoic and Mesozoic rocks of northeast Hungary. Journal of Metamorphic Geology 9, 723-734.

Árkai, P., Sassi, F.P., Sassi. R., 1995. Simultaneous measurement of chlorite and illite crystallinity: a more reliable tool for monitoring low- to very low-grade metamorphism in metapelites. A case study from the Southern Alps (NE Italy). European Journal of Mineralogy 7, 1115-1128.

Auclair, M., Lamothe, M., Huot, S., 2003. Measurement of anomalous fading for feldspar IRSL using SAR. Radiation Measurements 37, 487–492.

Boero, V., Schwertmann, U., 1987. Occurence and transformations of iron and manganese in a colluvial terra rossa toposequence of northern Italy. Catena 14, 519-531.

Boero, V., Schwertmann, U., 1989. Iron oxide mineralogy of terra rossa and its genetic implications. Geoderma 44, 319-327.

Bognar, A., 1997. "Lesni otoci" Kvarnera. In: Arko-Pijevac, M. Kovačić, M., Crnković, D. (Eds.), Prirodoslovna istraživanja riječkog područja. Rijeka, Prirodoslovni muzej Rijeka, pp. 303-322 (in Croatian).

Bognar, A., Klein, V., Tončić-Gregl, R., Šercelj, A., Magdalenić, Z., Culiberg, M., 1983. Kvartarne naslage otoka Suska i Baške na otoku Krku i njihovo geomorfološko značenje u tumačenju morfološke evolucije kvarnerskog prostora. Geografski glasnik 45, 7-32.

Bognar, A., Schweitzer, F., Szöőr, G., 2003. Susak - environmental reconstruction of a loess island in the Adriatic. Geographical Research Institute, Hungarian Academy of Sciences. Budapest. 141 pp.

Bognar, A., Zámbó, L., 1992. Some new data of the loess genesis on Susak Island. In: Bognar, A. (Ed.), Proceedings of the International Symposium "Geomorphology and Sea". University of Zagreb, Croatia, pp. 65-72.

Chiesa, S., Coltorti, M., Cremaschi, M., Ferraris, M., Floris, B., Prosperi, L., 1990. Loess sedimentation and quaternary deposits in the Marche province. In: Cremaschi, M. (Ed.), The loess in northern and central Italy: a loess basin between the Alps and the Mediterranean region. Guide-book to the excursion in Northern and Central Italy. INQUA Commission on Loess. C.N.R. Quaderni di Geodinamica Alpina e Quaternaria 1, Milano, 187 pp.

Clemens, S. C., 1998. Dust response to seasonal atmospheric forcing: Proxy evaluation and calibration. Paleoceanography 13, 471–490.

Cremaschi, M., 1990a. The loess in northern and central Italy: a loess basin between the Alps and the Mediterranean region. In: Cremaschi, M. (Ed.), The loess in northern and central Italy: a loess basin between the Alps and the Mediterranean region. Guide-book to the excursion in Northern and Central Italy. INQUA Commission on Loess. C.N.R. Quaderni di Geodinamica Alpina e Quaternaria 1, Milano, 187 pp.

Cremaschi, M., 1990b. Stratigraphy and palaeoenvironmental significance of the loess deposits on Susak Island (Dalmatian archipelago). Quaternary International 5, 97-106.

Cremaschi, M., Ferraro, F., 2007. The Upper Pleistocene in the Paglicci Cave (Gargano, Southern Italy): Loess and tephra in the anthropogenic sequence. Atti della Societa Toscana di Scienze Naturali, Memorie, Serie A, 112, 153-163.

Crnjaković, M., 1994. The detrital versus authigenic origin and provenance of mineral particles in Mesozoic carbonates of Central Croatian karst area. Geologia Croatica 47 (2), 167-179.

De Vivo, B., Rolandi, G., Gans, P.B., Calvert, A., Bohrson, W.A., Spera, F.J., Belkin, H.E., 2001. New constraints on the pyroclastic eruptive history of the Campanian volcanic Plain (Italy). Mineralogy and Petrology 73, 47-65.

Durn, G., 2003. Terra rossa in the Mediterranean region: Parent materials, composition and origin. Geologia Croatica 56 (1), 83-100.

Durn, G., Ottner, F, Slovenec, D., 1999. Mineralogical and geochemical indicators of the polygenetic nature of terra rossa in Istria, Croatia. Geoderma 91, 125-150.

Durn, G., Slovenec, D., Čović, M., 2001. Distribution of iron and manganese in terra rossa from Istria and its genetic implications. Geologia Croatica 54 (1), 27-36.

Durn, G., Aljinović, D., Crnjaković, M., Lugović, B., 2007. Heavy and light mineral fractions indicate polygenesis of extensive terra rossa soils in Istria, Croatia. In: Mange, M.A., Wright, D.T. (Eds.), Heavy minerals in use. Developments in Sedimentology, Elsevier, 58, pp. 701-737.

Ferraro, F., 2009. Age, sedimentation and soil formation in the Val Sorda loess sequence, Northern Italy. Quaternary International 204, 54-64.

Folk, R.L., Ward, W.C., 1957. Brazos river bar: a study in the significance of grain size parameters. Journal of Sedimentary Petrology 27 (1), 3-26.

Frechen, M., Horváth, E., Gábris, G., 1997. Geochronology of Middle and Upper Pleistocen Loess Sections in Hungary. Quaternary Research 48, 291-312.

Galović, L., Frechen, M., Halamić, J., Durn, G., Romić, M., 2009. Loess chronostratigraphy in Eastern Croatia—A first luminescence dating approach. Quaternary International 198 (1-2), 85 -97.

Garzanti, E., Andò, S., 2007. Plate tectonics and heavy mineral suites of modern sands. In: Mange, M.A., Wright, D.T. (Eds.), Heavy minerals in use. Developments in Sedimentology, Elsevier, 58, pp. 741-763.

Hubert, J.F., 1962. A zircon-tourmaline-rutile maturity index and the interdependence of the composition of heavy minerals assemblages with the gross composition and texture of sandstones. Journal of Sedimentary Petrology 32, 440-450.

Huntley, D. J., Lamothe, M., 2001. Ubiquity of anomalous fading in K-feldspars, and the measurement and correction for it in optical dating. Canadian Journal of Earth Sciences 38, 1093-1106.

JCPDS, 1996. Powder Diffraction File PDF-2 Database Sets. International Centre for Diffraction Data, Philadelphia.

Kisch, H.J., 1990. Calibration of the anchizone: a critical comparison of illite "crystallinity" scales used for definition. Journal of Metamorphic Geology 8, 31-46.

Kisch, H.J., 1991. Ilite "crystallinity": recommendations on sample preparation, X-ray diffraction settings and interlaboratory samples. Journal of Metamorphic Geology 9, 665-670.

Kišpatić, M., 1910. Der Sand von der Insel Sansego (Susak) bei Lussin und dessen Herkunft. Verhandlungen geologisches Reichsanstaldt, Wien, 13, 294-305.

Kübler, B., 1967. Anchimétamorphisme et schistosité. Bulletin Du Centre De Recherches Pau – SNPA 1, 259-278.

Kübler, B., 1968. Evaluation quantitative du métamorphisme par la cristallinité de l'illite. Bulletin Du Centre De Recherches Pau SNPA 2, 385-397.

Kübler, B., 1990. "Cristalinité" de l'illite et mixed-layers: breve revision. Schweizer Mineralogische und Petrographische Mitteilungen 70, 89-93.

Kretz, R., 1983. Symbols for rock-forming minerals. American Mineralogist 68, 277-279.

Le Maitre, R.W., 1989. A classification of igneous rocks and glossary of terms. Blackwell, Oxford, 193 pp.

Lužar-Oberiter, B., Babić, Lj., Crnjaković, M., 2007. Sources of modern beach sands from two islands in the eastern Adriatic (Croatia). Book of Abstracts Patras: International Association of Sedimentologists, 2007. 268 pp.

Lužar-Oberiter B., Mikulčić Pavlaković, S., Crnjaković, M., Babić, Lj., 2008. Variable sources of beach sands of north Adriatic islands: examples from Rab and Susak. Geologia Croatica 61 (2-3), 379-384.

Mamužić, P., 1973. Basic geological map of SFRY 1:100 000. Geology of the Lošinj Sheet. Federal Geological Institute, Belgrade, 34 pp.

Mange, M.A., Maurer, H.F.W., 1992. Heavy minerals in colour. Chapman & Hall. London. 142 pp.

Marchesetti, C., 1882. Cenni geologici sul'isola di Sansego. Boll. Soc. adratica sc. nat. Trieste, 7, 289-304.

Marković-Marjanović, J., 1966. Loess stratigraphy of Susak Island in the northern part of the Adriatic Sea. Bjulleten komisii po izučeniju četvertičnogo perioda, Moskow 31, 32-41 (in Russian).

Marković-Marjanović, J., 1976. Kvartarni sedimenti ostrva Hvara – Srednji Jadran. Glasnik prirodnjačkog muzeja A/31, 199-214, Beograd.

McDonough, W.F., Sun, S., Ringwood, A.E., Jagoutz, E., Hofmann, A.W., 1991. K, Rb and Cs in the earth and Moon and the evolution of the Earth's mantle. Geochimica et Cosmochimica Acta, Rossaylor Symposium volume.

Mehra, O.P., Jackson, M.L., 1960. Iron oxides removal from soils and clays by a dithionite-citrat-bicarbonate system buffered with sodium bicarbonate. Clays and Clay Minerals 7, 317-327.

MGI, 1977. Topographic map 1:25 000. 417-4-3, Military Geographical Institute, Belgrade, SFRJ.

Micromeritics, 2002. SediGraph 5100 Particle size analysis system operator' manual. Micromeritics Instrument Corporation, Norcross, Georgia.

Mikulčić Pavlaković, S., 2006. Mineralogical characteristics of sands and pyroclastics from Susak Island. Unpublished Master Thesis, University of Zagreb, 126 pp, Zagreb (in Croatian).

Mikulčić Pavlaković, S., Crnjaković, M., Tibljaš, D., 2005. Redetermination of the Samples of Susak Island Quaternary Sediments from the Petrographic Collection of the Croatian

Natural History Museum. 3. Croatian Geological Congress, Opatija, Book of Abstracts, 103-104.

Munsell Soil Color Charts, 1994. Revised Edition, Munsell Color, GretagMacbeth, New Windsor, NY.

Mutić, R., 1967. Pijesak otoka Suska. Geološki vijesnik 20, 41-57.

Nickling, W.G., 1983. Grain-size characteristics of sediments transported during dust storms. Journal of Sedimentary Petrology 53, 1011-1024.

Novothny, Á., Frechen, M., Horváth, E., Bradák, B., Oches, E.A., McCoy, W.D., Stevens, T., 2009. Luminescence and amino acid recemization chronology of the loess-palaeosol sequence at Sütto, Hungary. Quaternary International 198 (1-2), 62-76.

Novothny, Á., Horváth, E., Frechen, M., 2002. The loess profile at Albertirsa, Hungary - improvements in loess stratigraphy by luminescence dating. Quaternary International 95–96, 155–163.

Peccerillo, A., 2005. Plio-Quaternary Volcanism in Italy-Petrology, Geochemistry, Geodynamics. Springer, Berlin, 365 pp.

Pettijohn, F.J., 1957. Sedimentary Rocks. Harper & Brothers, New York, 718 pp.

Pettijohn, F.J.; Potter, P.E., Siever, R., 1972. Sand and Sandstones. Springer-Verlag, New York, 618 pp.

Philips Analytical B.V., 2001. X'Pert High Score, Version 1.0, Almelo.

Rollinson, H.R., 1993. Using Geochemical Data: Evaluation, Presentation, Interpretation. Longman Group UK Limited, Essex, 352 pp.

Ruchin, L.B., 1958. Grundzüge der lithologie. Akademie-Verlag, Berlin, 806 pp.

Salmojraghi, F. 1907. Sull' origine padana della sabbia di Sansego nel Quarnero. Rend. R. Ist. Lomb., sci. lett. (2), Milano, 40, 867-887.

Stache, G., 1872. Geologische Reisenotizen aus Istrien. 2. Der Sand von Sansego an der südlichen Küste Istriens. Verhandlungen geologisches Reichsanstaldt, Wien, 10, 215-223.

Šandor, F., 1912. Istraživanja prapora iz Vukovara, Bilo gore i sa Rajne. Vijesti geološkog povjerenstva 2, 103-107, Zagreb.

Štamol, V., Poje, M., 1998. The fossil and recent malacofauna of the island of Susak (Croatia) (Gastropoda: Prosobranchia, Basammatophora, Stylommatophora). Staatliches Museum fur Tierkunde Dresden, Dresden, 19/11, 103-117.

Starkey, H.C., Blackmon, P.D., Hauff, P.L., 1984. The Routine Mineralogical Analysis of Clay-Bearing Samples. U.S. Geological Survey Bulletin 1563, 1-32.

Thunell, R., Federman, A., Sparks, S., Williams, D.,1979. The age origin and volcanological significance of the Y5 ash layer in the Mediterranean. Quaternary Research 12, 241-253.

Trefethen, J.M., 1950. Classification of sediments. American Journal of Science 248, 55-62.

Tröger, W.E., 1967. Optische Bestimmung der gesteinsbildenden Minerale – Teil 2. E. Schweizerbart'sche Verlagsbuchhandlung, Stuttgart, 822 pp.

Tućan, F., 1911. Die Kalksteine und Dolomite des Kroatischen Karstgebietes. Geološki anali Balkanskoga poluostrva 6, fasc. 2, 609 – 813.

Wacha, L., Mikulčić Pavlaković, S., Novothny Á., Crnjaković, M., Frechen, M., 2011 Luminescence Dating of Upper Pleistocene Loess from the Island of Susak in Croatia. Quaternary International 234, 1-2, 50-61.

Warr, L.N, Rice, A.H.N., 1994. Interlaboratory standardization and calibration of clay mineral crystallinity and crystallite size data. Journal of Metamorphic Geology 12, 141-152.

Wein N., 1977. Die Lössinsel Susak - eine naturgeographische Singularität in der jugoslawischen Inselwelt. Petermanns geographische Mitteilungen, Gotha/Lepzig, 2, 123-132.

Wentworth, C.K., 1922. A scale of grade and class terms for clastic sediments. The Journal of Geology 30, 377–392.

Winchester, J.A., Floyd, P.A., 1977. Geochemical discrimination of different magma series and their differentiation products using immobile elements. Chemical Geology 20, 325-343.

Wintle, A.G., 1997. Luminescence dating: laboratory procedures and protocols. Radiation Measurements 27, 769–817.

Wintle, A. G., Packman, S. C., 1988. Thermoluminescence ages for three sections in Hungary. Quaternary Science Reviews 7, 315–320.

Wood, D.A., 1979. A variably veined suboceanic upper mantle - Genetic significance for mid-ocean ridge basalts from geochemical evidence. Geology 7, 499-503.

CHAPTER 4

Quaternary Science Journal (Eiszeitalter und Gegenwart) (2010), accepted for publishing

The Loess Chronology of the Island of Susak, Croatia

Lara Wacha[1, 2], Snježana Mikulčić Pavlaković[3], Manfred Frechen[1], Marta Crnjaković[3]

[1]Leibniz Institute for Applied Geophysics, S3 Geochronology and Isotope Hydrology, Stilleweg 2, D-30655 Hannover, Germany

[2] Croatian Geological Survey, Sachsova 2, HR-10000 Zagreb, Croatia

[3] Croatian Natural History Museum, Department of Mineralogy and Petrography, Demetrova 1, HR-10000 Zagreb, Croatia

Abstract

A high-resolution infrared stimulated luminescence (IRSL) and radiocarbon dating study was performed on the loess-palaeosol sequence from the island of Susak, situated in the North Adriatic Sea in Croatia. The dating results show that a detailed Late Pleistocene record is preserved on Susak, correlating to the marine Oxygen Isotope Stages (OIS) 5 to 2, with a very thick Middle Pleniglacial record predominating. Due to its extraordinary thickness (which is recorded to be up to 90 metres), the loess on Susak is unique in this area. The numerous palaeosols intercalated in the loess give evidence for climate variations which were warmer than in other loess regions (e.g. the Carpathian Basin). The great thickness of the OIS3 deposits correlates to the general increased dust accumulation in Europe during that time. Based on numerical ages a correlation of the loess on Susak with the loess in North Italy and the Carpathian basin, a more detailed time-based reconstruction of climate and environment changes in the study area was achieved.

Keywords: Susak, Croatia, loess-palaeosol sequence, geochronology, IRSL dating, radiocarbon dating

4.1. Introduction

Evidence of Pleistocene climatic changes can be found in more or less continuous terrestrial sediment records like loess-palaeosol sequences. Great efforts are made into the high resolution sampling and investigation of loess records using different disciplines and methods with the purpose of identifying climate oscillations and environmental changes (Buylaert et al., 2008; Stevens et al., 2008; Bokhorst and Vandenberghe, 2009). The correlation with oxygen isotope stages (OIS) and the GRIP data (GRIP Members, 1993) is a common practice. However, a robust and detailed chronology is mandatory to make a reliable correlation possible.

Loess and loess-like deposits in the North Adriatic region are found along the fringes of mountain chains like the Alps and the Apennines in Italy and along the coast and islands of Croatia. During the last Glacial period, the sea level of the Mediterranean was about 100 metres lower than today (Van Straaten, 1970; Cremaschi, 1987; Amorosi, et al., 1999). Therefore, the North Adriatic was an extended and closed basin exposed to a strong input of fluvial Alpine material carried by the river Po and other tributaries. The thickness of the loess and loess-like deposits in the North Adriatic area is relatively small, only up to a few meters (Ferraro, 2009), but the deposits are widely distributed. In Italy, loess and loess derivatives can be found on fluvial terraces (Cremaschi et al., 1990), on moraines and fluvioglacial deposits e.g. Val Sorda (Ferraro, 2009; Ferraro et al., 2004), or on the carbonate platform (Coudé-Gaussen, 1990) where they cover the carbonate basement and fill caves and shelters (Cremaschi, 1987; Peresani et al., 2008). Along the Croatian coast and on the islands loess and loess derivatives are common. In Istria loess can be found in the south, in Premantura and Mrlera, and in the north-west, in Savudrija (Durn, et al., 1999; 2007) as well as on the islands of Unije, Velike and Male Srakane, Krk and Lošinj in the Kvarner region and on the islands Hvar and Mljet in South Dalmatia, with reported thickness ranging from a few meters up to about 20 m (Bognar, 1979). In Savudrija loess is up to 4 m thick and covers terra rossa (Durn et al., 1999, 2003; 2007). The influence of loess was recognised by Durn et al. (1999; 2007) in the upper parts of terra rossa profiles in Istria. The most extraordinary loess-palaeosol record of this area is the one found on the island of Susak in Croatia (Fig. 4.1.). The genesis and the composition of the deposits on the island have been a matter of interest and discussion for a long time, since the past centuries (Fortis, 1771; Marchesetti, 1882; Kišpatić, 1910; Šandor, 1914; Mutić, 1967; Wein, 1977; Bognar, 1979; Bognar et al., 1983; Cremaschi, 1987; 1990;

Bognar and Zámbó, 1992; Bognar et al., 2002, 2003; Lužar-Oberiter et al., 2008; Mikulčić Pavlaković et al., 2011; Wacha et al., 2011). Based on the mineralogical investigations of the deposits from Susak, most of the researchers concluded that the provenance of the material is the river Po plain, situated in the northern part of Italy. Cremaschi (1990) stated that the deposition of loess on Susak is related to the 100 metres drop of the sea level in the Mediterranean during the last glacial period. Recently, the loess-palaeosol record on Susak has been successfully dated using infrared stimulated luminescence (Wacha et al., 2011). These first results showed that most of the loess-palaeosol record correlates to Oxygen Isotope Stage (OIS) 3, but the deposition age of the stratigraphically older and younger part of the sequence has not yet been determined.

In Croatia, loess and loess- like deposits are well known from the north of the country, on the Bilogora Mountain, around Đakovo, and the eastern part of the country along the river Danube, in Baranja, Srijem and on the Fruška gora (gora = mountain). Loess deposits in this region were investigated by Šandor (1912), Gorjanović-Kramberger (1912, 1915, 1922), Bronger (1976, 2003), Bognar (1979), Galović and Mutić (1984), Poje (1985, 1986), Mutić (1990) etc. The first age estimates of these deposits were presented by Singhvi et al. (1989), using the thermoluminescence (TL) dating method, and by Galović et al. (2009) using the infrared stimulated luminescence (IRSL).

In this study the geochronological framework of the loess record from the island of Susak presented in Wacha et al. (2011) is significantly improved by new infrared stimulated luminescence (IRSL) and radiocarbon data. Furthermore, the detailed loess-palaeosol sequence is compared with the contemporaneous loess deposits from the North Adriatic Basin and the Pannonian (Carpathian) Basin and an attempt of a chronostratigraphical correlation is given. The loess provinces mentioned above differ in many ways. The loess in the Adriatic region is often neglected when major correlations of loess in Europe are made. In this study the differences and similarities of these two genetically different loess provinces are summarized and they are correlated based only on their chronology.

The aim of this study is to establish a more detailed geochronological framework for the unique loess record on the Island of Susak in the North Adriatic Sea as a basis for further high-resolution proxy studies including grain-size and palaeomagnetic approaches (Wacha et al., in preparation) and to settle the Quaternary sediment succession of the Island in a wider context, that of the North Mediterranean and Pannonian (Carpathian) area.

4.2. Geological setting and the sediment succession

The island of Susak is situated in the western part of the Kvarner Archipelago in the North Adriatic Sea in Croatia (Fig. 4.1.). It is the outermost and quite isolated island with an area of 3.8 km^2. The highest peak is at 96 m above sea level (asl). Susak is located between 44.50° and 44.52° N and 14.28° and 14.32°E. The geomorphology of the island has all characteristics of a loess plateau (Bognar et al., 2003) dissected by numerous gorges, steep bluffs and gullies (Fig. 4.2.). Human activity during historical times had and still has a major influence on the morphology and erosion of the island because the island is a vine yard area since Roman times resulting in numerous artificial plateaus.

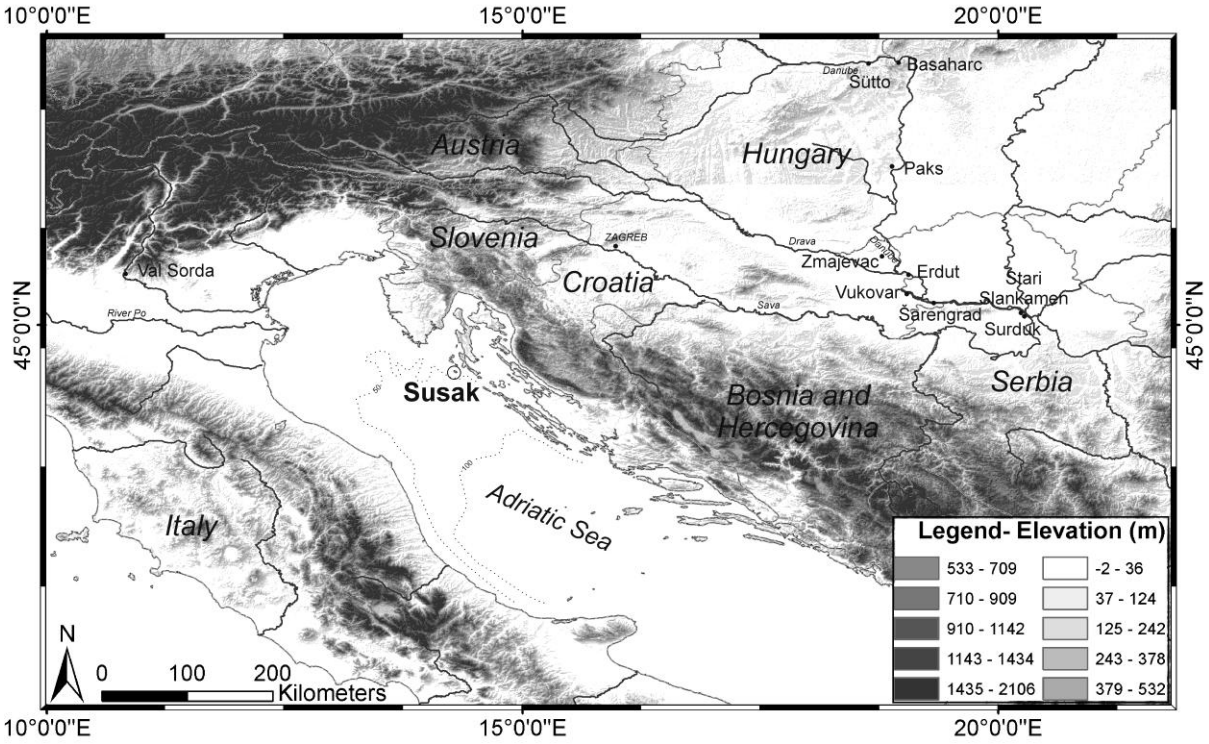

Figure 4.1. Geographical setting of the Island of Susak in Croatia and its relation to the river Po in North Italy and to the Danube loess region with indicated locations of loess-palaeosol sections used for correlation. Elevation map for the area is prepared using the DEM image obtained from ASTER GDEM (product of METI and NASA).

Geotectonically, Susak belongs to the West Istrian autochton of the Northern Adriatic Carbonate Platform (Mamužić, 1973). The basement of the island is made of Upper Cretaceous limestones (Fig. 4.3. and 4.4.). On the northern coast, Eocene limestones can be found (Mamužić, 1973). The bedrock is covered by up to 90 metres of Quaternary sediments, recently described by Cremaschi (1990), Bognar et al. (2003), Mikulčić Pavlaković et al.

(2011) and Wacha et al. (2011). Pliocene and Pleistocene sediments are usually transgressive on the Jurassic and Cretaceous carbonates of the Istrian platform, and on Neogene or Paleogene deposits in the Po basin as seen in cores from the North Adriatic Sea (Kalac, et al., 1995). The Quaternary deposits on Susak are made of loess, loess derivatives and sand, and are intercalated by numerous palaeosols and at least three tephra layers (Fig. 4.5.).

Figure 4.2. Photo of Kalučica bay on the easternmost cape of the island, with the characteristic dissected morphology of the Susak loess sequence.

Wacha et al. (2011) and Mikulčić Pavlaković et al. (2011) described altogether four smaller sections from the Eastern part of the island in more detail (Fig. 4.3.). In the bay of Bok (Fig. 4.3.) a red palaeosol, overlain by a second red palaeosol, covers the carbonate basement (Fig. 4.4.). The thickness of these red palaeosols is up to 100 cm but changes laterally. On some locations on the island only one red palaeosol is exposed. The palaeosols are separated with septarian carbonate concretions, up to 20 cm in diameter. Sandy loess covers the red palaeosols and is in its lower part lithified forming a sandstone bench. In the upper part of the sandy loess horizon vertical carbonate concretions up to 10 cm long are found. Secondary carbonates are described in more detail by Bognar and Zámbó (1992) and Mikulčić Pavlaković et al. (2011) and indicate strong water percolation from the upper part of the section. The lower part of the loess-palaeosol sequence on Susak is dominated by three about 1 metre thick palaeosols, two of them brown and one orange-brown in colour. In the upper part of the loess sequence numerous thin brown palaeosols are exposed, some of them

containing dispersed charcoal and charcoal pieces (Fig. 4.6.). The charcoal pieces found in two horizons were investigated by Bognar et al. (2003). They concluded that these remains are the results of forest fires, caused by self-inflammation or human activity and determined the Pinus sylvestris group of tree species from the charcoal. In the middle part of the loess-palaeosol record homogenous and laminated sand can be found, in a form of a few centimetres thick layers and dune sand. The sand indicates stronger wind activity, a near-distance transport and a very likely local source of the material. The transition from sand into loess is mostly gradual. The general trend of loess coarsening upwards was observed by Mikulčić Pavlaković et al. (2011) and is supported by the results of grain-size analysis from an ongoing study (Wacha et al., in preparation). Three tephras were detected intercalating the loess of Susak; two in a form of continuous layers (TF1 and TF3) and one as accumulations (pockets) in a thin brown palaeosol (TF2) (Fig. 4.5.). The sedimentological, geochemical and mineralogical properties of loess, sand, palaeosols and the tephras are presented in more detail by Mikulčić Pavlaković et al. (2011). In Fig. 4.7. all the investigated and sampled sections are presented along with the indicated sample positions and IRSL and radiocarbon ages.

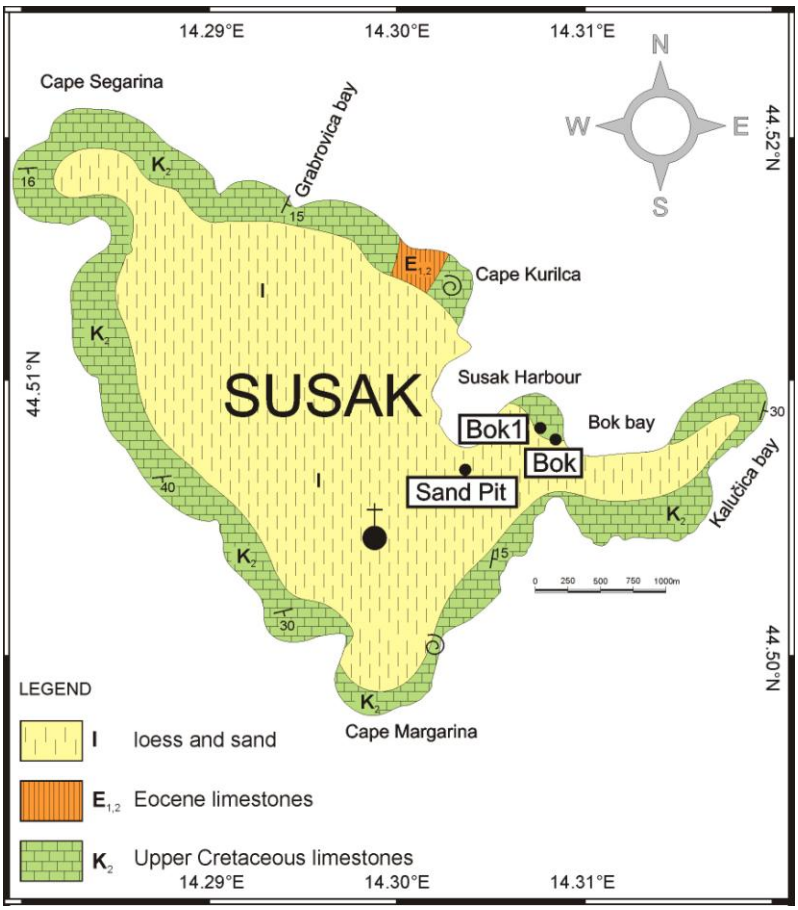

Figure 4.3. Geological map of the Island of Susak (simplified after Mamužić, 1965).

Figure 4.4. Carbonate basement covered with the red palaeosol which represents the beginning of the Quaternary loess-palaeosol sequence on Susak. (Photo by E. Schmidt.)

Figure 4.5. Three macroscopically visible tephra layers were detected intercalating the Susak loess-palaeosol sequence, described in more detail by Mikulčić Pavlaković et al. (2011). a) TF1 – a thin yellow layer of the lowermost, oldest tephra; b) the thin brown palaeosol with patches of orange-yellow middle tephra (TF2); c) TF3 – the uppermost and younger most tephra intercalating loess on Susak is found as a thin olive green layer.

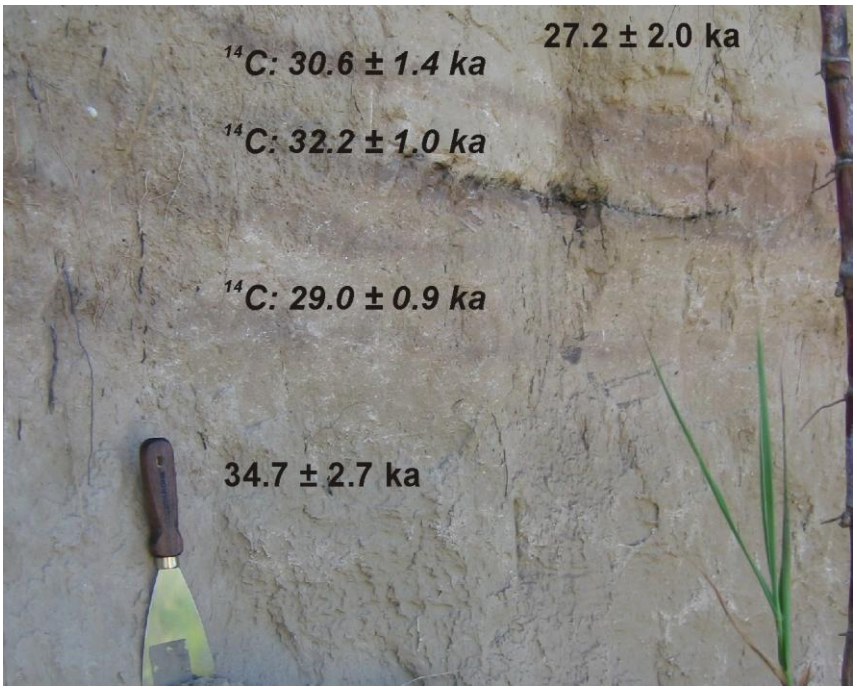

Figure 4.6. A detail from the upper part of the Sand Pit section showing the weakly developed brown palaeosols with dispersed charcoal remains and the IRSL and radiocarbon dating results.

4.3. Dating methods

4.3.1. Luminescence dating

Loess has proved to be excellent material for luminescence dating (Frechen et al., 1997; Lu et al., 2007; Roberts et al., 2003; Roberts, 2008; Novothny et al., 2002, 2009, 2010; Schmidt et al., 2010) because it fulfils the basic dating assumption which is the bleaching of the latent signal in the mineral grains (quartz and feldspar) prior to deposition. Aeolian transportation of dust is a good mechanism for the fulfilment of such an assumption because during transport the particles are exposed to sunlight which releases most of the trapped charges in the crystal lattice of the minerals and resets the dosimeter to zero. After the deposition and after the material had been buried, the minerals are again exposed to the natural radioactivity of the surrounding sediment. This ionizing radiation moves the charges from their original position into charge traps caused by impurities or crystal lattice defects, from where they can only be released by additional energy. Releasing these electrons from the traps and their recombination with the positive charges in the crystal lattice results in the emission of light (luminescence), and can be measured with a photomultiplier in the laboratory. With time the amount of such dislocated charge grows, meaning that the luminescence signal is proportional to the depositional age of the sediment. The intensity of the luminescence signal increases with the deposition age of the sediment. The equivalent dose (D_e) is a measure of the past radiation and, if divided by the dose rate, gives the time elapsed since the last exposure of the sediment to sunlight, i. e. the deposition. The principles of luminescence dating are given in detail by Aitken (1985, 1998), Wintle (1997), Bøtter-Jensen et al. (2003) and Preusser et al (2008, 2009) and a more recent review about luminescence dating of loess is presented by Roberts (2008).

Twenty-one sample was collected in 2008 using light-proof plastic tubes, by pushing or hammering into a previously cleaned loess wall. Additional material was taken for dose rate determination by gamma spectrometry. In this study we applied the same sample preparation procedure for the extraction of the polymineral fine-grained material, as described in Wacha et al. (2011).

The same protocols and measurement procedures were used as presented in Wacha et al. (2011), as they have proved to be satisfactory. All measurements were performed using two automated Risø TL/OSL-DA15 readers at the Leibniz Institute for Applied Geophysics

equipped with a $^{90}Sr/^{90}Y$ β-source, with dose rates of 0.101 Gy/s and 0.096 Gy/s, respectively, for fine grains mounted on aluminium discs.

Fading tests were performed on the same aliquots which were previously used for D_e measurements for all samples using the suggestion of Huntley and Lamothe (2001) and Auclair et al. (2003). The same measuring conditions were used as for the D_e evaluation. The mean of the six aliquots was used for fading corrections and their standard errors. The fading rates (g-values) were calculated according to Huntley and Lamothe (2001) using the same integration limits as for the D_e calculation. The g-values were used for age corrections.

The dose rates of the sediment were measured by gamma spectrometry with a HPGe (High-Purity Germanium) N-type coaxial detector in the laboratory at the Leibniz Institute for Applied Geophysics. 700 g of dried and homogenized material was used for the measurements. The sample was placed into a Marinelli-beaker and cap sealed to avoid the loss of ^{222}Rn in the ^{238}U decay chain and stored for a minimum of four weeks in order to re-establish the radioactive equilibrium. The measuring time was one day. The measured activities of ^{40}K; and ^{210}Pb, ^{234}Th, ^{214}Bi and ^{214}Pb radionuclides from the ^{238}U; and ^{228}Ac, ^{208}Tl and ^{212}Pb radionuclides from the ^{232}Th decay chains were used for the calculation of potassium, uranium and thorium contents, respectively. The radioactive equilibrium was assumed for the decay chain, which is normally the case for loess; no radioactive disequilibrium was detected by gamma spectrometry. Cosmic dose rates were corrected for the altitude and sediment thickness (Prescott and Hutton, 1994). The alpha efficiency was estimated to a mean value of 0.08 ± 0.02 for polymineral IRSL (Rees-Jones, 1995). The water content was assumed to be from 15 ± 5% to 20 ± 5%, depending on the depth (Pécsi, 1990). For the calculation of the total dose rate the conversion factors published by Adamiec and Aitken (1998) were used. A systematic error of 2 % is included for the gamma spectrometry. An error of 10 % is estimated for the cosmic dose. The uranium, thorium and potassium contents, as well as the total dose rates, the cosmic dose rates, the g-values, the uncorrected and corrected ages are given in Table 4.1.

Table 4.1. Sample list with depth below surface, results from the dosimetry, the SAR IRSL measurements, g-values, the uncorrected and corrected ages for fine-grained feldspar. The dose rate is the sum of the dose rates of the alpha, beta, gamma and cosmic radiation.

	Sample name	Sample ID	Depth (m)	Uranium (ppm)	Thorium (ppm)	Potassium (%)	Cosmic dose (mGy/a)	Dose rate (mGy/a)	De (Gy)	g-value (%/decade)	Uncorrected age (ka)	Corrected age (ka) *
Bok Section	Sus08-16	1753	2.00	3.30 ± 0.01	9.87 ± 0.03	1.23 ± 0.01	0.150 ± 0.015	3.16 ± 0.19	49.1 ± 2.5	1.7 ± 0.2	15.5 ± 1.2	18.1 ± 1.4
	Sus13	1438	8.00	3.84 ± 0.05	11.90 ± 0.13	1.28 ± 0.02	0.062 ± 0.006	3.48 ± 0.20	65.4 ± 3.3	2.1 ± 0.1	18.8 ± 1.5	22.8 ± 1.7
	Sus08-15	1752	8.50	4.10 ± 0.02	13.89 ± 0.04	1.61 ± 0.01	0.062 ± 0.006	4.03 ± 0.22	74.5 ± 3.7	2.1 ± 0.3	18.5 ± 1.4	22.4 ± 1.8
	Sus08-14	1751	13.00	3.84 ± 0.02	12.02 ± 0.06	1.51 ± 0.01	0.036 ± 0.004	3.66 ± 0.21	77.0 ± 3.9	1.7 ± 0.03	21.0 ± 1.6	24.6 ± 1.8
	Sus08-13	1750	15.00	3.50 ± 0.01	9.72 ± 0.03	1.31 ± 0.01	0.030 ± 0.003	3.16 ± 0.19	67.8 ± 3.4	1.8 ± 0.1	21.4 ± 1.7	25.3 ± 1.9
	Sus12	1437	15.80	4.52 ± 0.05	14.48 ± 0.12	1.70 ± 0.02	0.028 ± 0.003	4.26 ± 0.24	106.1 ± 5.4	2.0 ± 0.1	24.9 ± 1.9	29.9 ± 2.2
	Sus11	1436	16.30	4.15 ± 0.05	13.26 ± 0.13	1.68 ± 0.03	0.027 ± 0.003	4.01 ± 0.22	104.6 ± 5.3	1.9 ± 0.1	26.1 ± 2.0	31.0 ± 2.3
	Sus08-12	1749	17.00	3.99 ± 0.02	12.69 ± 0.04	1.67 ± 0.01	0.026 ± 0.003	3.90 ± 0.22	88.6 ± 4.4	1.8 ± 0.03	22.7 ± 1.7	26.8 ± 2.0
	Sus08-11	1748	17.60	3.81 ± 0.03	12.12 ± 0.06	1.62 ± 0.01	0.025 ± 0.002	3.74 ± 0.21	84.2 ± 4.2	1.7 ± 0.1	22.5 ± 1.7	26.3 ± 2.0
	Sus08-10	1747	18.80	2.94 ± 0.02	10.57 ± 0.06	1.31 ± 0.01	0.023 ± 0.002	3.06 ± 0.17	79.6 ± 4.0	1.9 ± 0.1	26.0 ± 2.0	31.0 ± 2.3
	Sus08-9	1746	19.80	4.11 ± 0.02	13.27 ± 0.04	1.60 ± 0.01	0.022 ± 0.002	3.92 ± 0.22	110.3 ± 5.6	1.7 ± 0.1	28.1 ± 2.1	32.9 ± 2.5
	Sus10	1435	20.80	4.19 ± 0.08	13.33 ± 0.14	1.76 ± 0.03	0.021 ± 0.002	4.09 ± 0.23	128.8 ± 6.5	2.3 ± 0.4	31.5 ± 2.4	39.0 ± 3.3
	Sus9	1434	21.30	3.50 ± 0.05	10.04 ± 0.12	1.40 ± 0.02	0.021 ± 0.002	3.26 ± 0.19	108.4 ± 5.5	2.3 ± 0.4	33.2 ± 2.6	41.2 ± 3.6
	Sus08-8	1745	23.00	3.48 ± 0.01	11.06 ± 0.03	1.43 ± 0.01	0.019 ± 0.002	3.20 ± 0.18	130.6 ± 6.6	1.8 ± 0.1	40.8 ± 3.1	48.2 ± 3.6
	Sus08-7	1744	23.60	2.71 ± 0.01	9.24 ± 0.03	1.38 ± 0.01	0.019 ± 0.002	2.77 ± 0.16	124.8 ± 6.4	1.7 ± 0.1	45.0 ± 3.5	52.8 ± 4.0
	Sus08-6	1743	25.00	2.58 ± 0.02	8.38 ± 0.05	1.14 ± 0.01	0.018 ± 0.002	2.46 ± 0.15	112.8 ± 5.7	1.8 ± 0.02	45.9 ± 3.6	54.3 ± 4.9
	Sus08-18	1755	26.70	3.27 ± 0.01	11.28 ± 0.03	1.46 ± 0.01	0.018 ± 0.002	3.18 ± 0.18	261.2 ± 13.1	1.9 ± 0.1	82.1 ± 6.2	98.3 ± 7.3
	Sus08-17	1754	27.00	3.38 ± 0.02	11.33 ± 0.06	1.44 ± 0.01	0.018 ± 0.002	3.20 ± 0.18	249.7 ± 12.6	1.9 ± 0.1	77.9 ± 5.9	93.3 ± 7.0
	Sus08-5	1742	28.00	4.09 ± 0.03	15.67 ± 0.08	1.91 ± 0.01	0.018 ± 0.002	4.18 ± 0.22	276.9 ± 14.0	1.9 ± 0.02	66.2 ± 4.8	79.1 ± 5.7
Bok1	Sus08-4	1741	21.90	2.17 ± 0.01	7.63 ± 0.04	1.36 ± 0.01	0.020 ± 0.002	2.58 ± 0.15	140.2 ± 7.8	2.3 ± 0.2	54.3 ± 4.4	67.6 ± 5.5
	Sus08-3	1740	23.00	3.48 ± 0.03	12.02 ± 0.06	1.44 ± 0.01	0.019 ± 0.002	3.47 ± 0.19	193.7 ± 11.1	2.5 ± 0.4	55.8 ± 4.5	70.7 ± 6.3
	Sus08-2	1739	23.50	3.55 ± 0.03	11.92 ± 0.06	1.43 ± 0.01	0.019 ± 0.002	3.47 ± 0.20	177.3 ± 10.0	2.4 ± 0.2	51.0 ± 4.1	64.1 ± 5.3
	Sus08-1	1738	24.70	3.83 ± 0.02	12.80 ± 0.06	1.50 ± 0.01	0.019 ± 0.002	3.70 ± 0.21	181.8 ± 10.1	2.7 ± 0.2	49.1 ± 3.9	63.5 ± 5.1
Sand Pit section	Sus8	1433	10.00	4.16 ± 0.05	13.32 ± 0.14	1.60 ± 0.03	0.050 ± 0.005	3.97 ± 0.22	80.0 ± 4.0	2.0 ± 0.1	20.1 ± 1.5	24.2 ± 1.8
	Sus08-24	1761	14.00	3.57 ± 0.02	11.17 ± 0.04	1.55 ± 0.01	0.033 ± 0.003	3.53 ± 0.20	106.2 ± 7.7	2.0 ± 0.2	26.1 ± 2.0	31.3 ± 2.5
	Sus5	1430	14.50	4.74 ± 0.05	14.99 ± 0.14	1.73 ± 0.03	0.032 ± 0.003	4.40 ± 0.24	105.7 ± 5.3	2.0 ± 0.1	24.0 ± 1.8	28.8 ± 2.1
	Sus4	1429	15.30	4.40 ± 0.05	13.44 ± 0.10	1.71 ± 0.02	0.030 ± 0.003	4.14 ± 0.23	101.1 ± 5.1	1.5 ± 0.2	24.5 ± 1.8	28.0 ± 2.1
	Sus3	1428	16.20	4.30 ± 0.05	12.81 ± 0.12	1.68 ± 0.03	0.028 ± 0.003	4.02 ± 0.23	94.8 ± 4.8	1.6 ± 0.1	23.6 ± 1.8	27.2 ± 2.0

* After calibration of the Risø Reader for fine-grained material mounted on Al discs, the data from samples presented in Wacha et al. (2011) were recalculated because the new dose rates of the reader were lower than previously used. In the table the complete Susak data set is presented.

Sample name	Sample ID	Depth (m)	Uranium (ppm)	Thorium (ppm)	Potassium (%)	Cosmic dose (mGy/a)	Dose rate (mGy/a)	De (Gy)	g-value (%/decade)	Uncorrected age (ka)	Corrected age (ka) *
Sus2	1427	17.00	2.32 ± 0.04	7.77 ± 0.11	1.31 ± 0.02	0.027 ± 0.003	2.61 ± 0.16	75.9 ± 3.8	1.9 ± 0.1	29.1 ± 2.3	34.7 ± 2.7
Sus1	1426	18.00	2.31 ± 0.04	8.12 ± 0.09	1.15 ± 0.02	0.024 ± 0.002	2.50 ± 0.15	79.0 ± 4.0	2.0 ± 0.1	31.7 ± 2.5	38.1 ± 2.9
Sus7	1432	19.50	3.57 ± 0.04	11.03 ± 0.11	1.37 ± 0.02	0.023 ± 0.002	3.35 ± 0.19	91.4 ± 4.6	2.4 ± 0.5	27.3 ± 2.1	34.1 ± 3.1
Sus6	1431	20.70	3.71 ± 0.05	11.09 ± 0.12	1.40 ± 0.03	0.022 ± 0.002	3.42 ± 0.20	96.6 ± 4.9	1.9 ± 0.1	28.2 ± 2.2	33.6 ± 2.6
Sus08-23	1760	20.80	3.50 ± 0.02	10.85 ± 0.04	1.50 ± 0.01	0.021 ± 0.002	3.42 ± 0.20	93.2 ± 4.9	2.4 ± 0.2	27.2 ± 2.1	34.1 ± 2.7
Sus08-22	1759	22.20	3.56 ± 0.02	11.86 ± 0.04	1.51 ± 0.01	0.020 ± 0.002	3.54 ± 0.20	105.7 ± 5.6	2.7 ± 0.2	29.8 ± 2.3	38.5 ± 3.0
Sus08-21	1758	23.80	4.18 ± 0.02	13.86 ± 0.04	1.64 ± 0.01	0.019 ± 0.002	4.03 ± 0.22	126.9 ± 6.7	2.2 ± 0.1	31.5 ± 2.4	38.6 ± 2.9
Sus08-20	1757	25.40	4.11 ± 0.05	13.27 ± 0.12	1.57 ± 0.03	0.018 ± 0.002	3.90 ± 0.22	122.6 ± 7.4	2.4 ± 0.3	31.5 ± 2.6	39.3 ± 3.4
Sus08-19	1756	26.80	3.83 ± 0.01	12.05 ± 0.03	1.74 ± 0.01	0.018 ± 0.002	3.65 ± 0.20	113.2 ± 5.7	1.3 ± 0.3	31.0 ± 2.3	34.9 ± 2.7

4.3.2. Radiocarbon dating

In this study seven new radiocarbon ages are presented, six from the Bok section and one from the Sand Pit section. Among them four samples were molluscs (Hv 25895 – 25898) and three were charcoal remains (Hv 25899 – 25901). The specific activity of ^{14}C was measured radiometrically by proportional counters (Geyh, 1990, 2005) at the Leibniz Institute for Applied Geophysics (LIAG). The radiocarbon ages were converted into calibrated calendar ages using the radiocarbon calibration curve based on coral samples and program after Fairbanks et al. (2005). The sample positions are shown in Fig. 4.7. and the calibrated and uncalibrated ages are given in Table 4.2. The radiocarbon ages presented in Wacha et al. (2011) are shown as well.

Table 4.2. Uncalibrated and calibrated radiocarbon dating results. The results were calibrated using the Fairbanks et al (2005) calibration curve spanning from 0 to 50.000 years BP and transferred in ka B. P. in order to make the radiocarbon results better comparable with luminescence ages. * radiocarbon dating results presented in Wacha et al. (2011). $^{+}$ Radiocarbon ages are by definition "Age before 1950".

Sample name	Radiocarbon age ka B.P.$^{+}$	Calendar age cal. B.P.	Calendar age ka cal. B.P.	Material type
Hv 25696*	24215 ± 750	29023 ± 923	29.0 ± 0.9	charcoal
Hv 25697*	26890 ± 950	32176 ± 1042	32.2 ± 1.0	charcoal
Hv 25698*	26810 ± 200	32103 ± 261	32.1 ± 0.3	charcoal
Hv 25699*	23040 ± 600	27650 ± 696	27.7 ± 0.7	charcoal
Hv 25700*	27150 ± 910	32458 ± 986	32.5 ± 1.0	charcoal
Hv 25701*	25515 ± 1170	30602 ± 1390	30.6 ± 1.4	charcoal
Hv 25895	1510 ± 60	1391 ± 60	1.4 ± 0.1	molluscs
Hv 25896	16240 ± 200	19365 ± 202	19.4 ± 0.2	molluscs
Hv 25897	12950 ± 290	15073 ± 371	15.1 ± 0.4	molluscs
Hv 25898	24095 ± 900	28888 ± 1092	28.9 ± 1.1	molluscs
Hv 25899	24300 ± 455	29097 ± 571	29.1 ± 0.6	charcoal
Hv 25900	21765 ± 420	26156 ± 546	26.2 ± 0.6	charcoal
Hv 25901	20755 ± 640	24814 ± 836	24.8 ± 0.8	charcoal

4.4. Dating results

Altogether 37 luminescence and 13 radiocarbon samples were measured from the loess sequence on Susak to set up a chronological framework for the very detailed sediment archive. Results from the dosimetry, the equivalent doses, g-values, the uncorrected and corrected age estimates are given in Table 4.1. and the dating results are given in Fig. 4.7. The uncalibrated and calibrated radiocarbon dating ages are given in Table 4.2.

The uranium, thorium and potassium contents range from 2.17 to 4.74 ppm, 7.63 to 15.67 ppm and 1.14 to 1.91 %, respectively. The dose rates of the sediment for the fine-grained material range from 2.46 to 4.40 mGy/a, with a mean value of 3.53 ± 0.20 mGy/a which is typical for European loess (see Frechen et al., 1997; Galović et al., 2009; Novothny et al. 2009; Schmidt et al., 2010).

The D_e values from fine-grain feldspar are between 49.1 ± 2.5 Gy to 276.9 ± 14.0 Gy. For the samples collected at the Bok section, the D_e values show a systematic increase with depth, with a few exceptions and inversions. None of the dose response curves indicated luminescence signal saturation. The calculated age estimates are in good stratigraphic order. For the Sand Pit section the D_e values and the calculated ages are quite uniform with a slight increase of age with depth.

Fading corrections were performed for all samples indicating only low anomalous fading. The calculated g-values range from 1.3 to 2.7 %/decade which is very low compared to other locations (e.g. Serbian loess (Schmidt et al., 2010) or Hungarian loess (Novothny et al., 2010)). Fading corrections were done, and the uncorrected and corrected ages, as well as the g-values, are presented in Table 4.1.

At the Bok section an almost continuous increase of age with depth can be seen (Fig. 4.8.). The lowermost loess with the abundant carbonate accumulations and intercalated by the oldest tephra (TF1; Fig 4.5.a and 4.7.) yielded age estimates ranging from 98.3 ± 7.3 ka to 79.1 ± 5.7 ka. According to the IRSL dating results from the loess underlying and covering the oldest tephra (TF1), the age of the tephra is between 98.3 ± 7.3 ka and 93.3 ± 7.0 ka. The sample collected from the same loess horizon, but a few metres away from the investigated section gave an age of 79.1 ± 5.7 ka. This horizon is covered by an orange-brown palaeosol. The latter soil formation took place prior to 54.3 ±4.9 ka, which is the IRSL age of the loess

covering the orange-brown palaeosol. The next 4 metres of the sequence are made of three brown palaeosols, one of them containing the middle tephra (TF2; Fig. 4.5.b and 4.7.). In the middle part of this interval a sand layer is present, giving an IRSL age of 52.8 ± 4.0 ka. The age of the thin brown palaeosol with the tephra patches (TF2) is between 41.2 ± 3.6 ka and 39.0 ± 3.3 ka (Fig 4.5.b). Above this palaeosol about 20 metres of loess is exposed. The IRSL ages from the loess range from 39.0 ± 3.3 ka to 18.1 ± 1.4 ka, for the loess immediately covering the palaeosol with the tephra (TF2), and the stratigraphically youngest loess collected at this section, respectively. In this interval, four thin brown palaeosols, some of them with charcoal remains, and another tephra layer (TF3) (Fig. 4.5.c) are intercalated in the loess. IRSL age estimates from the loess below and above this thin tephra are between 31.0 ± 2.3 ka and 29.9 ± 2.2 ka. The radiocarbon ages of charcoal remains collected from the thin brown palaeosols gave calibrated ages of 26.2 ± 0.6 ka and 29.1 ± 0.6 ka and are in excellent agreement with the IRSL ages. The radiocarbon age of molluscs collected from below TF3 is in agreement with IRSL ages and calibrated radiocarbon ages from charcoal, whereas the mollusc sample taken from the top of TF3 shows an age of 15.1 ± 0.4 ka, which is very likely underestimated for this part of the sequence, probably due to contamination with younger mollusc species. Two mollusc samples were collected in the uppermost part of the section, from the youngermost exposed loess. The radiocarbon age of 19.4 ± 0.2 ka is in excellent agreement with the uppermost collected IRSL sample. The radiocarbon age of 1.4 ± 0.06 ka from molluscs collected on top of the section correlates to modern species which were very probably washed out from the modern soil.

Mikulčić Pavlaković et al. (2011) described a second section in the bay of Bok. At the Bok1 section, four luminescence samples were collected from the loess covering the orange brown palaeosol (Fig 4.7.). The IRSL age estimates range from 70.7 ± 6.3 ka to 63.5 ± 5.1 ka. This interval of the section - loess intercalated with brown palaeosol - gave a little higher ages than the stratigraphical equivalent at the Bok section. These horizons fill the time gap between the orange-brown palaeosol and the brown palaeosol at the Bok section and can hence be correlated with each other and interpolated. The differences between these two nearby sections could be a result of a different paleorelief evolution and possible erosion.

The Sand Pit section starts with a thick brown palaeosol which is covered by about 8 metres of loess. This loess gave age estimates ranging from 39.3 ± 3.4 ka to 33.6 ± 2.6 ka. The thin brown soil on the top of this loess horizon containing charcoal yielded a calibrated radiocarbon age of 32.5 ± 1.0 ka and is in excellent agreement with the IRSL ages. Loess is

covered by a few meters thick laminated sand horizon which gave an IRSL age estimate of 34.1 ± 3.1 ka. Within error limits, the age is in agreement with the calibrated radiocarbon age. Another sample from this laminated sand horizon was taken from the South wall of the investigated section and yielded an age of 38.1 ± 2.9 ka. The charcoal collected from the thin brown palaeosols, yielded radiocarbon ages ranging from 32.2 ± 1.0 ka to 24.8 ± 0.8 ka (Fig. 4.6. and 4.7.). A deposition of the laminated sand during a very short time period is very likely. The cross-laminated sand is of aeolian origin (Mikulčić Pavlaković et al., 2011) and probably represents a dune (Cremaschi, 1990). The upper part of the Sand Pit section consists of loess which is in its lower part intercalated by the youngest tephra (TF3; Fig. 4.5.c) and 4.7.). IRSL age estimates of the loess from below and above the tephra gave 28.0 ± 2.1 ka and 28.8 ± 2.1 ka, respectively, and within error limits correlate to the IRSL ages from samples taken from the stratigraphically same position at the Bok section. The uppermost sample collected from the Sand Pit section gave an IRSL age of 24.2 ± 1.8 ka. About ten metres of loess is still covering the investigated section, but unfortunately this part of the section was not reachable for sampling during our fieldwork. In Fig. 4.7., the IRSL and the radiocarbon dating results are presented. They show an excellent correlation for both sections.

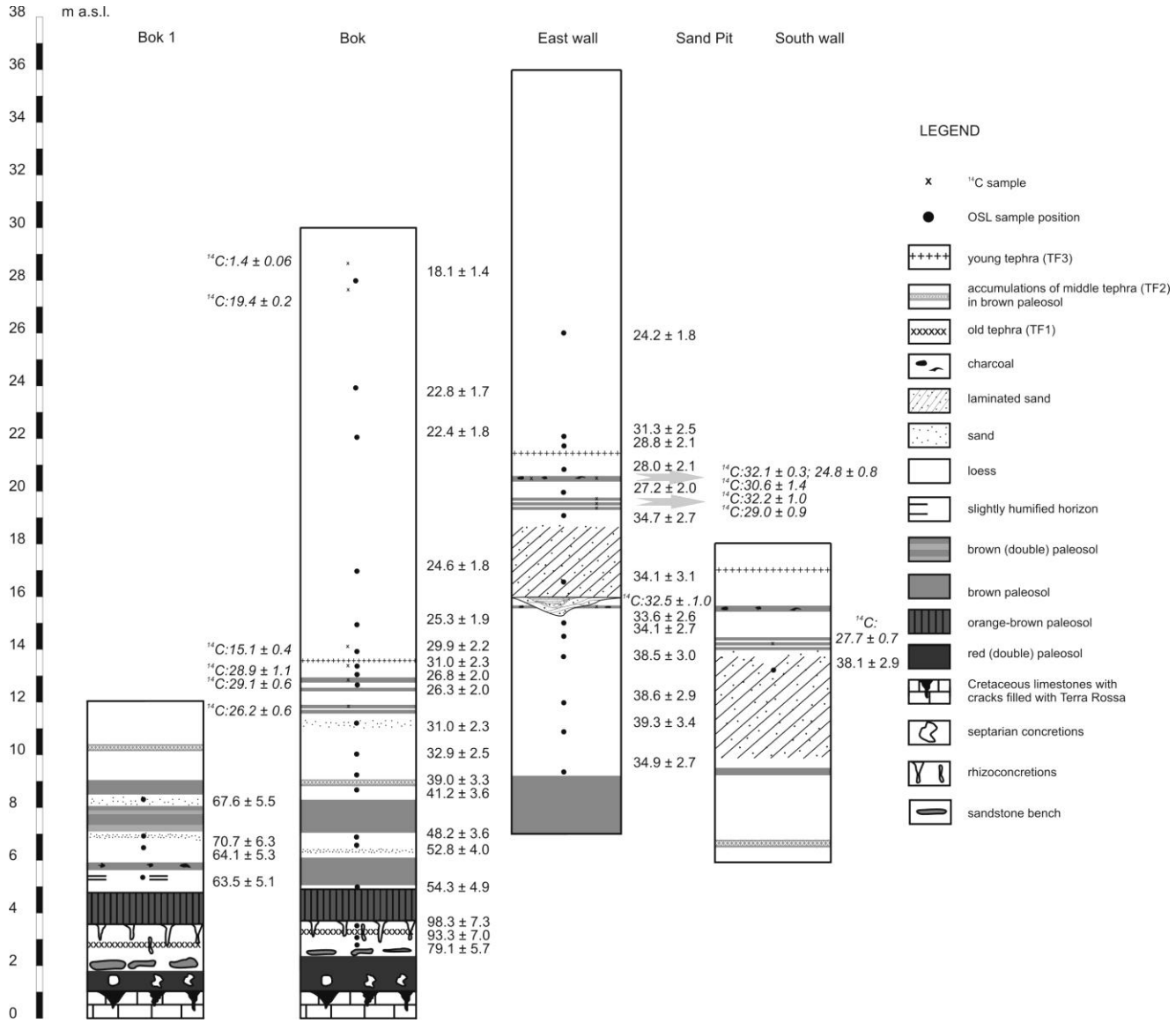

Figure 4.7. The investigated loess-palaeosol sections on Susak, with indicated IRSL and radiocarbon sampling positions and age estimates, and their correlation.

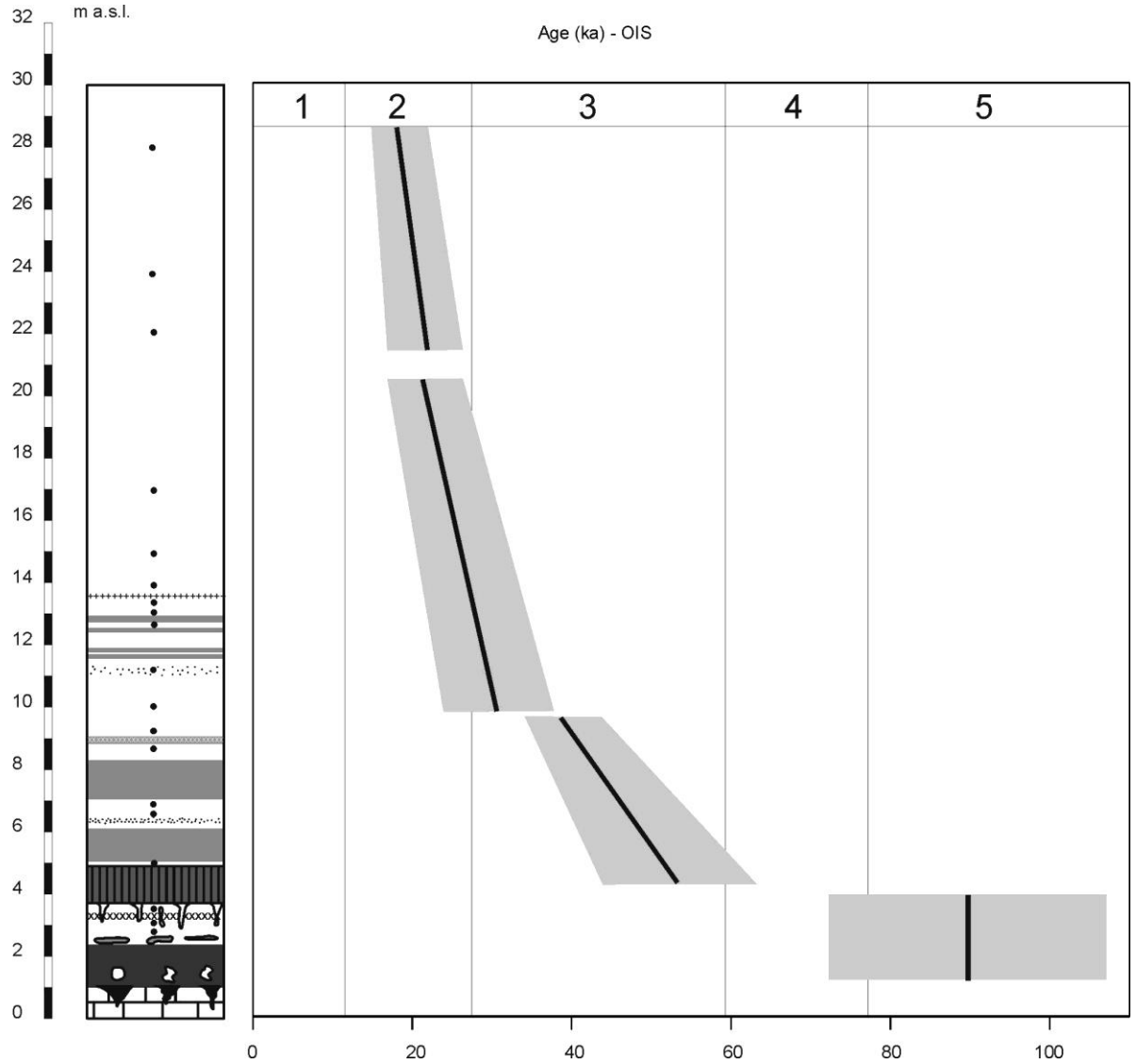

Figure 4.8. The sketch of all IRSL dating results from the Bok section. A continuous increase with depth is evident, showing an increased accumulation of loess during the OIS3. Part of the OIS4 deposits are missing in this section but can be found at the Bok1 section (see legend in Fig. 4.7.).

4.5. Discussion

Wacha et al. (2011) presented the first infrared stimulated luminescence (IRSL) dating results for the loess from Susak including thirteen samples. In their study a part of the loess-palaeosol sequence was investigated only from the easternmost part of the island. The present study gives an improved, precise and very detailed geochronological framework of the investigated loess-palaeosol sequence which resulted from denser sampling.

Wacha et al. (2011) used the single aliquot regenerative-dose (SAR) protocol on polymineral fine-grained material separated from loess for the determination of the equivalent doses (D_e). Furthermore, fading tests and fading corrections were carried out and a few samples were additionally measured using the older multiple aliquot additive-dose (MAAD) protocol for an easier correlation with previously published data, like recently published in Galović et al. (2009). The results showed that the loess-palaeosol record on Susak correlates to the Oxygen Isotope Stage (OIS) 3 with the fading corrected data ranging from 50.3 ± 3.5 ka to 27.5 ± 3.5 ka. The ages calculated after the MAAD protocols are between 38.0 ± 2.2 ka and 15.1 ± 1.1 ka and hence underestimating the results of the SAR measurements and the true deposition age of the deposits. Underestimation of these ages is expected due to the anomalous fading of feldspar infrared stimulated (IRSL) signals (Wintle, 1973; Spooner, 1994). Nevertheless, both protocols gave data which lead to the same conclusion, that the loess-palaeosol record on Susak is an amazing and very detailed OIS3 record. Mikulčić Pavlaković et al. (2011) presented four more IRSL ages from a further nearby section in the bay of Bok on Susak. This IRSL dating study used the same methodological approach as discussed in Wacha et al. (2011) as it proved to be successful. The IRSL ages range from 90.0 ± 6.8 ka to 80.8 ± 5.0 ka. The results presented in these previous publications do not cover the complete loess sequence but concentrate only on the middle part. Therefore, additional samples were collected with the aim to fill previous sampling gaps and to extend the numerical framework to the oldest and youngest deposits and so get a very detailed geochronological record of the last interglacial/glacial cycle.

The stratigraphically oldest soil found on the island is the fossil terra rossa, named that way by Bognar et al. (2003) (FTR according to Mikulčić Pavlaković et al., 2011), seen in the cracks of the limestone basement. Bognar et al. (2003) assumed the age of the fossil terra rossa to be 3 to 4 million years BP, but no evidence was provided for such statement. It is still

not known, i.e. there are still no exact data about the age of the thick red palaeosols which cover the carbonate basement of the island. Bognar et al. (2003) suggested that the red palaeosol presents the lower or the lowermost Pleistocene. Paleomagnetic measurements carried out by Bognar et al. (2003) showed negative inclination in the red palaeosol, so they correlated the apparent polarity change to the Brunhes-Matuyama boundary (0.78 Ma; Spell and McDougall, 1992; OIS19). They also correlated the red palaeosol with the Paks Double (PD) type palaeosol from the Hungarian loess stratigraphy. The PD type palaeosol belongs to the Hungarian "old loess series", also called Paks series, corresponding to OIS 9-24 (Pécsi, 1993). In loess from below this PD palaeosol in the type locality at the Paks section the Brunhes-Matuyama boundary was identified (Pécsi, 1993). There is no evidence for such pedostratigraphical correlation of palaeosols from Susak with palaeosols from Hungary key loess sections and hence this approach is questionable. Durn et al. (1999, 2007) and Durn (2003) investigated terra rossa and loess from Istria (Savudrija) and based on similarities with loess deposits on Susak described by Cremaschi (1990) tentatively proposed an Eemian age of the red palaeosol below the loess complex in Savudrija, but without any dating results. They also showed the importance of Late Pleistocene loess as parent material of these palaeosols in Istria. Mikulčić Pavlaković et al. (2011) concluded that the source material of the thick red palaeosol which covers the carbonate and can be seen in the basement of the loess sequence in the bay of Bok on Susak is of a predominantly aeolian origin (loess) with a minor influence of material remained after limestone karstification and that they are similar to Istrian terra rossa. Loess covering the red palaeosol on Susak showed age estimates ranging from 98.3 ± 7.3 ka to 79.1 ± 5.7 ka and so numerically correlates to OIS5c-a and 4, respectively. Based on these dating results, and the assumed aeolian origin of the red palaeosols covering the carbonate basement on Susak and similar red palaeosols below loess from Istria, we can conclude that soil formation on Susak took place during the last interglacial optimum or any older interglacial period and that loess deposited prior to OIS5e, probably in OIS6 or any other glaciation predating the Eemian. The OIS5 interglacial was marked by three distinct high sea level stands (Surić and Juračić, 2010). During OIS5e the sea level stand was the highest, up to a few meters higher than today (Lambeck and Chappell, 2001). The OIS5a is characterized by two sea level high stands, around 84 ka and 77 ka BP, with sea level above -14 m, and low sea-stand in between, at around 80 ka BP (Surić and Juračić, 2010). The sea level of the Adriatic Sea was about 100 metres lower than today (Cremaschi, 1990; Amorosi et al., 1999; Lambeck et al., 2004) during a part of the Upper

Pleistocene making the North Adriatic a vast basin exposed to various sedimentary processes as well as to aeolian activity during the glacials which resulted in loess deposition.

Red palaeosols are often reported to underlie loess in the Pannonian basin in Hungary (Kovács, 2008) and in China (e.g. Bronger and Heinkele, 1989) and are found on different rock type basements, representing the beginning of loess deposition. The origin of such palaeosols is still under discussion (e.g. Kovács, 2008) but the aeolian origin is probable (Yang and Ding, 2004). The age of these palaeosols very likely belongs to the Pliocene (Bronger and Heinkele, 1989; Ding et al., 1999; Kovács, 2008). Such red palaeosols are the result of specific climatic conditions and should be correlated only in that context. Correlating these palaeosols based only on their physical properties, without any dating results, can lead to wrong geochronological conclusions.

The age of the tephra (TF1) found in loess covering the red palaeosol is between 98.3 ± 7.3 ka and 93.3 ± 7.0 ka (Fig. 4.5.a). Based on these ages, the mineral and geochemical characteristics (Mikulčić Pavlaković et al., 2011), the tephra could be related to the Middle and South Italian volcanic provinces.

The oldest loess is covered by an orange-brown palaeosol up to 150 cm thick. The pedogenesis of this palaeosol took place after 93.3 ± 7.0 ka (or 79.1 ± 5.7 ka, if the sample Sus08-5 is considered, which was not collected directly from the investigated outcrops but a few meters away) and before 54.3 ± 5.7 ka, which is the age estimate from the thin loess horizon covering the thick orange-brown palaeosol in the Bok section. This orange-brown palaeosol is widespread over the island and with a more or less constant thickness. Bognar et al. (2003) correlated this orange-brown palaeosol with the Mende Base (MB)-type palaeosol from Hungarian stratigraphy. Wintle and Packman (1988) and Frechen et al. (1997) proved that the age of the MB palaeosol is significantly older than the last interglacial (OIS5e). At the Süttő section in Hungary, the OIS5 is represented by a MB-type palaeosol (Novothny et al., 2009). The results from this study discarded such correlation completely. The orange-brown palaeosol is covered by 4 to 5 metres thick loess. This loess is intercalated by brown palaeosols and sand layers and a thin brown palaeosol containing patches of the orange-yellow middle tephra (TF2). At the Bok section two, up to 100 cm thick, brown palaeosols are developed while at the Bok 1 section the situation differs. There, alterations of loess and sand are intercalated by two brown palaeosols, one of them containing charcoal pieces, and one double palaeosol i.e. a brown palaeosol directly overlain by another brown palaeosol. This horizon gave IRSL age estimates ranging from 54.3 ± 4.9 ka, measured from loess collected

between the orange-brown and the first brown palaeosol at the Bok section, and 41.2 ± 3.6 ka, sample collected below the TF2 containing palaeosol. At the Bok 1 section the IRSL age estimates showed slightly older ages ranging from 70.7 ± 6.3 ka to 63.5 ± 5.1 ka. Based on the IRSL results we can conclude that this sequence very likely correlates to OIS4. The differences between these two investigated sections are probably due to the differences in the paleorelief. It is very likely that a part of the record is missing at the Bok section. A layer of thin loess covering the orange-brown palaeosol at the Bok section might be the evidence for the later statement.

The brown palaeosol covering the thin loess horizon was correlated to the Basaharc Lower (BA)-type palaeosol from the Hungarian loess stratigraphy by Bognar et al. (2003). When compared to the new IRSL dating results of this study and data presented by Frechen et al. (1997), who showed that the BA palaeosol formed during the antepenultimate interglacial, such a statement can be discarded.

The IRSL age estimates of loess from below and above the palaeosol containing the middle tephra (TF2) range from 41.2 ± 3.6 ka and 39.0 ± 3.3 ka (Fig 4.5.b). This tephra layer was found on several locations on the island and hence is an excellent marker horizon for better correlation. The tephra layer was investigated by Mikulčić Pavlaković et al. (2011) and could be correlated to the Campanian Ignimbrite eruption of the Phlegraean Fields, which was dated around 39 ka (De Vivo et al., 2001).

On top of the palaeosol with TF2 patches about 20 metres of loess is exposed. In the lower part of this loess a sand layer and four thin brown palaeosols are present. The IRSL ages are in stratigraphic order, as presented in Figs. 4.7. and 4.8., showing a continuous loess deposition during OIS3. Four radiocarbon samples were collected: two charcoal samples from the thin brown palaeosols and two samples from loess molluscs. The radiocarbon ages are in agreement with the IRSL dating results. The youngest tephra (TF3) (Fig 4.5.c), which is exposed in this part of the sequence, has IRSL age estimates ranging from 31.0 ± 2.3 ka to 29.9 ± 2.2 ka and could be related to the Middle and South Italian volcanic provinces based on the geochemical analysis, mineral composition and vitroclast morphology (Mikulčić Pavlaković et al., 2011). The youngest sample collected from the top of the section, at the highest accessible position, gave an IRSL age estimate of 18.1 ± 1.4 ka and represents the loess accumulated during a period of increased dust accumulation most likely during the last glacial maximum (OIS2). This IRSL age is in agreement with the radiocarbon dating results of molluscs collected from loess.

The steep loess wall of the Sand Pit sections shows similarities with the upper part of the Bok section. There, only loess and laminated sand are exposed correlating to OIS3. The contact with the carbonate basement is not exposed; the sequence starts with a thick brown palaeosol which is older than 34.9 ± 2.7 ka and 39.3 ± 3.4 ka, which are IRSL age estimates of the loess covering the brown palaeosol. This palaeosol very likely correlates with the second brown palaeosol (the upper one) from the Bok section. At the Sand Pit section the middle tephra (TF2) was previously found in the South Wall but was not exposed during our fieldwork. The main difference between the two investigated sections (Bok and Sand Pit) is the predominance of cross-laminated sand in the Sand Pit section which probably represents a dune. Such aeolian sands are often seen on the islands in the Adriatic Sea (Marković-Marjanović, 1976; Borović et al., 1977; Korolija et al., 1977; Bognar et al., 1992; Pavelić et al., 2006) but they have scarcely been investigated (Pavelić et al., 2011). The sand on Susak very likely came from a proximal source. An erosional channel which was seen in the Sand Pit section on the East Wall was a result of local, short and intensive water activity. Four brown palaeosols containing charcoal remains, which can be seen in the lower part of the loess covering the dune sands, gave calibrated radiocarbon age estimates ranging from 32.2 ± 1.0 ka to 24.8 ± 0.8 ka and are in excellent agreement with IRSL dating results (Fig. 4.6.); the loess below the first palaeosol gave an IRSL age of 34.7 ± 2.7 ka and the loess above the fourth, the uppermost palaeosol yielded an IRSL age of 28.0 ± 2.1 ka. The youngest tephra layer (TF3) is clearly visible above the uppermost palaeosol. Its IRSL age estimates range from 28.8 ± 2.1 ka to 28.0 ± 2.1 ka and is in agreement with the IRSL ages from the samples collected at the Bok section. The uppermost collected loess gave an age estimate of 24.2 ± 1.8 ka and so correlates to OIS3. This sample location is covered by at least 10 metres of loess; this part of the sequence probably correlates to OIS2.

When comparing both major investigated sections, a strong similarity is evident. Minor differences are very likely due to the evolution and shape of the paleorelief. Such sediment succession is representative for the eastern part of the island and a similar situation was exposed on the southern part of the island. But still no outcrops are available on the northern and the western part, the part of the island which morphologically forms a plateau. It would be interesting to know the succession of the deposits in the thickest location and its relations to the carbonate basement. The question about the great thickness of the deposits and the sediment succession in the northern part of the island and its relation to the carbonate bedrock still remains open.

In northern Italy, the Val Sorda loess-palaeosol sequence is located in the river Po basin. Along the Danube, the Zmajevac section in eastern Croatia, Stari Slankamen and Surduk sections in Serbia and the Süttő section in Hungary were chosen for correlation and comparison (Fig. 4.9.). These sections were selected because of their detailed geochronological studies allowing a correlation with the last interglacial-glacial cycle. These two major loess areas differ in climatic conditions during periods of increased dust deposition in the Upper Pleistocene, hence providing different loess evolution.

If we place Susak in a wider perspective and compare it with coeval loess-palaeosol sequences from nearby regions, the most amazing thing is the great thickness of the deposits on such a small island in the Northern Adriatic Sea and the fact that such a sequence remained preserved. Loess has been found on other nearby islands in the area (Unije, Velike and Male Srakane, Lošinj), but only as a few metres thick local appearances. Durn et al. (1999, 2003) recognised the influence of Upper Pleistocene loess in upper parts of terra rossa profiles from Istria. Further north, in the river Po plain region, loess can also be found, but there no such amazing thicknesses have been registered. The most representative loess-palaeosol sequence in North Italy is the Val Sorda sequence (Ferraro et al., 2004, Ferraro, 2009; Fig. 4.9.). This section is about 6 metres thick, starts with a rubefied clayey palaeosol covering fluvioglacial deposits and consists of about 4 metres of loess intercalated by three chernosem palaeosols (Ferraro et al., 2004; Ferraro, 2009). Ferraro et al. (2004) concluded that the periods of loess deposition alternated with three stable phases of interstadial pedogenesis under steppe climate. Loess has been dated by means of radiocarbon and IRSL methods and gave age estimates ranging from 63.3 ± 6.7 ka to 18.7 ± 2.1 ka. These data presented in Ferraro (2009) were measured using the multiple aliquot additive dose (MAAD) method and may require a correction for anomalous fading. The published IRSL ages can be compared and are in agreement with those from the study on Susak. Dating results of artefacts from the Fumane Cave in Northern Italy, also containing loess, were correlated with the Aurignacian cultural layer which represents the OIS3 (Peresani et al., 2008). At the Bagaggera loess sequence TL dating results of artefacts also showed an OIS4 to OIS2 age (Cremaschi et al., 1990), with soil formation during most of OIS3. The rubefied clayey palaeosol at the bottom of the Val Sorda sequence can very likely be correlated with the red palaeosols covering the carbonate basement on Susak and the red palaeosol described in Savudrija in Istria (Durn et al., 2003). The OIS 5 (5e – Last Interglacial palaeosol) palaeosols in the Carpathian basin are usually chernozem-type palaeosols. At the Zmajevac section the second palaeosol from the top is correlated to OIS5 (Galović et al., 2009). In the Serbian stratigraphy the OIS5 palaeosol is

termed S1 and is also of chernozem-type (Antoine et al., 2009; Marković et al., 2007, 2009). In the Hungarian loess sections, the OIS5 palaeosol is a forest steppe-type palaeosol (Frechen et al., 1997; Novothny et al., 2002). At the Süttő section (Novothny et al., 2011), based on a detailed geochronological investigation and grain-size analysis, the palaeosols correlated to OIS5 were divided into interstadials and the reddish-brown palaeosol, below the chernozem-like palaeosol, was correlated to OIS5e (Fig. 4.9.). The overlying chernozem-like palaeosol was correlated to OIS5c, which was a warm and drier interstadial. The two thinner brown steppe-like palaeosols intercalated by a thin loess layer, indicate a shorter and/or less warm and humid interstadial period, most likely correlating to the 5a substage. The subdivision of the red palaeosols on Susak is still not possible; detailed investigations are required. These different palaeosol types in different geographical regions are a clear evidence for different paleoclimatic conditions during coeval periods.

In the Carpathian (Pannonian) basin OIS4 is represented only by loess deposition (Fig. 4.9.), while on Susak the Early Pleniglacial record is probably incomplete. A thin loess horizon intercalated with thin brown palaeosols and occasionally with sand is exposed at the Bok section. The loess covering the orange-brown palaeosol in the Bok 1 section (Fig 4.7.) can also be correlated to OIS4. Loess accumulation during OIS4 is also evidenced in the Val Sorda section in a small amount (Ferraro, 2009). Novothny et al. (2010b) reported an increase in sand content for the Lower Pleniglacial (OIS4) loess due to a colder and drier climate and increased wind intensity in Süttő.

In the Pannonian (Carpathian) basin OIS3 is characterised by soil development during the interstadials alternating with loess accumulation during stadials. In Zmajevac (Fig. 4.9.) in Eastern Croatia, one weakly developed palaeosol correlates to OIS3 (Galović et al., 2009). In loess from Serbia the middle pleniglacial (OIS3) is represented by a weakly developed palaeosol complex (called L1S1 in Serbian stratigraphy, Marković et al., 2004a, b, 2005, 2006, 2007, 2008, 2009). A single, weakly developed chernozem is described from the Ruma section (Marković et al., 2006), a weakly developed double palaeosol at the Petrovaradin brickyard (Marković et al, 2005), the Batajnica (Marković et al., 2009) and Irig sections (Marković et al., 2007) and multiple palaeosol at the Stari Slankamen (Schmidt et al., 2010) and Surduk (Antoine et al., 2009) sections (Fig. 4.9.). In Hungary, Novothny et al. (2011) reported a brown palaeosol in Süttő, previously termed MF1 in the Hungarian loess stratigraphy (Novothny et al., 2002; Frechen et al., 1997). On Susak, increased dust deposition interrupted by many soil forming periods is evidenced for the Middle Pleniglacial

period. In the bay of Bok on Susak at least five thin brown palaeosols are intercalated in the loess but it is even very likely that more of such weak palaeosols are present. Beside these weakly developed palaeosols, two thick brown palaeosols are present as well, possibly correlating with the Hengelo or Denekamp Interstadials of the NW European stratigraphy, both correlating to OIS3. The great thickness of the OIS3 deposits on Susak is the result of the generally increased dust accumulation in Europe (Frechen et al., 2003; Machalett et al., 2008) as well as a suitable geographical and morphological position in the North Adriatic basin, which was very likely a vast plateau with a large material input from the extended floodplain of the river Po and its tributaries. The numerous palaeosols give evidence that the climate on Susak was milder than in the Carpathian basin. Three brown palaeosols are described in the Val Sorda sequence in North Italy (Ferraro et al, 2004; Ferraro, 2009). Novothny et al. (2011) concluded that at Süttő the climate had an intermediate character, which was between the wetter climate in the Western European loess sequences and the drier loess successions in the southern Carpathian basin. A relatively "warmer" climate was proposed for the Irig section in Vojvodina by Marković et al. (2007). On Susak, loess deposition was continuous and intensive from OIS3 to 2, if compared with the Carpathian basin. Based on the numerous palaeosols found intercalating aeolian deposits on Susak an even "warmer" climate is assumed for the North Adriatic area.

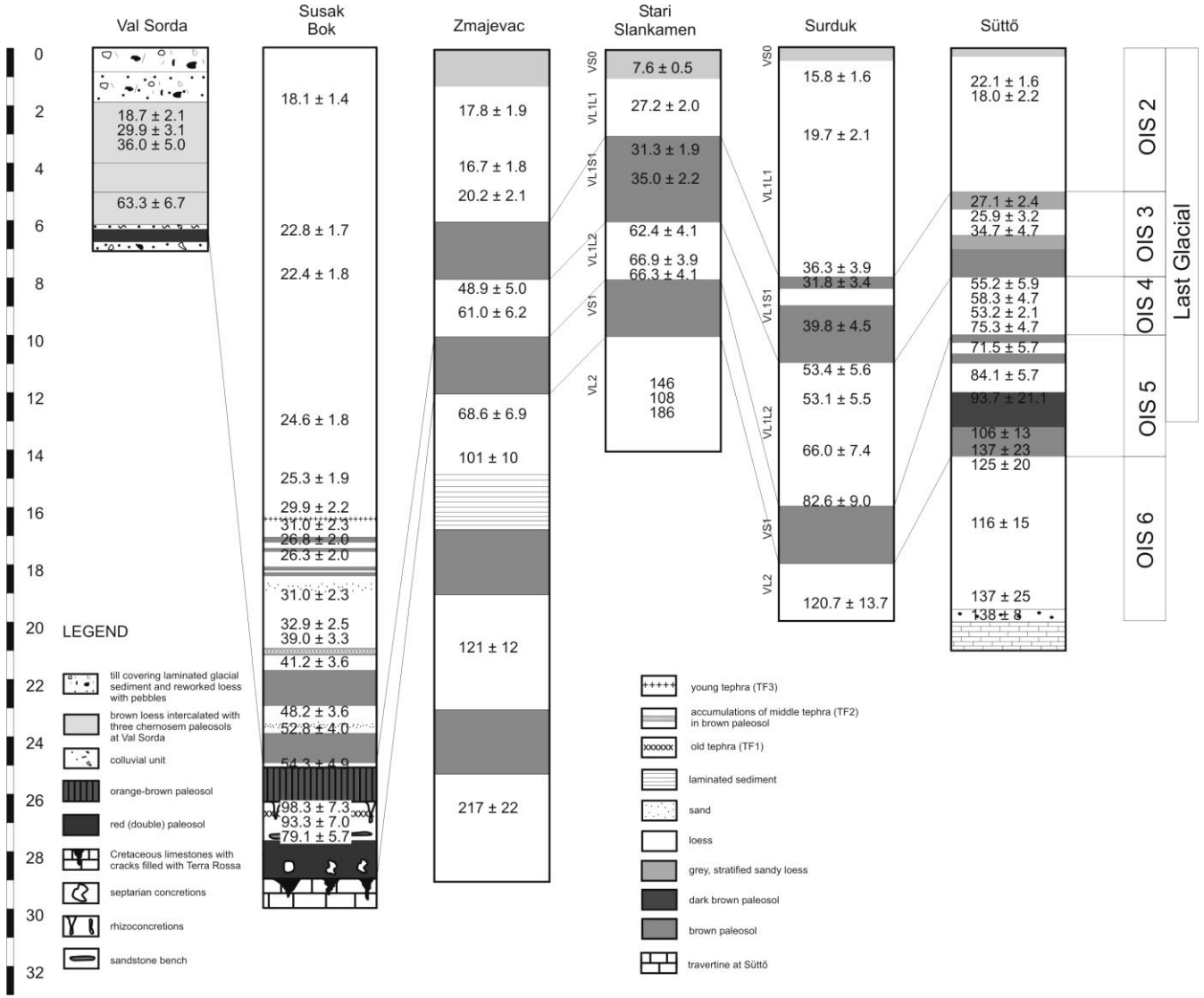

Figure 4.9. Bok section, selected to be the most representative section on Susak, correlated with the Val Sorda section in North Italy (Ferraro, 2009), Zmajevac in East Croatia (Galović et al., 2009), Stari Slankamen (Schmidt et al, 2010) and Surduk (Antoine et al., 2009; Fuchs et al., 2008) in Serbia and Süttő in Hungary (Novothny et al., 2009; 2010).

4.6. Conclusion

As a part of an ongoing multidisciplinary study, IRSL dating of loess-palaeosol sequences from Susak was applied to provide a detailed geochronological framework. The results indicate that the deposits on Susak are a very detailed Last Glacial-Interglacial record. Within error limits, the results are in stratigraphic order, showing a continuous record spanning from OIS5 (and possibly OIS6 or older) to OIS2. The most impressive sequence is the Middle Pleniglacial (OIS3) record, including evidence for intensive dust accumulation, interrupted by numerous soil forming processes and two volcanic events. The IRSL dating results are in excellent agreement with the radiocarbon dating results. Although dating results are consistent for both dating methods, a more precise method should be used for estimating the volcanic activity. The grain size of the tephras on Susak does not allow the use of the Ar-Ar dating method. Nevertheless, mineralogical and geochemical investigations of the tephras (Mikulčić Pavlaković et al., 2011) showed that the volcanism involved could be related to the Italian volcanic provinces. The red palaeosol covering the carbonate basement on Susak correlates at least to OIS5 but an older age is not excluded. A more detailed investigation regarding the age of the oldest exposed palaeosol is needed. Such red palaeosols are typical for the whole North Adriatic area.

If the loess record on Susak is correlated with the Danube loess-palaeosol sequences in the Carpathian basin, the differences are obvious. Loess deposition in the Carpathian basin was continuous, interrupted by interglacial or interstadial pedogenetical processes which are evident in thick continuous palaeosol layers. On Susak the deposition of aeolian sediment was more often interrupted by soil forming processes, as evidenced by the numerous palaeosols, some of them are well developed, some probably representing only initial pedogenesis. The same major climatic shifts during the Last Glacial are responsible for the development of the deposits on Susak, as in the Carpathian, Pannonian basin. The main difference is the aridity of the climate involved. The climate on Susak was very likely more humid and milder than in other regions.

The detailed geochronological framework presented in this work is an excellent base for future high-resolution investigations of climate proxies. Such studies are in progress.

The loess-palaeosol succession on Susak proves that the North Adriatic region is a separate and unique periglacial environment and should not be neglected when investigating the global Glacial-Interglacial evolution.

4.7. Acknowledgements

This research has been financed by the DAAD (German Academic Exchange Service); the Leibniz Institute for Applied Geophysics (LIAG), Hannover, Germany; the Croatian Ministry of Science, Education and Sports, Projects Nr. 0181001, 0183008 and 183-0000000-3201. This work could not be possible without the help of colleagues of S3 from LIAG, especially Linto Alappat and Alexander Kunz. The authors wish to thank Dr. Lidija Galović for many fruitful discussions and her support and to Ira Wacha-Biličić for correcting English. Help from Dr. Francesca Ferraro and Prof. Dr. Davor Pavelić, who supplied us with the needed literature, is appreciated. We are grateful to Prof. Dr. Goran Durn and Dr. Ágnes Novothny for their criticism and constructive comments of an earlier version of the manuscript.

4.8. References

Adamiec, G., Aitken, M.J., 1998. Dose-rate conversion factors: update. Ancient TL 16, 37-50.

Aitken, M.J., 1985. Thermoluminescence Dating. Academic Press, London, 351 pp.

Aitken, M.J., 1998. An introduction to optical dating. Oxford University Press, Oxford, 280 pp.

Amorosi, A., Colalongo, M.L., Pasini, G., Preti, D., 1999. Sedimentary response to Late Quaternary sea-level changes in the Romagna plain (northern Italy). Sedimentology 46, 99-121.

Antoine, P., Rousseau, D.D., Fuchs, M., Hatté, C., Gauthier, C., Marković, S.B., Jovanović, M., Gaudenyi, T., Moine, O., Rossignol, J., 2009. High-resolution record of the last climatic

cycle in the southern Carpathian Basin (Surduk, Vojvodina, Serbia). Quaternary International 198, 19-36.

Auclair, M., Lamothe, M., Huot, S., 2003. Measurement of anomalous fading for feldspar IRSL using SAR. Radiation Measurements 37, 487–492.

Bognar, A., 1979. Distribution, properties and types of loess and loess-like sediments in Croatia. Acta Geologica Academiae Scientiarium Hungaricae 22, 267-286.

Bognar, A., Klein, V., Tončić-Gregl, R., Šercelj, A., Magdalenić, Z., Culiberg, M., 1983. Kvartarne naslage otoka Suska i Baške na otoku Krku i njihovo geomorfološko značenje u tumačenju morfološke evolucije kvarnerskog prostora. Geografski glasnik 45, 7-32.

Bognar, A., Klein, V., Mesić, I., Culiberg, M., Bogunović, M., Sarkotić-Šlat, M., Horvatinčić, N., 1992. Quaternary sands at the south-eastern part of the Mljet Island. In: Bognar, A. (ed.): Proceedings of the International Symposium "Geomorphology and Sea" and the Meeting of the Geomorphological Commission of the Carpatho-Balcan Countries, 99-110; Zagreb (University of Zagreb).

Bognar, A., Zámbó, L., 1992. Some new data of the loess genesis on Susak island. In: Bognar, A. (ed.): Proceedings of the International Symposium ‘‘Geomorphology and Sea’’ and the Meeting of the Geomorphological Commission of the Carpatho-Balcan Countries, 65–72; Zagreb (University of Zagreb).

Bognar, A., Schweitzer, F., Kis, E., 2002. The Reconstruction of the Paleoenvironmental History of the Northern Adriatic Region Using of the Granulometric Properties of Loess Deposits on Susak Island, Croatia. Special issue of the fifth International Conference on geomorphology Loess and eolian dust 23/5, 795-810.

Bognar, A., Schweitzer, F., Szöőr, G., 2003. Susak – environmental reconstruction of a loess island in the Adriatic. Geographical Research Institute, Hungarian Academy of Sciences, Budapest, 141 pp.

Bokhorst, M., Vandenberghe, J., 2009. Validation of wiggle matching using a multi-proxy approach and its palaeoclimatic significance. Journal of Quaternary Science 24/8, 937-947.

Borović, I., Marinčić, S., Majcen, Ž., Magaš, N., 1977. Osnovna geološka karta SFRJ 1:100 000. Tumač za listove Vis K 33-33 Jelsa 33-34 Biševo 33-35. Institut za geološka istraživanja, Zagreb 1968, Savezni geološki zavod Beograd, Beograd, 67 pp.

Bøtter-Jensen, L., McKeever, S.W.S., Wintle, A.G., 2003. Optically stimulated luminescence dosimetry. Elsevier, Amsterdam, 355 pp.

Bronger, A., 1976. Zur quartaeren Klima- und Landschaftsentwicklung des Karpatenbeckens auf (palaeo)-pedologischer und bodengeographischer Grundlage. Kieler Geographische Schriften 45, Kiel, 268 pp.

Bronger, A., 2003. Correlation of loess-paleosol sequences in East and Central Asia with SE Central Europe: towards a continental Quaternary pedostratigraphy and paleoclimatic history. Quaternary International 106/107, 11–31.

Bronger, A., Heinkele, Th., 1989. Micromorphology and Genesis of Paleosols in the Luochuan Loess Section, China: Pedostratigraphic and Environmental Implications. Geoderma 45, 123-143.

Buylaert, J.P., Murray, A.S., Vandenberghe, D., Vriend, M., De Corte, F., Van den haute, P., 2008. Optical dating of Chinese loess using sand-sized quartz: Establishing a time frame for Late Pleistocene climate changes in the western part of the Chinese Loess Plateau. Quaternary Geochronology 3/1-2, 99-113.

Coudé-Gaussen, G., 1990. The loess and loess-like deposits along the sides of the western Mediterranean Sea: genetic and palaeoclimatic significance. Quaternary International 5, 1–8.

Cremaschi, M., 1987. Loess deposits of the Po plain and the adjoining Adriatic basin (Northern Italy). In: Pécsi, M. and French, H.D. (eds.): Loess and Periglacial Phenomena: 125-140, Akademiai Kiado, Budapest.

Cremaschi, M., 1990. Stratigraphy and palaeoenviromental significance of the loess deposits on Susak Island (Dalmatian archipelago). Quaternary International 5, 97-106.

Cremaschi, M., Fedoroff, N., Guerreschi, A., Huxtable, J., Colombi, N., Castelletti, L., Maspero, A., 1990. Sedimentary and pedological processes in the Upper Pleistocene loess of North Italy. The Bagaggera sequence. Quaternary International 5, 23-38.

De Vivo, B., Rolandi, G., Gans, P.B., Calvert, A., Bohrson, W.A., Spera, F.J., Belkin, H.E., 2001. New constraints on the pyroclastic eruptive history of the Campanian volcanic Plain (Italy). Mineralogy and Petrology 73, 47-65.

Ding, Z.L., Xiong, S.F., Sun, J.M., Yang, S.L., Gu, Z.Y., Liu, T.S., 1999. Pedostratigraphy and paleomagnetism of a ~7.0 Ma eolian loess–red clay sequence at Lingtai, Loess Plateau,

north-central China and the implications for paleomonsoon evolution. Palaeogeography, Palaeoclimatology, Palaeoecology 152, 49–66.

Durn, G., Ottner, F., Slovenec, D., 1999. Mineralogical and geochemical indicators of the polygenetic nature of terra rossa in Istria, Croatia. Geoderma 91/1–2, 125–150.

Durn, G., 2003. Terra rossa in the Mediterranean region: Parent materials, composition and origin. Geologia Croatica 56/1, 83-100.

Durn, G., Ottner, F., Tišljar, J., Mindszenty, A., Barudžija, U., 2003. Regional Subaerial Unconformities in Shallow-Marine Carbonate Sequences of Istria: Sedimentology, Mineralogy, Geochemistry and Micromorphology of Associated Bauxites, Palaeosols and Pedo-sedimentary Complexes. In: Vlahović, I. and Tišljar, J. (eds): Evolution of depositional environments from the Palaeozoic to the Quaternary in the Karst Dinarides and the Pannonian Basin. Field trip guidebook of the 22nd IAS Meeting of Sedimentology, Institute of Geology, Zagreb, 209-255.

Durn, G., Aljinović, D., Crnjaković, M., Lugović, B., 2007. Heavy and light mineral fractions indicate polygenesis of extensive terra rossa soils in Istria, Croatia. In: Mange, M. and Wright, D. (eds.): Heavy Minerals in Use, Developments in Sedimentology 58, Elsevier, Amsterdam, 701–737.

Fairbanks, R.G., Mortlock, R.A., Chiu, T.-C., Cao, L., Kaplan, A., Guilderson, T.P., Fairbanks, T.W., Bloom, A.L., 2005. Marine radiocarbon calibration curve spanning 0 to 50,000 years B.P. based on paired 230Th/234U/238U and 14C dates on pristine corals. Quaternary Science Reviews 24, 1781–1796.

Ferraro, F., 2009. Age, sedimentation and soil formation in the Val Sorda loess sequence, Northern Italy. Quaternary International 204, 54-64.

Ferraro, F., Terhorst, B., Ottner, F., Cremaschi, M., 2004. Val Sorda: an upper Pleistocene loess–palaeosol sequence in northeastern Italy. Revista Mexicana de Ciencias Geológicas 24/1, 30–47.

Fortis, A., 1771. Saggio d´osservazioni sopra l´isola di Cherso ed Osero. Venezia, 167 pp.

Frechen, M., Horváth, E., Gábris, G., 1997. Geochronology of Middle and Upper Pleistocene loess sections in Hungary. Quaternary Research 48/3, 291–312.

Frechen, M., Oches, E.A., Kohfeld, K.E., 2003. Loess in Europe - mass accumulation rates during the Last Glacial Period. Quaternary Science Reviews 22/18–19, 1835–1857.

Fuchs, M., Rousseau, D.-D., Antoine, P., Hatté, C., Gauthier, C., Marković, S., Zoeller, L., 2008. Chronology of the Last Climatic Cycle (Upper Pleistocene) of the Surduk loess sequence, Vojvodina, Serbia. Boreas 37, 66-73.

Galović, L., Frechen, M., Halamić, J., Durn, G., Romić, M., 2009. Loess chronostratigraphy in Eastern Croatia - A first luminescence dating approach. Quaternary International 198/1-2, 85 -97.

Galović, I., Mutić, R., 1984. Gornjopleistocenski sedimenti istočne Slavonije (Hrvatska). Rad JAZU 411, 299–356, Zagreb.

Geyh, M.A., 1990. ^{14}C dating of loess. Quaternary International 7/8, 115-118.

Geyh, M.A., 2005. ^{14}C dating - still a challenge for users? Zeitschrift für Geomorphologie, Neue Folge, Supplementband 139, 63–86.

Gorjanović-Kramberger, D., 1912. Iz prapornih predijela Slavonije. Vijesti geološkog povjerenstva 2, 28–30, Zagreb.

Gorjanović-Kramberger, D., 1915. Die Hydrographischen Verhältnisse der Lössplateaus Slavoniens. Glasnik hrvatskoga prirodoslovnoga društva 27, 70-75 Zagreb.

Gorjanović-Kramberger, D., 1922. Morfologijske i hidrografijske prilike prapornih predjela Srijema, te pograničnih česti županije virovitičke. Glasnik hrvatskoga prirodoslovnoga društva 34, 111-164, Zagreb.

Greenland Ice-Core Project (GRIP) Members, 1993. Climate instability during the last interglacial period recorded in the GRIP ice core. Nature 364, 203–207.

Huntley, D. J., Lamothe, M., 2001. Ubiquity of anomalous fading in K-feldspars, and the measurement and correction for it in optical dating. Canadian Journal of Earth Sciences 38, 1093-1106.

Kalac, K., Bajraktarević, Z., Marković, Z., Barbić, Z., Gušić, I., 1995. Stratigrafija pliocensko-pleistocenskih sedimenata u bušotinama podmorja Jadrana. In: Vlahović, I., Velić, I., Šparica, M.: Proceedings of the First Croatian Geological Congress 1, 281-284, Croatian Geological Institute, Zagreb.

Kišpatić, M., 1910. Der Sand von der Insel Sansego (Susak) bei Lussin und dessen Herkunft. Verhandlungen geologischer Reichsanstalt 13, 294-305, Wien.

Korolija, B., Borović, I., Marinčić, S., Jagačić, T., Magaš, N., Milanović, M., 1977. Osnovna geološka karta SFRJ 1:100 000. Tumač za list Lastovo K 33-46 Korčula K 33-47 Palagruža K 33-57, Institut za geološka istraživanja Zagreb 1968, Savezni geološki zavod Beograd, Beograd, 53 pp.

Kovács, J., 2008. Grain-size analysis of the Neogene red clay formation in the Pannonian Basin. International Journal of Earth Sciences 97, 171-178.

Lambeck, K., Chappell, J., 2001. Sea level change through the Last Glacial Cycle. Science 292, 679-686.

Lambeck, K., Antonioli, F., Purcell, A., Silenzi, S., 2004. Sea-level change along the Italian coast for the past 10.000 yr. Quaternary Science Reviews 23, 1567-1598.

Lu, Y.C., Wang, X.L., Wintle, A.G., 2007. A new OSL chronology for dust accumulation in the last 130,000 yr for the Chinese Loess Plateau. Quaternary Research 67, 152–160.

Lužar-Oberiter, B., Mikulčić Pavlaković, S., Crnjaković, M., Babić, Lj., 2008. Variable sources of beach sands of north Adriatic islands: examples from Rab and Susak. Geologia Croatica 61/2-3, 379-384.

Machalett, B., Oches, E.A., Frechen, M., Zöller, L., Hambach, U., Mavlyanova, N.G., Marković, S.B., Endlicher, W., 2008. Aeolian dust dynamics in central Asia during the Pleistocene: Driven by the long-term migration, seasonality, and permanency of the Asiatic polar front. Geochemistry, Geophysics, Geosystems 9, Q08Q09.

Mamužić, P., 1965. Osnovna geološka karta SFRJ 1:100 000. List Lošinj L 33-155. Institut za geološka istraživanja, Zagreb, Savezni geološki zavod, Beograd.

Mamužić, P., 1973. Osnovna geološka karta SFRJ 1:100 000. Tumač za list Lošinj L 33-155. Institut za geološka istraživanja, Zagreb, Savezni geološki zavod, Beograd, Beograd, 34 pp.

Marchesetti, C., 1882. Cenni geologici sul'isola di Sansego. Bollettino della Societa´ adriatica di Scienze Naturali 7, 289-304, Trieste.

Marković, S.B., Kostić, N.S., Oches, E.A., 2004a. Palaeosols in the Ruma loess section (Vojvodina, Serbia). Revista Mexicana de Ciencias Geológicas 21, 79–87.

Marković, S.B., Oches, E.A., Gaudenyi, T., Jovanović, M., Hambach, U., Zöller, L., Sümegi, P., 2004b. Paleoclimate record in the late Pleistocene loess-palaeosol sequence at Miseluk (Vojvodina, Serbia). Quaternaire 15, 361–368.

Marković, S.B., McCoy, W.D., Oches, E.A., Savić, S., Gaudenyi, T., Jovanović, M., Stevens, T., Walther, R., Ivanisević, P., Galić, Z., 2005. Paleoclimate record in the upper Pleistocene loess-palaeosol sequence at Petrovaradin brickyard (Vojvodina, Serbia). Geologica Carpathica 56, 545–552.

Marković, S.B., Oches, E., Sümegi, P., Jovanović, M., Gaudenyi, T., 2006. An introduction to the middle and upper Pleistocene loess-palaeosol sequence at Ruma brickyard, Vojvodina, Serbia. Quaternary International 149, 80–86.

Marković, S.B., Oches, E.A., McCoy, W.D., Frechen, M., Gaudenyi, T., 2007. Malacological and sedimentological evidence for ‘‘warm’’ glacial climate from the Irig loess sequence, Vojvodina, Serbia. Geochemistry Geophysics Geosystems 8, Q09008.

Marković, S.B., Bokhorst, M.P., Vandenberghe, J., McCoy, W.D., Oches, E.A., Hambach, U., Gaudenyi, T., Jovanović, M., Stevens, T., Zöller, L., Machalett, B., 2008. Late Pleistocene loess-palaeosol sequences in the Vojvodina region, North Serbia. Journal of Quaternary Science 23/1, 73–84.

Marković, S.B., Hambach, U., Catto, N., Jovanović, M., Buggle, B., Machalett, B., Zöller, L., Glaser, B., Frechen, M., 2009. The middle and late Pleistocene loess palaeosol sequences at Batajanica, Vojvodina, Serbia. Quaternary International 198, 255–266.

Marković-Marjanović, J., 1976. Kvartarni sedimenti ostrva Hvara – Srednji Jadran. Glasnik prirodnjačkog muzeja A/31, 199-214, Beograd.

Mikulčić Pavlaković, S., Crnjaković, M., Tibljaš, D., Šoufek, M., Wacha, L., Frechen, M., Lacković, D., 2011. Mineralogical and Geochemical Characteristics of Quaternary Sediments from the Island of Susak (Northern Adriatic, Croatia). Quaternary International 234, 1-2, 32-49.

Mutić, R., 1967. Pijesak otoka Suska. Geološki Vjesnik 20, 41–57.

Mutić, R., 1990. Korelacija kvartara istočne Slavonije na osnovi podataka mineraloško-petrografskih analiza (Istočna Hrvatska, Jugoslavija) - Dio II: Lesni ravnjak. Acta Geologica 20/2, 29–80, Zagreb.

Novothny, Á., Horváth, E., Frechen, M., 2002. The loess profile at Albertirsa, Hungary - improvements in loess stratigraphy by luminescence dating. Quaternary International 95–96, 155–163.

Novothny, Á., Frechen, M., Horváth, E., Bradák, B., Oches, E.A., McCoy, W.D., Stevens, T., 2009. Luminescence and amino acid recemization chronology of the loess-palaeosol sequence at Süttő, Hungary. Quaternary International 198/1-2, 62-76.

Novothny, Á., Frechen, M., Horváth, E., Krbetschek, M., Tsukamoto, S., 2010. Infrared stimulated luminescence and radiofluorescence dating of aeolian sediments from Hungary. Quaternary Geochronology 5, 114-119.

Novothny, A., Frechen, M., Horváth, E., Wacha, L., Rolf, C., 2011. High resolution grain size and magnetic susceptibility record of the (penultimate and) last glacial cycles in the Süttő loess section, Hungary. Quaternary International 234, 1-2, 75-85.

Pavelić, D., Kovačić, M., Vlahović, I., 2006. Periglacial aeolian-alluvial interaction: Pleistocene of the Island of Hvar (Eastern Adriatic, Croatia). In: Hoyanagi, K., Takano, O. and Kano, K. (eds.): From the Highest to the Deepest. Abstracts book of the 17th International Sedimentological Congress, Volume A, Fukuoka.

Pavelić, D., Kovačić, M., Vlahović, I., Wacha, L., 2011. Pleistocene calcareous aeolian-alluvial deposition in a steep relief karstic coastal belt (Island of Hvar, eastern Adriatic, Croatia). Sedimentary Geology, doi: 10.1016/j.sedgeo.2011.05.005.

Pécsi, M., 1990. Loess is not just the accumulation of dust. Quaternary International 7/8, 1-21.

Pécsi, M., 1993. Quaternary and loess research. In: Bassa, L., Keresztesi, Zs., Lóczy, D. (eds.): Loess in Form, 2, Hungarian Academy of Science, Budapest, 82 pp.

Peresani, M., Cremaschi, M., Ferraro, F., Falguères, C., Bahain, J.-J., Gruppioni, G., Sibilia, E., Quarta, G., Calcagnile, L., Dolo, J.-M., 2008. Age of the final Middle Palaeolithic and Uluzzian levels at Fumane Cave, Northern Italy, using 14C, ESR, 234U/230Th and thermoluminescence methods. Journal of Archaeological Science 35, 2986–2996.

Poje, M., 1985. Praporne naslage vukovarskog profila i njihova stratigrafska pripadnost. Geološki Vjesnik 38, 45–66.

Poje, M., 1986. Ekološke promjene na vukovarskom prapornom ravnjaku proteklih cca 500.000 godina. Geološki Vjesnik 39, 19–42.

Prescott, J.R., Hutton, J.T., 1994. Cosmic ray contributions to dose rates for luminescence and ESR dating: large depths and long-term time variations. Radiation Measurements 23, 497-500.

Preusser, F., Degering, D., Fuchs, M., Hilgers, A., Kadereit, A., Klasen, N., Krbetschek, M., Richter, D., Spencer, J.Q.G., 2008. Luminescence dating: basics, methods and applications. Eiszeitalter und Gegenwart (Quaternary Science Journal) 57/1-2, 95-149.

Preusser, F., Chithambo, M.L., Götte, T., Martini, M., Ramseyer, K., Sendezera, E.J., Susino, G.J., Wintle, A.G., 2009. Quartz as a natural luminescence dosimeter. Earth-Science Reviews 97, 184-214.

Rees-Jones, J., 1995. Optical dating of young sediments using fine-grain quartz. Ancient TL 13, 9–14.

Roberts, H.M., 2008. The development and application of luminescence dating to loess deposits: a perspective on the past, present and future. Boreas 37, 483-507.

Roberts, H.M., Muhs, D.R., Wintle, A.G., Duller, G.A.T., Bettis III, E.A., 2003. Unprecedented last-glacial mass accumulation rates determined by luminescence dating of loess from western Nebraska. Quaternary Research 59, 411–419.

Schmidt, E., Machalett, B., Marković, S.B., Tsukamoto, S., Frechen, M., 2010. Luminescence chronology of the upper part of the Stari Slankamen loess sequence (Vojvodina, Serbia). Quaternary Geochronology 5, 137-142.

Singhvi, A.K., Bronger, A., Sauer, W., Pant, R.K., 1989. Thermoluminescence dating of loess-paleosol sequences in the Carpathian basin (East-Central Europe): a suggestion for a revised chronology. Chemical Geology: Isotope Science Section 73, 307–317.

Spell, T.L., McDougall, I., 1992. Revisions to the age of the Brunhes - Matuyama Boundary and the Pleistocene geomagnetic polarity timescale. Geophysical Research Letters 19/12, 1181–1184.

Spooner, N.A., 1994. The anomalous fading of infrared-stimulated luminescence from feldspars. Radiation Measurements 23, 2/3, 625-632.

Stevens, T., Lu, H., Thomas, D.S.G., Armitage, S.J., 2008. Optical dating of abrupt shifts in the late Pleistocene East Asian Monsoon. Geology 36/5, 415-418.

Surić, M., Juračić, M., 2010. Late Pleistocene-Holocene environmental changes – records from submerged speleothems along the Eastern Adriatic coast (Croatia). Gelogia Croatica 63/2, 155-169.

Šandor, F., 1912. Istraživanja prapora iz Vukovara, Bilo gore i sa Rajne. Vijesti geološkog povjerenstva 2, 103-107, Zagreb.

Šandor, F., 1914. Praporasti nanos otoka Suska. Vijesti geološkog povjerenstva Hrvatske i Slavonije 3-4, Zagreb.

Van Straaten, L.M.J.U., 1970. Holocene and Late Pleistocene sedimentation in the Adriatic Sea. Geologische Rundschau 60, 106-131.

Wacha, L., Mikulčić Pavlaković, S., Novothny Á., Crnjaković, M., Frechen, M., 2011. Luminescence Dating of Upper Pleistocene Loess from the Island of Susak in Croatia. Quaternary International 234, 1-2, 50-61.

Wacha, L., Rolf, C., Frechen, M., Galović, L., Duchoslav, M., Hambach, U. The OIS 3 loess record on Susak: the high resolution grain-size, rock magnetic and palaeomagnetic approach. (in preparation).

Wein N., 1977. Die Lössinsel Susak - eine naturgeographische Singularität in der jugoslawischen Inselwelt. Petermanns geographische Mitteilungen 2, 123-132, Gotha/Leipzig.

Wintle, A.G., 1973. Anomalous fading of thermoluminescence in mineral samples. Nature 245, 143–144.

Wintle, A.G., 1997. Luminescence dating: laboratory procedures and protocols. Radiation Measurements 27, 769–817.

Wintle, A.G., Packman, S.C., 1988. Thermoluminescence ages for three sections in Hungary. Quaternary Science Reviews 7, 315–320.

Yang, S.L., Ding, Z.L., 2004. Comparison of particle size characteristics of the Tertiary “red clay” and Pleistocene loess in the Chinese Loess Plateau: implications for origin and sources of the “red clay”. Sedimentology 51, 77-93.

CHAPTER 5

Quaternary International, doi: 10.1016/j.quaint.2011.04.010

The Geochronology of the "Gorjanović loess section" in Vukovar, Croatia

Lara Wacha[1, 2], Manfred Frechen[2]

[1] Croatian Geological Survey, Sachsova 2, HR-10000 Zagreb, Croatia

[2] Leibniz Institute for Applied Geophysics, S3 Geochronology and Isotope Hydrology, Stilleweg 2, D-30655 Hannover, Germany

Abstract

Along the right bank of the Danube River in Croatia up to 30 m thick loess-palaeosol sequences are exposed. A detailed geochronological study was performed on the "Gorjanović loess section" at Vukovar by the means of infrared stimulated luminescence (IRSL) dating. The section consists of loess intercalated by three palaeosols and a tephra layer. Fourteen samples were collected and dated using the elevated temperature post-IR IRSL protocol, a modified single aliquot regenerative dose (SAR) protocol, for the equivalent dose (D_e) determination on fine-grained polymineral material. Both the IRSL signal at 50°C as well as the post-IR IRSL signal at 225°C were recorded. Fading tests were performed for both signals and the ages were fading corrected. The loess/palaeosol sequence can be correlated to the penultimate glacial – last interglacial - last glacial period (OIS6 – OIS2). An even older loess record at the site under study was previously described but is not exposed anymore owing to the embankment. The fading corrected IRSL and the fading corrected post-IR IRSL results are in excellent agreement. The post-IR IRSL signal at 225°C shows less fading than the IRSL signal at 50°C and can successfully be used for the dating of older loess.

Keywords: Gorjanović loess section, Vukovar, Croatia, luminescence dating, post-IR IRSL protocol, fading

5.1. Introduction

Loess-palaeosol sequences give evidence for Quaternary climatic changes and can be used for the reconstructions of atmospheric dust flux, palaeotemperature and palaeoprecipitation (Zoeller, 2010, and papers therein) applying high-resolution sampling and multi-proxy analytical approaches by means of granulometry, stable isotopes and environmental magnetism (Antoine et al., 2009; Bokhorst and Vandenberghe, 2009; Bokhorst et al., 2011; Novothny et al., 2011). A reliable and robust chronology is of major importance for a quantitative interpretation of such high-resolution multi-proxy data. Luminescence dating method is the most appropriate approach when it comes to establishing a reliable chronological framework for loess-palaeosol sequences (Roberts, 2008; Frechen et al., 1997; Novothny et al., 2002, 2009, 2010; Schmidt et al., 2010; Fuchs et al., 2008; Galović et al., 2009; Wacha et al., 2010a, 2011). Furthermore, the latter dating method is applicable for a wide span of ages, ranging from a few years (Ballarini et al., 2003; Kunz et al., 2010) to several hundred thousand years (Thiel et al., 2010b, c, submitted).

The "Gorjanović loess section" is an about 30 m high loess-palaeosol sequence exposed along the Danube in Vukovar, Croatia (Fig. 5.1.). It has been a matter of interest since the last century (Gorjanović-Kramberger, 1912, 1914, 1915, 1922) and because of that and its location; it was selected for a detailed geochronological study. Furthermore, the loess palaeosol sequence from Vukovar is as detailed as those loess records investigated in detail further downstream the Danube and thus does act as a Pleistocene key site in Croatia.

The first detailed investigations of the Vukovar loess-palaeosol section, as well as loess exposures in the surrounding area, and a preliminary chronological interpretation were done by Gorjanović-Kramberger in the first half of the twentieth century (Gorjanović-Kramberger, 1910, 1912, 1914, 1915, 1922). His primary interest were the hydrographical properties of the deposits. Furthermore, in his work Gorjanović-Kramberger divided the loess area of eastern Croatia into smaller units (plateaus) and correlated the changes in the quite uniform loess deposits ("brown zones spreading through the loess plateau") to changing climatic conditions (Gorjanović-Kramberger, 1910, 1922). He also proposed a hypothetical age of the sediments. He concluded that, if loess in China is 200-600 metres thick and 2000 year-old graves are covered with 2 meters of loess which very likely indicates that the complete loess coverage in China is about 200,000 years old, than loess in Eastern Croatia, which is about 30 metres

thick, must be 20,000-30,000 years old or even older if the dust, which fell into swamps and lakes, is taken into account in such hypothetical calculations. In China, loess began to accumulate around the Gauss-Matuyama palaeomagnetic boundary which is around 2.58 Ma (Liu et al., 1993). In the same study, Gorjanović-Kramberger (1922) also correlated several loess-palaeosol sequences from the Srijem area in Serbia and Croatia. Besides Gorjanović-Kramberger (1922), the loess-palaeosol sequence in Vukovar, near the St. Filip and Jacob's church and the water tower (Fig. 5.1. and 5.2.), was investigated by means of mineralogy, palaeontology, pedology, palaeoclimatology etc., by Šandor (1912), Bronger (1976, 2003), Rukavina (1983), Galović and Mutić (1984), Poje (1985, 1986) and Mutić (1990). Galović and Mutić (1984) presented radiocarbon ages of carbonate concretions found in loess from the Vukovar loess section yielding ^{14}C ages between 33,000 years and 16,000 years. But these ages very likely do not present the actual depositional age of the sediment because carbonate concretions can be formed long after the deposition of loess, which would give too small apparent ages, or they can contain fossil carbonate which would give a too large age (Geyh, 1990). Furthermore, the upper age limit of the method is around 45,000 years (Walker, 2005).

The first numerical dating approach of loess-palaeosol sequences in Croatia by means of the thermoluminescence (TL) dating method was presented by Singhvi et al. (1989). More recently infrared stimulated luminescence (IRSL) dating was applied on loess from Eastern Croatia by Galović et al. (2009). Wacha et al. (2010a, 2011) presented a detailed geochronological framework of the loess-palaeosol sequence from the island of Susak in the North Adriatic Sea. These two studies were the first high resolution geochronological investigations of loess deposits in Croatia and in the North Adriatic region. A detailed geochronology is mandatory for any future research and correlation with other loess regions and sedimentary environments. The aim of this research is to propose a detailed and reliable geochronological framework for the Gorjanović loess section (first called that way by Galović and Mutić (1984)) in Vukovar based on the luminescence dating method which will be a base for future multidisciplinary research. Furthermore, the results will be correlated with data from loess-palaeosol sequences in the region (Serbia and Hungary). Results presented in this work are the first part of an ongoing study.

5.2. Geological setting and the sediment succession

In Croatia, the thickest Quaternary deposits can be found in the Eastern part of the country (Fig. 5.1.) including clastic deposits, fluvial and alluvial sediments, marsh and lake deposits (Fig. 5.2.). During the Pleistocene glacial times a large amount of dust was available which was transported by wind and subsequently deposited covering river and lake sediments and forming loess plateaus at the confluences of large river systems, such as the Danube along with the Drava and Sava rivers in Eastern Croatia. Along the Danube River in the Pannonian basin, the thickness of such deposits varies between 0.5 m and about 60 m (Bognar, 1979). In the eastern part of Croatia the Vukovar loess plateau continues into the Fruška gora (gora=mountain) where numerous loess-palaeosol sequences were recently described and investigated by Marković et al. (2004a, b; 2005; 2006; 2007; 2008; 2009) and a detailed loess stratigraphy is established.

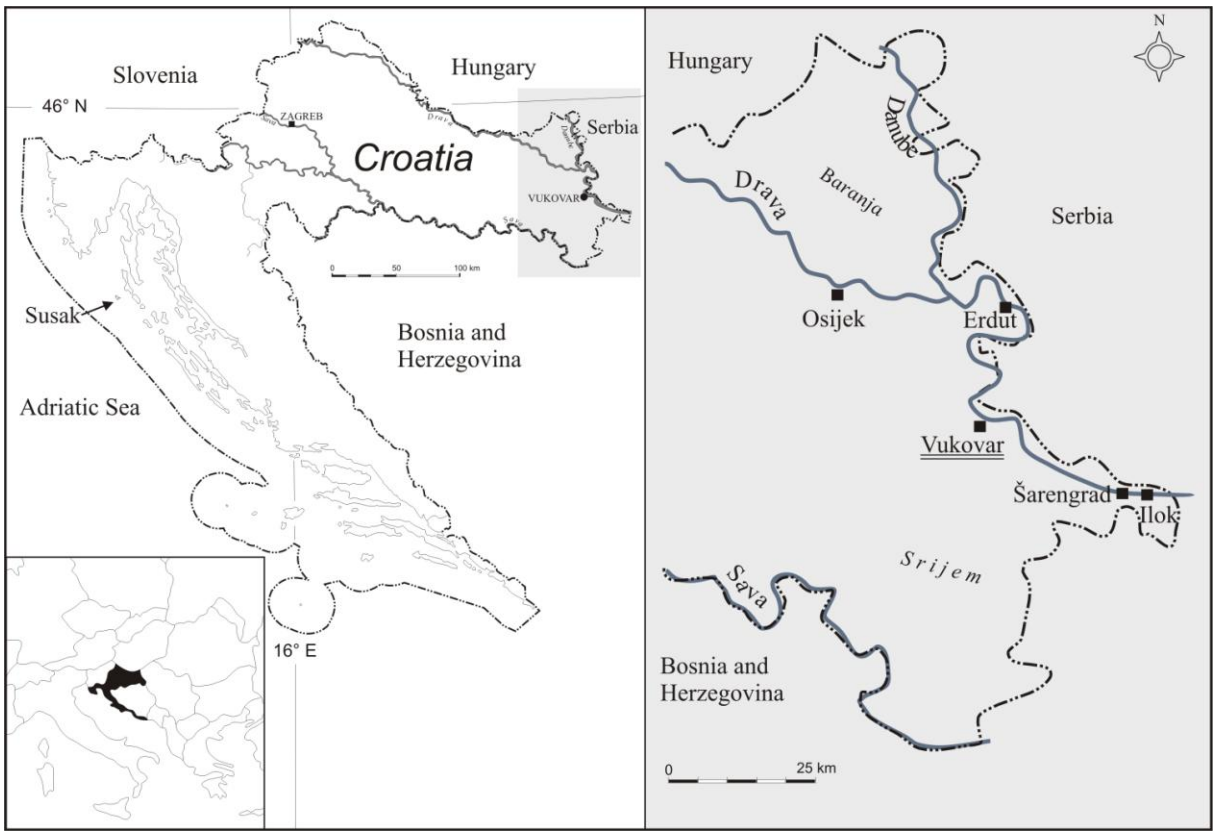

Figure 5.1. Map showing the location of the section at Vukovar in Srijem, eastern Croatia.

The Gorjanović loess section is situated on the right bank of the Danube River (45.3453N; 19.0123E) in Vukovar (Fig. 5.1. and 5.2.), just below the water tower and near the church of St Filip and Jakov (Fig. 5.3., 5.4.). From Vukovar to Vučedol a steep loess wall is exposed with a height up to 30 m. At Vučedol the famous Eneolithic archaeological site can be seen for which a reliable geochronological framework was presented by the means of thermoluminescence and radiocarbon dating methods (Benkö et al., 1989). Several palaeosol layers can be followed along the way from Vukovar to Vučedol. Gorjanović-Kramberger (1922) and Poje (1985) reported three palaeosol layers while Bronger (1976) reported four palaeosols (F5 to F2) along the Danube in Vukovar (Fig. 5.5.).

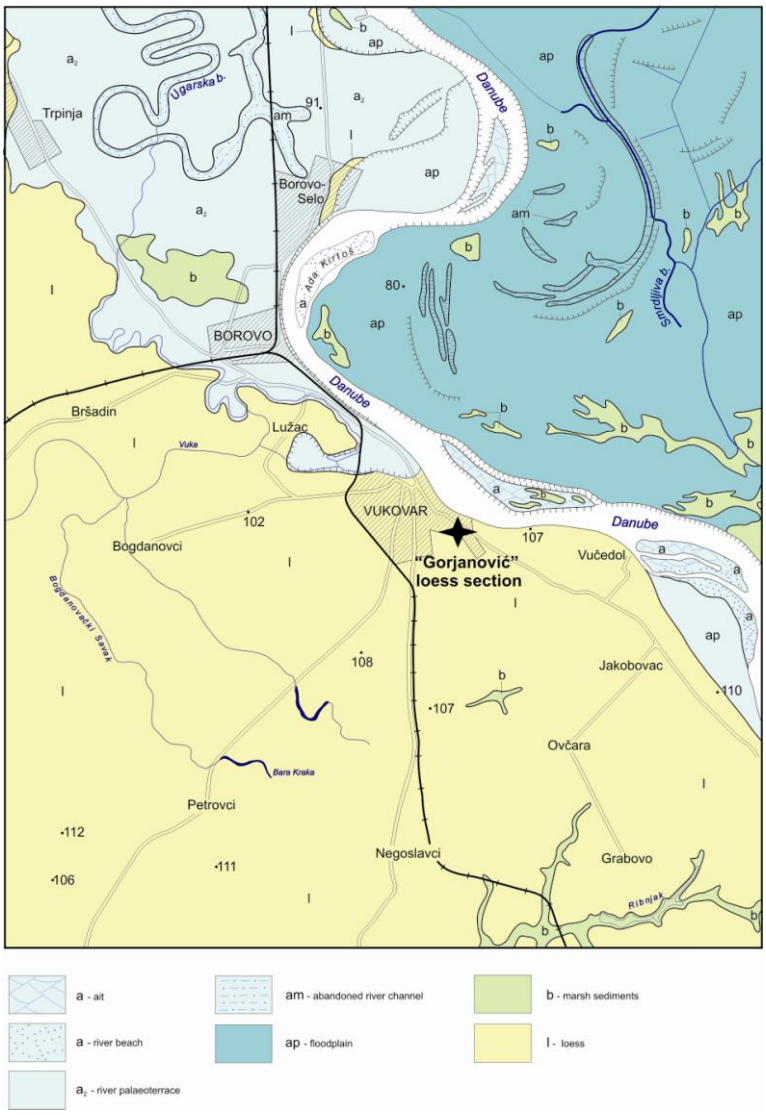

Figure 5.2. Geological map of the surrounding area of Vukovar (simplified after Trifunović, 1983; Magaš, 1987; Čičulić-Trifunović and Galović, 1984; Brkić et al., 1989).

Gorjanović-Kramberger (1922) described yellow sandy clay from the bottom of the investigated loess-palaeosol sequence which he correlated to the upper diluvium. On top of the sandy clay a horizon of carbonate concretions was exposed, the latter one covered with 22.6 m of loess which he subdivided into four loess layers, L_1 to L_4 (counting from the stratigraphically oldest to the youngest), intercalated by three horizons of fossil soils (S_1 to S_3 counting again from the stratigraphically oldest to the youngest) (Fig. 5.5.). Galović and Mutić (1984) reported that the basement of the section was covered during their field-work but reported yellow sands from the lowermost part of the sequence south of the studied section along the Danube. Below these sands, which very likely correlate to the Quaternary, Pliocene fossils were found from a borehole near Vukovar (Galović and Mutić, 1984). Today around 8 m high embankment along the Danube coast covers the lower part of the sequence and only the upper two brown palaeosols intercalating the loess are exposed. The present height of the exposed loess wall is about 20 m.

Only about two meters of the lowermost loess unit is exposed at the investigated location (Fig. 5.3. and 5.4.). This loess horizon has abundant up to few mm long Fe-Mn accumulations and carbonate concretions. In the upper part of this homogenous loess a 60 cm thick horizon enriched with carbonate concretions up to 12 cm long is exposed. The loess is overlain by a brown (7.5YR4/4) palaeosol up to 80 cm thick. The lower boundary of the palaeosol is bioturbated and up to a few cm long crotovinas filled with the same soil material can be seen. The palaeosol gradually transitions into loess. This second loess horizon is up to 8 m thick and homogenous; it consists of yellow (2.5Y6/6) silt with secondary carbonates up to few mm long. The upper 2 m of this thick loess horizon is enriched with carbonate concretions up to 10 cm long. This loess layer is covered by a thick brown (5YR4/3) palaeosol with distinguishable spots in its upper part having a somewhat lighter brown colour. Bronger (1976) described the second palaeosol from the top (F_2) from Vukovar as a *Braunerde-Tschernosem* with a striking mottled horizon containing red-brown cm long spots of a dark brown soil material in the upper part of the A-horizon. Based on the similarities from Bronger`s report and the descriptions in this study, it can be concluded that the thick brown palaeosol in the Gorjanović loess section is most likely the F_2 palaeosol described by Bronger (1976). Numerous crotovinas can be seen near the lower boundary of the palaeosol. About 80 cm below the thick brown palaeosol an up to one cm thick discontinuous yellow layer was detected which disappears laterally. This thin yellow layer very likely represents a tephra. Galović and Mutić (1984) made mineralogical investigations of the Gorjanović loess section and determined volcanogenic minerals in the same loess horizon. Similar tephra layers

intercalating the penultimate glacial loess were found in the Carpathian basin as well (Marković et al., 2009; Horváth, 2001). The palaeosol overlying the loess with the assumed tephra layer is covered by another loess horizon (2.5Y7/3). This loess contains secondary carbonates but not as abundant as the lower loess horizons. In this uppermost loess horizon, about 2 m above the thick brown palaeosol, a 50 cm thick grey humic horizon was detected. This grey humic horizon is covered approximately by 4 m of loess. Bronger (1976) described a thin humic horizon in the uppermost loess which he called F_1.

A detailed investigation of the palaeosols seen in the Gorjanović loess section was done by Bronger (1976). Palaeontological investigations of the section were done by Galović and Mutić (1984) and a detailed malacological study of the same deposits was presented by Poje (1985).

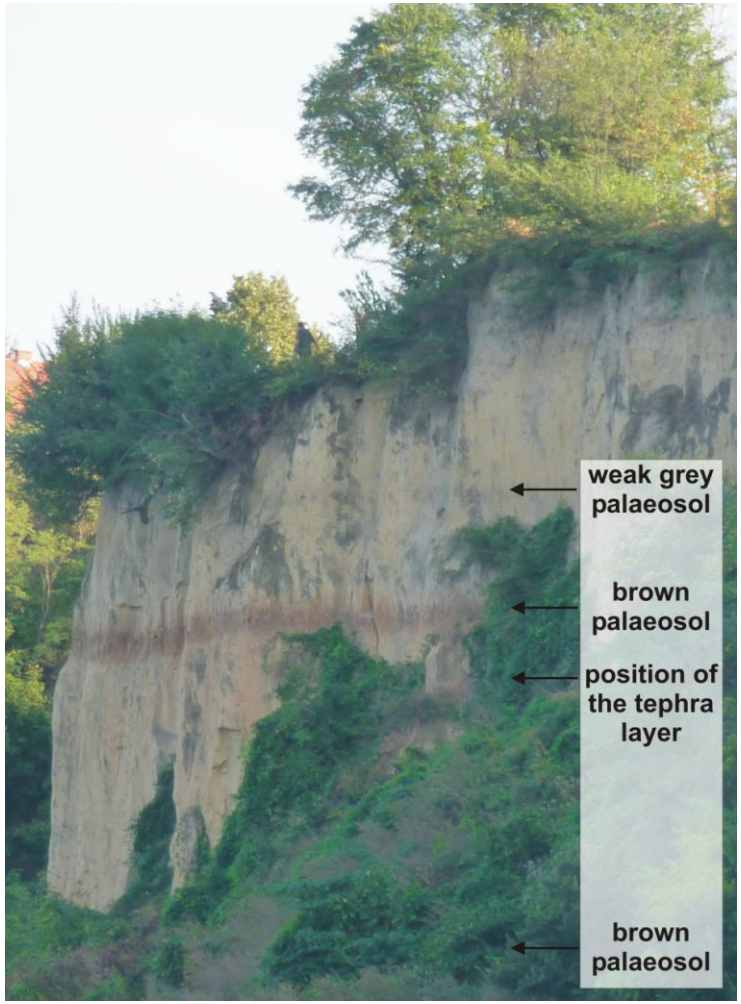

Figure 5.3. The investigated loess-palaeosol section along the bank of the River Danube in Vukovar (the Gorjanović loess section). The lower part of the section (the lower most palaeosol) is covered by vegetation.

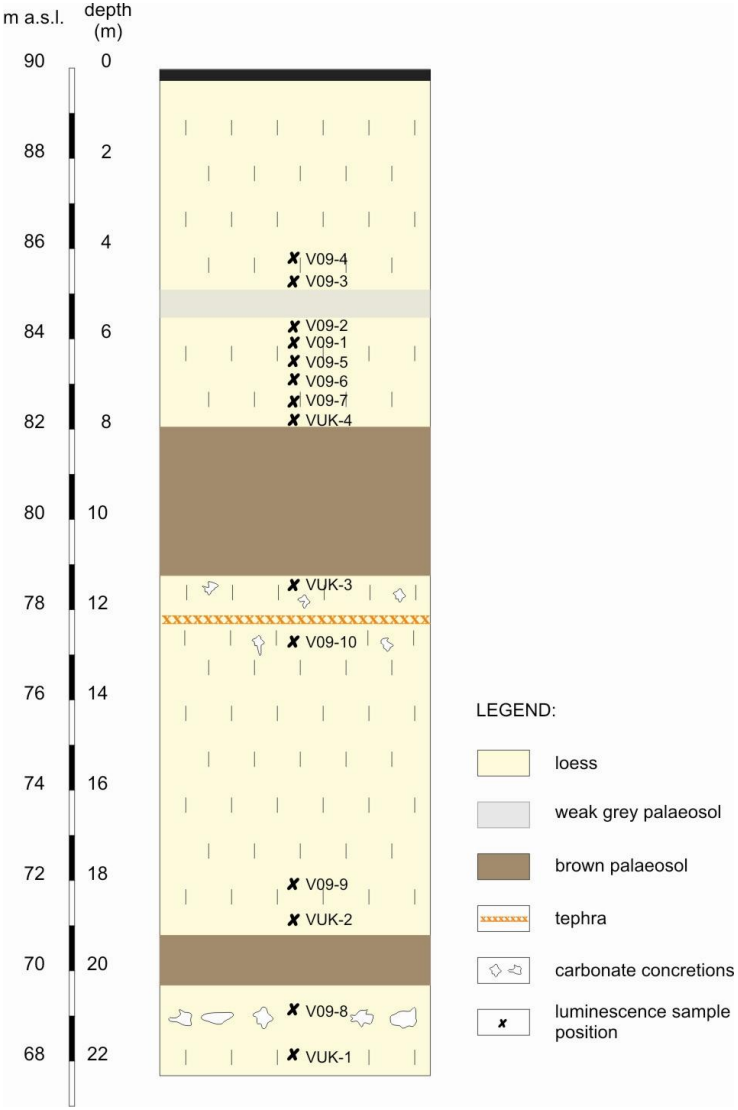

Figure 5.4. The sketch of the Gorjanović loess section with indicated sampling locations and samples names.

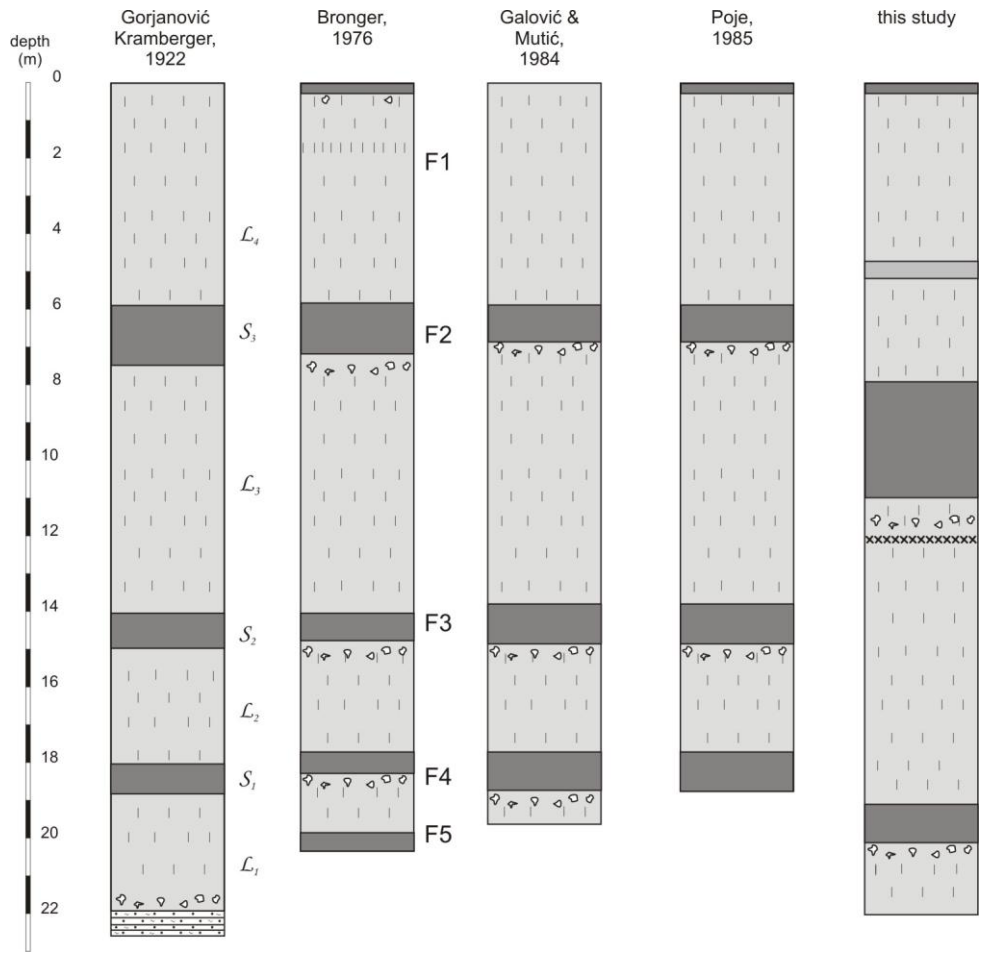

Figure 5.5. A comparison of the Vukovar loess section as described by Gorjanović Kramberger (1922), Bronger (1976), Galović and Mutić (1984) with indicated radiocarbon ages, Poje (1985) and this study. Refer to text for details.

5.3. Luminescence dating

The optically stimulated luminescence (OSL) dating method is based on the assumption that the latent luminescence signal in the sediments grains, which is the result of the natural radioactivity, is bleached (zeroed) prior to deposition (Aitken, 1998). The natural radioactivity of the surrounding sediment moves charges from their original position into traps in the mineral crystal. These charges are subsequently stimulated with light in the laboratory and recorded in the form of the luminescence signal. This amount of luminescence is described as the equivalent dose (D_e) and presents the dose absorbed by the sample since its last exposure to light or the last bleaching process. Aeolian transportation fulfils the assumption of bleaching because long aeolian transport exposes the material to sunlight which releases trapped charge from the crystal lattice of the minerals and hence resets the dosimeter to zero. The dosimeters used for luminescence dating are quartz and feldspar, which are the two most abundant detrital grains in the loess. The optically stimulated luminescence (OSL) signal of quartz shows saturation at lower doses than the infrared stimulated luminescence (IRSL) signal of feldspar, which means that quartz is not suitable for dating older material. Therefore, a lot of effort has been recently invested in testing feldspar luminescence properties and its application for dating (Wallinga et al., 2000a, b). In contrast, the disadvantage of the feldspar signal is the effect of anomalous fading (Wintle, 1973; Spooner, 1994) an athermal loss of signal from feldspar which causes age underestimation, despite a much higher saturation dose. This problem can be minimised by applying fading corrections, as proposed by Huntley and Lamothe (2001). Such fading corrections are strictly spoken only applicable for the linear part of the growth curve, i.e. for younger samples, although age underestimation was still reported by Wallinga et al. (2007). The alternative option for avoiding age underestimation as well as fading corrections is measuring more stable luminescence signals. Thomsen et al (2008) made tests on various sedimentary feldspar samples using different stimulation and detection conditions. They concluded that stimulation at elevated temperatures (IRSL at 110°C, 170°C and 225°C after an IR bleach at 50°C) reduces the fading rate. They also concluded that the later part of the post-IR IRSL curve at 225°C is apparently the most stable and thus likely to be the most accurate dosimeter (Thomsen et al., 2008). It was Buylaert et al. (2009) who, based on the work of Thomsen et al. (2008), tested and compared signals obtained after IR bleaching at 50°C and after the stimulation on an elevated temperature (225°C) on a variety of potassium feldspars from different depositional environments. They showed that the fading

rates of the elevated temperature signal are significantly lower than those measured by the standard 50°C signal and that, when fading corrected, the fading corrected ages of the IRSL at 50°C signal are in agreement with the fading corrected ages of the post-IR IRSL signal. Based on experiments and conclusions of Thomsen et al. (2008), Buylaert et al. (2009) and Murray et al. (2009), numerous post-IR IRSL protocols have been developed and tested for dating (Reimann et al., 2011; Thiel et al., 2010a, b, c, 2011, submitted; Wacha et al., 2010b) and proved to be satisfactory. Thiel et al. (2010a) investigated shallow marine and aeolian sediments from Sardinia using a post-IR IRSL protocol, as proposed by Buylaert et al. (2009). The observation of Murray et al. (2009) that the main charge traps in feldspar are not significantly eroded by heating on high temperatures (up to 320°C) and that higher preheat and stimulation temperatures could even more reduce fading rates, inspired Thiel et al. (2011) in using a high preheat temperature (320°C) and hence stimulation temperature of 290°C after an IR bleach at 50°C for dating of a Middle and Late Pleistocene loess site from Lower Austria. Polymineral fine grains extracted from loess from Lower Austria and Japan were dated by Thiel et al. (2010a, b, c) and loess from Croatia (Wacha et al. 2010b). Thiel et al. (2010b) used and compared two post-IR IRSL protocols (post-IR IRSL protocol using the 225°C signal after an IRSL bleach at 50°C with a preheat at 250°C and the 290°C signal after an IR bleach at 50°C with a preheat at 320°C) on same samples on prominent Austrian loess sections. They concluded that both post-IR IRSL signals (at 225°C and 290°C) can be used for dating and that the 290°C signal is preferable because no fading corrections are necessary. Reimann et al. (2011) successfully applied a modified elevated post-IR IRSL protocol on K-rich feldspar from late Pleistocene and Holocene coastal sediments using a preheat at 200°C and a post-IR IRSL stimulation at 180°C for D_e measurements.

5.3.1. Sampling and sample preparation

The samples were collected using light-proof metal tubes from a previously cleaned loess wall. The sample numbers and depths are presented in Table 5.1. and 5.3. and on Fig. 5.4. Laboratory preparation took place under subdued red light. The material was treated with 10% HCl to remove the carbonates, Na-oxalate against coagulation and H_2O_2 to remove organic matter. The material was refined into the fine silt fraction (4-11 μm) (Frechen et al., 1996).

For the dosimetry measurements, the material surrounding the luminescence sample location was collected. The samples were dried and exactly 700 g was filled into Marinelli-beaker and cap-sealed to avoid the loss of ^{222}Rn in the ^{238}U decay chain. The samples were stored for at least four weeks in order to re-establish the radioactive equilibrium due to the radon loss.

Altogether 14 samples for infrared stimulated luminescence dating (IRSL) were collected throughout the section. The sampling positions are indicated in Fig. 5.4.

5.3.2. Dose rate determination

The dose rates of the sediment were measured by high-resolution gamma spectrometry using a HPGe (High-Purity Germanium) N-type coaxial detector in the laboratory (Leibniz Institute for Applied Geophysics, Hanover, Germany). Measuring time was one day per sample. For the calculation of potassium, thorium and uranium contents, the measured activities of ^{40}K; and ^{210}Pb, ^{234}Th, ^{214}Bi and ^{214}Pb radionuclides from the ^{238}U decay chain; and ^{228}Ac, ^{208}Tl and ^{212}Pb radionuclides from the ^{232}Th decay chain were used. Radioactive equilibrium was assumed for the decay chain. Cosmic dose rates were corrected for the altitude and sediment thickness (Prescott and Hutton, 1994). The alpha efficiency was estimated to a mean value of 0.08 ± 0.02 for polymineral IRSL (Rees-Jones, 1995). The water content was assumed to be 15 ± 5% (Pécsi, 1990). For the calculation of the total dose rate the conversion factors published by Adamiec and Aitken (1998) were used. A systematic error of 5 % is included for the gamma spectrometry. An error of 10 % is estimated for the cosmic dose. The uranium, thorium and potassium contents, as well as the total dose rates and the cosmic dose rates are given in Table 5.1.

Table 5.1. Results from the dosimetry. The dose rate is the sum of the dose rates from alpha, beta, gamma and cosmic radiation. For the calculation of the total dose rate the conversion factors published by Adamiec and Aitken (1998) were used. A systematic error of 5% is included for the gamma spectrometry. An error of 10% is estimated for the cosmic dose.

Sample name	Sample ID (LUM)	Depth below surface (m)	U (ppm)	Th (ppm)	K (%)	Cosmic dose (mGy/a)	Doserate (mGy/a)
Vuk1	1654	22.0	2.89 ± 0.02	12.10 ± 0.06	1.73 ± 0.01	0.020 ± 0.002	3.54 ± 0.20
Vuk2	1655	19.0	3.32 ± 0.03	11.95 ± 0.06	1.71 ± 0.02	0.023 ± 0.002	3.65 ± 0.21
Vuk3	1656	11.9	2.78 ± 0.02	10.26 ± 0.06	1.44 ± 0.01	0.041 ± 0.004	3.11 ± 0.19
Vuk4	1657	7.8	3.47 ± 0.02	12.35 ± 0.06	1.77 ± 0.01	0.065 ± 0.007	3.83 ± 0.21
V09-1	2079	6.4	3.17 ± 0.04	11.76 ± 0.09	1.79 ± 0.00	0.079 ± 0.008	3.71 ± 0.21
V09-2	2080	5.9	4.51 ± 0.06	15.26 ± 0.13	2.28 ± 0.03	0.084 ± 0.008	4.89 ± 0.26
V09-3	2081	4.6	3.95 ± 0.05	13.10 ± 0.12	2.19 ± 0.03	0.102 ± 0.010	4.45 ± 0.24
V09-4	2082	4.0	3.22 ± 0.02	10.04 ± 0.04	1.75 ± 0.01	0.111 ± 0.011	3.57 ± 0.21
V09-5	2083	7.0	3.12 ± 0.04	10.51 ± 0.08	1.61 ± 0.00	0.072 ± 0.007	3.42 ± 0.20
V09-6	2084	7.3	3.23 ± 0.02	10.50 ± 0.04	1.62 ± 0.01	0.070 ± 0.007	3.46 ± 0.20
V09-7	2085	7.7	3.34 ± 0.02	10.98 ± 0.06	1.72 ± 0.01	0.066 ± 0.007	3.62 ± 0.21
V09-8	2086	21.3	2.83 ± 0.02	10.79 ± 0.06	1.43 ± 0.01	0.021 ± 0.002	3.14 ± 0.19
V09-9	2087	18.3	3.22 ± 0.02	11.55 ± 0.04	1.74 ± 0.01	0.024 ± 0.002	3.61 ± 0.21
V09-10	2088	12.9	2.85 ± 0.06	10.41 ± 0.15	1.66 ± 0.00	0.037 ± 0.004	3.33 ± 0.19

5.3.3. Elevated temperature post-IR IRSL protocol – Equivalent dose measurements and luminescence characteristics

All measurements were performed using an automated Risø TL/OSL-DA15 reader (Bøtter-Jensen et al., 2000) at the Leibniz Institute for Applied Geophysics during 2009 and 2010 equipped with a $^{90}Sr/^{90}Y$ beta source, with a dose rate of 0.094 Gy/s for fine grain material mounted on aluminium discs. The feldspar was stimulated with infrared light diodes and the luminescence signal was detected in the blue wavelength using a Schott BG39/Corning 7-59 filter combination between aliquots and photomultiplier.

For the equivalent dose (D_e) determination a modified elevated temperature post-IR IRSL protocol was used (Buylaert et al., 2009; Thiel et al., 2010a, c). For the measurements a preheat of 250°C (10s), IR stimulation at 50°C (200s) and IR stimulation at 225°C (200s) on the same aliquot were applied. The response to the test dose was measured the same way. The measuring protocol is shown in Table 5.2. Both signals were recorded and used for D_e calculations for better correlation with other published data and for comparison. The dose

response and decay curves for both signals of sample VUK3 (LUM 1656) are presented as an example in Fig. 6. The signal intensity of the IRSL at 50°C is much greater than the post-IR IRSL signal at 225°C (Fig. 5.6.a) for all samples. Same relations between the 50°C and 225°C signal intensities were detected by Thiel et al. (2010b) for loess from Lower Austria. Dose response curves of all samples were fitted using exponential and linear curve fitting and no evidence for saturation was detected for the older samples with all the D_e values smaller than $2D_0$ (Wintle and Murray, 2006). Dose response curves show similar patterns for both the IRSL signal at 50°C and the post-IR IRSL signal at 225°C (Fig. 5.6.b). Same was observed by Buylaert et al. (2009) for coarse grain feldspar and Thiel et al. (2010b) for fine grain material from various regions.

Table 5.9. Flowchart of the post-IR IRSL SAR protocol (after Buylaert et al., 2009).

Step	Treatment	Observed
1	Give dose	
2	Preheat, 250°C (10s)	
3	IR stimulation @ 50°C (200s)	$L_{x(50°C)}$
4	IR stimulation @ 225°C (200s)	$L_{x(225°C)}$
5	Give test dose	
6	Preheat, 250°C (10s)	
7	IR stimulation @ 50°C (200s)	$T_{x(50°C)}$
8	IR stimulation @ 225°C (200s)	$T_{x(225°C)}$
9	Return to 1	

The D_e-s were calculated using different integration limits, from the initial part of the curve (0-1 s) and the middle (5-20 s) part of the curve, for both signals IRSL at 50°C and post-IR IRSL at 225°C with the aim to find the more stable part of the curve with lower fading. For the IRSL at 50°C signal the background was subtracted from the last 50 s of the curve while for the post-IR IRSL at 225°C signal the middle 20 s of the curve were selected for background subtraction. The intensity of this part of the post-IR IRSL 225°C signal curve was more like the background intensity of the IRSL at 50°C signal and was hence selected for subtraction. For the age calculation the D_e values calculated from the part of the curve which showed lowest fading was selected (see section 5.3.4. and results). The results of the D_e-s calculated using different integration limits are presented in Table 5.3.

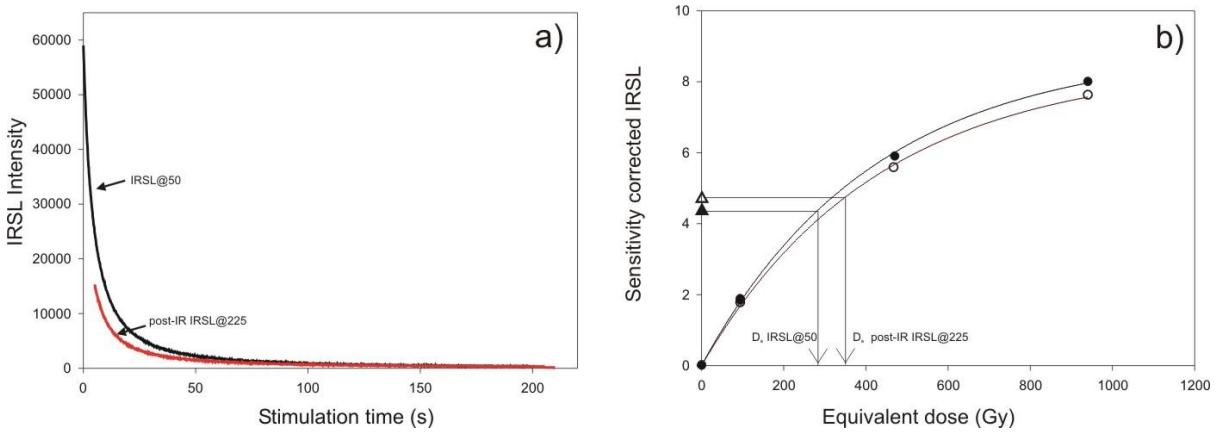

Figure 5.6. Comparison of luminescence characteristics of the measured IRSL signals of sample VUK-3 (1656). a) Signal intensity (decay) curves and b) dose response curves with indicated De values for both the IRSL at 50°C and post-IR at 225°C signals.

The quality of the performance of the measuring protocol was investigated before any D_e calculations by checking the recycling ratios, recuperation and performing the dose recovery tests (Wallinga et al., 2000b). The recycling ratios range from 0.97 ± 0.04 to 1.00 ± 0.04 and from 0.98 ± 0.04 to 1.00 ± 0.04 for the IRSL at 50°C signal and for the post-IR IRSL at 225°C signal, respectively. Recuperation is under 5% for all samples and both signals. To test whether the measured dose actually represents the real dose and can be successfully recovered artificially, dose recovery tests were performed. Eight aliquots were bleached for 4 hours in the Hönle SOL 2 solar simulator for the dose recovery test. Five aliquots were irradiated with a fixed beta- dose close to the expected equivalent dose and then measured using the same protocol as for the D_e measurements. Three aliquots were used for measuring residuals after bleaching. The dose recovery ratios for sample LUM 2082 (representative for younger samples) are around 1.0 for both the IRSL and the post-IR IRSL signal. For sample LUM 2088 the dose recovery ratios are 1.2 for the IRSL at 50°C signal and 1.0 for the post-IR IRSL at 225°C signal. For the representative of the oldest samples (2086) the dose recovery ratio for the IRSL at 50°C signal was 1.4 and for the post-IR IRSL at 225°C signal 1.1. These results represent the applicability of the measuring protocol and show that the post-IR IRSL at 225°C signal can be recovered more precisely than the IRSL at 50°C signal and hence give more accurate results. Scattered and high dose recovery results were reported by Thiel et al. (submitted) for the IR 50°C and post-IR IRSL 290°C signal although the results were in agreement with independent age control. Residual doses of ~ 1 Gy were measured for the 50°C as well as for the 225°C signals for sample LUM 2082, 1 Gy for the IRSL at 50°C signal and 2 Gy for the post-IR IRSL at 225°C signal for sample LUM 2088 and 2 Gy for the

IRSL at 50°C signal and 3 Gy for the post-IR IRSL at 225°C signal for sample LUM 2086. The values are considered as insignificant and were neglected and not subtracted prior to age calculations. The results of the dose recovery tests, the recycling ratios as well as the measured residuals are presented in Table 5.4.

5.3.4. Fading tests and fading corrections

IRSL of feldspars suffers from anomalous fading (Wintle, 1973; Spooner, 1994), an unwanted loss of signal which causes age underestimation. To overcome this problem fading test and fading corrections, according to Huntley and Lamothe (2001) and Auclair et al. (2003), were performed. After the D_e measurements same aliquots (three per sample) were irradiated with a beta-dose close to the natural D_e value. The same SAR sequence was used as for the D_e measurements with varying storage times, inserted immediately after irradiation and the preheat (Auclair et al., 2003). The g-values used for fading corrections were obtained from the mean of g-values of the three aliquots and their standard error because the results of the fading tests did not show any aliquot to aliquot scatter. Recently, Novothny et al. (2010) tested different fading rates for different IRSL decay curve components and concluded that the lowest fading rates can be seen for the middle part of the curve. Based on their experiments and results, the g-values were calculated for different parts of the decay curve (0-1 s and 5-20 s) for both the IRSL at 50°C signal as well as for the post-IR IRSL at 225°C signal for comparison. The summary of the calculated g-values for different integrating limits is presented in Table 5.5.

Table 5.3. Summary of the dating results (IRSL @ 50°C and post-IR IRSL @ 225°C). Five aliquots per sample were used for D_e calculation. Fading corrected ages were calculated after Huntley and Lamothe (2001).

Sample name	Sample ID (LUM)	De (Gy)				Uncorrected age (ka)				Fading corrected age (ka)			
		IRSL @ 50°C		IRSL @ 225°C		IRSL @ 50°C		IRSL @ 225°C		IRSL @ 50°C		IRSL @ 225°C	
		(0-1 s)	(5-20 s)	(0-1 s)	(5-20 s)	(0-1 s)	(5-20 s)	(0-1 s)	(5-20 s)	(0-1 s)	(5-20 s)	(0-1 s)	(5-20 s)
Vuk1	1654	384.4 ± 22.9	407.9 ± 24.7	474.6 ± 39.3	450.2 ± 41.6	108.6 ± 8.9	115.1 ± 9.5	134 ± 13	127 ± 14	163 ± 20	156 ± 15	151 ± 19	141 ± 19
Vuk2	1655	324.7 ± 17.0	343.3 ± 18.0	457.0 ± 24.5	422.6 ± 21.9	89.0 ± 6.9	94.0 ± 7.3	125 ± 10	116 ± 9	142 ± 11	133 ± 10	151 ± 12	138 ± 11
Vuk3	1656	289.9 ± 15.1	306.3 ± 15.6	379.7 ± 21.7	367.6 ± 19.4	93.5 ± 7.3	98.5 ± 7.7	123 ± 10	118 ± 9	149 ± 12	139 ± 11	147 ± 12	141 ± 11
Vuk4	1657	179.0 ± 9.0	185.2 ± 9.3	226.2 ± 11.6	216.2 ± 11.0	46.7 ± 3.5	48.4 ± 3.6	59.1 ± 4.4	56.5 ± 4.3	72.8 ± 5.4	65.8 ± 4.8	69.1 ± 5.1	64.1 ± 4.7
V09-1	2079	147.7 ± 7.5	154.2 ± 8.1	172.6 ± 9.5	170.4 ± 9.0	39.8 ± 3.0	41.5 ± 3.2	46.5 ± 3.7	45.9 ± 3.5	58.4 ± 5.2	56.5 ± 5.0	52.8 ± 4.8	54.2 ± 4.3
V09-2	2080	135.0 ± 7.6	142.1 ± 8.0	148.2 ± 8.7	154.3 ± 9.2	27.6 ± 2.1	29.1 ± 2.3	30.3 ± 2.4	31.6 ± 2.5	40.7 ± 3.2	37.7 ± 2.9	35.7 ± 2.9	37.1 ± 2.9
V09-3	2081	85.4 ± 4.7	89.8 ± 4.8	97.1 ± 6.2	96.7 ± 5.9	19.2 ± 1.5	20.2 ± 1.6	21.8 ± 1.8	21.7 ± 1.8	29.8 ± 2.4	27.0 ± 2.1	25.4 ± 2.1	24.9 ± 2.0
V09-4	2082	81.6 ± 4.3	83.9 ± 4.4	96.1 ± 4.8	97.0 ± 5.0	22.9 ± 1.8	23.5 ± 1.8	26.9 ± 2.1	27.2 ± 2.1	31.9 ± 2.9	30.2 ± 2.5	31.7 ± 2.5	30.0 ± 2.4
V09-5	2083	168.9 ± 8.7	174.6 ± 8.9	198.7 ± 11.5	194.1 ± 10.8	49.4 ± 3.9	51.1 ± 3.9	58.1 ± 4.8	56.8 ± 4.6	75.3 ± 5.9	68.9 ± 5.3	68.0 ± 5.5	66.4 ± 5.4
V09-6	2084	186.0 ± 10.3	191.0 ± 10.7	218.5 ± 11.0	214.4 ± 11.6	53.8 ± 4.3	55.3 ± 4.5	63.2 ± 4.8	62.0 ± 4.9	83.0 ± 6.9	77.0 ± 6.3	75.4 ± 5.8	75.4 ± 6.6
V09-7	2085	204.6 ± 13.4	212.5 ± 14.0	238.7 ± 14.3	242.3 ± 16.0	56.5 ± 4.9	58.7 ± 5.1	65.9 ± 5.5	67.0 ± 5.9	85.3 ± 8.0	79.2 ± 7.4	77.9 ± 6.6	79.1 ± 7.2
V09-8	2086	356.2 ± 19.6	366.2 ± 21.4	524.9 ± 28.5	476.3 ± 31.9	113.4 ± 9.3	116.5 ± 9.7	167 ± 14	152 ± 14	186 ± 15	164 ± 14	204 ± 17	182 ± 17
V09-9	2087	334.0 ± 19.8	353.5 ± 21.3	441.7 ± 32.0	407.6 ± 31.0	92.5 ± 7.7	97.9 ± 8.2	122 ± 11	113 ± 11	161 ± 14	144 ± 12	151 ± 14	139 ± 13
V09-10	2088	311.4 ± 18.8	332.9 ± 20.2	416.9 ± 24.8	407.6 ± 26.9	93.5 ± 7.8	100.0 ± 8.4	125 ± 10	122 ± 11	157 ± 14	145 ± 12	153 ± 13	145 ± 13

Table 5.4. Recycling ratios, dose recovery ratios and measured residuals for samples 2082, 2088 and 2086, selected to be representative for the upper, middle and lower part of the investigated section, respectively. Doses given for the dose recovery tests were 94 Gy, 373 Gy and 466 Gy to samples 2082, 2088 and 2086, respectively..

Sample ID (LUM)	Depth (m)	Nr. of aliquots	Recycling ratio		Dose recovered		Residuals	
			IRSL@50°C	post-IR IRSL@225°C	IRSL@50°C	post-IR IRSL@225°C	IRSL@50°C (Gy)	post-IR IRSL@225°C (Gy)
2082	4	5	1.02 ± 0.04	1.03 ± 0.04	0.9 ± 0.02	1.0 ± 0.01	~1	~1
2088	12.9	5	0.97 ± 0.04	0.98 ± 0.04	1.2 ± 0.02	1.0 ± 0.02	~1	~2
2086	21.3	5	0.98 ± 0.04	0.98 ± 0.04	1.4 ± 0.04	1.0 ± 0.01	~2	~3

Table 5.5. Results of the fading tests and the calculated g-values. The average of three aliquots per sample was used. The g-values from the middle part of the curve (5-20 s) were selected for age calculations for both the IRSL at 50°C signal and the post-IR IRSL at 225°C signal because it showed less fading.

Sample ID (LUM)	g-value (%/decade)			
	IR at 50°C		post-IR IRSL at 225°C	
	0-1 s	5-20 s	0-1 s	5-20 s
1654	4.0 ± 0.7	3.1 ± 0.4	1.3 ± 0.7	1.1 ± 0.8
1655	4.5 ± 0.1	3.5 ± 0.1	2.0 ± 0.1	1.9 ± 0.1
1656	4.5 ± 0.1	3.4 ± 0.2	1.9 ± 0.2	1.8 ± 0.2
1657	4.4 ± 0.1	3.2 ± 0.0	1.7 ± 0.1	1.4 ± 0.1
2079	3.9 ± 0.4	3.2 ± 0.4	1.4 ± 0.5	1.8 ± 0.2
2080	4.0 ± 0.1	2.8 ± 0.0	1.8 ± 0.2	1.6 ± 0.2
2081	4.5 ± 0.3	3.1 ± 0.1	1.7 ± 0.1	1.5 ± 0.2
2082	3.5 ± 0.4	2.7 ± 0.3	1.8 ± 0.2	1.1 ± 0.2
2083	4.2 ± 0.1	3.1 ± 0.1	1.7 ± 0.1	1.7 ± 0.2
2084	4.3 ± 0.2	3.4 ± 0.2	1.9 ± 0.2	2.1 ± 0.4
2085	4.1 ± 0.3	3.1 ± 0.3	1.8 ± 0.2	1.8 ± 0.3
2086	4.7 ± 0.1	3.4 ± 0.1	2.1 ± 0.2	1.9 ± 0.2
2087	5.2 ± 0.2	3.8 ± 0.2	2.2 ± 0.1	2.2 ± 0.1
2088	4.9 ± 0.2	3.7 ± 0.2	2.1 ± 0.1	1.8 ± 0.1

5.4. Results

Results from the dosimetry, the equivalent doses, g-values, and the uncorrected and corrected ages, as well as the results of the performance tests, from all measured luminescence signals are given in Tables 5.1., 5.3., 5.4. and 5.5.. The final ages used for stratigraphic interpretation are presented in Figure 5.7. and 5.8.

Uranium, thorium and potassium content range from 2.78 to 4.51 ppm, from 10.04 to 15.26 ppm and from 1.43 to 2.28 %, respectively. The total dose rates range from 3.11 to 4.89 mGy/a. The average value of 3.67 ± 0.21 mGy/a for all samples is typical for European loess (e.g. Frechen et al., 1997; Galović et al., 2009; Novothny et al., 2009, Wacha et al., 2010a, 2011).

The g-values were calculated for the initial part as well as for the middle part of the decay curve, for both luminescence signals (IRSL at 50°C and post-IR IRSL at 225°C). The initial part of the curve gave the largest fading rates (g-values ranging from 3.5 to 4.9%/decade for the IRSL at 50°C signal and from 1.3 to 2.2%/decade for the post-IR IRSL at 225°C signal). The medium part of the decay curve showed lower fading rates (g-values ranging from 2.8 to 3.8%/decade for the IRSL at 50°C signal and 1.1 to 2.2%/decade for the post-IR IRSL at 225°C signal) except for samples 2083, 2085 and 2087 where same values within error limits were calculated for both the initial and the middle part of the decay curve for the post-IR IRSL at 225°C signal (Table 5.3. and 5.5.). Furthermore, as seen from Table 5.5., the g-values calculated for the post-IR IRSL at 225°C signal for the initial and middle part of the decay curve are quite uniform within error limits. For the calculation of the D_e the part of the curve which showed lowest fading was selected. The D_e values range from 83.9 ± 4.4 Gy to 407.9 ± 24.7 Gy for the IRSL at 50°C signal and from 96.7 ± 5.9 Gy to 450.2 ± 41.6 Gy for the post-IR IRSL at 225°C signal.

Saturation was not seen in the growth curves. Reliable D_e-s can be obtained up to a dose value of $2D_0$ which corresponds to 86% of saturation (Wintle and Murray, 2006). All D_e values in this study are much less than $2D_0$ and range from 388 Gy to 620 Gy for the IRSL at 50°C signal and from 374 Gy to 642 Gy for the post-IR IRSL signal. This suggests that for samples in this study it is possible to measure D_e-s up to about ~ 620 Gy. The ratio of the sensitivity-corrected natural signal to the laboratory saturation level was calculated as 0.30 ± 0.02 to 0.75 ± 0.08 and 0.37 ± 0.02 to 0.78 ± 0.15 for the IRSL at 50°C and the post-IRSL at 225°C signal,

respectively. The fading correction method after Huntley and Lamothe (2001) was applied for all samples and both signals even though Huntley and Lamothe (2001) stated that the method is successful only for the linear part of the curve. In Table 5.4. the uncorrected and corrected ages are summarized, for both signals and both integration limits. The fading corrected ages of both the 50°C signal and the 225°C signal are in excellent agreement although the results of older samples are considered as minimum ages due to the limits of the fading corrections which are not appropriate for the exponential part of the growth curve. Sample Vuk-1 (LUM 1654) from the oldest loess shows age underestimation, if compared to the sample above (V09-8/LUM 2086). The reason for this age inversion and underestimation is very likely related to sediment mixing due to numerous crotovinas found in the loess or the restrictiveness of the fading corrections for old samples.

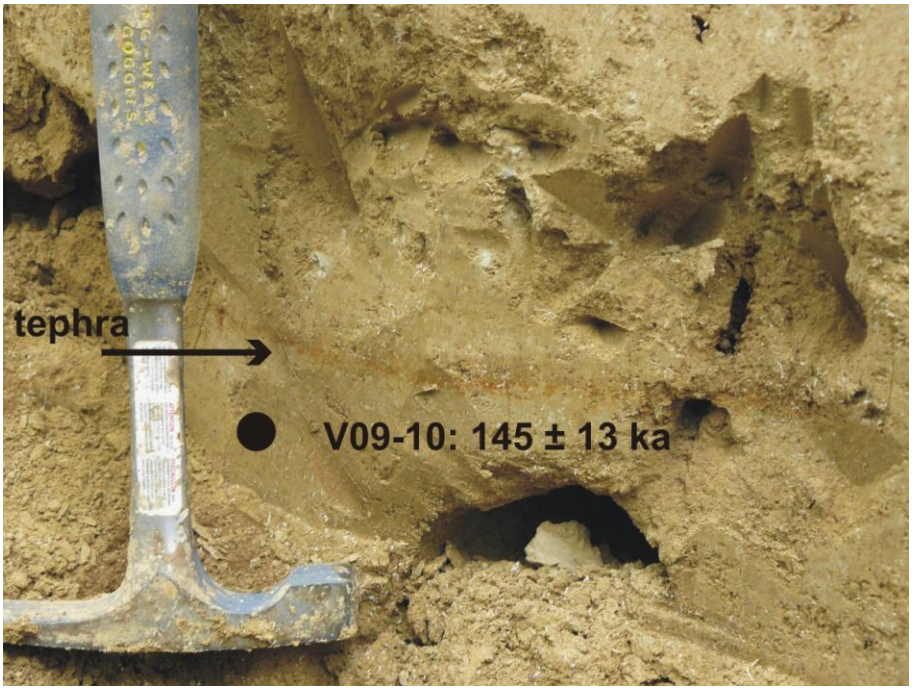

Figure 5.7. The detail of the thin yellow assumed tephra layer with indicated dating results of the loess below.

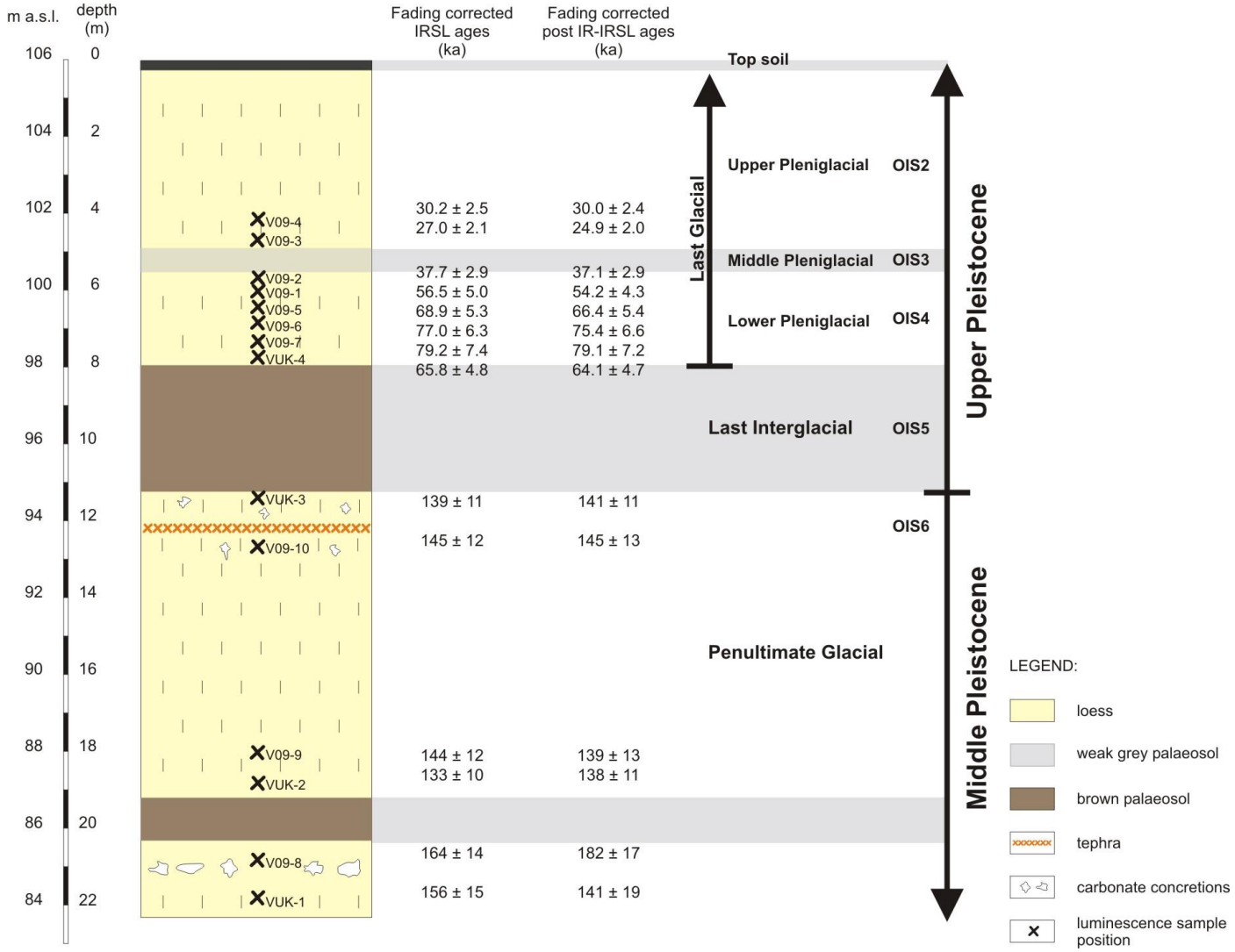

Figure 5.8. The summary of the dating results of the investigated loess-palaeosol section, the Gorjanović loess section in Vukovar, with indicated fading corrected ages of the IRSL at 50°C signal and the post-IR IRSL at 225°C signal and the interpretation. The ages presented here are calculated integrating the middle part of the luminescence decay curve which showed less fading.

5.5. Discussion

In recent years luminescence dating was carried out on numerous loess-palaeosol sections in the Carpathian (Pannonian) basin (Novothny et al., 2002, 2009, 2010; Marković et al., 2007; Fuchs et al., 2008; Bokhorst and Vandenberghe, 2009; Schmidt et al., 2010) providing new data and unravelling the geochronology and stratigraphy of loess sequences in the Danubian area. In Eastern Croatia, Singhvi et al. (1989) presented thermoluminescence (TL) dating results of the Erdut loess section. Galović et al. (2009) presented infrared stimulated luminescence (IRSL) dating results for three loess sections (Erdut, Zmajevac and Šarengrad) from eastern Croatia. In order to minimise anomalous fading, Galović et al. (2010) delayed IRSL measurements at least for four weeks after irradiation and used the middle part of the IRSL decay curves for D_e determination. However, age underestimation due to anomalous fading cannot be excluded and will be investigated in an ongoing study. In this study a detailed geochronological framework is presented for the Vukovar loess-palaeosol sequence in Eastern Croatia.

In his 1976 work, Bronger described five fossil soils in Vukovar ($F_1 – F_5$) which he correlated to the complete last interglacial/glacial cycle; he correlated the F_5 palaeosol with the Riss/Würm interglacial. In the work of Galović and Mutić (1984) radiocarbon dating results of carbonate concretions found in loess were presented. Their results supported the conclusion of Bronger (1976) that the complete sequence correlates to the last glacial period although only three palaeosols were described in their study. However, these radiocarbon results must be taken with caution because of the limited applicability of the radiocarbon dating method on secondary carbonates in loess. The time of the formation of the carbonate concretions found in loess may be long after the deposition of loess. Furthermore, they can be contaminated with detrital carbonates and other types of secondary carbonates (Geyh, 1990). Poje (1985) accepted the geochronology and stratigraphy from Bronger (1976) and from Galović and Mutić (1984) and provided a palaeoclimatic interpretation of the loess-palaeosol sequences based on detailed malacological investigations. Thermoluminescence dating of loess-palaeosol sequences in the Carpathian basin, as presented by Singhvi et al. (1989), showed that the F_5 palaeosol is much older than the last interglacial period and that only the F_2 and F_3 palaeosols correlate to the last interglacial period (oxygen isotope stage (OIS) 5). However, TL dating results are very likely underestimated owing to the lack of fading corrections. The dating results of samples collected from the Gorjanović loess section presented in this study

clearly show that the complete section correlates to loess from at least two last glacials intercalated by soil forming processes which can be correlated to interglacials and interstadials (OIS 5). If the descriptions of Gorjanović-Kramberger (1922) are considered about the deposits underlying the loess sequence of this study, an even older record was previously exposed but is covered by an embankment nowadays. Gorjanović–Kramberger (1922) reported a further brown palaeosol and sandy clays and sands in the lower part of the loess sequence, which are not exposed today. A similar Quaternary sediment succession is described from the nearby location in Šarengrad (Hupuczi et al., 2010; Wacha et al., 2010b; in preparation).

The lowermost exposed loess of the described section at Vukovar shows age estimates ranging from 164 ± 14 ka to 156 ± 15 ka, when fading corrected 182 ± 17 ka to 141 ± 19 ka, respectively (Fig. 5.8.). Fading corrections are successful only for the linear part of the curve (Huntley and Lamothe, 2001) which means that they are applicable only for young samples (up to around 50 ka). Although the fading corrections are questionable for the exponential part of the curve the same fading correction procedure was performed for all samples, to obtain more accurate age estimates. Equivalent dose calculation was based on the middle part of the IRSL and post-IR IRSL signal curve which gave the most reliable results and showed lowest fading. Nevertheless, the fading corrected ages for the stratigraphically older samples must be considered as minimum age estimates indicating that the lowermost exposed loess very likely correlates to the Penultimate Glacial period (OIS6) or any older glaciation (Fig. 5.8.). More data is needed for a more precise correlation. This lowermost and oldest exposed loess is about 10 m thick and homogenous and gave fading corrected age estimates which range from 182 ± 17 ka to 141 ± 11 ka (Fig. 5.8.) and is in its lower part intercalated with a one meter thick brown palaeosol, developed under interglacial (very likely during OIS7) or interstadial climatic conditions, and an orange-brown thin discontinuous layer which is assumed to be a tephra (Fig. 5.7. and 5.8.). Tephra remains were also reported by Marković et al. (2009) in the Batajnica section, approximately 90 km away from Vukovar, in Vojvodina in the middle part of the penultimate glacial loess. The fading corrected age estimates of the loess surrounding the tephra horizon range from 141 ± 11 ka to 145 ± 13 ka (Fig. 5.7. and 5.8.) but the exact age and the origin of the tephra is still unknown. The thick brown palaeosol in the middle part of the section can be correlated to OIS5 based on luminescence dating results of loess from below and above the palaeosol which gave fading corrected post-IR IRSL ages ranging from 141 ± 11 ka to 64.1 ± 4.7 ka. According to Bronger (2003) OIS5 in Serbian loess-palaeosol sequences (Stari Slankamen and Mosorin/Titel) is represented by two palaeosols F_2 and F_3,

which gave fading uncorrected thermoluminescence (TL) ages of about 125 ka for the F_3 palaeosol and 75 ka for the F_2 palaeosol (Singhvi et al., 1989). Bronger (2003) correlated the F_3 palaeosol to the Riss/Würm interglacial, which corresponds with OIS5e, and the F_2 palaeosol to substage 5a. In the Serbian loess-palaeosol stratigraphy Marković et al. (2004a, b; 2005; 2006; 2007; 2008; 2009) correlated the V-S1 pedocomplex, which is the stratigraphically uppermost and youngest intercalated pedocomplex in the loess/palaeosol sequence, to the complete OIS5 period. This stratigraphic model is supported by recent IRSL dating results from the Surduk section (Fuchs et al., 2008) where the age estimates of the upper part of the penultimate glacial loess and the loess covering the OIS5 palaeosol ranged from 121 ± 14 ka to 82.7 ± 9.6 ka and the results from the upper part of the Stari Slankamen section (Schmidt et al., 2010) where the post-IR OSL age estimates range from 148 ± 9 ka for the penultimate glacial loess to 60.5 ± 3.9 ka for loess covering the V-S1 pedocomplex. In the Hungarian loess chronostratigraphy the MF_2 palaeosol, which is a chernozem type palaeosol described at the Middle Pleistocene type locality Mende in Hungary, is suggested to correlate with OIS5 (Wintle and Packman, 1988; Frechen et al., 1997). At the Süttő section, the last interglacial record consists of four palaeosols. The lowermost pedocomplex is composed of a well-developed, reddish-brown palaeosol and covered by a well-developed dark-brown chernozem-like palaeosol (Novothny et al., 2009, 2010, 2011). This pedocomplex is covered by a transitional loess layer and two brownish palaeosols intercalated by another transitional loess layer (Novothny et al., 2011). Based on IRSL age estimates presented in Novothny et al. (2010) it is very likely that the reddish-brown palaeosol correlates to OIS5e, whereas the chernozem-like palaeosol correlates to OIS5c, while the transitional loess layer overlying the pedocomplex at Süttő correlates to OIS5b. The two thin brownish steppe-like palaeosol intercalated with a transitional loess layer very likely give evidence for a period of short and/or less warm and humid interstadial period interrupted by a colder period during OIS5a (Novothny et al., 2011). At the Zmajevac section located in eastern Croatia, the second brown intercalated palaeosol from the top very likely correlates to OIS5 (Galović et al., 2009). Based on the dataset presented in Galović et al. (2009) a subdivision into interstadials (i.e. OI substages 5e, 5c or 5a) is not possible and needs further investigation, especially the chronological framework needs to be improved, as fading correction has not yet been applied to this data set.

The Last Glacial loess covering the OIS5 palaeosol at the Gorjanović loess section shows fading corrected post-IR IRSL age estimates ranging from 64.1 ± 4.7 ka to 30.0 ± 2.4 ka, for samples collected from loess directly covering the thick brown palaeosol and from loess

collected from the stratigraphically youngest accessible position, respectively. In this loess horizon a weakly developed greyish palaeosol is intercalated. This palaeosol very likely correlates with F_1 by Bronger (1976, 2003). Based on TL age estimates the F_1 palaeosol in Erdut formed between 45-29 ka (Singhvi et al., 1989) and hence can be correlated to OIS3. Based on the results of the present study the humic horizon detected in the Vukovar loess section formed between 37.1 ± 2.9 ka and 24.9 ± 2.0 ka, if the fading corrected post-IR IRSL dating results are considered (Fig. 5.8.), and hence correlates to OIS3. At the Süttő section in Hungary a brownish palaeosol and two grey laminated horizons are correlated to OIS3 (Novothny et al., 2011). In loess-palaeosol sections from Serbia the middle pleniglacial (OIS3) is called L1S1 (Marković et al., 2004a, b, 2005, 2006, 2007, 2008, 2009). In the Ruma section a single, weakly developed chernozem is described (Marković et al., 2006), at the Petrovaradin brickyard (Marković et al., 2005), the Batajnica section (Marković et al., 2009) and Irig section (Marković et al., 2007) a weakly developed double chernozem-like palaeosol, and at Stari Slankamen and Surduk sections (Schmidt et al., 2010; Antoine et al., 2009) multiple brown palaeosols were described. At the island of Susak which belongs to the river Po loess province, several brown palaeosols can be correlated to the middle pleniglacial. The Susak loess/palaeosol sequences are regarded to be one of the most detailed loess records of the Po river system correlating to OIS3 (Wacha et al., 2010a, 2011). The uppermost loess exposed at the Gorjanović loess section very likely correlates to the last glacial maximum (OIS2) but no samples were collected for this study.

The loess record of eastern Croatia provides a high-resolution sediment archive enabling the reconstruction of mid- and long-term regional climate forcing. The present chronological framework for the Vukovar section makes it possible to study the palaeodust content of the atmosphere more precisely and to understand long-term trends of atmospheric circulation, which is a part of an ongoing study in the Carpathian basin.

5.6. Conclusion

In this study a detailed and robust chronological framework for the Gorjanović loess section in Vukovar was set up by means of infrared stimulated luminescence dating. The elevated temperature post-IR IRSL protocol (Buylaert et al., 2009) was used for the equivalent dose (D_e) determination. Tests performed for this protocol confirmed its applicability especially for

the post-IR IRSL at 225°C signal. Within error limits, the calculated ages are in stratigraphic order and can be correlated to the penultimate glacial – last interglacial - last glacial period (OIS6 – OIS2) but the existence of an even older record is not excluded. The fading corrected IRSL and the fading corrected post-IR IRSL results are in excellent agreement. The post-IR IRSL ages show less fading than the IRSL data and can hence be successfully used for the dating of older loess although there is still no appropriate fading correction method proposed for older samples.

At the investigated section three palaeosols are intercalated in the loess; the lowermost palaeosol very likely correlates to an interglacial or interstadial period predating to OIS5, probably to OIS7, the middle thick brown palaeosol is very likely the result of warm climatic conditions during the last interglacial while the upper weakly developed palaeosol indicates climatic fluctuations during OIS3. Traces of volcanic activity can be seen in a thin discontinuous tephra layer. Similar tephras were detected in the Carpathian basin. For better correlation a detailed tephra analysis is necessary and in progress. The Gorjanović loess section can be correlated to similar loess-palaeosol sections in the region and provides an excellent record for unravelling palaeoclimatic and environmental conditions from the penultimate glacial until the upper pleniglacial of the Pannonian basin.

5.7. Acknowledgements

This research has been financed by the DAAD (German Academic Exchange Service); the Leibniz Institute for Applied Geophysics (LIAG), Hanover, Germany and the Croatian Ministry of Science, Education and Sports (project Nr. 0181001). This work could not be possible without the help of colleagues from the S3 from LIAG, especially Dr. Sumiko Tsukamoto and Dr. Christine Thiel. The authors wish to thank Dr. Lidija Galović for support and to Ivo Suša for Figure 2. Special thanks to Dr. Géza Chikán who accompanied and helped L.W. in the first Vukovar expedition.

5.8. References

Adamiec, G., Aitken, M.J., 1998. Dose-rate conversion factors: update. Ancient TL 16, 37-50.

Aitken, M.J., 1998. An Introduction to Optical Dating. Oxford University Press, Oxford, 280 pp.

Antoine, P., Rousseau, D.D., Fuchs, M., Hatté, C., Gauthier, C., Marković, S.B., Jovanović, M., Gaudenyi, T., Moine, O., Rossignol, J., 2009. High-resolution record of the last climatic cycle in the southern Carpathian Basin (Surduk, Vojvodina, Serbia). Quaternary International 198, 19-36.

Auclair, M., Lamothe, M., Hout, S., 2003. Measurement of anomalous fading for feldspar IRSL using SAR. Radiation Measurement 37, 487-492.

Ballarini, M., Wallinga, J., Murray, A. S., Heteren, S. v., Oost, A. P., Bos, A. J. J., Eijk, C. W. E. v., 2003. Optical dating of young coastal dunes on a decadal time scale. Quaternary Science Reviews 22, 1011-1017.

Benkö, L., Horváth, F., Horvatinčić, N., Obelić, B., 1989. Radiocarbon and thermoluminescence dating of Prehistoric sites in Hungary and Yugoslavia. Radiocarbon 31, 992-1002.

Bognar, A., 1979. Distribution, properties and types of loess and loess-like sediments in Croatia. Acta Geologica Academiae Scientiarium Hungaricae 22, 267-286.

Bokhorst, M.P., Vandenberghe, J., 2009. Validation of wiggle matching using a multi-proxy approach and its palaeoclimatic significance. Journal of Quaternary Sciences 24 (8), 937-947.

Bokhorst, M.P., Vandenberghe, J., Sümegi, P., Łanczont, M., Gerasimenko, N.P., Matviishina, Z.N., Marković, S.B., Frechen, M., 2011. Atmospheric circulation patterns in central and eastern Europe during the Weichselian Pleniglacial inferred from loess grain-size records. Quaternary International 234, 1-2, 62-74.

Bøtter-Jensen, L., Bulur, E., Duller, G.A.T., Murray, A.S., 2000. Advances in luminescence instrument systems. Radiation Measurements 32, 523-528.

Brkić, M., Galović, I., Buzaljko, R., 1989. Osnovna geološka karta SFRJ 1:100.000 list Vinkovci L 34-98. Geološki zavod – Zagreb i Geoinženjering – Sarajevo, Savezni geološki zavod, Beograd.

Bronger, A., 1976. Zur quartären Klima- und Landschaftsentwicklung des Karpatenbeckens auf (palaeo)-pedologischer und bodengeographischer Grundlage. Kieler Geographische Schriften 45, 268 pp.

Bronger, A., 2003. Correlation of loess-paleosol sequences in East and Central Asia with SE Central Europe: towards a continental Quaternary pedostratigraphy and paleoclimatic history. Quaternary International 106/107, 11–31.

Buylaert, J.P., Murray, A.S., Thomsen, K.J., Jain, M., 2009. Testing the potential of an elevated temperature IRSL signal from K-feldspar. Radiation Measurements 44, 560-565.

Čičulić-Trifunović, S., Galović, I., 1983. Osnovna geološka karta SFRJ 1:100.000 list Bačka Palanka L 34–99. Geološki institut Beograd i Geološki zavod Zagreb, Savezni geološki zavod, Beograd.

Frechen, M., Schweitzer, U., Zander, A., 1996. Improvements in sample preparation for the fine grain technique. Ancient TL 14 (2), 15-17.

Frechen, M., Horváth, E, Gábris, G. 1997. Geochronology of Middle and Upper Pleistocene loess sections in Hungary. Quaternary Research 48/3, 291–312.

Fuchs, M., Rousseau, D.-D., Antoine, P., Hatté, C., Gauthier, C., Marković, S., Zoeller, L., 2008. Chronology of the Last Climatic Cycle (Upper Pleistocene) of the Surduk loess sequence, Vojvodina, Serbia. Boreas 37, 66-73.

Galović, I., Mutić, R., 1984. Gornjopleistocenski sediment istočne Slavonije (Hrvatska). Rad JAZU 411, 299–356, Zagreb.

Galović , L., Frechen, M., Halamić, J., Durn, G., Romić, M., 2009. Loess chronostratigraphy in Eastern Croatia – A first luminescence dating approach. Quaternary International 198, 85–97.

Geyh, M., 1990. ^{14}C dating of loess. Quaternary International 7/8, 115-118.

Gorjanović-Kramberger, D., 1910. Die Klimaschwankungen zur Zeit der Lössbildung in Kroatien-Slavonien. Stockholm, Postglaziale Klimaveränderungen, 139-141.

Gorjanović-Kramberger, D., 1912. Iz prapornih predjela Slavonije. Vijesti geološkoga povjerenstva 2, 28–30, Zagreb.

Gorjanović-Kramberger, D., 1914. Iz prapornih predjela Slavonije. Vijesti geološkoga povjerenstva 3-4, 21-26, Zagreb.

Gorjanović-Kramberger, D., 1915. Die Hydrographischen Verhältnisse der Lössplateaus Slavoniens. Glasnik hrvatskoga prirodoslvnoga društva XXVII, 71-75, Zagreb.

Gorjanović-Kramberger, D., 1922. Morfologijske i hidrografijske prilike prapornih predjela Srijema, te pograničnih česti županije virovitičke. Glasnik hrvatskoga prirodoslovnog društva XXXIV, 111-164, Zagreb.

Horváth, E., 2001. Marker horizons in the loesses of the Carpathian Basin. Quaternary International 76/77, 157-163.

Huntley, D.J., Lamothe, M., 2001. Ubiquity of anomalous fading in K-feldspars, and the measurement and correction for it in optical dating. Canadian Journal of Earth Sciences 38, 1093-1106.

Hupuczi, J., Molnár, D., Galović, L., Sümegi, P., 2010. Preliminary malacological investigation of the loess profile at Šarengrad, Croatia. Central European Journal of Geosciences 2 (1), 57-63.

Kunz, J.A., Frechen, M., Ramachandran, R., Urban, B., 2010. Revealing the coastal event-history of the Andaman Islands (Bay of Bengal) during the Holocene using radiocarbon and OSL dating. International Journal of Earth Sciences 99, 1741-1761.

Liu, T., Zhongli, D., Zhiwei, Y., Rutter, N., 1992. Susceptibility time series of the Baoji section and the bearings on paleoclimatic periodicities in the last 2.5 Ma. Quaternary International 17, 33-38.

Magaš, N., 1987. Osnovna geološka karta SFRJ List Osijek L 34-86. Geološki zavod Zagreb, Savezni geološki zavod, Beograd.

Marković, S.B., Kostić, N.S., Oches, E.A., 2004a. Palaeosols in the Ruma loess section (Vojvodina, Serbia). Revista Mexicana de Ciencias Geológicas 21, 79–87.

Marković, S.B., Oches, E.A., Gaudenyi, T., Jovanović, M., Hambach, U., Zöller, L., Sümegi, P., 2004b. Paleoclimate record in the late Pleistocene loess-palaeosol sequence at Miseluk (Vojvodina, Serbia). Quaternaire 15, 361–368.

Marković, S.B., McCoy, W.D., Oches, E.A., Savić, S., Gaudenyi, T., Jovanović, M., Stevens, T., Walther, R., Ivanisević, P., Galić, Z., 2005. Paleoclimate record in the upper Pleistocene loess-palaeosol sequence at Petrovaradin brickyard (Vojvodina, Serbia). Geologica Carpathica 56, 545–552.

Marković, S.B., Oches, E., Sümegi, P., Jovanović, M., Gaudenyi, T., 2006. An introduction to the middle and upper Pleistocene loess-palaeosol sequence at Ruma brickyard, Vojvodina, Serbia. Quaternary International 149, 80–86.

Marković, S.B., Oches, E.A., McCoy, W.D., Frechen, M., Gaudenyi, T., 2007. Malacological and sedimentological evidence for ‘‘warm’’ glacial climate from the Irig loess sequence, Vojvodina, Serbia. Geochemistry Geophysics Geosystems 8/9, Q09008.

Marković, S.B., Bokhorst, M.P., Vandenberghe, J., McCoy, W.D., Oches, E.A., Hambach, U., Gaudenyi, T., Jovanović, M., Stevens, T., Zöller, L., Machalett, B., 2008. Late Pleistocene loess-palaeosol sequences in the Vojvodina region, North Serbia. Journal of Quaternary Science 23/1, 73–84.

Marković, S.B., Hambach, U., Catto, N., Jovanović, M., Buggle, B., Machalett, B., Zöller, L., Glaser, B., Frechen, M., 2009. The middle and late Pleistocene loess palaeosol sequences at Batajanica, Vojvodina, Serbia. Quaternary International 198, 255–266.

Murray, A.S., Buylaert, J.P., Thomsen, K.J., Jain, M., 2009. The effect of preheating on the IRSL signal from feldspar. Radiation Measurements 44, 554-559.

Mutić, R., 1990. Korelacija kvartara istočne Slavonije na osnovi podataka mineraloško-petrografskih analiza (Istočna Hrvatska, Jugoslavija) - Dio II: Lesni ravnjak. Acta Geologica 20 (2), 29–80, Zagreb.

Novothny, Á., Horváth, E., Frechen, M., 2002. The loess profile at Albertirsa, Hungary - improvements in loess stratigraphy by luminescence dating. Quaternary International 95–96, 155–163.

Novothny, Á., Frechen, M., Horváth, E., Bradák, B., Oches, E.A., McCoy, W.D., Stevens, T., 2009. Luminescence and amino acid recemization chronology of the loess-palaeosol sequence at Sütto, Hungary. Quaternary International 198/1-2, 62-76.

Novothny, Á., Frechen, M., Horváth, E., Krbetschek, M., Tsukamoto, S., 2010. Infrared stimulated luminescence and radiofluorescence dating of aeolian sediments from Hungary. Quaternary Geochronology 5, 114-119.

Novothny, Á., Frechen, M., Horváth, E., Wacha, L., Rolf, Ch., 2011. Investigating the penultimate and last glacial cycles of the Süttő loess section (Hungary) using luminescence dating, high resolution grain size, and magnetic susceptibility data. Quaternary International 234, 1-2, 75-85.

Pécsi, M., 1990. Loess is not just the accumulation of dust. Quaternary International 7/8, 1-21.

Poje, M., 1985. Praporne naslage vukovarskog profila i njihova stratigrafska pripadnost. Geološki Vjesnik 38, 45–66.

Poje, M., 1986. Ekološke promjene na vukovarskom prapornom ravnjaku proteklih cca 500.000 godina. Geološki Vjesnik 39, 19–42.

Prescott, J.R., Hutton, J.T., 1994. Cosmic ray contributions to dose rates for luminescence and ESR dating: large depths and long-term time variations. Radiation Measurements 23, 497-500.

Rees-Jones, J., 1995. Optical dating of young sediments using fine-grain quartz. Ancient TL 13, 9–14.

Reimann, T., Tsukamoto, S., Naumann, M., Frechen, M., 2011. The potential of using feldspars for optical dating of young coastal sediments – a test case from Darss-Zingst peninsula (southern Baltic Sea coast). Quaternary Geochronology 6, 207-222.

Roberts, H.M., 2008. The development and application of luminescence dating to loess deposits: a perspective on the past, present and future. Boreas 37, 483-507.

Rukavina, D., 1983. O stratigrafiji gornjeg pleistocena s osvrtom na topla razdoblja i njihov odraz u naslagama na području Jugoslavije. Rad JAZU 19, 199–221, Zagreb.

Schmidt, E., Machalett, B., Marković, S.B., Tsukamoto, S., Frechen, M., 2010. Luminescence chronology of the upper part of the Stari Slankamen loess sequence (Vojvodina, Serbia). Quaternary Geochronology 5, 137-142.

Singhvi, A.K., Bronger, A., Sauer, W., Pant, R.K., 1989. Thermoluminescence dating of loess-paleosol sequences in the Carpathian basin (East-Central Europe): a suggestion for a revised chronology. Chemical Geology (Isotope Science Section) 73, 307–317.

Spooner, N.A., 1994. The anomalous fading of infrared-stimulated luminescence from feldspars. Radiation Measurements 23, 2/3, 625-632.

Šandor, F., 1912. Istraživanje prapora iz Vukovara, Bilo gore i sa Rajne, Vijesti geološkoga povjerenstva 2, 103-108, Zagreb.

Thiel, C., Coltorti, M., Tsukamoto, S., Frechen, M., 2010a. Geochronology for some key sites along the coast of Sardinia (Italy). Quaternary International 222, 36-47.

Thiel, C., Buylaert, J.-P., Murray, A.S., Terhorst, B., Tsukamoto, S., Frechen, M., 2010b. Investigating the chronostratigraphy of prominent palaeosols in Lower Austria using post-IR IRSL dating. Quaternary Science Journal (E&G).

Thiel, C., Terhorst, B., Jaburová, I., Buylaert, J.-P., Murray, A.S., Fladerer, F.A., Damm, B., Frechen, M., Ottner, F., 2010c. Sedimentation and erosion processes to late Pleistocene sequences exposed in the brickyard of Langenlois/Lower Austria. Geomorphology, doi: 10.1016/j.geomorph.2011.02.011.

Thiel, C., Buylaert, J.-P., Murray, A., Terhorst, B., Hofer, I., Tsukamoto, S., Frechen, M., 2011. Luminescence dating of the Stratzing loess profile (Austria) – Testing the potential of an elevated temperature post-IR IRSL protocol. Quaternary International 234, 1-2, 23-31.

Thiel, C., Buylaert, J.-P., Murray, A.S., Tsukamoto, S., submitted. On the applicability of post-IR IRSL dating to Japanese loess. Geochronometria.

Thomsen, K.J., Murray, A.S., Jain, M., Bøtter-Jensen, L., 2008. Laboratory fading rates of various luminescence signals from feldspar-rich sediment extracts. Radiation Measurements 43, 1474-1486.

Trifunović, S., 1983. Osnovna geološka karta SFRJ 1:100.000 List Odžaci L 34-87. Geološki institut Beograd i Nafta-gas Novi Sad, Savezni geološki zavod, Beograd.

Wacha, L., Mikulčić Pavlaković, S., Frechen, M., Crnjaković, M., 2010a. The Loess Chronology of the Island of Susak, Croatia. Quaternary Science Journal (E&G).

Wacha, L., Koloszár, L., Chikán, G., Galović, L., Magyari, Á., Marsi, I., Tsukamoto, S., 2010b. IRSL Dating of a Quaternary Sediment Succession in Šarengrad, Eastern Croatia. In: Horvat, M.: Abstracts book, 4th Croatian Geological Congress, 380-381, Croatian Geological Survey, Zagreb.

Wacha, L., Mikulčić Pavlaković, S., Novothny, Á., Crnjaković, M., Frechen, M., 2011. Luminescence Dating of Upper Pleistocene Loess from the Island of Susak in Croatia. Quaternary International 234, 1-2, 50-61.

Walker, M., 2005. Quaternary Dating Methods. John Wiley & Sons, London, 286 pp.

Wallinga, J., Murray, A.S., Wintle, A.G., 2000a. The single-aliquot regenerative-dose (SAR) protocol applied to coarse-grain feldspar. Radiation Measurement 31, 529-533.

Wallinga, J., Murray, A., Duller, G., 2000b. Underestimation of equivalent dose in single-aliquot optical dating of feldspars caused by preheating. Radiation Measurement 31, 691-695.

Wallinga, J., Bos, A.J.J., Dorenbos, P., Murray, A.S., Schokker, J., 2007. A test case for anomalous fading correction in IRSL dating. Quaternary Geochronology 2, 216-221.

Wintle, A.G., 1973. Anomalous fading of thermoluminescence in mineral samples. Nature 245, 143-144.

Wintle, A.G., Murray, A.S., 2006. A review of quartz optically stimulated luminescence characteristics and their relevance in single-aliquot regeneration dating protocols. Radiation Measurements 41, 369-391.

Wintle, A.G., Packman, S.C., 1988. Thermoluminescence ages for three sections in Hungary. Quaternary Science Reviews 7, 315–320.

Zoeller, L., 2010. New approaches to European loess: a stratigraphic and methodical review of the past decade. Central European Journal of Geosciences 2(1), 19-31..

CHAPTER 6

Conclusion

The main topic of the PhD study was luminescence dating of loess-palaeosol sequences from Croatia. It was the first time that detailed and systematic optically stimulated luminescence (OSL) dating was applied to Croatian loess deposits. Two genetically different types of loess deposits were studied; the loess-palaeosol sequences found in the river Po loess region, represented by the aeolian deposits found on the Island of Susak in the North Adriatic Sea, and loess-palaeosol sequences from the Danube loess region, represented by the famous "Gorjanović loess section" from Vukovar. Establishing a geochronological framework of these similar loess deposits from different locus typicus in Croatia helps us to understand the evolution of the palaeoclimatic conditions during the Middle and Late Pleistocene, and so enable us to reconstruct the environmental conditions and changes for this time period. One of the milestones of this study is the setting up of a detailed stratigraphy of Quaternary deposits in Croatia based on numerical dating. Furthermore, the results of these detailed and systematically investigated loess-palaeosol sequences can be used for a better local as well as regional correlation.

The island of Susak is a unique and extraordinary example for loess accumulation in the Po river system. Its very detailed preservation of sediments is unique giving us the most detailed terrestrial Late Pleistocene loess-palaeosol record in the Po river system and so in the North Adriatic region. The loess from Susak became the focus of a multi-disciplinary study. Three chapters of this thesis (Chapter 2, 3 and 4) deal with the geochronology of the deposits, as well as with the detailed mineralogy and geochemistry of the sediments under study. For the first time a high-resolution dating approach was applied for the sections under study on Susak, with altogether 37 samples collected for luminescence dating and 13 for radiocarbon dating. The very detailed geochronological framework using two numerical dating methods but also geological field-evidence shows that the loess and loess-like deposits from Susak correlate to the Upper Pleistocene. The material proved to have excellent luminescence properties (Chapter 2 and 4), as seen from the performance tests, and so gave reliable results. For the dating of the samples the single aliquot regenerative (SAR) protocol was used on polymineral fine-grained material separated from the loess and the feldspar signal was

registered. Besides the SAR protocol the multiple aliquot additive dose (MAAD) protocol, which is a somewhat older measuring principle, was used as well, to be able to compare the data with previously published literature. The MAAD dating results are comparable (more or less in good agreement) with the uncorrected SAR results. Since feldspar shows anomalous fading, fading tests were performed and the SAR dating results were corrected (Huntley and Lamothe, 2001) giving more reliable results. Within error limits, the results are in stratigraphical order, correlating the investigated loess-palaeosol sections to the last glacial-interglacial cycle (and possibly older). The most interesting is the Middle Pleniglacial record (OIS3), which is characterised by a great thickness of the deposits giving evidence for intensive dust accumulation during that time. The loess is intercalated by numerous palaeosols and two tephra layers indicating climatic fluctuations which resulted in pedogenetical processes as well as volcanic activity during that time. The luminescence dating results are in excellent agreement with independent age control, as provided by the radiocarbon dating method.

The dating results of the investigated sections can be correlated to the Last Glacial-Interglacial period and do not at all present the (almost) complete Pleistocene like previously assumed by Bognar et al. (2003). The possibility that loess deposited on Susak in the Penultimate Glacial exists but the assumption of Bognar et al. (2003) that the red palaeosols covering the carbonate basement belong to the Early-Middle Pleistocene and that the Brunhes-Matuyama palaeomagnetic inversion was detected in these palaeosols can very likely be discarded. Furthermore, the dating results of this study and their interpretation are in good agreement with similar studies from North Italy (Ferraro, 2009).

The results of the heavy minerals analysis of the deposits on Susak show that the source material most likely originates from the area of the Alpine collisional orogen and the river Po sediments and its tributaries (Chapter 3). Furthermore, based on the mineralogy and morphology of the volcanic particles found in the tephra layers, as well as the age estimates, the possible sources of the tephras were detected in the Campanian Province and the Aeolian arc in Italy.

The research of the palaeomagnetic and grain-size properties of the sections under study is in progress (Wacha et al., in preparation). The first results of the current palaeomagnetic studies show a clear, well defined palaeomagnetic signal with dominant normal magnetization for the entire loess sequence. In the upper part of the investigated sections smaller palaeomagnetic inversions are detected which can be correlated to the Mono Lake and Laschamp events dated

around 34.6 ka and 41 ka (Laj et al., 2004), respectively. This conclusion is supported by the OSL-based geochronology presented in this PhD. Furthermore, detailed investigations of the red palaeosols covering the carbonate basement and from the lower part of the section is in progress as well.

In Chapter 5 a detailed geochronological study was presented for the "Gorjanović loess section" at Vukovar in eastern Croatia. This is the first detailed high-resolution OSL dating study in this loess region of Croatia, although first luminescence dating results from loess of the same region were presented by Singhvi et al. (1989) using the thermoluminescence (TL) dating method and by Galović et al. (2009) using infrared optically stimulated luminescence (IRSL). In this study the recently developed post-IR IRSL protocol was used for measuring the D_e-s needed for age calculations. In recent times the dating method is going to be developed for dating of older deposits (>100ka) as well as with the aim to overcome problems connected to fading of the feldspar IRSL signal (Thomsen et al., 2008; Buylaert et al., 2009; Thiel et al., 2010a, b, c, 2011, submitted). This study is an example that the post-IR IRSL protocol has potential of dating older samples what significantly helps unravelling Penultimate Glacial loess sequences.

The dating results presented in Chapter 5 show us that the section under study represent loess deposition during the last two glacials intercalated by palaeosols which developed under interglacial and interstadial periods. The lowest exposed palaeosol form the "Gorjanović loess section" very likely correlates to OIS7, the thick brown palaeosol from the middle part of the sequence can be correlated to OIS5 while the thin gray palaeosol found in the upper part correlates to OIS3. These results can be correlated and compared to similar studies from the Carpathian basin (Serbia and Hungary) (Figure 4.1.). Furthermore, a tephra horizon was detected intercalated in the loess below the OIS5 palaeosol which can be used as a marker horizon in this area. Similar evidences of volcanic activity were found in the Carpathian basin as well. On Figure 6.1. the loess-palaeosol sequences investigated in this PhD research are compared with similar last glacial-interglacial sequences from the nearby area, i.e. from North Italy (Val Sorda - Ferraro, 2009), Eastern Croatia (Zmajevac - Galović et al., 2009), Serbia (Stari Slankamen - Schmidt et al., 2010; Surduk – Fuchs et al., 2008; Antoine et al., 2009) and Hungary (Süttő – Novothny et al., 2009, 2010). These sections have a detailed luminescence dating – based geochronological framework established. In Eastern Croatia, as seen in the loess-palaeosols sequence from Vukovar, there were two major loess accumulation phases during the last Glacial, correlating to OIS4 and 2. Especially high mass accumulation rates

were calculated for the Last Glacial Period (OIS2) in Europe (Frechen et al., 2003; Újvári et al., 2010) The weak palaeosol found intercalating the last glacial loess correlates to an interstadial during OIS3. A similar stratigraphic situation was found at the Zmajevac section (Galović et al., 2009). Based on the results of this study it is very likely that the dating results from the Zmajevac section have to be revised, especially from the lower part of the sequence (for which fading correction was not applied by Galović et al., 2009), due to the progress in the dating method which significantly will improve the chronological framework and the interpretation. The same conclusion is valid for the Carpathian basin as seen on Figure 6.1. The Penultimate Glacial loess is exposed in many sections and more investigations are required with the more robust and newly developed protocol for dating of older loess. This will significantly improve and help understanding of the palaeoclimatic conditions during the Penultimate Glacial as well.

While the OIS3 record in the Carpathian basin seems simple and uniform, the situation in the North Adriatic loess region is more complex and completely different. There, OIS3 includes numerous palaeosols of different types and evolution. Although a part of the OIS3 record on Susak is re-deposited, as seen from the grain-size analyses (Wacha et al., in preparation), the great thickness of the deposits due to the increased dust dynamics in this area during that time, the types of palaeosols, the great input of coarser-grained material and the volcanic influence all indicate that the North Adriatic loess area is a separate and specific loess region which deserves to be studied in more detail.

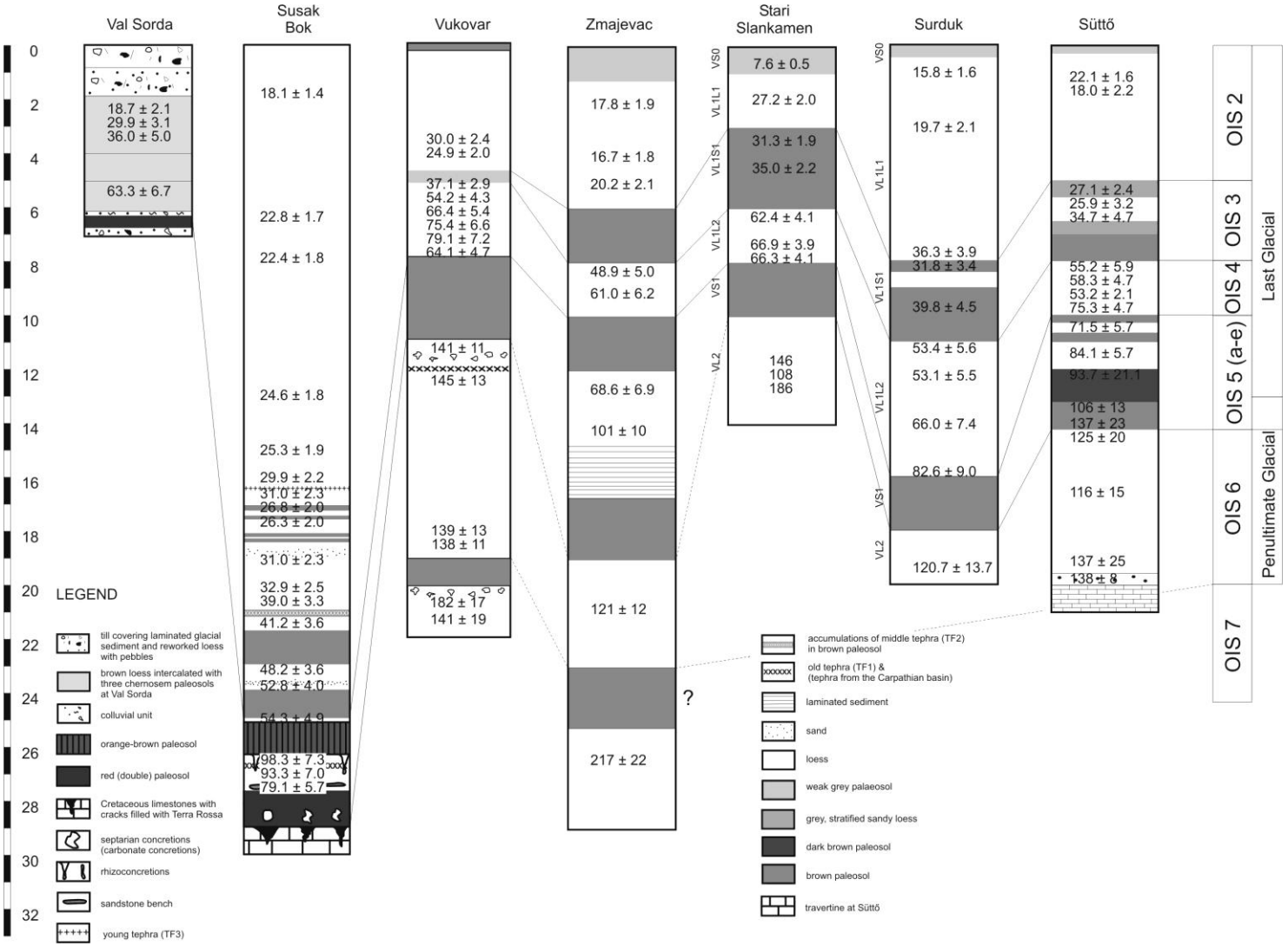

Figure 6.1. The Bok section, selected to be the most representative section on Susak, and the "Gorjanović loess section" from Vukovar correlated with coeval loess-palaeosol sections from Italy (Val Sorda – Ferraro, 2009), East Croatia (Zmajevac – Galović et al., 2009), Serbia (Stari Slankamen – Schmidt et al., 2010 and Surduk – Antoine et al., 2009; Fuchs et al., 2008) and Hungary (Süttő – Novothny et al., 2009, 2010).

References

Antoine, P., Rousseau, D.D., Fuchs, M., Hatté, C., Gauthier, C., Marković, S.B., Jovanović, M., Gaudenyi, T., Moine, O. and Rossignol, J., 2009. High-resolution record of the last climatic cycle in the southern Carpathian Basin (Surduk, Vojvodina, Serbia). Quaternary International 198, 19-36.

Bognar, A., Schweitzer, F., Szöőr, G., 2003. Susak – environmental reconstruction of a loess island in the Adriatic. Geographical Research Institute, Hungarian Academy of Sciences, Budapest, 141 pp.

Buylaert, J.P., Murray, A.S., Thomsen, K.J., Jain, M., 2009. Testing the potential of an elevated temperature IRSL signal from K-feldspar. Radiation Measurements 44, 560-565.

Ferraro, F., 2009. Age, sedimentation and soil formation in the Val Sorda loess sequence, Northern Italy. Quaternary International 204, 54-64.

Fuchs, M., Rousseau, D.-D., Antoine, P., Hatté, C., Gauthier, C., Marković, S., Zoeller, L. 2008. Chronology of the Last Climatic Cycle (Upper Pleistocene) of the Surduk loess sequence, Vojvodina, Serbia. Boreas 37, 66-73.

Frechen, M., Oches, E.A., Kohfeld, K.E., 2003. Loess in Europe – mass accumulation rates during the Last Glacial Period. Quaternary Science Reviews 22, 1835-1857.

Galović, L., Frechen, M., Halamić, J., Durn, G., Romić, M., 2009. Loess chronostratigraphy in Eastern Croatia - A first luminescence dating approach. Quaternary International 198 (1-2), 85 -97.

Huntley, D.J., Lamothe, M., 2001. Ubiquity of anomalous fading in K-feldspars, and the measurement and correction for it in optical dating. Canadian Journal of Earth Sciences 38, 1093-1106.

Laj, C., Kissel, C., Beer, J., 2004. High Resolution Global Paleointensity Stack Since 75 kyr (GLOPIS-75) Calibrated to Absolute Values. Timescales of the Geomagnetic Field (American Geophysical Union, Washington, C, 2004), vol. Geophysical Monograph 145, 255–265.

Novothny, Á., Frechen, M., Horváth, E., Bradák, B., Oches, E.A., McCoy, W.D., Stevens, T., 2009. Luminescence and amino acid recemization chronology of the loess-palaeosol sequence at Sütto, Hungary. Quaternary International 198/1-2, 62-76.

Novothny, Á., Frechen, M., Horváth, E., Krbetschek, M., Tsukamoto, S., 2010. Infrared stimulated luminescence and radiofluorescence dating of aeolian sediments from Hungary. - Quaternary Geochronology 5, 114-119.

Schmidt, E., Machalett, B., Marković, S.B., Tsukamoto, S., Frechen, M., 2010. Luminescence chronology of the upper part of the Stari Slankamen loess sequence (Vojvodina, Serbia). Quaternary Geochronology 5, 137-142.

Singhvi, A.K., Bronger, A., Sauer, W., Pant, R.K., 1989. Thermoluminescence dating of loess-paleosol sequences in the Carpathian basin (East-Central Europe): a suggestion for a revised chronology. Chemical Geology (Isotope Science Section) 73, 307-317.

Thiel, C., Coltorti, M., Tsukamoto, S., Frechen, M., 2010a. Geochronology for some key sites along the coast of Sardinia (Italy). Quaternary International 222, 36-47.

Thiel, C., Terhorst, B., Jaburová, I., Buylaert, J.-P., Murray, A.S., Fladerer, F.A., Damm, B., Frechen, M., Ottner, F., 2010b. Sedimentation and erosion processes to late Pleistocene sequences exposed in the brickyard of Langenlois/Lower Austria. Geomorphology, doi: 10.1016/j.geomorph.2011.02.011.

Thiel, C., Buylaert, J.-P., Murray, A.S., Terhorst, B., Tsukamoto, S., Frechen, M., 2010c. Investigating the chronostratigraphy of prominent palaeosols in Lower Austria using post-IR IRSL dating. Quaternary Science Journal (E&G).

Thiel, C., Buylaert, J.-P., Murray, A., Terhorst, B., Hofer, I., Tsukamoto, S., Frechen, M., 2011. Luminescence dating of the Stratzing loess profile (Austria) – Testing the potential of an elevated temperature post-IR IRSL protocol. Quaternary International 234, 1-2, 23-31.

Thiel, C., Buylaert, J.-P., Murray, A.S., Tsukamoto, S., submitted. On the applicability of post-IR IRSL dating to Japanese loess. Geochronometria.

Thomsen, K.J., Murray, A.S., Jain, M., Bøtter-Jensen, L., 2008. Laboratory fading rates of various luminescence signals from feldspar-rich sediment extracts. Radiation Measurements 43, 1474-1486.

Újvari, G., Kovács, J., Varga, G., Raucsik, B., Marković, S.B., 2010. Dust flux estimates for the Last Glacial Period in East Central Europe based on terrestrial records of loess deposits: a review. Quaternary Science Review 29, 3157-3166.

Wacha, L., Rolf, C., Frechen, M., Galović, L., Duchoslav, M., Hambach, U. The OIS 3 loess record on Susak: the high resolution grain-size, rock magnetic and palaeomagnetic approach. (in preparation).

CURRICULUM VITAE

For reasons of data protection, the curriculum vitae is not included in the online version.

PUBLICATIONS LIST

- **Wacha, L**., Rolf, C., Frechen, M., Galović, L., Duchoslav, M., Hambach, U. The OIS 3 loess record on Susak: the high resolution grain-size, rock magnetic and palaeomagnetic approach. (in preparation).

- **Wacha, L**., Frechen, M., 2011. The geochronology of the "Gorjanović loess section" in Vukovar, Croatia. Quaternary International, doi: 10.1016/j.quaint.2011.04.010.

- Pavelić, D., Kovačić, M., Vlahović, I., **Wacha, L.**, 2011. Pleistocene calcareous aeolian-alluvial deposition in a steep relief karstic coastal belt (Island of Hvar, eastern Adriatic, Croatia). Sedimentary Geology, doi: 10.1016/j.sedgeo.2011.05.005.

- **Wacha, L.**, Mikulčić Pavlaković, S., Frechen, M., Crnjaković, M., 2010. The Loess Chronology of the Island of Susak, Croatia. Quaternary Science Journal (E&G).

- Novothny, A., Frechen, M., Horváth, E., **Wacha, L**., Rolf, C., 2011. High resolution grain size and magnetic susceptibility record of the (penultimate and) last glacial cycles in the Süttő loess section, Hungary. Quaternary International 234, 1-2, 75-85.

- Mikulčić Pavlaković, S., Crnjaković, M., Tibljaš, D., Šoufek, M., **Wacha, L.**, Frechen, M., Lacković, D., 2011. Mineralogical and geochemical characteristics of Quaternary sediments from the Island of Susak (Northern Adriatic, Croatia), Quaternary International 234, 1-2, 32-49

- **Wacha, L.,** Mikulčić Pavlaković, S., Novothny, Á., Crnjaković, M., Frechen, M., 2011. Luminescence Dating of Upper Pleistocene Loess from the Island of Susak in Croatia. Quaternary international 234, 1-2, 50-61.

- Hajek-Tadesse, V., Belak, M., Sremac, J., Vrsaljko, D., **Wacha, L**., 2009. Lower Miocene ostracods from the Sadovi section (Mt. Požeška gora, Croatia). Geologica Carpathica. 60/3; 251-262.

CONFERENCE PARTICIPATION

- Novothny, Á., Horváth, E., Frechen, M., Thiel, Ch., **Wacha, L**., Rolf, Ch., 2010. Complex investigation of the penultimate and last glacial cycles of the Süttő loess section (Hungary). In: Lassu, T. (ed.): International workshop on loess research and geomorphology 2010., Book of Abstracts, 23-23, University of Pécs, Faculty of Sciences, Institute of Geography, Pécs, Hungary.

- Novothny, Á., Horváth, E., Frechen, M., Königer, P., Thiel, Ch., **Wacha, L.**, Rolf, Ch., Krolopp, E., Barta, G., Bajnóczi, B., 2010. Detailed chronological and high resolution grain size, geochemical and palaeomagnetic study of the Süttő loess-palaeosol sequence, Hungary. XIX Congress of the Carpathian Balkan Geological Association. Thessaloniki, Greece.

- Mikulčić Pavlaković, S., Crnjaković, M., Tibljaš, D., Šoufek, M., **Wacha., L**., Frechen, M., 2010, Tefra u pleistocenskim lesnim naslagama otoka Suska (sjeverni Jadran, Hrvatska) –karakterizacija i problematika. In: Horvat, M. (ed.): 4th Croatian Geological Congress, Šibenik, Abstracts book, 22-23, Croatian Geological Survey, Zagreb.

- **Wacha, L.,** Koloszár, L., Chikán, G., Galović, L., Magyari, Á., Marsi, I., Tsukamoto, S., 2010. IRSL Dating of a Quaternary Sediment Succession in Šarengrad, Eastern Croatia. In: Horvat, M. (ed.): 4th Croatian Geological Congress, Šibenik, Abstracts book, 380-381, Croatian Geological Survey, Zagreb.

- **Wacha, L.,** Mikulčić Pavlaković, S., Frechen, M., Crnjaković, M., Rolf, Ch., Hambach, U., 2010. Geochronological and Palaeoenvironmental Reconstruction of the Loess-Palaeosol Sequence on the Island of Susak In: Horvat, M. (ed.): 4th Croatian Geological Congress, Šibenik, Abstracts book, 382-383, Croatian Geological Survey, Zagreb.

- Hambach, U., Duchoslav, M., Rolf, Ch., **Wacha, L**., Frechen, M., Galović, L., 2010. The rock magnetic characteristics of last glacial cycle loess from the island of Susak (Adriatic Sea, Croatia) EGU General Assembly 2010, Wienna, Austria.

- Thiel, Ch., Königer, P., Ostertag-Henning, Ch., Scheeder, G., Novothny, Á., Horváth, E., **Wacha, L**., Techmer, A., Frechen, M., 2010. Multi-proxy approach for palaeoclimate reconstruction using a loess-palaeosol sequence from Süttő, Hungary. EGU General Assembly 2010, Wienna, Austria.

- Koeniger, P., **Wacha, L.**, Thiel, Ch., Ostertag-Henning, Ch., Scheeder, G., Novothny, Á., Bajnóczi, B., Horváth, E., Techmer, A., Frechen, M., 2010. Evaluation of bulk carbonate stable isotope composition from the Süttő loess sequence (Hungary) - What can we interpret with an existing chronology? - 10th International Conference "Methods of Absolute Chronology", Gliwice, Poland.

- **Wacha, L.**, Frechen, M., Novothny, Á., Mikulčić Pavlaković, S., Crnjaković, M., 2009. Luminescence and Radiocarbon dating of Three Loess Sections on the Island of Susak, Croatia. German Meeting on Luminescence and Electron Spin Resonance Dating 2009, Hannover, Germany.

- **Wacha, L**., Mikulčić Pavlaković, S., Novothny, Á., Crnjaković, M., Frechen, M., 2009. The Loess Record on the Island of Susak, Croatia. Loessfest2009, Novi Sad, Serbia.

- Mikulčić Pavlaković, S., Crnjaković, M., Šoufek, M., **Wacha, L**., Frechen, M., 2009. Morphology of volcanic particles from Quaternary loess deposits of Susak Island, Croatia // XL. Ifjú Szakemberek Ankétja – XL. Meeting of Young Geoscientists, 46-47., Keszthely, Hungary.

- **Wacha, L.,** Novothny, Á., Kunz, A., Frechen, M., 2008. Luminescence Dating of Loess on the Island of Susak, Croatia. - German Meeting on Luminescence and Electron Spin Resonance Dating 2008, Leipzig, Germany.

- Avanić, R., Bakrač, K., Grizelj, A., **Wacha, L.,** Šimić-Stanković, M., Hećimović, Lj., Tibljaš, D., Kruk, B., 2006. Ivošević Gaj ceramic clay deposit in the vicinity of Vojnić. In: Vlahović, I., Tibljaš, D., Durn, G. (eds.) 3rd Mid European Clay conference, Opatija, Field Trip Guidebook: Ceramic and brick clays deposits and excesive flysch erosion, 39-47.

- Kovačić, M., Miknić, M., Bakrač, K., Grizelj, A., **Wacha, L.**, Vrsaljko, D., 2005. Gornjomiocenska regresija u jugozapadnom rubnom području Panonskog bazena (Žumberak, Republika Hrvatska). In: Ed. Velić, I., Vlahović, I., Biondić, R., (eds.): 3rd Croatian Geological Congress, Opatija, Abstracts book, 75-76, Croatian Geological Survey, Zagreb.

- Avanić, R., Pécskay, Z., **Wacha, L**., Palinkaš, L. 2005. K-Ar dating of glauconitic sediments in Macelj Mt. (NW Croatia). In: Ed. Velić, I., Vlahović, I., Biondić, R., (eds.): 3rd Croatian Geological Congress, Opatija, Abstracts book, 5-6, Croatian Geological Survey, Zagreb.

Erklärung

Hiermit erkläre ich, Lara Wacha, dass ich die Arbeit eigenständig angefertigt habe. Alle Stellen, die dem Wortlaut oder dem Sinn nach anderen Werken entnommen sind, wurden durch Angabe der Quellen als solche kenntlich gemacht.

Die Bearbeitungsanteile der in dieser Dissertation eingegliederten Manuskripte sind in den entsprechenden Kapiteln aufgeführt.

Lara Wacha

Zagreb, Februar 2011

This work has been financed by the DAAD (German Academic Exchange Service); the Leibniz Institute for Applied Geophysics (LIAG), Hannover, Germany, the Croatian Geological Survey, Zagreb, Croatia and by the Croatian Ministry of Science, Education and Sports (project nr. 0181001).
A lot of people helped, supported, and inspired me during my work. I hope I will have the opportunity to say thanks to every single last one of you…

L.